The function and regulation of IL-17A-producing T cell subsets in central nervous system autoimmunity

Trinity College Dublin
Coláiste na Tríonóide, Baile Átha Cliath
The University of Dublin

Charlotte Leane

B.A. (Mod.) Immunology

A thesis submitted to

Trinity College Dublin

As completion of the degree of Doctor of Philosophy

2024

Supervisor: Professor Kingston Mills

Immune Regulation Research Group

School of Biochemistry and Immunology

Trinity College Dublin

Declaration of Authorship

I declare that this thesis has not been submitted as an exercise for a degree at this or any other university and it is entirely my own work.

I agree to deposit this thesis in the University's open access institutional repository or allow the Library to do so on my behalf, subject to Irish Copyright Legislation and Trinity College Library conditions of use and acknowledgement.

I consent to the examiner retaining a copy of the thesis beyond the examining period, should they so wish.

_____

Charlotte Leane

School of Biochemistry and Immunology

Trinity College Dublin

Abstract

Multiple sclerosis (MS) is a chronic progressive autoimmune disease of the central nervous system (CNS). MS is characterised by the presence of demyelinating lesions in the CNS and is the leading cause of disability among young adults between the ages of 20-30. Experimental autoimmune encephalomyelitis (EAE) is the murine model for MS and is a crucial tool for dissecting the immune responses that mediate pathology in this disease. EAE is a T cell-mediated autoimmune disease that results in ascending paralysis of the mouse. Autoantigen-specific IL-17A-producing CD4 T (Th17) cells and γδ T cells have emerged as central players in the pathogenesis of EAE. Activation of naïve CD4 T cells and their differentiation into IL-17A-producing antigen-specific Th17 cells requires several signals, provided by antigen presenting cells (APCs). APCs present the myelin antigen, myelin oligodendrocyte glycoprotein (MOG) to CD4 T cells, hence regulating the differentiation of Th17 cells. Conversely, IL-17A-producing γδ T cells can be activated with the cytokines IL-1β and IL-23, in the absence of T cell receptor (TCR) engagement, thereby becoming activated under less stringent conditions than CD4 T cells. γδ T cells are a crucial early source of IL-17A that precipitate CNS autoimmunity. As CD4 T cells require antigen to be presented to them in the context of MHC molecules expressed by APCs, they are subject to regulatory T (Treg) cell-mediated suppression. Furthermore, the expression of checkpoints, such as programmed cell death protein-1 (PD-1) by CD4 T cells contributes to the regulation of the antigen-specific immune response. Engagement of PD-1 expressed by CD4 T cells negatively regulates T cell function. Immune checkpoint inhibitors (ICIs) are used in the treatment of cancer, but patients that respond to this immunotherapy develop autoimmune diseases. Since γδ T cells can be activated without TCR engagement with MHC and co-stimulatory molecules expressed by APCs we hypothesised that IL-17A-producing γδ T cells are not subject to the same regulatory mechanisms that control CD4 T cell function. This lack of conventional regulation may allow γδ T cells to become activated in an unrestrained manner enabling them to precipitate autoimmunity.

The present study revealed that $CD27^-$ Vγ4-expressing γδ T cells express high levels of the immune checkpoint, PD-1 in the lymph node (LN) of naïve mice and this expression is further augmented during EAE. Anti-PD-1 treatment during EAE significantly enhanced the severity of disease in wildtype mice, but not in $TCR\delta^{-/-}$ mice. Furthermore, anti-PD-1 enhanced IL-17A production by Vγ4 γδ T cells in the LN at the induction phase of EAE and also promoted the development of Th17 cells. However, anti-PD-1 treatment did not enhance the severity of EAE

or the development of Th17 cells in TCRδ$^{-/-}$ mice. Studies using recombinant PD-L1 demonstrated that Vγ4 γδ T cells activated via their TCR were regulated by PD-1 engagement *in vitro* whereas PD-1 engagement of IL-1β+IL-23-activated Vγ4 γδ T cells did not impact their function. Additionally, the anti-PD-1-mediated increase in IL-17A production by Vγ4 γδ T cells was dependent on MOG, which suggests that during EAE, IL-17A-producing Vγ4 γδ T cells are MOG-specific and are regulated via PD-1 in a TCR-dependent manner.

An examination of the role of IL-10 in regulating T cell responses during EAE revealed that neutralisation of the IL-10R enhanced the severity of disease and was associated with enhanced expression of the integrins LFA-1 and VLA-4 by CD4, CD8, and γδ T cells in the LN early in disease. Furthermore, neutralisation of the IL-10R enhanced the infiltration of VLA-4-expressing CD4, CD8, and CD27^{-} γδ T cells into the brain at the peak of EAE. MOG-specific type 1 regulatory T (Tr1) cells regulated IL-17A-and IFN-γ-producing MOG-specific CD4 T cells in an IL-10-dependent manner. In contrast, IL-17A production by IL-1β+IL-23 activated CD27^{-} γδ T cells was not regulated by MOG-specific Tr1 cells demonstrating that innately activated γδ T cells escape the regulatory mechanisms of TCR-activated T cells.

An examination of the role of TGF-β in regulating the development of IL-17A-producing CD4 and γδ T cells during EAE has demonstrated that IL-17A production by IL-1β+IL-23-activated CD27^{-} γδ T cells was not suppressed, but rather enhanced by TGF-β, whereas IFN-γ production by IL-12+IL-18-stimulated CD27^{+} γδ T cells was suppressed by TGF-β. Neutralisation of TGF-β-mediated signalling during EAE reduced the severity of disease and this was associated with decreased infiltration of IL-17A and TNF-producing γδ and CD4 T cells into the CNS at the peak of EAE and increased IFN-γ and GM-CSF production by CNS-infiltrated γδ and CD4 T cells. Neutralisation of IFN-γ reversed the suppressive effect of TGF-β neutralisation on IL-1β+IL-23-activated CD27^{-} γδ T cells, suggesting that TGF-β supports IL-17A production by γδ and CD4 T cells in an IFN-γ-dependent manner.

The findings of this study have demonstrated that IL-17A-producing γδ T cells are resistant to suppression mediated by TGF-β and IL-10. However, PD-1 engagement significantly suppressed IL-17A production by Vγ4 γδ T cells during EAE, highlighting the therapeutic potential of PD-1 agonistic monoclonal antibodies for the treatment of autoimmunity.

Acknowledgements

First and foremost, I would like to thank Kingston enormously for all the support and patience over the past number of years. I really appreciate the time you have taken to help me with writing my thesis and I hope I have done you justice. It has been an incredible experience training with you and I can't thank you enough for your advice and guidance on matters both inside and outside of the lab when things have been challenging. I will always think of these years fondly and I am very proud of what I have managed to accomplish under your supervision. Your excitement and passion for research is truly inspiring.

Aoife, I can't thank you enough for your help at the very beginning of my time in the lab. From supervising my undergrad project to teaching me how to induce EAE and to now being a really good friend, I appreciate every bit of it. Thank you so much for being a fantastic science role model and also just a really fun person to be around.

I have so much appreciation for the post-docs that have been in the lab throughout my years here. I would like to especially thank Caroline, Davoud, Lisa, and Mieszko for being great mentors and providing us with such excellent examples of what great scientists look like. I will always appreciate you all for being so helpful and insightful. I feel really lucky to have learned from you all. I would also like to massively thank Barry and Aoife for all the FACS help over the past number of years. Barry, we are so fortunate to have you here to help us. I have never met a more patient person before, and you never make anything seem like a problem. I am so appreciative to you for your help and advice.

I have made so many incredible friends in the lab over the years and I am so grateful to now also call you real-life friends! To Lucy, I miss you so so much since you have moved on, but I am so excited to see the amazing work you do next! You have been a fantastic friend and I appreciate your light heartedness and kindness so much. I feel very fortunate that we met during our PhDs and I thank you for showing me a fabulous example of how to work hard and play even harder! Thank you, Kyle, for being a great PhD role model from when I started in the lab. I have always admired how balanced you are in your approach to research, and I have learned so much from you over the years. Caitlín, you are a superstar and I count myself very lucky to have met you during this journey. You have such a bright and kind energy, which is so lovely to be around, and I can't imagine

the lab without you! We have shared some very cool experiences over the past couple of years and I'm extremely glad that you were a part of them. Béré and Pauline, you have been such amazing ladies to work with. I have learned an enormous amount from you both and I can't thank you both enough for your time, but more importantly your kindness. To Karen, I am so glad we met! You are such an amazing person and I do not know how you make it all look so easy. I hope to see you soon for a glass/ bottle of wine to celebrate us both finishing! Thank you so much to Catherine and Paula for helping with all lab matters and for always keeping everything running smoothly. Mag, thank you so much for being so helpful and for never making things feel like a problem. You are such a gift to have and I have really enjoyed getting to know you.

I would like to thank the Loane lab so much for being really great to work with! To David, thank you for your advice on the project and also for your neuroscience insight, which has been greatly appreciated. To Janeen and Isabella, you are both such fab girls. Isabella, I miss you so much! Janeen, you are such a fabulous friend! I feel like I have known you for years and years. You are so fun to be around and I appreciate not only your stunning energy but also your amazing work ethic. You are really very impressive and I know that you will do amazing things. To Carly, Gloria, Nathan, and Sahil, it has been really great to meet you all and you have brought so much fun to the lab, which I absolutely love!

Stephen, where do I start? Thank you so so much for being the most hilarious and fantastic friend. We have been through so much over the last few years and I feel like we kind of became best friends accidentally? All good though because it has worked out pretty well. It began with New York, then Beverly Hills, and even Dubai, all the way to Pearse Square. What a time! I'm glad you didn't actually go to prison because I would miss you far too much.

Luke!!! It feels so strange to actually be writing this right now especially when I know you are doing the same thing. We have had such hilarious times over the past few years and I am glad that our time living together didn't end in Worcester! I am always intrigued to find out what you are about to send me when I hear you cackle down the hallway of 26B. Love you so very much and I really appreciate your friendship. I am so lucky to have you and Stephen and I never laugh more than when I am with you both.

Hannah, you are such a sweetheart and I count myself very lucky to be friends with you. You are such a caring person but equally able to say what is really on your mind. It has been so nice to get advice from you when I know you have gone through it all before and with such ease. Thank you for being a great friend (for life I hope).

To my friends from home, Adam, Darragh, Eimear, Kara, and Maria. I am so lucky to have had you all by my side for over a decade! Thank you all for being there even if we don't speak as often as we would like. You are all true friends and I look forward to seeing more of you all now that this chapter is coming to an end.

I have been so so lucky to meet the most amazing people over the past few years that have helped me greatly outside of work. To Lorraine, I can't believe I met you almost 4 years ago! Thank you so much for pushing me when I need it but also for knowing when to pull back. You are an inspiration to me! Thanks for helping me to be strong both physically and mentally. To my teachers at Reformation and The Space Between especially Eszter, Gill, and Lucybloom. Beyond learning about immunology, I have learned so much about life in the past number of years and you have been a major part of that. Thank you all so much for being a part of the journey and for helping me to stay grounded throughout this whole process but above all thank you for showing me that some things need to be believed to be seen.

Most importantly I can't express enough gratitude to my family for all their support throughout this journey. Mom, you are my rock. Thank you for being there through every up and every down. I couldn't have done it without you. To Dad, thank you so much for being the most chill human being on the planet. Your support has always made anything seem possible and I don't know how I will ever repay you (please don't make me repay you!). To Elana, I have loved you being in Dublin with me. I kind of hate to say it but I think you might be funnier than me! I love your humour and I'm very lucky to have you and Mom as the best example of super strong ladies. To Gavin and Jaden, you are both so funny in very different ways and I really love being around you both. Thanks for the distractions in stressful times over the past few years. To my grandparents of whom I have lost three, I would not be the person I am today without your influence. I have learned different things from each of you and I count myself extremely lucky to have known you and experienced your strength.

Publications

McGinley, AM, Sutton, CE, Edwards SC, **Leane, CM**, DeCourcey, J, Teijeiro, A, Hamilton, JA, Boon, L, Djouder, N and Mills, KHG (2020) Interleukin-17A Serves a Priming Role in Autoimmunity by Recruiting IL-1β-Producing Myeloid Cells that Promote Pathogenic T Cells. Immunity 2(52)

List of abbreviations

AAV	Adeno-associated virus
ADCC	Antibody-dependent cellular cytotoxicity
AHR	Aryl hydrocarbon receptor
AML	Acute myeloid leukaemia
AMP	Anti-microbial peptide
AMPK	AMP-activated protein kinase
AP-1	Activator protein-1
APC	Antigen presenting cell
AREG	Amphiregulin
B_2m	β_2 microglobulin
BALF	Bronchoalveolar lavage fluid
BBB	Blood brain barrier
BCR	B cell receptor
BM	Bone marrow
BMDC	Bone marrow-derived dendritic cells
Breg	Regulatory B cell
BSA	Bovine serum albumin
BTN	Butyrophilin
CAF	Cancer-associated fibroblast
Ceacam-1	Carcinoembryonic-antigen-related cell adhesion molecule1
CFA	Complete Freund's adjuvant
CIA	Collagen-induced arthritis
CLP	Common lymphoid progenitor
CMC	Chronic mucocutaneous candidiasis
CMU	Comparative Medicine Unit
CNS	Central nervous system
CRC	Colorectal cancer
CSF	Cerebrospinal fluid
CSF	Colony-stimulating factor
CTL	Cytotoxic lymphocytes
CTLA4	Cytotoxic T lymphocyte-associated antigen-4
DAG	Diacylglycerol
DAMP	Damage-associated molecular pattern
DC	Dendritic cell
DETC	Dendritic epidermal T cell
DMSO	Dimethyl sulfoxide
DMT	Disease-modifying treatment
DN	Double negative
DNase	Deoxyribonuclease
DOT	Delta One T

DP	Double positive
EAE	Experimental autoimmune encephalomyelitis
eATP	Extracellular adenosine triphosphate
EBAO	Ethidium bromide acridine orange
EBI3	EBV-induced gene 3
EBV	Epstein-Barr virus
EDSS	Expanded disability status scale
ELISA	Enzyme-linked immunosorbent assay
EOMES	Eomesodermin
ERK	Extracellular signal-related kinase
FACS	Fluorescence-associated cell sorting
FCS	Fetal calf serum
FMO	Fluorescence minus one
FoxP3	Forkhead box protein 3
GARP	Glycoprotein A repetitions predominant protein
G-CSF	Granulocytes colony-stimulating factor
GI	Gastrointestinal
GITR	Glucocorticoid-induced TNF receptor
GM-CSF	Granulocyte macrophage colony-stimulating factor
GvHD	Graft versus host disease
HIF-1α	Hypoxia-inducible factor-1α
HMGR	Hydroxy-methylglutaryl-CoA reductase
HRP	Horseradish peroxidase
i.p	Intraperitoneal
ICI	Immune checkpoint inhibitor
IFN	Interferon
IL	Interleukin
ILC3	Innate lymphoid cell type 3
IP_3	Inositol triphosphate
irAE	Immune-related adverse event
IRF4	Interferon regulatory factor 4
ITAM	Immunoreceptor tyrosine-based activation motif
ITSM	Immunoreceptor tyrosine-based switch motif
JC virus	John Cunningham virus
LAG-3	Lymphocyte-activation gene-3
LAP	Latency-associated peptide
LAT	Linker for activation of T cells
Lcn2	Lipocalin-2
LFA-1	Leukocyte function-associated antigen-1
LN	Lymph node
MACS	Magnetic activated cell sorting

MAIT	Mucosal-associated invariant T
MAPK	Mitogen-activated protein kinase
MBP	Myelin basic protein
MFI	Mean fluorescence intensity
MHC	Major histocompatibility complex
MM	Multiple myeloma
MMP	Matrix metalloproteinase
MMRd	Mismatch repair deficient
MOG	Myelin oligodendrocyte protein
MS	Multiple sclerosis
Mtb	*Mycobacterium tuberculosis*
NCR	Natural cytotoxicity receptor
NFAT	Nuclear factor of activated T cells
NF-κB	Nuclear factor-κ-light-chain-enhancer of activated B cells
NK	Natural killer
NLR	NOD-like receptor
NSCLC	Non-small cell lung carcinoma
OVA	Ovalbumin
PAg	Phosphoantigen
PAMP	Pathogen-associated molecular pattern
PBS	Phosphate-buffered saline
PD-1	Programmed cell death protein-1
PDAC	Pancreatic ductal adenocarcinoma
PD-L1	Programmed cell death-ligand 1
PEC	Peritoneal exudate cell
PI	Propidium iodide
PI3K	Phospatidylinositol-3-kinase
PIP_2	Phosphatidylinositol bisphosphate
PKC	Protein kinase C
PLC	Phospholipase C
PLP	Proteolipid peptide
PLZF	Promyelocytic leukemia zinc finger
PMA	Phorbol myristate acetate
pMHC	MHC-peptide
PML	Progressive multifocal leukoencephalopathy
PPMS	Primary progressive multiple sclerosis
PRR	Pathogen recognition receptor
PT	Pertussis toxin
PTEN	Phosphatase and TENsin homologue
pTreg	Peripheral Treg
PVR	Poliovirus receptor

RA	Retinoic acid
RhA	Rheumatoid arthritis
RBC	Red blood cell
RLR	RIG-I-like receptor
RORγt	Retinoic acid receptor-related orphan receptor γt
RPMI	Roswell Park Memorial Institute
RRMS	Relapsing remitting multiple sclerosis
RT-qPCR	Real-time quantitative polymerase chain reaction
s.c	Subcutaneous
SCFA	Short chain fatty acid
SCID	Severe combined immunodeficiency
SD	Standard deviation
SEFIR	SEF/IL-17R
SEM	Standard error of the mean
SLT	Secondary lymphoid tissue
SNP	Single nucleotide polymorphism
SP	Single positive
sPD-L1	Secretory programmed cell death ligand-1
SPF	Specific pathogen free
SPM	Small peritoneal macrophage
SPMS	Secondary progressive multiple sclerosis
STAT	Signal transducer and activator of transcription
TCR	T cell receptor
TEC	Thymic epithelial cells
Tfh	T follicular helper cell
TGF-β	Transforming growth factor-β
Th	T helper
TIGIT	T cell immunoreceptor with Ig and ITIM domains
Tim3	T cell Ig and mucin domain-containing protein3
TLR	Toll-like receptor
TMB	Tetramethylbenzidine
TME	Tumour microenvironment
TNF	Tumour necrosis factor
Tr1	Type 1 regulatory T
TRAF	Tumour necrosis factor receptor-associated factor
Treg	Regulatory T
TSA	Tumour specific antigen
tTreg	Thymic Treg
VCAM-1	Vascular cellular adhesion molecule-1
VLA-4	Very late antigen-4
WT	Wildtype

Table of Contents

Chapter 1
General Introduction

1.1 The immune system

The immune system is composed of networks of immune cells and signalling molecules, which communicate with each other with the common goal of protecting the host from invading pathogens. The immune system has evolved to protect the body against a variety of pathogens including bacteria, viruses, and parasites. The lymphatic system consists of a network of tissues that includes the lymphoid organs; spleen, lymph nodes (LNs), bone marrow (BM) and thymus. The lymphoid organs are the main sites of immune cell production and differentiation. Immune cells use the lymphatic and circulatory systems to migrate around the body in lymphatic vessels and blood to infiltrate affected tissues where they induce an immune response against a particular pathogen. The immune system coordinates a complex set of interactions, which work to induce a controlled immune response followed by resolution of inflammation [1].

1.1.1 The innate immune system

The innate immune system represents the front-line of defence to pathogens and is made up of a variety of immune cells including monocytes, macrophages, dendritic cells (DCs), and neutrophils. Innate immune cells express surface receptors called pattern recognition receptors (PRRs) which have evolved to recognise conserved sequences that are referred to as pathogen-associated molecular patterns (PAMPs). PAMPs are non-specific microbial components that are expressed across a wide range of micro-organisms and allow for direct recognition of pathogens by the innate immune system. The innate immune system uses PRRs to discriminate between “infectious non-self and non-infectious self” [2]. There are various types of PRRs including Toll-like receptors (TLRs), NOD-like receptors (NLRs), and RIG-I-like receptors (RLRs). PRRs recognise molecules that are necessary for the survival of microbes such as lipids, nucleic acids and glycoproteins, which are not expressed by the host [3]. Damage-associated molecular patterns (DAMPs) are also recognised by the innate immune system. DAMPs are endogenous danger molecules that are generally released from dead or dying cells and their presence outside of the cell alerts the innate immune system to possible ’danger’. Examples of DAMPs include S100

proteins, uric acid, and interleukin-1α (IL-1α) [4]. PRR engagement by either PAMPs or DAMPs leads to a series of downstream signalling events that result in innate immune cell activation and production of inflammatory mediators, including cytokines and chemokines. The cytokine network includes interleukins, interferons (IFNs) and colony stimulating factors (CSFs). Cytokine-mediated inflammation activates a range of different cell types and allows for communication within the innate immune system and subsequent initiation of adaptive immune responses [5].

1.1.2 Antigen presenting cells

Antigen presenting cells (APCs) are cells of the innate immune system that present antigen to T cells and help to direct adaptive immune responses driving the appropriate antigen-specific immune response required to clear the pathogen. DCs are the key APC required for activation of naïve T cells [6]. DCs constantly survey peripheral tissues and take up antigen. Expression of the chemokine receptor CCR7 is upregulated upon activation of DCs. CCR7 binds to its ligands CCL19 and CCL21 resulting in migration of the DC to local draining lymph nodes (LNs). DCs make contact with naïve T cells in the LN where they present antigen and provide signals necessary for T cell activation and polarisation. DCs present antigen to CD4 and CD8 T cells in the context of major histocompatibility complexes (MHC) II and I, respectively. DCs also provide co-stimulatory signals via CD80 and CD86 that interact with CD28 expressed by T cells, which are necessary for T cell activation. The cytokines produced by DCs also help to polarise T cell responses to shape functional subtypes [7].

1.1.3 The adaptive immune system

The adaptive immune system is composed of T cells and B cells. A hallmark of adaptive immunity is its extreme specificity and associated memory, characteristics lacking in the innate immune system. T cells and B cells express T cell receptors (TCRs) and B cell receptors (BCRs), respectively. TCRs and BCRs are formed by somatic recombination of germ-line encoded antigen receptor genes to produce an extensive range of genetically

variable TCRs and BCRs. This process allows for the generation of many TCRs with varying affinity for MHC-peptide (pMHC) complexes expressed on the surface of APCs. T cell activation is initiated when a particular TCR clone interacts with a pMHC complex with very high affinity. The diversity of the TCR resulting from the somatic recombination process allows for extensive diversity and specificity in the T cell pool. Once a specific T cell response has been generated, memory T cells persist and can remain in tissues where they are poised to react instantly to previously encountered pathogens and prevent re-infection. Memory T cells have less stringent criteria for subsequent activation allowing for rapid antigen-specific reactivation and proliferation [8].

1.2 T cells

1.2.1 T cell development

T cell development occurs in the thymus and results in the production of mature T lymphocytes with diverse antigen specificity. The thymus is an immune organ composed of thymic epithelial cells (TECs) that form an epithelial microenvironment necessary to support T cell differentiation [9]. Common lymphoid progenitors (CLPs) express the chemokine receptors CCR7 and CCR9, which allow them to enter the thymus from the BM. $CD4^-CD8^-$ double negative (DN) T cell precursors enter the thymus and undergo various stages of T cell development as defined by the expression of CD4, CD8 and the αβ TCR [10]. DN cells move through four stages of development referred to as DN1-4 and these stages of development are defined by cell surface expression of CD25 and CD44. DN1 cells ($CD44^+CD25^-$) enter the thymus and migrate from the cortex to the medulla moving through DN1-4 stages with TCR gene rearrangement of both the α and β chains [11]. $CD4^-$ $CD8^-$ DN thymocytes can give rise to both αβ or γδ T cells and lineage commitment is dependent on signals received via expression of functional surface receptors. $CD4^+CD8^+$ double positive (DP) αβ TCR-expressing cells undergo positive and negative selection in the thymus to ensure that cells expressing self-reactive TCRs are not released into the periphery. Positive selection is a process whereby DP αβ T cells successfully signal in response to self-MHC molecules presenting self-peptide. Strong signalling via the αβ TCR in response to self-recognition results in deletion of these cells from the T cell repertoire

by a process called negative selection [12]. The decision between positive and negative selection of immature thymocytes is determined by the intensity of the signal received via the TCR in response to self-pMHC complexes [13]. T cells with functional TCRs that are not deleted by positive or negative selection down-regulate the expression of either CD4 or CD8 and leave the thymus as mature single positive (SP) thymocytes. The CD4 or CD8 lineage decision depends on whether the thymocyte reacts with a self-pMHC-II or self-pMHC-I molecule, respectively [14].

CD4 T cells recognise peptide presented in the context of MHC-II molecules by APCs and are termed T helper (Th) cells because of their capacity to produce cytokines and chemokines that help to orchestrate immune responses. Cytokines produced by Th cells facilitate B cell class switching to allow for antibody production tailored to a specific infection type [15]. CD8 T cells recognise peptide presented in the context of MHC-I molecules expressed by all nucleated cells and are called cytotoxic T lymphocytes (CTLs). CTLs are crucial for fighting viral infection as well as killing abnormal host cells. CD8 T cells function by producing the cytotoxic effectors perforin and granzymes and the inflammatory cytokine interferon-γ (IFN-γ) [16]. After TCR engagement, antigen-specific T cells produce large amounts of IL-2 and also upregulate the IL-2 receptor α chain (CD25) to undergo intense rounds of proliferation [17]. These rounds of proliferation result in large numbers of T cells expressing identical TCRs specific for a particular antigen in a process known as clonal expansion.

1.2.2 TCR signalling

Upon binding of the TCR to its relevant pMHC ligand, a series of downstream signalling events are triggered. Zap70 and the ζ chains of CD3 are phosphorylated on immunoreceptor tyrosine-based activation motif (ITAM) tyrosine residues by Lck [18]. Zap70 then phosphorylates the linker for activation of T cells (LAT) on one of four major LAT phosphorylation sites [19]. Phosphorylation of tyrosine 132 on LAT recruits phospholipase Cγ (PLCγ) that provides intracellular calcium (Ca^{2+}) for Ras and mitogen-activated protein kinase (MAPK) pathway activation [20]. Phosphorylation of tyrosine 171, 191, or 226 of LAT by Zap70 activates Ras [21]. TCR signalling also induces

phosphatidylinositol 3-kinase (PI3K)-Akt signalling. PI3K signalling can be regulated by dephosphorylation mediated by phosphatase and TENsin homologue (PTEN) [22]. PLCγ increases cytosolic levels of Ca^{2+} by hydrolysis of phosphatidylinositol bisphosphate (PIP_2) to inositol triphosphate (IP_3) and diacylglycerol (DAG) [23]. Elevated Ca^{2+} levels allow for the activation of the transcription factor nuclear factor of activated T cells (NFAT), which activates T cell subset gene expression profiles [24]. Furthermore, PLCγ activates protein kinase C (PKC) which targets nuclear factor κ-light-chain-enhancer of activated B cells (NF-κB) and activator protein-1 (AP-1) [25]. Phorbol myristate acetate (PMA) activates PKC and ionomycin is a calcium ionophore that drives NFAT activation [26]. Stimulation with PMA and ionomycin is a commonly used method to restimulate T cells *ex vivo* to examine their cytokine production.

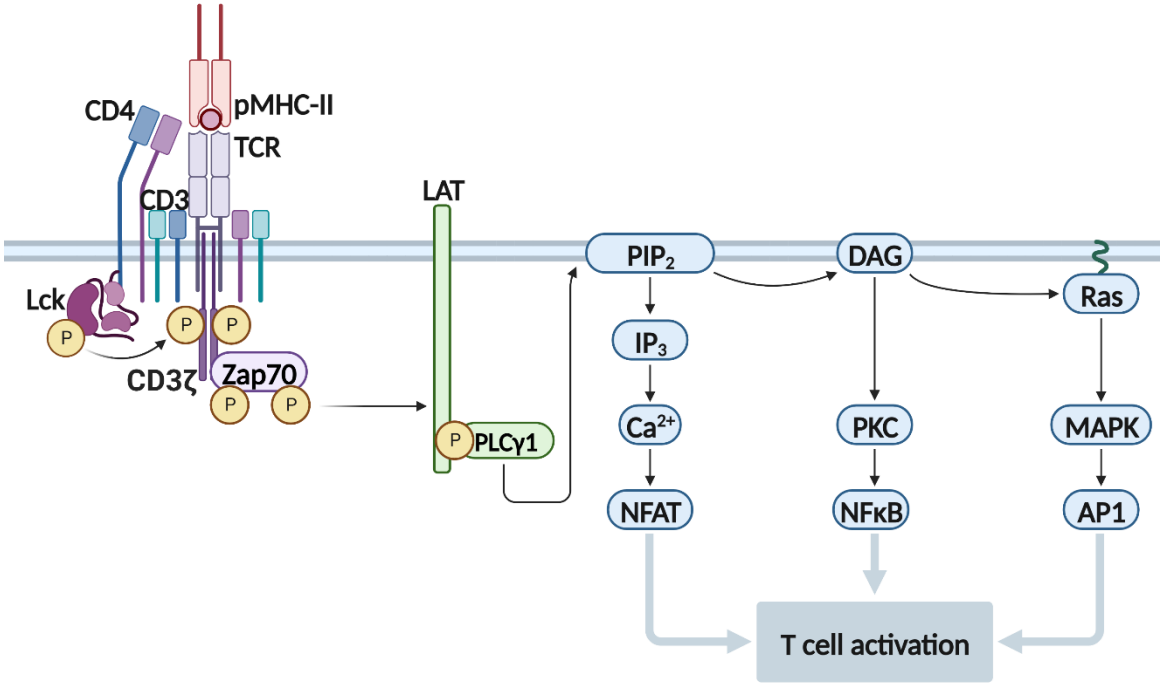

Figure 1.1 TCR signalling cascade. Upon TCR triggering by pMHC binding, The CD3ζ chains are phosphorylated by Lck. Phosphorylation of the ITAMs on the CD3ζ chains allow for the recruitment and phosphorylation of Zap70. Activated Zap70 phosphorylates LAT, which forms the TCR signalosome. PLCγ is recruited by LAT and its activation facilitates signalling via three main pathways. PIP_2 is hydrolysed into IP_3 and DAG which increases intracellular Ca^{2+} levels and activates NFAT. DAG activates PKC and Ras which targets NF-κB and AP1. *Figure adapted from Brownlie et al, Nature Reviews Immunology, 2013 [27] and created with Biorender.com 2023.*

1.2.3 Th cell activation

CD4 T cells require three signals to become activated. These signals are provided by myeloid cells, including APCs that present processed antigen to CD4 T cells in the context of MHC-II. The second signal results from CD28, a co-stimulatory molecule expressed by the T cell, with CD80 or CD86, which are co-stimulatory molecules expressed by APCs. The third signal required for CD4 T cell activation is crucial in determining differentiation into specific Th cell lineages. This final signal is provided by cytokines in the immediate microenvironment which are produced by APCs and other myeloid cells [7].

Th1 cells mediate immune responses against intracellular pathogens and are induced in response to IL-12 and IFN-γ produced by innate immune cells. TLR signalling induced by innate recognition of bacterial, viral, or protozoan infections results in activation of NF-κB signalling and IL-12p40 production. Type I IFNs can be produced by TLR-stimulated DCs, activated natural killer (NK) cells and Th1 cells. Type I IFN signalling results in IL-12p35 transcription by APCs. Mature IL-12, IL-12p70, is composed of both IL-12p40 and IL-12p35 subunits and is the active heterodimeric cytokine which induces Th1 cell differentiation [28]. IL-12 signalling in naïve T cells induces signal transducer and activator of transcription 4 (STAT4) transcription and results in expression of Tbet which is the master transcription factor for Th1 cells [29]. IFN-γ production by Th1 cells induces classical activation of macrophages necessary to kill intracellular pathogens.

Th2 cells play an important role in the immune response to extracellular parasitic infections and differentiate in response to IL-4. Specific TLR signalling in response to parasite antigens such as TLR-2 engagement, promotes activation of extracellular signal-related kinase (ERK) in DCs, which subsequently phosphorylates c-Fos and inhibits IL-12p70, inducing Th2 cell development. STAT6 activation in naïve T cells is promoted by IL-4 signalling and induces high levels of expression of GATA-3, which is the master transcriptional regulator of Th2 cell differentiation [30]. Th2 cells produce cytokines IL-4, IL-5, and IL-13, which are important cytokines in anti-helminth and extracellular parasitic immunity. IL-4 induces antibody class switching to IgE and promotes alternative activation of macrophages, resulting in tissue repair. IL-13 drives mucin production and smooth

muscle contraction in the small intestine to allow for expulsion of parasites. Th2 cells also mediate pathology in allergy and asthma.

In 1986, Mossman and Coffman described the Th1/Th2 paradigm of Th cell differentiation. This principle described the transcription factors Tbet and GATA-3 as the master regulators of Th1 and Th2 cell differentiation, respectively. It was demonstrated that these transcription factors are mutually inhibitory of each other [31]. However, it was established that Th cell differentiation was in fact not limited to the biphasic model proposed by Mossman and Coffman and the discovery of further Th subsets including Th17, regulatory T (Treg) cells, Th9, Th22, and T follicular helper (Tfh) followed [32].

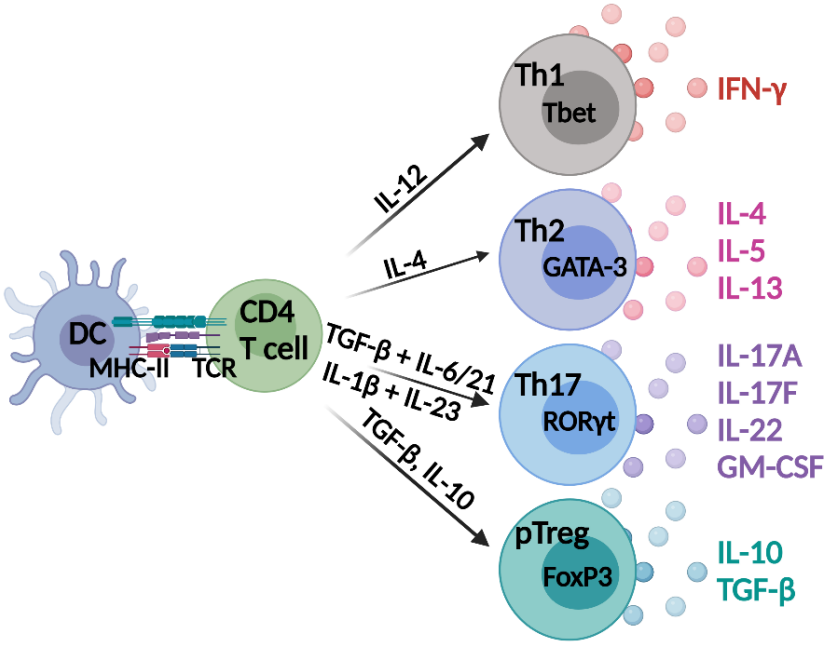

Figure 1.2 T cell differentiation in response to DC-derived cytokines. DCs present antigenic peptide, in the context of MHC-II, to the TCR on the surface of a naïve CD4 T cell. Differentiation of various Th subsets is dependent on the cytokines produced by DCs. Th1 cells differentiate in response to IL-12 stimulation which induces Tbet expression. Th1 cells produce IFN-γ upon activation. IL-4 enhances GATA-3 expression in naïve CD4 T cells and induces differentiation of Th2 cells. Th2 cells produce IL-4, IL-5, and IL-13. Differentiation of Th17 cells is dependent on RORγt expression which is induced by transforming growth factor-β (TGF-β) in combination with either IL-6, or IL-21. Further exposure to cytokines IL-1β and IL-23 enhances differentiation of pro-inflammatory Th17 cells, which produce IL-17A, IL-17F, GM-CSF, and IL-22. Treg cells that are induced in the periphery are referred to as pTreg cells and differentiate outside of the thymus in response to cytokines IL-10 and TGF-β which induces FoxP3 expression. pTreg cells produce IL-10 and TGF-β upon activation and differentiation. *Figure created with Biorender.com 2023.*

1.2.4 Th17 cells

Th17 cells are critical for controlling immune responses against extracellular bacteria and fungi. The master transcriptional regulator of Th17 cells is retinoic acid receptor-related orphan receptor (ROR) γt [33]. Activation of STAT3 is a crucial step for the development of Th17 cells. STAT3 mediates IL-6, IL-21, and IL-23 cytokine signalling and induces expression of IL-23R on CD4 T cells. IL-6 and IL-21 in combination with TGF-β are required to induce Th17 cells and this process is enhanced in the presence of IL-1β [34, 35]. IL-1β and IL-23 are involved in further differentiation and maintenance of a distinct, more inflammatory population of Th17 cells that are pathogenic in autoimmunity [36]. The less pro-inflammatory group of Th17 cells produce IL-17A, IL-17F, and IL-10 and have important homeostatic functions, as well as having important roles in maintaining host defence at mucosal barriers [37]. This population of Th17 cells is induced when naïve CD4 T cells are stimulated with IL-6 and TGF-β [38]. IL-24 also regulates the function of Th17 cells via an IL-10-dependent mechanism [39]. Th17 cells produce IL-24, which induces IL-10 production by Th17 cells and limits their pathogenicity in experimental autoimmune encephalomyelitis (EAE). Autocrine IL-17A signalling also induces IL-24 production by Th17 cells and regulates their function [40].

STAT3 signalling induces expression of genes including *rorc, il17a, il17f, il23r,* and *il1r1* [41]. Subsequent stimulation with IL-1β activates interferon regulatory factor (IRF) 4, which plays a role in the reinforcement of RORγt expression [42]. Further IL-23 exposure allows for the development of a hyper-inflammatory population of Th17 cells that produce a range of different cytokines including IL-17A, IL-17F, IL-21, IL-22, IFN-γ, granulocytes-macrophage colony-stimulating factor (GM-CSF), and tumour necrosis factor (TNF). This inflammatory population produces IL-21, which creates a strong positive feedback loop further reinforcing this pathogenic population of Th17 cells that are critical for driving autoimmunity [43]. IL-23 signalling induces further expression of IL-23R via STAT3 signalling and maintains RORγt and IL-17A expression, thereby stabilising the inflammatory phenotype of Th17 cells [44].

The requirement of TGF-β for the development of Th17 cells represents a reciprocal development pathway between Th17 cells and Treg cells. TGF-β induces expression of the

transcription factor forkhead box protein 3 (FoxP3) in CD4 T cells to drive Treg cell development but TGF-β in combination with IL-6 or IL-21 induces differentiation of RORγt-expressing Th17 cells. Further studies have demonstrated that TGF-β indirectly promotes Th17 cell differentiation by suppressing the development of Th1 and Th2 cells [45].

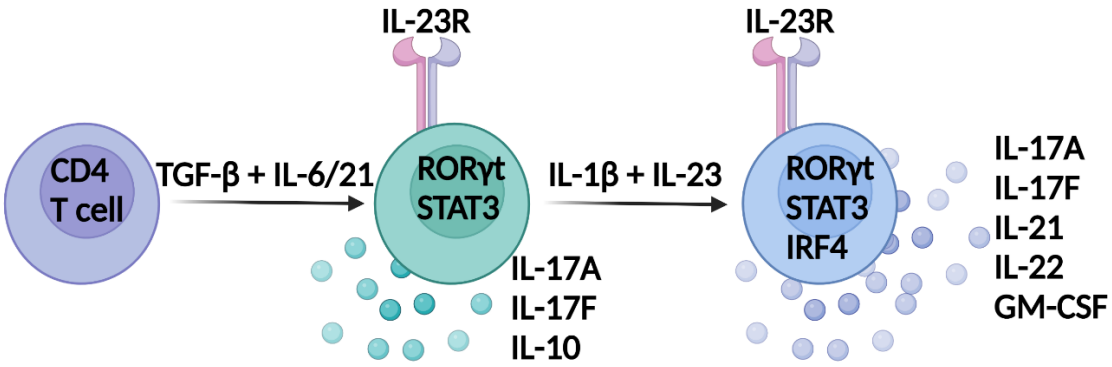

Figure 1.3 Th17 cell differentiation. Th17 cells differentiate in response to TGF-β stimulation in combination with either IL-6 or IL-21. RORγt-expressing Th17 cells produce cytokines IL-17A, IL-17F, and IL-10. Upon further exposure to cytokines IL-1β and IL-23, RORγt expression is stabilised and leads to development of a pro-inflammatory population of Th17 cells that produce a range of inflammatory cytokines including, IL-17A, IL-17F, GM-CSF, IL-21, and IL-22. *Figure created with Biorender.com 2023.*

1.3 Regulatory T cell subtypes

1.3.1 Treg cells

Treg cells are a population of T cells responsible for controlling inflammation and reducing the risk of autoimmunity and immunopathology caused by aberrant immune responses. Sakaguchi et al. discovered that depletion of CD25-expressing CD4 T cells from a normal CD4 T cell pool could induce a range of autoimmune diseases when transferred to an immunocompromised recipient. It was also shown that transfer of this CD25-expressing population of CD4 T cells was protective against the development of autoimmunity [46]. Treg cells are defined by expression of the transcription factor FoxP3 and can be generated in the thymus (tTreg) or in the periphery (pTreg). tTreg cells develop in response to high affinity reactions by naïve CD4 T cells via the TCR to MHC-II-restricted self-peptide complexes presented by APCs. IL-2 signalling via CD25 is then required to induce FoxP3 expression in these cells and results in the induction of a population of

FoxP3-expressing CD4 T cells called Treg cells. pTreg cells are induced in response to antigen presentation under tolerogenic conditions, including TGF-β, retinoic acids (RAs) and short chain fatty acids (SCFAs) [47]. The role of tTreg cells is to control the immune responses to self-antigens, whereas pTreg cells are considered to be involved in restraining immune responses to non-self-antigens, such as the commensal microbiota [48]. Subpopulations of pTreg cells include type 1 regulatory T (Tr1), Th3, and Th35 cells [49]. Tr1 cells are a $FoxP3^-$ subpopulation of Treg cells that are induced in response to IL-10 signalling and produce large amounts of IL-10 with or without, TGF-β [50]. Th3 cells produce large amounts of TGF-β *in vivo* [51]. Th35 cells secrete IL-35, a recently described immunosuppressive cytokine [52].

The major mechanisms whereby Treg cells execute their suppressive functions include (a) secretion of the suppressive cytokines IL-10, TGF-β, and IL-35, (b) consumption of large amounts of IL-2, (c) production of perforin and granzymes, and (d) cell contact involving suppressive cell surface receptors. Treg cells carry out suppressive functions by acting directly on effector T cells, but also target the APC to induce bystander suppression of T cell responses [53].

Treg cells express a range of cell surface receptors associated with their suppressive functions. Such receptors include CD25, cytotoxic T lymphocyte-associated protein 4 (CTLA-4), glucocorticoid-induced TNF receptor (GITR), lymphocyte-activation gene 3 (LAG-3) and programmed cell death protein-1 (PD-1). High expression of CD25 allows Treg cells to compete with effector T cells for IL-2 and results in cytokine-mediated deprivation and apoptosis of effector T cells [54]. Treg cells are the only T cell population that constitutively expresses CTLA-4, a CD28 homologue that functions to engage co-stimulatory molecules CD80 and CD86 on APCs, thereby blocking effector T cell activation [55]. PD-1 is also a member of the CD28 family and delivers negative signals to T cells upon ligand binding [56]. LAG-3 is a CD4 homologue that can bind MHC-II molecules with very high affinity thereby suppressing APC maturation [57]. GITR has a crucial role in maturation and expansion of tTreg cells and neutralisation of GITR on Treg cells has been shown to abrogate their suppressive capacity [58]. Immune checkpoint inhibitors (ICIs) exploit suppressive receptors by preventing them from delivering inhibitory signals to effector T cells thereby enhancing T cell responses [59].

1.3.2 Tr1 cells

Tr1 cells are a population of FoxP3$^-$ CD4 T cells that are induced in response to the cytokines IL-10 and IL-27 and are characterised by expression of CD49b and LAG3 in both mice and humans [60]. Expression of CD49b and LAG3 differentiates IL-10-producing Tr1 cells from other IL-10-producing CD4 T cells [61]. Tr1 cells are induced in the periphery in response to antigen, unlike natural Treg cells that develop in the thymus [62]. Repeated antigenic stimulation of T cells isolated from ovalbumin (OVA)-specific TCR transgenic mice with IL-10 expanded a population of IL-10-producing Tr1 cells that prevented the development of colitis in severe combined immunodeficiency (SCID) mice [63]. Infection with the respiratory pathogen *Bordetella pertussis* induced development of antigen-specific Tr1 cells at mucosal surfaces that suppressed IFN-γ-producing pathogen-specific Th1 cells [64].

The main mechanism of Tr1 cell-mediated suppression is via production of the immunosuppressive cytokine IL-10. In humans, IL-10 acts on monocytes to down-regulate their expression of MHC-II and subsequent induction of antigen-specific T cell responses [65]. In addition to CD49b and LAG3, Tr1 cells can also express the inhibitory receptors CTLA-4 and PD-1 [66]. Neutralisation of either CTLA-4 or PD-1 can reverse Tr1 cell-mediated suppression of allergen-specific T cell responses in humans [67]. Tr1 cells also express ectonucleoside triphosphate diphosphohydrolase-1 (CD39) under the control of the aryl hydrocarbon receptor (AHR) [68]. CD39 depletes extracellular adenosine triphosphate (eATP) and allows hypoxia-inducible factor-1α (HIF-1α) to promote the differentiation of Tr1 cells. Conditional ablation of CD39 by IL-10-producing Tr1 cells reversed their protective effect in EAE. Antigen-specific Tr1 cells can also be induced using the immunomodulatory metabolite RA as an adjuvant [69]. In this study from the Mills lab, autoantigen-specific Tr1 cells were induced in response to immunisation with myelin oligodendrocyte glycoprotein (MOG), RA, and IL-2. The MOG-specific Tr1 cells produced IL-10 and adoptive transfer of the MOG-specific Tr1 cells into mice with EAE reduced the severity of EAE in an antigen-specific manner.

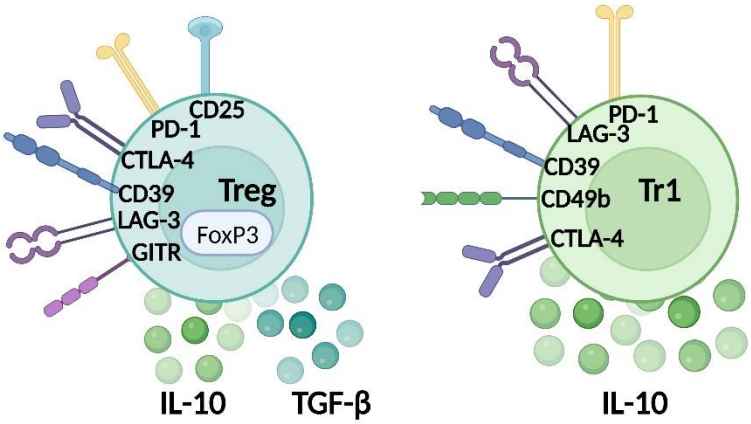

Figure 1.4 Regulatory T cell subsets. Treg cells and Tr1 cells are populations of regulatory T cells that can be differentiated based on expression of FoxP3. Treg cells develop in the thymus and express FoxP3 and CD25. Treg cells express many inhibitory receptors including CTLA-4, GITR, LAG-3, and PD-1. Treg cells make the immunosuppressive cytokines IL-10 and TGF-β. Tr1 cells are antigen-specific Treg cells that develop in the periphery and can be identified based on surface expression on CD49b and LAG-3. Tr1 cells can also express the inhibitory receptors CD39, CTLA-4, and PD-1 and are potent sources of IL-10. *Figure created with Biorender.com 2023.*

1.4 Immunosuppressive cytokines

1.4.1 IL-10

The main regulatory cytokines are IL-10, IL-27, IL-35, and TGF-β. IL-10 signals via the IL-10R (CD210), comprising of IL-10RA and IL-10RB subunits [70]. IL-10R is expressed by most hematopoietic cells, but its expression is upregulated on immune cells under inflammatory conditions. Th17 cells have low expression of IL-10R at rest, but expression is augmented following activation with anti-CD3 [71]. IL-10 signals via STAT1, STAT3, and STAT5, but STAT3 is the crucial transcription factor required for downstream transcription of IL-10 target genes [72]. IL-10 can be produced by both innate and adaptive immune cells, including DCs, macrophages, T cells, NK cells, and B cells [73]. IL-10 plays an essential role in limiting pathology in the immune response to infection but this can impede pathogen clearance [74]. Increased IL-10 production in mice was associated with higher bacterial burden in a model of *Mycobacterium tuberculosis* infection [75]. IL-10 also has a role in tumour progression. There was increased IL-10 and IL-10R expression in tumour biopsies from glioma patients [76] and IL-10 increased proliferation of glioma cells *in vitro*

[77]. In a murine model of ovarian cancer, dual blockade of PD-1 and IL-10 enhanced the infiltration of activated T cells into the tumour which delayed tumour growth [78].

1.4.2 IL-27

IL-27 is a heterodimeric cytokine consisting of the p28 subunit and Epstein-Barr virus-induced gene 3 (EBI3) [79]. IL-27 signals via the IL-27Ra and gp130 subunits and induces phosphorylation of STAT1 and STAT3 [80]. IL-27R is expressed by T cells and NK cells. IL-27 is produced mainly by myeloid cells, including macrophages, monocytes, and DCs [81]. IL-27 produced by myeloid cells signals via the IL-27R expressed by T cells to induce IL-10 production via STAT3 signalling [80]. Down-regulation of gp130 expression by CD8 T cells inhibited their responsiveness to IL-27, which suppressed their production of IL-10 [82]. Nasal colonisation with *Staphylococcus aureus* induced production of IL-27 by innate immune cells, which acted upstream of IL-10 to impede bacterial clearance [83]. In the adoptive transfer model of EAE, IL-27 induced IL-10 production by T cells that decreased the severity of disease [84]. IL-27 has been demonstrated to mediate the therapeutic benefit of IFN-β in multiple sclerosis (MS) patients by inhibiting pathogenic Th17 cells [85].

1.4.3 IL-35

IL-35 is an inhibitory cytokine that is a member of the IL-12 family of cytokines and is composed of the p35 subunit and EBI3, which also forms part of the immunosuppressive cytokine, IL-27 [52]. Maximal IL-35 signalling occurs via the IL-35R, which is composed of IL-12RB2 and gp130 subunits [86]. IL-35 signals via STAT1 and STAT4, which form a unique heterodimer to elicit the downstream effects of IL-35. IL-35 is produced by Treg cells, regulatory B (Breg) cells, macrophages, and DCs [52, 87-89]. IL-35 is also capable of inhibiting T cell proliferation and inducing Treg cells that are a potent source of IL-35 (iTr35) [90]. In a murine model of melanoma, tumour cells produced IL-35 and promoted tumour growth by enhancing the infiltration of myeloid cells [91]. Increased IL-35 concentrations in serum have been significantly associated with progression of non-small cell lung carcinoma (NSCLC) [92]. Conversely, mice that lack IL-35-mediated signalling had

stronger Th17 cell responses and were more susceptible to EAE, suggesting that IL-35 is protective in autoimmunity [93].

1.4.4 TGF-β

The TGF-β family of cytokines includes TGF-β1, TGF-β2, and TGF-β3 and these cytokines are secreted in a latent form [94]. Latent TGF-β is synthesised in complex with the latency-associated peptide (LAP) and can be cleaved into its active form by furin [95]. Latent TGF-β can be expressed on the cell surface through interactions with glycoprotein A repetitions predominant protein (GARP) [96]. TGF-β can also be activated by the integrins $\alpha_V\beta_6$ [97] and $\alpha_V\beta_8$ [98]. Mature TGF-β, which has been cleaved from LAP, signals via the TGF-βR complex. The TGF-βR complex consists of two TGF-βRI subunits and two TGF-βRII subunits [99]. Binding of mature TGF-β to its receptor induces downstream signalling involving SMAD family proteins [100]. Phosphorylation and dimerisation of SMAD2 and SMAD3 allows complex formation with SMAD4. This SMAD complex translocates to the nucleus and regulates gene expression. TGF-β is produced by Treg cells and tumour cells and has a broadly pro-tumour role in the tumour microenvironment (TME) [101]. In colorectal cancer (CRC), cancer-associated fibroblasts (CAFs) produced large amounts of TGF-β in the tumour which prevented the infiltration of cytotoxic T cells [102]. TGF-β exerts its immunosuppressive effects by inducing FoxP3-expressing Treg cells and inhibiting proliferation of cytotoxic immune cells [103]. Increasing TGF-β-mediated signalling specifically in T cells protected mice from the development of EAE [104]. Galunisertib is a small molecule inhibitor of TGF-β that reduced tumour burden in a murine model of CRC by increasing T cell infiltration into the tumour and Th1 cell differentiation [105].

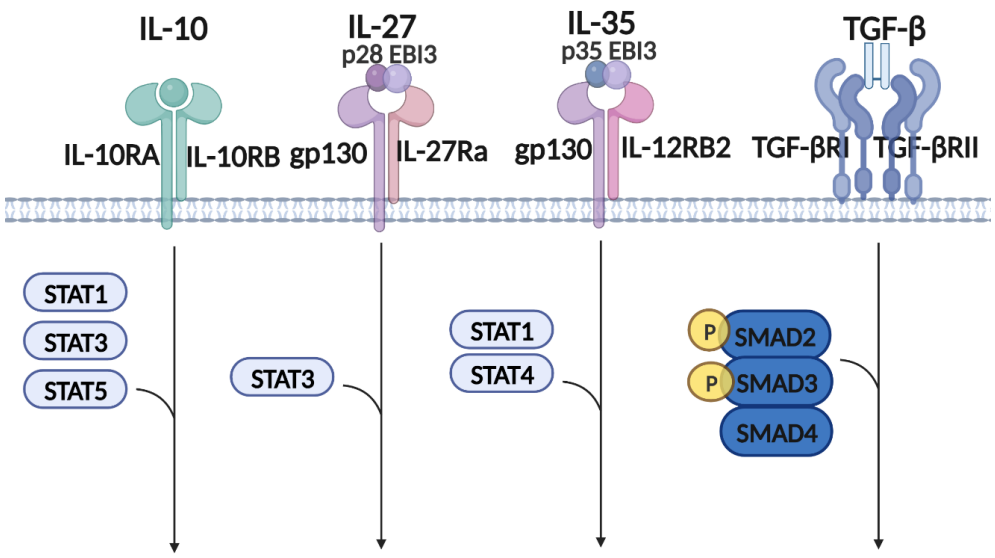

Figure 1.5 Immunosuppressive cytokine receptors and downstream signalling. IL-10 signals via the IL-10R, comprising of the IL-10RA and IL-10RB subunits. IL-10 signalling is mediated by STAT1, STAT3, and STAT5. IL-27 is a heterodimeric cytokine that consists of the p28 subunit and EBI3. IL-27 signals via the IL-27R, which is composed of gp130 and IL-27Ra. Signalling downstream of IL-27 occurs via STAT3. IL-35 is composed of the p35 subunit and EBI3. IL-35 signals via the IL-35R, which is composed of IL-12RB2 and gp130. STAT1 and STAT4 mediate IL-35-induced signalling. Active TGF-β binds to the TGF-βR which is composed of two TGF-βRI subunits and two TGF-βRII subunits. Binding of mature TGF-β to its receptor induces phosphorylation and dimerisation of SMAD2 and SMAD3, which then forms a complex with SMAD4. *Figure created with Biorender.com 2023.*

1.5 Immune checkpoints

Immune checkpoints are suppressive receptors expressed by T cells that limit activation and prevent aberrant immune responses [106]. The checkpoints that have been studied as suppressive immunoreceptors expressed by T cells include CTLA-4, LAG-3, PD-1, T cell immunoreceptor with Ig and ITIM domains (TIGIT), and T cell immunoglobulin and mucin domain-containing protein-3 (Tim-3).

1.5.1 CTLA-4

CTLA-4 was one of the first inhibitory receptors shown to have a role in the suppression of T cell responses [107]. CTLA-4 acts by binding competitively to CD28 at a higher affinity

than CD80 or CD86, which sends a negative signal to the T cell and limits activation. CTLA-4 is constitutively expressed by Treg cells and activated effector T cells [108]. CTLA-4 expression by Treg cells allows them to inhibit activation, cytokine production and proliferation of effector T cells. Adeno-associated virus (AAV) delivery of CTLA-4 Ig significantly reduced the severity of EAE by suppressing CD4 T cell activation and subsequent infiltration of encephalitogenic T cells into the CNS [109].

1.5.2 LAG-3

LAG-3 exerts its inhibitory effects in a similar manner to CTLA-4. LAG-3 binds to MHC-II with higher affinity than CD4, thereby preventing CD4 T cell activation and effector function [110]. Upon binding, LAG-3 provides inhibitory signals by disrupting the signalling of Lck and thereby inhibiting TCR signalling [111]. Other ligands for LAG-3 exist which explains how LAG-3 expression does not exclusively suppress CD4 T cell responses. LSECtin and galectin-3, expressed in the context of melanoma and pancreatic ductal adenocarcinoma (PDAC), respectively, [112, 113] have been shown to bind LAG-3 expressed by CD8 T cells, which suppressed the anti-tumour immune response. The specific signalling cascade induced by LAG-3 binding has not yet been fully elucidated, but has been associated with suppression of TCR signalling [114].

1.5.3 PD-1

PD-1 is expressed by activated T cells, B cells, and myeloid cells. In T cells, engagement of PD-1 with either of its ligands, programmed cell death ligand-1 (PD-L1) or programmed cell death ligand-2 (PD-L2), suppresses TCR-mediated T cell activation, proliferation, and cytokine production [56]. PD-1 binding induces recruitment of phosphatases, including SHP2, to the immunoreceptor tyrosine-based switch motif (ITSM) in the PD-1 tail [115]. SHP2 can dephosphorylate kinases that are associated with CD28 and TCR signalling [116] and inhibit PI3K-Akt, Ras, ERK and PLCγ [117]. SHP2 can also inhibit T cell signalling by inhibiting phosphorylation of CD3ζ and Zap70 [118]. Inhibition of these signalling cascades ultimately results in suppression of T cell activation, proliferation, cytokine

production, and survival [119]. B cells also express PD-1, however they are not thought to be involved in the anti-tumour activity of anti-PD-1 treatment as in the absence of B cells anti-PD-1 treatment is still a successful anti-cancer immunotherapy [120]. In contrast to CTLA-4, which functions to suppress early T cell responses, PD-1 functions primarily to limit immune responses in the periphery upon binding to PD-L1 or PD-L2. PD-L1 is expressed by a broad range of immune cells and non-immune cells. Expression of PD-L1 can be increased in response to inflammatory signals, as demonstrated by the IL-6-induced increase in PD-L1 expression by tolerogenic APCs [121]. In the CNS, PD-L1 is expressed by astrocytes with PD-L1 expression increasing during Alzheimer's disease in APP/PS1 mice [122]. PD-L1-expressing astrocytes are also present in the CNS during EAE and can interact with PD-1-expressing microglia to suppress their pathogenicity [123]. PD-1 has an important role in preventing autoimmunity and *pdcd1*$^{-/-}$ mice develop lupus-like symptoms over time [124]. Blockade of PD-1 signalling enhanced the severity of EAE [125].

1.5.4 TIGIT

TIGIT is expressed by Treg cells and NK cells as well as activated and memory T cells [126]. TIGIT binds poliovirus receptor (PVR), also known as CD155 or poliovirus receptor-related 2 (PVRL2), which is also known as CD112, expressed by APCs and tumour cells [127]. In a similar manner to CTLA-4 and LAG-3, TIGIT binds PVR with higher affinity than its activating ligand, CD226, and delivers a negative signal to the target cell [128]. In NK cells, TIGIT engagement inhibits IFN-γ production and cytotoxicity [129]. In T cells, TIGIT engagement can block T cell activation and proliferation by downregulating the TCR complex and suppressing PLCγ [130]. TIGIT-expressing Treg cells are highly suppressive and have been demonstrated to inhibit Th1 and Th17 cell responses in a murine colitis model [131].

1.5.5 Tim-3

Tim-3 was discovered in 2002 and was identified as a suppressive receptor expressed by IFN-γ-producing CD4 and CD8 T cells [132]. Further studies have demonstrated Tim3

expression by Treg cells, NK cells, monocytes, and DCs [126]. IL-27 can induce Tim-3 and IL-10 expression by CD4 T cells [133]. Galectin-9 is a ligand for Tim-3 [134] that can be expressed by acute myeloid leukaemia (AML) cells [135]. Carcinoembryonic-antigen-related cell adhesion molecule-1 (Ceacam-1) is also a ligand for Tim-3 that can be co-expressed with Tim-3 by CD4 and CD8 T cells [136]. Binding of either galctin-9 or Ceacam-1 to Tim-3 increases the amount of catalytically inactive Lck in T cells, thereby suppressing TCR signalling [137]. Tim-3 signalling via galectin-9 induces cell death [134]. Treatment of mice with galectin-9 protected against EAE as it depleted IFN-γ-producing Th1 cells.

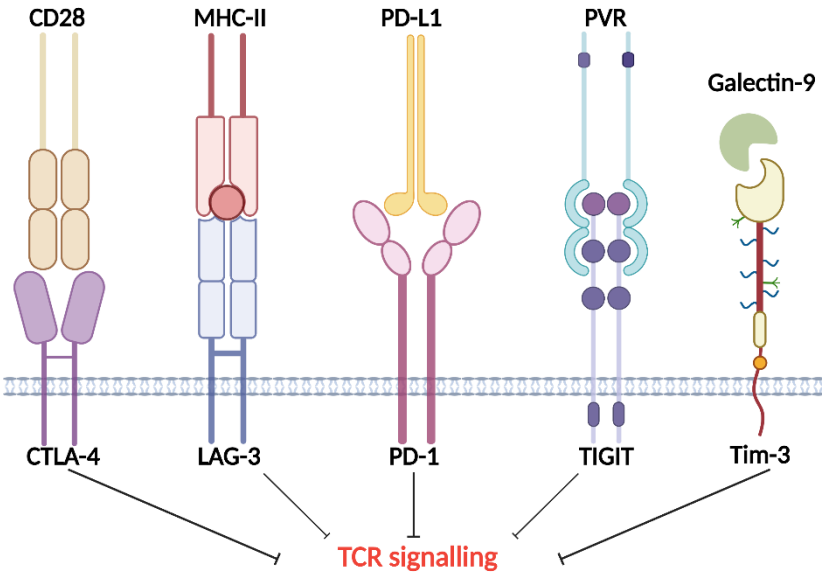

Figure 1.6 Immune checkpoints inhibit T cell responses upon binding to their respective ligands. CTLA-4 binds competitively to CD28 at a higher affinity than CD80 or CD86 which sends a negative signal to the T cell and limits effector T cell activation. LAG-3 binds to MHC-II with higher affinity than CD4 thereby preventing CD4 T cell activation and effector function. Upon binding, LAG-3 provides inhibitory signals by disrupting the signalling of Lck, thereby inhibiting TCR signalling. PD-1 binds to PD-L1, which suppresses downstream TCR-mediated activation, proliferation, and cytokine production. TIGIT binds PVR with a higher affinity than the PVR activating ligand CD226 and delivers a negative signal to the target cell resulting in suppression of activation. Tim-3 binding by galectin-9 suppresses TCR-mediated signalling and downstream activation. *Figure created with Biorender.com 2023.*

1.5.6 Immune checkpoints inhibitors (ICIs)

The action of immune checkpoints can be inhibited with blocking antibodies that target either the receptor or the checkpoint ligand. Immune checkpoints are highly expressed in

the tumour and blocking checkpoint-mediated signalling promotes anti-tumour immunity [138]. ICIs have been approved for the treatment of cancers including CRC, NSCLC, and melanoma.

Early pre-clinical studies showed that blockade of CTLA-4 in combination with a therapeutic vaccine in the B16 murine melanoma model led to tumour eradication [139]. This seminal study showed that treatment with anti-CTLA-4 increased infiltration of CD8 T cells and NK cells into the tumour. Ipilimumab is a monoclonal antibody that targets CTLA-4, which was the first ICI approved for the treatment of melanoma and subsequently multiple types of cancer including, CRC and NSCLC [140]. Pooled analysis of clinical trials has revealed that ipilimumab treatment can extend survival for up to 10 years in patients with advanced melanoma [141]. Furthermore, blockade of CTLA-4 increased T cell activation in melanoma patients [142]. CTLA-4 is expressed by Treg cells and its expression is augmented in breast tumours [143].

ICIs targeting PD-1 have also been approved for the treatment of a range of cancers. Pembrolizumab, nivolumab, and cemiplimab are monoclonal antibodies that target PD-1 and atezolizumab, durvalumab and avelumab are ICIs that targets PD-L1 [144]. Each of these drugs blocks PD-1-mediated signalling. PD-L1 is highly expressed by tumour cells in the MC38 murine CRC model and treatment with either anti-PD-1 or anti-PD-L1 promoted tumour clearance by increasing CD8 T cell cytotoxicity in the tumour [145]. Furthermore, increased PD-L1 expression and CD8 T cell numbers at the invasive tumour margin are associated with response to pembrolizumab treatment in melanoma patients [146]. Patients that responded to pembrolizumab treatment had increased infiltration of proliferating CD8 T cells into the tumour.

Combination therapy with two different ICIs targeting CTLA-4 and PD-1 has greater efficacy in the treatment of advanced melanoma, but combination therapy is associated with increased immune related adverse events (irAEs) as a consequence of ablating multiple immunoregulatory pathways [147]. The most common manifestations of irAEs present in the skin, gastro-intestinal (GI) tract, and endocrine system [148]. The manifestation of irAEs in patients treated with ICIs highlights the important role that the CTLA-4 and PD-1 pathways have in preventing autoimmunity.

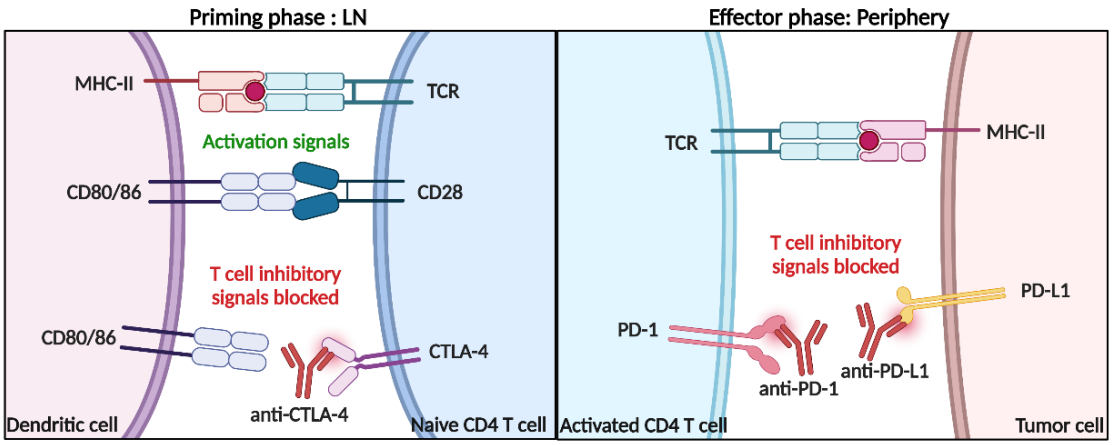

Figure 1.7 ICIs block CTLA-4, PD-1, or PD-L1-mediated suppression of T cell activation. During the induction of antigen-specific T cell responses in the LN, anti-CTLA-4 treatment prevents inhibitory signals being delivered to effector T cells, thereby increasing T cell priming. In the periphery, anti-PD-1 or anti-PD-L1 treatment prevents PD-1 engagement and the downstream suppression of effector T cell activation. ICIs are used to treat cancer as they can block inhibitory signals in T cells and enhance the anti-tumour immune response. *Figure created with Biorender.com 2023.*

1.6 γδ T cells

γδ T cells are a minor unconventional population of T cells present in both humans and mice that express a TCR composed of a γ and a δ chain. The γ chain is located on the same chromosome as the TCRβ chain and the TCRδ chain is located within the gene encoding the TCRα chain [149].

1.6.1 Human γδ T cells

Human γδ T cells are separated into subpopulations based on differential Vδ chain usage designated Vδ1, Vδ2, and Vδ3. Vδ1 γδ T cells are the main tissue-resident γδ T cell subset in humans and express various activating ligands, which allow them to recognise cellular stress in an innate-like manner [150]. Expression of multiple natural cytotoxicity receptors (NCRs) including Nkp30 and Nkp44 by Vδ1 γδ T cells allows them to recognise virally-infected or transformed cells in an NK cell-like manner [151]. The cytotoxic capacity of Vδ1 γδ T cells has led to the development of an adoptive cell therapy termed Delta One T (DOT) cells that are being developed for the treatment of AML [152]. Conversely, Vδ1 γδ

T cells can also have pro-tumour roles in CRC, via production of amphiregulin (AREG) [153].

The Vδ2 chain preferentially pairs with the Vγ9 chain to form Vγ9Vδ2 γδ T cells, which are the predominant subtype of γδ T cell found in the blood, where they can account for up to 5% of circulating T cells [154]. Vγ9Vδ2 γδ T cells can be activated in a TCR-dependent manner, through recognition of phosphoantigens (PAgs) that are produced by tumour cells via the mevalonate pathway [155]. Intracellular PAg such as hydroxy-methylglutaryl-CoA reductase (HMGR), produced by tumour cells, bind to butyrophilin-2A1 (BTN2A1) and butyrophilin-3A1 (BTN3A1) [156]. The resulting conformational change in BTN2A1 and BTN3A1 facilitates binding to the Vγ9Vδ2 TCR and subsequent activation [157]. A recent study identified AMP-activated protein kinase (AMPK) expression in tumour cells as a positive regulator of BTN2A1 and BTN3A1 expression which subsequently increased Vγ9Vδ2 γδ TCR-mediated killing of tumour cells [158]. Vγ9Vδ2 γδ T cells have cytolytic functions in the tumour via production of TNF, IFN-γ, and increased NK-mediated antibody-dependent cellular cytotoxicity (ADCC) [159]. Conversely, under the influence of the TME, Vγ9Vδ2 γδ T cells can promote tumour growth, via expression of IL-17A and AREG [160].

1.6.2 Murine γδ T cells

Murine γδ T cell subsets are defined by their expression of particular γ chains according to the Heilig and Tonegawa nomenclature [161]. γδ T cells are found primarily at barrier sites where they are poised to respond rapidly to infection or damage. In the mouse, γδ T cells are enriched in the skin, intestine, and genitourinary tract and account for 3-5% of all lymphoid cells found in secondary lymphoid tissues (SLTs) and the blood [162].

1.6.3 Murine γδ T cell development

Development of γδ T cells occurs in the fetal thymus and different subsets of γδ T cells emerge from the thymus in successive waves to seed various tissues guided by chemokine

receptor expression. The first wave produces skin-resident γδ T cells, termed dendritic epidermal T cells (DETCs) which express Vγ5 TCRs [163]. The second wave seeds the vaginal epithelium and these cells express Vγ6 TCRs [164]. The first two waves of γδ T cells to emerge from the fetal thymus have restricted Vγ gene usage and pair preferentially with the Vδ1 chain thereby producing clones of γδ T cells with limited TCR diversity. Subsequent groups of γδ T cells emerge from the thymus postnatally and express TCRs with much larger diversity [165]. Encountering antigen in the thymus in the context of MHC molecules has been shown to be neither necessary nor inhibitory to the development of antigen-specific γδ T cells [166].

γδ T cells differentiate into effector subsets that can produce cytokines and cytolytic molecules. Cell surface receptor expression directs differentiation and activation of γδ T cells that produce IL-17A or IFN-γ in response to a range of stimuli. IFN-γ and IL-17A-producing γδ T cells can be segregated into two distinct populations based on cell surface marker expression. IFN-γ-producing γδ T cells express CD27, CD122, and NK1.1, whereas IL-17A-producing γδ T cells are $CD27^-$ and express CCR6 on their surface [167, 168]. IFN-γ^+ γδ T cells are biased towards Vγ1, Vγ5, or Vγ7 γ chain usage and IL-$17A^+$ γδ T cells have enriched Vγ4 and Vγ6 γ chain usage. Research has demonstrated that IFN-γ-producing $CD27^+$ γδ T cells are antigen experienced and require signals via their TCR for development. IL-17A-producing $CD27^-$ γδ T cells are described as being antigen-naïve as they do not require TCR stimulation for their development [166]. Furthermore, CD70 is the ligand for CD27 and is expressed by TECs thereby implicating both TCR and CD27 signalling in the development of $CD27^+$ γδ T cells.

1.6.4 Murine γδ T cell activation

γδ T cells can be activated by cytokine stimulation alone, in the absence of TCR engagement, and this has been referred to as innate activation. Stimulation of $CD27^-$ γδ T cells with IL-1β and IL-23 promotes production of IL-17A, whereas IL-12 and IL-18 stimulation induces IFN-γ production by $CD27^+$ γδ T cells [169]. The ability of γδ T cells to become activated under less stringent conditions than conventional CD4 T cells allows them to kickstart the immune response and amplify inflammation. Although γδ T cells

represent a small population of T cells, they have the capacity to produce large amounts of IL-17A rapidly in response to pathogens [170] and are a vital early source of IL-17A critical to initiating inflammation in central nervous system (CNS) autoimmunity [171].

In addition to innate-activated γδ T cells, memory γδ T cells have also been described. In a model of infection with an upper respiratory pathogen, *Bordetella pertussis,* IL-17A-producing γδ T cells accumulate in the lung in two waves, at 2 hours and 2 weeks post-challenge. Vγ4 γδ T cells isolated from the lungs of mice two weeks post challenge with *B. pertussis* produced IL-17A *in vitro* in response to re-stimulation with the pathogen in the presence of APCs. Upon reinfection in convalescent mice, this IL-17A-producing population of Vγ4 γδ T cells expanded, demonstrating that they develop a memory response to infection with *B. pertussis* [172]. A similar phenotype was demonstrated in a model of *S. aureus* infection, where a population of IL-17A-producing $CD27^{-}CD44^{+}$ γδ T cells expanded upon encounter with the pathogen and expanded upon reinfection [173]. Due to their placement at barrier sites and rapid effector function, γδ T cells are important responders to a host of different pathogens and can develop into tissue resident memory populations in response to specific pathogens.

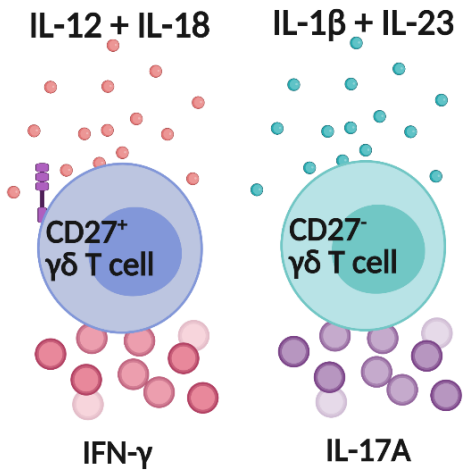

Figure 1.8 Cytokine-mediated activation of murine γδ T cells. Murine γδ T cells can be separated into two subpopulations based on expression of CD27. $CD27^{+}$ γδ T cells produce IFN-γ in response to IL-12 and IL-18. $CD27^{-}$ γδ T cells produce IL-17A in response to IL-1β and IL-23 *Figure created with Biorender.com 2023.*

1.6.5 Regulation of murine γδ T cell function

γδ T cell subsets have distinct activatory signals to CD4 or CD8 T cells and therefore are not regulated in the same manner as conventional T cells. Studies on the regulation of γδ T cells have demonstrated that multiple mechanisms including immunosuppressive

cytokines, immune checkpoints, and Treg cells may be involved. There is evidence to support the hypothesis that the immunosuppressive cytokines IL-27 and IL-10 may suppress the function of γδ T cells. IL-27-induced IL-10 suppressed the expansion of IL-17A-producing γδ T cells in the nasal tissue of *S. aureus*-infected mice [83]. Infected IL-$10^{-/-}$ mice had increased numbers of IL-17A and IL-22-producing γδ T cells in the nasal tissue, which was accompanied by lower bacterial load suggesting that IL-17A and IL-22-producing γδ T cells are suppressed by IL-10 during infection with *S. aureus*. IFN-γ and IL-17A-proudcing γδ T cells were also suppressed by RA via downregulation of STAT3 [174]. In the adoptive transfer model of EAE, treatment of γδ T cells with RA prior to cell transfer significantly decreased the severity of disease.

Treg cells inhibit CD4 and CD8 T cell responses by modulating APC function. As γδ T cells can be activated to produce IL-17A by IL-1β and IL-23 without TCR engagement with MHC expressed by APCs, Treg cells inhibit γδ T cell function by alternative mechanisms. In a murine model of aeroallergen exposure, IL-33 activated $ST2^{+}$ Treg cells to produce IL-35 that suppressed IL-17A production by γδ T cells [175]. Furthermore, ablation of IL-33 signalling in Treg cells in this model exacerbated allergic inflammation in the lung by increasing γδ T cell-mediated infiltration of eosinophils and neutrophils. Another study demonstrated that Treg cells can suppress proliferation and cytokine production by γδ T cells, which was partially reversed by blocking signalling via the immune checkpoint GITR [176].

Immune checkpoints can also regulate γδ T cell effector function. In a murine model of metastatic breast cancer, Vγ4 γδ T cells were regulated by expression of the checkpoint Tim-3 and Vγ6 γδ T cells were regulated by PD-1 expression [177]. Treatment with anti-Tim-3 in this model increased infiltration of IL-17A-producing Vγ4 γδ T cells into the pre-metastatic lung. Similarly, treatment with anti-PD-1 increased infiltration of Vγ6 γδ T cells into the pre-metastatic lung. Expansion of these pro-tumour γδ T cells conferred resistance to ICIs. In another study, PD-1-expressing γδ T cells were identified in the murine colon. The microbiota sustained PD-1 expression by γδ T cells in this model and limited IL-17A production in a protective manner [178].

1.7 IL-17

IL-17A is the key member of the IL-17 family of cytokines and is the signature cytokine of the Th17 cell subset of CD4 T cells [179]. The IL-17 family of cytokines includes; IL-17A, IL-17B, IL-17C, IL-17D, IL-17E (IL-25), and IL-17F [180]. IL-17 family cytokines signal via the IL-17R family which comprises five receptor subunits, IL-17RA-IL-17RE [181]. IL-17A and IL-17F are the best characterised cytokines of the IL-17 family and are usually co-produced by type 17 cells. IL-17A and IL-17F form covalent homodimers and signal through IL-17RA and IL-17RC. IL-17A and IL-17F can also form covalent heterodimers [182]. IL-17A and IL-17F homodimers, as well as IL-17A/IL-17F heterodimers, signal via an obligate dimer IL-17RA/IL-17RC complex [183]. IL-17RA is expressed ubiquitously, but has particularly concentrated levels of expression on epithelial cells, endothelial cells, and fibroblasts [180].

1.7.1 IL-17 signalling

IL-17R complexes encode SEF/IL-17R (SEFIR) domains, which allow them to interact with the SEFIR-domain containing adaptor protein Act1. Act1 is required for recruitment of TNFR-associated factor 6 (TRAF6), an essential upstream activator of NF-κB [180]. Act1 is a crucial adaptor protein required for IL-17 signalling, and mutations in Act1 enhances susceptibility to chronic mucocutaneous candidiasis (CMC) in humans [184]. IL-17 signalling also results in activation of MAPK pathways, particularly ERK, which leads to further activation of AP-1. A key role for MAPK activation in response to IL-17 signalling is mRNA stabilisation [185]. IL-17A is not itself a potent inducer of NF-κB but can synergise with other cytokines to exert its effects. There have been several reports of IL-17A acting as an mRNA stabilising factor for TNF-induced targets, resulting in more potent signal transduction [186, 187]. IL-17A is also capable of upregulating TNF-R expression to further enhance the synergistic effects of these two inflammatory cytokines [188].

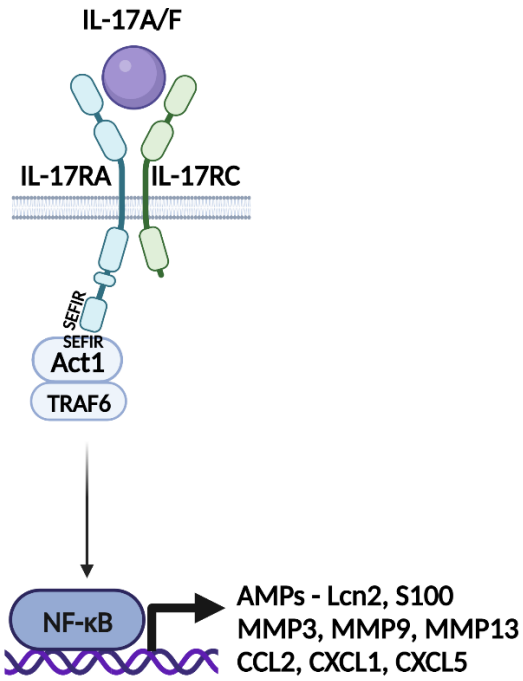

Figure 1.9 IL-17-mediated signalling. IL-17A and IL-17F can bind to the IL-17R which is a heterodimeric receptor composed of IL-17RA and IL-17RC. The intracellular domain of the IL-17R encodes a SEFIR region. Upon binding of IL-17 to the IL-17R, the SEFIR domain-containing adaptor protein, Act1 binds to the intracellular domain of the IL-17R. Act1 recruits TRAF6 which facilitates NF-κB activation. IL-17 signalling induces production of AMPs, MMPs, and chemokines by epithelial cells and fibroblasts. *Figure created with Biorender.com 2023.*

1.7.2 IL-17 effector functions

IL-17A and IL-17F are crucial cytokines for host defence at mucosal and epithelial barriers. Downstream signalling of IL-17RA/IL-17RC heterodimers results in the induction of the expression of anti-microbial peptides (AMPs); β-defensins, S100 proteins and lipocalin-2 (Lcn2). AMPs can directly limit bacterial growth by various mechanisms. IL-17 signalling also induces the expression of matrix metalloproteinases (MMPs) and chemokines, factors important for mediating activation and recruitment of immune cells to epithelial and endothelial surfaces [189]. Induction of granulocyte-colony stimulating factor (G-CSF) as well as chemokines CXCL1, CXCL5, and CCL2, by IL-17 is important for the expansion and recruitment of neutrophils to the site of inflammation [190]. MMPs induced by IL-17A include MMP3, MMP9, and MMP13 [191]. IL-17 signalling is crucial for host defence and absence of IL-17RA signalling increased susceptibility to oropharyngeal candidiasis in mice [192]. IL-17R$^{-/-}$ mice were more susceptible to cutaneous *S. aureus* infection [193]. IL-17 signalling is also crucial in mediating protection from fungal pathogens in humans [184]. As well as promoting pathogen clearance and homeostatic protection, aberrant IL-17 signalling can induce immunopathology.

IL-17A can act in synergy with cytokines such as IL-22 and TNF to induce expression of CCL20, a chemokine that recruits CCR6-expressing Th17 cells and IL-17A producing type 3 innate lymphoid cells (ILC3s) [194]. IL-17A induces G-CSF, GM-CSF, and MMP production, which allows for the recruitment and expansion of inflammatory neutrophils. MMPs, in general, make the extracellular matrix more accessible to immune cell infiltration and allow IL-17A to signal further to recruit immune cell populations. IL-17A can induce sustained production of the inflammatory cytokines IL-1β, IL-6, TNF, and GM-CSF [195]. IL-17A and IL-17F are potent mediators of inflammation resulting from broad acting signalling events that lead to immune cell recruitment and activation as well as amplification of inflammatory networks. When inflammation is dysregulated, IL-17A and IL-17F are potent mediators of autoimmune pathology. Knockout mouse studies have shown that IL-17A signalling is crucial in the induction of collagen-induced arthritis (CIA) and EAE [171, 196].

1.8 Autoimmunity

The ability of the immune system to provide checkpoints at multiple stages during lymphocyte development, as well as the presence of specific regulatory networks keeps the immune response under control and prevents dysregulation. When the immune response becomes dysregulated it can lead to systemic autoimmunity [197]. Regulation of self-reactive receptors on adaptive lymphocytes is crucial for the development of self-tolerance. As a result of the generation of large diversity in TCRs and BCRs, self-reactive lymphocytes also develop. It is estimated that 20-50% of TCRs and BCRs generated in the thymus and spleen have a potentially dangerous affinity for self-antigens [198]. The regulatory arm of the immune system can induce apoptosis of self-reactive lymphocytes during negative selection in the thymus. Other mechanisms used by the immune system to prevent activation of self-reactive lymphocytes include downregulation of TCR expression and signalling, down-regulation of co-stimulatory receptor expression, and production of immunosuppressive cytokines [198]. Peripheral tolerance mechanisms exist as a second barrier to the activation of self-reactive T cells that may have escaped negative selection in the thymus. Potentially auto-reactive T cells are inhibited by induction of T

cell anergy and are also inhibited by the suppressive effects of Treg cells [199]. When auto-reactive T cells escape tolerance mechanisms and become activated in the peripheral tissues they can go on to precipitate autoimmunity. Dysregulated immune responses in various tissues lead to different autoimmune diseases, including rheumatoid arthritis (RA), type I diabetes, psoriasis, and MS.

1.8.1 Multiple sclerosis

MS is a chronic, progressive inflammatory disorder of the CNS. MS patients can initially present with a range of symptoms including, but not limited to, optic neuritis, double vision, facial sensory loss, or asymmetric limb weakness [200]. Following presentation with symptoms for MS an abnormal brain or spinal cord MRI featuring gadolinium-enhancing lesions leads to the diagnosis of clinically isolated syndrome [201]. A further clinical attack leads to the diagnosis of MS. Further examination of the CSF from patients presenting with suspected MS can reveal the presence of elevated white blood cell counts and IgG oligoclonal bands [202]. The most common form of MS is relapsing remitting MS (RRMS) which is characterised by acute episodes of neurological dysfunction, followed by periods of partial or complete remission [203]. Secondary progressive MS (SPMS) follows the initial course of RRMS when the periods of remissions cease [204]. Primary progressive MS (PPMS) is primarily progressive from the onset of disease without relapses [205]. Disability in MS is quantified using the expanded disability status scale (EDSS) [206]. The risk of acquiring MS is associated with exposure to certain environmental factors in genetically susceptible individuals. Environmental factors associated with increased risk of MS development include smoking, vitamin D deficiency, and infectious agents such as Epstein-Barr virus (EBV) [207]. MS is one of the world's most common neurological disorders and is the leading cause of neurologic disability in young adults. MS is a growing health burden with the number of people affected worldwide estimated to have increased from 2.3 million in 2013 to 2.9 million in 2022 [208]. Ireland has a high MS incidence rate with disease development being much more common in women than in men [209].

MS pathology is characterised by demyelinated lesions present in the CNS. These areas of focal demyelination are referred to as plaques and are associated with areas of axonal damage and oligodendrocyte loss. The myelin sheath, which functions to insulate axons, is damaged in these lesions, and prevents efficient transmission of nerve impulses. As disease progresses an increase in neuroaxonal loss is associated with increased patient disability [210]. The involvement of the immune system in MS disease pathology is supported by the fact that diverse methods of immunomodulatory treatments have efficacy as disease-modifying therapies (DMTs) for MS. IFN-β and glatiramer acetate are first-line therapeutics for the treatment of MS [211]. Natalizumab is a monoclonal antibody that targets the α_4 subunit of the very late antigen-4 (VLA-4) integrin to prevent T cell migration into the CNS. Natalizumab is a an effective treatment for highly active RRMS [212]. The immune-mediated pathology of MS includes CNS infiltration of innate and adaptive immune cells as well as a contribution from CNS-resident innate cells [213].

The success of therapies targeting B cells in the treatment of MS have highlighted a role for B cells in the pathogenesis of disease. Rituximab is a monoclonal antibody, which depletes CD20-expressing B cells. In RRMS, treatment with Rituximab significantly reduced the occurrence of gadolinium-enhancing lesions by MRI when compared with the placebo group [214]. B cell depletion therapies have also been successful in the treatment of PPMS. In addition to Rituximab, Ocrelizumab also depletes CD20-expressing B cells and it has been approved for the treatment of PPMS with trials showing that treatment with ocrelizumab slowed disability progression in patients when compared with the placebo group [215].

1.8.2 Experimental autoimmune encephalomyelitis model of MS

EAE is a murine model for MS which is an important tool used to dissect the role of T cells in precipitating CNS autoimmunity. EAE is characterised by ascending paralysis of the mouse beginning with a limp tail, followed by hind limb paralysis, and forelimb paralysis. The clinical severity of EAE is assessed using a 5 point scale [216]. EAE is induced by immunisation with encephalitogenic antigens, such as myelin basic protein (MBP), proteolipid peptide (PLP), or MOG, emulsified in complete Freund's adjuvant (CFA). CFA

is a mineral oil-based adjuvant supplemented with heat-inactivated *Mtb* and is a key adjuvant for the induction of cell-mediated immunity [217]. Mice are also injected with pertussis toxin (PT) on days 0 and 2 of active EAE and the addition of PT greatly improves the efficacy of the induction of EAE [218]. Early studies show that PT exerts its effects by increasing permeability of the blood brain barrier (BBB) [219]. More recent reports suggest that PT exerts effects directly on immune cells and can enhance the differentiation of Th17 cells by recruiting IL-1β-producing CCR2-expressing neutrophils and monocytes [220, 221].

1.8.3 Chronic relapsing EAE model of MS

The chronic relapsing EAE (CR-EAE) model of MS can be induced by immunisation of SJL mice with $PLP_{139-151}$ or $PLP_{178-191}$ [222]. In the PLP-induced relapsing-remitting model of MS SJL mice develop initial symptoms 6-20 days after induction with the first relapses occurring after 30-45 days. T cells are important pathogenic immune cells in the relapsing-remitting model of MS with relapse being caused by T cell specificity spreading to new myelin peptides determinants [223].

1.8.4 Viral models of MS

In addition to EAE, there are also murine models of MS that involve infection with viruses including, Theiler's virus, Semiliki Forest virus, and JHM coronavirus [224]. Intracerebral infection with Theiler's virus causes severe demyelinating disease in SJL mice characterized by flaccid paralysis of the hind limbs. Furthermore, Theiler's virus infects macrophages, oligodendrocytes, and astrocytes thereby inducing inflammatory demyelination, which causes progressive paralysis that is similar to that observed in human MS patients [225].

Semiliki Forest virus is a mosquito-transmitted RNA virus that when mutated to become avirulent can cause a non-lethal demyelinating disease [226]. Infection of BALB/c mice with the avirulent A7 strain of Semiliki Forest virus [227] causes immune-mediated

demyelination that involves both encephalitogenic CD8 T cells and B cell-derived anti-myelin [228].

Intracerebral infection with an avirulent strain of JHM coronavirus (MHV-J2.2-v1) also causes demyelinating disease in C57BL/6 mice. JHM virus-induced demyelination is immune-mediated as SCID mice die from encephalitis without signs of demyelination [229]. Both CD4 and CD8 T cells are required to induce demyelination in response to infection with JHM coronavirus [230].

Viral models of MS represent a powerful tool for studying the pathogenesis of the disease as they cause demyelination in plaques in the CNS in a similar manner to that observed in MS patients. Furthermore, this demyelination is in part T cell-mediated and macrophage infiltration into the CNS is also observed [231].

1.8.5 CD4 T cells in MS and EAE

EAE is a CD4 T cell-mediated autoimmune disease of the CNS and CD4 T cells are also enriched in the blood, cerebrospinal fluid (CSF) and CNS lesions of MS patients [213]. EAE was initially believed to be a Th1-dependent disorder, but characteristics of disease progression did not fully support this idea. IL-12p40$^{-/-}$ mice are resistant to the development of EAE and this was initially attributed to the failure of these mice to mount a Th1 response [232]. IFN-γ is also detectable in MS lesions and treatment of patients with IFN-γ leads to a worsened disease phenotype [233, 234]. IL-12 is a heterodimeric cytokine, composed of the IL-12p35 and IL-12p40 subunits. The discovery of IL-23, which is composed of the IL-12p40 chain and a unique p19 chain, led to a change in the belief that EAE was a Th1-mediated disease. Knockout studies revealed that IL-12p35$^{-/-}$ mice were susceptible to the induction of EAE, whereas IL-12p40$^{-/-}$ and IL-23p19$^{-/-}$ mice were resistant to disease [235]. This study revealed an essential role for IL-23, rather than IL-12, in the pathogenesis of EAE. Subsequent studies showed that IL-23 is required for the expansion of pathogenic, autoantigen specific IL-17A, IL-17F, TNF, and GM-CSF-producing CD4 T cells which were able to induce EAE when transferred to naïve mice [236]. These IL-

17A producing CD4 T cells were termed Th17 cells and are now established as being key pathogenic mediators of autoimmune diseases [237].

The induction of Th17 cells *in vivo* is dependent on IL-1 signalling; IL-1R1$^{-/-}$ mice failed to mount Th17 responses and were resistant to the induction of EAE. However, it was subsequently shown that the transfer of auto-reactive T cells to IL-1R1$^{-/-}$ mice restored disease susceptibility, highlighting the importance of IL-1 signalling in the induction of pathogenic Th17 cell responses [238]. IL-1 and IL-23 signalling are both essential for the induction of EAE. T cells from IL-23R$^{-/-}$ mice produce less IL-17A which suggests that IL-23 is required for the expansion of the pathogenic Th17 cell population [44]. The accepted view is that both IL-1 and IL-23 are critical to the stabilisation of inflammatory Th17 cells, which promotes disease progression via production of a number of inflammatory cytokines, including IL-17A, IL-17F, TNF, GM-CSF, and IFN-γ [239]. IL-17 and Th17 cells have also been implicated in the pathogenesis of MS [240]. IL-17 mRNA expression was elevated in the blood and CSF mononuclear cells of MS patients. Furthermore, IL-17 production by infiltrating CD4 and CD8 T cells is associated with active disease [241, 242].

Treg cells accumulate in the CNS during EAE, but fail to control autoimmune inflammation [243]. Other reports have shown that self-antigen induced Treg cells are dysfunctional as their expression of FoxP3 is unstable [244]. A pathogenic and inflammatory cytokine milieu also prevents the development of induced Treg cells in the periphery and instead favours the development of pathogenic Th17 cells. IL-6 in the presence of TGF-β enhances the development of Th17 cells and IL-6 also enhances the induction of IL-17A-producing γδ T cells [245]. Enhancement of TGF-β-induced SMAD3 signalling and inhibition of IL-6 and IL-23 signalling favours the development of FoxP3^{+} Treg cells [246]. Treg cells mediate recovery from EAE and can effectively inhibit autoantigen-specific T cell proliferation and motility in the CNS [247]. Accumulation of IL-10-producing CD4^{+}CD25^{+} T cells in the CNS correlated with recovery from EAE and these cells persisted and provided resistance from re-induction of EAE [248]. Furthermore, transfer of autoantigen-specific Tr1 cells on the day prior to induction of EAE significantly delayed the onset and severity of disease [69]. MS has also been associated with dysfunctional Treg cell populations and FoxP3 expression [249]. Pathogenic Th17 cells are resistant to Treg cell-mediated suppression in cells purified from peripheral blood and synovial fluid of RhA patients [250].

1.8.6 γδ T cells in MS and EAE

γδ T cells have a significant role in driving the pathogenesis of EAE. γδ T cells infiltrate the CNS in large numbers early during the development of EAE and these cells produce IL-17A. TCR-$\delta^{-/-}$ mice have significantly reduced disease severity and this phenotype is accompanied by reduced levels of IL-17A, demonstrating that γδ T cells are an important source of IL-17A during EAE. γδ T cells can be activated *in vitro* with the innate cytokines IL-1β and IL-23 to produce IL-17A, IL-21, and GM-CSF, in the absence of TCR engagement [169]. Early IL-17A is important for mobilising IL-1β-producing inflammatory monocytes and neutrophils that are crucial to the induction of EAE [171]. IL-17A produced by γδ T cells is also important for amplifying Th17 responses during CNS autoimmunity as TCR-$\delta^{-/-}$ mice have impaired MOG-specific CD4 T cell responses [169]. Furthermore, IL-1 and IL-23-induced GM-CSF is essential to the pathogenicity of Th17 cells and a subset of GM-CSF-producing Th17 cells have been shown to be crucial for monocyte invasion into the CNS during EAE [251].

IL-17A-producing γδ T cells have also been implicated in the progression of MS. Expanded γδ T cell clones were identified in the CSF of patients with recent onset disease but not in patients with chronic disease, suggesting a role for γδ T cells in the initiation of MS neuroinflammation [252]. $CD161^{hi}CCR6^{+}$ γδ T cells were enriched in the CSF of patients with MS [253] and RORγt was shown to be overexpressed in γδ T cells isolated from the peripheral blood of patients during relapse in relapsing-remitting MS (RRMS) [254].

γδ T cells can also enhance autoimmunity by suppressing early Treg cell responses. γδ T cells were the first cells to respond to IL-23 and promoted Th17 cell responses by preventing the development of Treg cell responses *in vitro*. IL-23-activated γδ T cells also prevented conversion of naïve CD4 T cells into $FoxP3^{+}$ Treg cells *in vivo* [255]. Myelin-specific Treg cells accumulated in the CNS during EAE, but they failed to control autoimmune inflammation [243]. Studies in TCR-$\delta^{-/-}$ mice have further elucidated the role that γδ T cells play in restraining Treg cell responses. Treg cell depletion in TCR-$\delta^{-/-}$ mice led to decreased severity of EAE suggesting that the presence of γδ T cells improved CD4 T cell responses and had an impact on Treg cell function [255].

1.9 Aims

The aims of this project were to:

- Characterise the expression of immune checkpoint molecules by T cell subsets including CD4 T cells, CD8 T cells, and γδ T cells during EAE.
- Determine the role of PD-1 signalling in the induction and severity of EAE.
- Examine the regulatory effect of immunosuppressive cytokines IL-10 and TGF-β on cytokine-activated γδ T cells.
- Determine the role of IL-10 and TGF-β-mediated signalling in regulating IL-17A-producing T cell subsets in EAE.
- Investigate the ability of Treg cells to suppress cytokine-activated γδ T cells and autoantigen-specific CD4 T cells.

Chapter 2
Materials and Methods

2.1 Materials

2.1.1 Buffers, media, and solutions

Complete Roswell Park Memorial Institute (cRPMI) medium

RPMI-1640 medium (Sigma-Aldrich)

10% heat inactivated fetal calf serum (FCS; Biosera)

100 mM L-glutamine (Sigma-Aldrich)

100 µg/mL penicillin/streptomycin (Gibco)

50 µM β-mercaptoethanol (Thermo Fisher)

γδ T cell medium

cRPMI medium

1 mM sodium pyruvate (Gibco)

10 mM HEPES (Gibco)

1X non-essential amino acids (Gibco)

Red blood cell lysis buffer

0.87% ammonium chloride (Sigma-Aldrich)

Dissolved in ddH_2O and filter sterilised

Ethidium bromide/ Acridine orange (EBAO)

5% Ethidium bromide (Sigma-Aldrich)

5% Acridine orange (Sigma-Aldrich)

Dissolved in 1X phosphate buffered saline (PBS; Sigma-Aldrich)

Magnetic-activated cell sorting (MACS) buffer

1XPBS (Sigma-Aldrich)

0.5% heat-inactivated FCS (Biosera)

2 mM EDTA (Sigma-Aldrich)

Fluorescence-activated cell sorting (FACS) buffer

1XPBS (Sigma-Aldrich)

2% heat-inactivated FCS (Biosera)

FACS sort buffer

1XPBS (Sigma-Aldrich)

3% heat-inactivated FCS (Biosera)

10 mM HEPES (Gibco)

2 mM EDTA (Sigma-Aldrich)

100 µg/mL penicillin/streptomycin (Gibco)

Stock isotonic Percoll

90% Percoll (GE Healthcare)

10% 10X PBS (Sigma-Aldrich)

20X PBS – dissolved in dH_2O, pH adjusted to 7.0

1.4 M Sodium chloride (NaCl; Sigma-Aldrich)

0.08 M Sodium hydrogen phosphate (Na_2HPO_4; Sigma-Aldrich)

0.01 M Potassium dihydrogen phosphate (KH_2PO_4; Sigma-Aldrich)

0.03 M Potassium chloride (KCl; Sigma-Aldrich)

ELISA wash buffer

0.5% Tween-20 (Sigma-Aldrich)

Prepared in 1X PBS

ELISA blocking buffer

1% w/v Bovine serum albumin (BSA; Sigma-Aldrich)

Dissolved in 1X PBS

ELISA stop solution

1M Sulfuric acid (H_2SO_4; Sigma-Aldrich)

Dissolved in dH_2O

2.1.2 General reagents

Reagent	Supplier
BSA	Sigma-Aldrich
CFA	Chondrex
Cottonseed oil	Sigma-Aldrich
DMSO	Sigma-Aldrich
EDTA	Sigma-Aldrich
HEPES	Gibco
Heat-inactivated FCS	Biosera
High-capacity cDNA reverse transcription kit	Applied Biosystems
MOG_{35-55} peptide	Genscript
Heat-killed *Mycobacterium tuberculosis* (*Mtb*)	Invivogen
PBS (1X and 10X)	Sigma-Aldrich
Pertussis toxin	Native Antigen Company
Retinoic acid	Stemcell
Streptavidin horseradish peroxidase (HRP)	BD Pharmigen

Streptavidin HRP	R&D Systems
RNase free H_2O	Invitrogen
RNeasy mini kit	Qiagen
SB431542	Biotechne
Tetramethylbenzidine (TMB)	Life Technologies

2.1.3 Cell separation kits

Reagent	Supplier
$CD4^+$ T cell isolation kit	Miltenyi Biotec
Magnisort mouse CD4 T cell enrichment kit	Invitrogen
Magnisort mouse T cell enrichment kit	Invitrogen
TCRγ/$δ^+$ T cell isolation kit	Miltenyi Biotec

2.1.4 *in vitro* antibodies

Reagent	Clone	Concentration	Application	Supplier
Anti-CD3ε	145-2C11	1 µg/mL	Plate bound	BD Pharmigen
Anti-CD28	37.51	2 µg/mL	Soluble	BD Pharmigen
Anti-IFN-γ	XMG1.2	10 µg/mL	Neutralising	Biolegend
Anti-IL-10	JES5-16E3	10 µg/mL	Neutralising	BD Pharmigen
Anti-TGF-β	1D11	5 µg/mL	Neutralising	Invitrogen
Anti-PD-1	RMP1-14	10 µg/mL	Neutralising	Invitrogen
Anti-TCRγ/δ	GL3	1 µg/mL	Plate bound	Biolegend
Anti-TCRγ/δ	UC7-13D5	1 µg/mL	Plate bound	Biolegend
Rat IgG1, κ isotype control	eBRG1	5 µg/mL	Neutralising	Invitrogen
Rat IgG2a, κ isotype control	eBR2A	10 µg/mL	Neutralising	Invitrogen
Rat IgG2b, κ isotype control	eB149/10H5	10 µg/mL	Neutralising	Invitrogen

2.1.5 *in vivo* monoclonal antibodies

Reagent	Clone	Dose	Supplier
Anti-PD-1 (CD279)	RMP1-14	200 µg/mouse	Assay Genie
Anti-CD210 (IL-10R)	1B1.3A	200 µg/mouse	Bio X Cell
Rat IgG1, κ isotype control	MOPC-21	200 µg/mouse	Bio X Cell
Rat IgG2a isotype control	1-1	200 µg/mouse	Assay Genie

2.1.6 Recombinant cytokines and proteins

Cytokine	Concentration *in vitro*	Supplier
GM-CSF	20 ng/mL	Peprotech
IL-1β	2.5 ng/mL	Biolegend
IL-2	10 ng/mL	Biolegend
IL-7	10 ng/mL	Biolegend
IL-12p70	5 ng/mL	Biolegend
IL-15	10 ng/mL	Biolegend
IL-18	5 ng/mL	Biolegend
IL-23	10 ng/mL	Biolegend
TGF-β	5 ng/mL	PeproTech
PD-L1-Fc	25 µg/mL	R&D Systems

2.1.7 ELISA antibodies

Cytokine	Blocking buffer	Top working standard	Supplier
GM-CSF	1% BSA	1000 pg/mL	R&D Systems
IFN-γ	1% BSA	10 ng/mL	BD Pharmigen
IL-1β	1% BSA	1000 pg/mL	R&D Systems
IL-10	1% BSA	2000 pg/mL	R&D Systems
IL-17A	1% BSA	1000 pg/mL	R&D Systems
IL-23	1% BSA	2500 pg/mL	R&D Systems
TNF	1% BSA	2000 pg/mL	R&D Systems

2.1.8 FACS antibodies

Specificity	Clone	Fluorochrome	Supplier
B220	RA3-6B2	BV650	Biolegend
B220	RA3-6B2	BV711	Biolegend
CD3ε	145-2C11	APC	Biolegend
CD3ε	17A2	PE-Dazzle594	Biolegend
CD4	RM4-5	APCeFluor780	Invitrogen
CD4	RM4-5	BV785	Biolegend
CD4	RM4-5	BV570	Biolegend
CD8	53-6.7	AlexaFluor700	Invitrogen
CD11a	M17/4	BB700	BD Biosciences
CD11b	M1/70	APCeFluor780	Invitrogen
CD11b	M1/70	BV711	Invitrogen
CD11c	N418	BV785	Biolegend
CD25	PC61.5	AlexaFluor700	Invitrogen
CD27	LG.3A10	PE	Biolegend
CD27	LG.3A10	PE-Dazzle594	Biolegend
CD27	LG.7F9	PE-Cy7	Invitrogen
CD44	IM7	BV605	Biolegend
CD45	30-F11	AlexaFluor700	Biolegend
CD45	30-F11	BV785	Biolegend
CD49b	DX5	APCeFluor780	Invitrogen
CD49d	R1-2	PerCPeFluor710	Invitrogen
CD210	1B1.3a	PE	Biolegend
F4/80	BM8	PE-Cy7	Invitrogen
FoxP3	FJK-16s	FITC	Invitrogen
FoxP3	FJK-16s	PE-Cy5	Invitrogen
FoxP3	FJK-16s	APC	Invitrogen
GM-CSF	MP1-22E9	PE	Invitrogen
IFN-γ	XMG1.2	BV711	Biolegend
IFN-γ	XMG1.2	PE-CF594	BD Biosciences

IFN-γ	XMG1.2	PE-Cy7	Invitrogen
IL-10 mRNA	PrimeFlow probe	AlexaFluor647	Invitrogen
IL-17A	TC11-18H10.1	FITC	Biolegend
IL-17A	TC11-18H10.1	PacificBlue	Biolegend
IL-17A	TC11-18H10.1	V450	BD Biosciences
LAG-3	C9B7W	BV785	Biolegend
Ly6c	AL-21	FITC	BD Biosciences
Ly6c	AL-21	BV605	BD Biosciences
Ly6g	1A8	BV650	Biolegend
MHC-II	M5/114.15.2	APC	Invitrogen
PD-1	29F.1A12	BV785	Biolegend
PD-L1	MIH5	PerCPeFluor710	Invitrogen
PD-L2	TZ25	PE-Dazzle594	Biolegend
pSMAD2/3	O72-670	PE-CF594	BD Biosciences
pSTAT3 (Y705)	13A3-1	PerCP/Cy5.5	Biolegend
RORγt	Q31-378	BV650	BD Biosciences
RORγt	Q31-378	PE	BD Biosciences
SiglecF	E50-2440	PE-CF594	BD Biosciences
Tbet	4B10	PE-Dazzle594	Biolegend
TCRβ	H57-597	BV570	Biolegend
TCRβ	H57-597	PE-Cy7	Invitrogen
TCRδ	GL3	FITC	Invitrogen
TCRδ	GL3	PerCPeFluor710	Invitrogen
TCR Vγ1.1	2.11	BV605	BD Biosciences
TCR Vγ4	UC3-10A6	PE	Invitrogen
TCR Vγ4	UC3-10A6	PE-Cy7	Biolegend
Tmem119	V3RT1G0sz	PE	Invitrogen
TNF	MP6-XT22	FITC	BD Biosciences
TNF	MP6-XT22	BV650	BD Biosciences

2.1.9 FACS reagents

Reagent	Supplier
Anti-mouse CD16/32 Fc block	BD Biosciences
Arc Amine reactive compensation beads	Invitrogen
Brefeldin A	Sigma-Aldrich
CellTrace Violet cell proliferation kit	Invitrogen
CountBright absolute counting beads	Invitrogen
Collagenase-D	Sigma-Aldrich
Deoxyribonuclease I (DNase I)	Sigma-Aldrich
FoxP3 transcription factor staining buffer kit	Invitrogen
Ionomycin	Sigma-Aldrich
Live/Dead fixable aqua dead cell stain kit	Invitrogen
Lyse/Fix buffer 5X	BD Biosciences
Paraformaldehyde (16%)	Invitrogen
Perm buffer III	BD Biosciences
PMA	Sigma-Aldrich
Primeflow RNA assay kit	Invitrogen
Zombie NIR fixable viability kit	Biolegend

2.1.10 Rt-PCR primers

Oligonucleotide	Product code	Supplier
Eukaryotic 18S rRNA	4319413E	Applied Biosystems
ifng	Mm01168134	Applied Biosystems
il17a	Mm00439618	Applied Biosystems
ptpn11	Mm00448434	Applied Biosystems
rorc	Mm01261022	Applied Biosystems
smad2	Mm00487530	Applied Biosystems
smad3	Mm01170760	Applied Biosystems
smad7	Mm00484742	Applied Biosystems
stat3	Mm01219775	Applied Biosystems
tbx21	Mm00450960	Applied Biosystems
tgfbr2	Mm00436977	Applied Biosystems

2.2 Methods

2.2.1 Mice

C57BL/6J mice and TCRδ$^{-/-}$ mice on a C57BL/6J background were bred by the Comparative Medicine Unit (CMU), Trinity College Dublin and were housed under specific-pathogen free (SPF) conditions. Mice were maintained under guidelines and regulations of the Health Products Regulatory Authority and experiments were carried out under license with the approval of Trinity College Dublin Animal Research Ethics Committee. Experiments were conducted with female 6–12-week-old mice. All mice within experiments were age matched. Mice were sacrificed by CO_2 asphyxiation followed by confirmation of death by cervical dislocation.

2.2.2 Induction and assessment of EAE

2.2.2.1 Active EAE

EAE was induced in C57BL/6J mice by subcutaneous (s.c) immunisation with 100 µg myelin oligodendrocyte glycoprotein$_{35-35}$ (MOG$_{35-55}$; Genscript, referred to as MOG throughout) peptide emulsified 1 in 2 in complete Freund's adjuvant (CFA; Chondrex) which contains 4 mg/mL of H37 Ra *Mycobacterium tuberculosis.* Mice were injected intraperitoneally (i.p) with 250 ng of pertussis toxin (PT; Native Antigen Company) on days 0 and 2 of EAE. In certain experiments mice were also injected with anti-PD-1 antibody, anti-CD210 antibody or isotype control antibody (200 µg/mouse) on the day prior to the induction of EAE and on days 2 and 5 post induction of EAE. In other experiments mice were also injected with the small molecule inhibitor of TGF-β-mediated signalling SB431542 or vehicle control (DMSO) as indicated.

Animals were monitored daily for clinical disease and their weights were recorded.

Disease severity was assessed according to percentage weight change and EAE clinical scores as follows:

0 – no clinical signs

1 - Limp tail

2 – Ataxic gait

3 – Hind limb weakness

4 – Hind limb paralysis

5 – Tetra paralysis

2.2.2.2 Adoptive transfer EAE model

EAE was induced by adoptive transfer of MOG-specific T cells from C57BL/6J mice. C57BL/6J mice were immunised with 100 µg MOG emulsified 1 in 2 in CFA. Donor mice did not receive PT. After 10 days, donor mice were sacrificed and spleen and axillary, brachial, and inguinal LNs were isolated and prepared into single cell suspension at a ratio of 70:30 spleen: LN.

In some experiments either CD4 T cells or γδ T cells were separated from the total culture by MACS and stimulated for 6 hours with SB431542 or vehicle control (DMSO). After 6 hours, the treated CD4 T cells or γδ T cells were washed thoroughly. Separated cells were recombined with the remaining $CD4^-$ or $TCR\delta^-$ cells before proceeding with the adoptive transfer protocol.

Cells were cultured with MOG (100 µg/mL), IL-1β (10 ng/mL) and IL-23 (10 ng/mL) at $10x10^6$ cells/mL in 6 well plates. After 72 hours, cells were harvested and washed thoroughly in PBS before counting. Cells were re-suspended in PBS at a concentration of 50-75 x 10^6 cells/mL. 10-15 x 10^6 viable cells were transferred into naïve recipient C57BL/6J mice by i.p immunisation. Recipient mice were not injected with PT. Animals were monitored daily for signs of clinical disease and their weights were recorded. Disease severity was measured according to percentage weight change and clinical score as described in 2.2.2.1.

2.2.3 Cell counting

Cells re-suspended in either MACS buffer or cRPMI were diluted 1 in 10 in EBAO. 10 µL of this cell suspension was loaded into a disposable haemocytometer (Hycor Biomedical).

Viable cells (green) were differentiated from dead cells (red) and counted using a fluorescent microscope (Leitz). Cell concentration (per mL) was determined using the following formula: (#cells/#squares) x EBAO dilution factor x 10^4 = #cells/mL.

2.2.4 Isolation of mononuclear cells from the spleen and lymph nodes

Mice were sacrificed by CO_2 anaesthesia and the spleen, axillary, brachial and inguinal LNs were harvested. Spleen and LN cells were processed by using the barrel of a 1 mL syringe to push the organs through a 70 µm filter washing through with cRPMI continuously. Cells were pelleted by centrifugation (342 g, 5 mins) and re-suspended in cRPMI.

2.2.5 Isolation of mononuclear cells from the peritoneal cavity

Mice were sacrificed by CO_2 anaesthesia and dissected to reveal the intact peritoneum. 5 mL ice cold PBS was injected into the peritoneal cavity using a 20G intravascular catheter. The mouse peritoneal wall was prodded mechanically to disrupt cells without removing the catheter. A syringe was attached to the catheter and the PBS was removed. The peritoneal exudate cells (PEC) were pelleted by centrifugation (342 g, 5 mins) and resuspended in PBS for staining and analysis by flow cytometry.

2.2.6 Isolation of mononuclear cells from the lung and nasal tissue

Mice were sacrificed by CO_2 anaesthesia and lung and nasal tissue was harvested into cRPMI. Lung tissue was mechanically disrupted using a scalpel. Chopped lung tissue and nasal tissue was digested with collagenase D and DNase I for 1 hour at 37^oC, continuously rotating to facilitate tissue break down and release of cells. Digested lung and nasal tissue samples were passed through a 70 µm strainer to obtain a single cell suspension. Cells were pelleted by centrifugation (342 g, 5 mins) and pellets were resuspended in 1 mL RBC lysis buffer for 2 minutes. The reaction was neutralised by adding 10 mL cRPMI. Cells were pelleted by centrifugation and resuspended in PBS for staining and analysis by flow cytometry.

2.2.7 Isolation of mononuclear cells from the CNS

Mice were sacrificed by CO_2 anaesthesia and perfused through the left ventricle with 20 mL of ice cold PBS before removal of the brain and spinal cord. Organs were lysed in 1 mL cRPMI using a tissue lyser (Qiagen) at 27.5 rpm/second for 5 minutes. The organ homogenate was re-suspended in 5 mL of 40% isotonic Percoll in cRPMI. This homogenate was layered over 5 mL of 70% Percoll in PBS. The Percoll gradients were centrifuged at 1600 rpm for 20 minutes at room temperature with the centrifuge brake off. The upper myelin layer was removed and discarded. Mononuclear cells were removed from the interface of the Percoll gradients using a Pasteur pipette and passed through a 70 µm filter. Cells were washed in cRPMI and immediately stained or alternatively stimulated with PMA, ionomycin and brefeldin A or brefeldin A alone for 4 hours at 37^{o}C before intracellular cytokine staining.

2.2.8 Isolation of bone marrow-derived cells

Mice were sacrificed by CO_2 anaesthesia and femurs and tibiae were aseptically removed and separated from the surrounding muscle and tissue. The tips of each bone were removed with a sterile scalpel to expose the bone marrow. The bone marrow was flushed out using a 27G needle attached to a 10 mL syringe containing cRPMI. A transfer pipette was used to break up cell aggregates in the bone marrow suspension. Cells were pelleted by centrifugation (342 g, 5 mins) and red blood cells were lysed as previously described. The RBC-lysed bone marrow was resuspended in 10 mL cRPMI to count.

2.2.9 Generation of bone marrow-derived dendritic cells (BMDCs)

Bone marrow cells were cultured (37^{o}C; 5% CO_2) at a concentration of 1 x 10^6 cells/mL (20 mL per T175 flask) in cRPMI supplemented with 20 ng/mL recombinant GM-CSF. After 3 days, a further 20 mL cRPMI supplemented with 20 ng/mL recombinant GM-CSF was added to each culture flask. After a further 3 days of culture, the cell culture supernatant was gently poured off and discarded. 20 mL sterile PBS, heated to 37^{o}C was added to each

flask and the flask was agitated to remove loosely adherent cells. The PBS suspension was transferred to falcon tubes containing 10 mL cRPMI. 20 mL sterile EDTA, heated to 37°C, was added to each flask, and incubated at 37°C for 10 minutes, after which the EDTA suspension was pipetted up and down and transferred into falcon tubes containing 10 mL cRPMI. PBS and EDTA suspensions were pelleted by centrifugation (342 g, 5 mins) and combined in 10 mL cRPMI for counting. Cells were re-cultured at a concentration of 1 x 10^6 cells/mL (20 mL per T175 flask) in cRPMI supplemented with 20 ng/mL recombinant GM-CSF. On day 8 of culture, a further 20 mL cRPMI supplemented with 20 ng/mL recombinant GM-CSF was added to each culture flask. On day 10 of the culture, loosely adherent cells were harvested by gentle repeat pipetting. BMDCs were pelleted by centrifugation (342 g, 5 mins) and resuspended in cRPMI supplemented with 20 ng/mL recombinant GM-CSF. BMDCs were plated at a concentration of 1 x 10^6 cells/mL in 96 well flat-bottomed plates. Cells were rested overnight before stimulation with heat-killed *Mtb* (10 µg/mL).

For co-culture experiments where BMDCs were used as APCs, BMDCs were resuspended in cRPMI supplemented with 20 ng/mL recombinant GM-CSF at a concentration of 2 x 10^6 cells/mL. 100 µL of the cell suspension (2 x 10^5 cells total) was seeded in each well of a 96 well round-bottomed plate. BMDCs were rested for 6 hours prior to co-culture with FACS-purified T cells.

2.2.10 Isolation of γδ T cells by magnetic-activated cell sorting (MACS)

γδ T cells were purified from mouse spleen and LNs by depletion of non-target cells and subsequent positive selection of cells expressing the γδ TCR using a TCR γ/$δ^+$ T cell isolation kit (Miltenyi Biotec) according to the manufacturer's protocol.

Mononuclear cells were isolated from the spleen and LNs of either naïve or MOG-immunised C57BL/6J mice and pelleted by centrifugation (342 g, 5 mins). The cell pellet was re-suspended in 1 mL RBC lysis buffer for 2 minutes to lyse the erythrocytes. Cells were washed in cRPMI and counted with EBAO. 1 x 10^8 cells were re-suspended in 450 µL of MACS buffer. 50 µL of non-T cell depletion cocktail was added to the cell suspension.

The cell suspension was vortexed well and then incubated for 15 minutes at 4°C. Cells were washed and re-suspended in 450 µL of MACS buffer. The cell suspension was applied to a pre-washed LD MACS column, placed in the magnetic field of a QuadroMACS separator. The flow through was collected and washed with MACS buffer. The cell suspension was centrifuged and re-suspended in 450 µL of MACS buffer. 50 µL of anti-biotin microbeads were added to the cell suspension which was mixed well by vortexing and incubated for 15 minutes at 4°C. Cells were washed with MACS buffer and then re-suspended in 500 µL of MACS buffer before being applied to a pre-washed MS MACS column, placed in the magnetic field of an OctoMACS separator. The column was removed from the separator and 1 mL MACS buffer was flushed through it using the supplied plunger. The second magnetic separation step was repeated using another pre-washed MS column and plunger. Cells flushed through the MS column were magnetically labelled γδ T cells. Separated cells were pelleted by centrifugation and re-suspended in 1 mL cRPMI to count.

2.2.11 Isolation of CD4 T cells by MACS

CD4 T cells were purified from mouse spleen and LNs by depletion of non-target cells and subsequent positive selection of cells CD4 using a $CD4^+$ T cell isolation kit (Miltenyi Biotec) according to the manufacturer's protocol.

Mononuclear cells were isolated from the spleen and LNs of either naïve or MOG-immunised C57BL/6J mice and pelleted by centrifugation (342 g, 5 mins). The cell pellet was re-suspended in 1 mL RBC lysis buffer for 2 minutes to lyse the erythrocytes. Cells were washed in cRPMI and counted with EBAO. 1 x 10^8 cells were re-suspended in 400 µL of MACS buffer. 100 µL of Biotin antibody cocktail was added to the cell suspension. The cell suspension was vortexed well and then incubated for 5 minutes at 4°C. A further 300 µL of MACS buffer was added to the cell suspension. 200 µL of anti-biotin microbeads were added to the cell suspension which was mixed well by vortexing and incubated for 10 minutes at 4°C. The cell suspension was mixed well and applied to a pre-washed LS MACS column, placed in the magnetic field of a QuadroMACS separator. The flow through was collected and contained the enriched CD4 T cells. The column was then removed from

the separator and 5 mL MACS buffer was flushed through it using the supplied plunger to remove the bound $CD4^-$ fraction from the column. Both fractions ($CD4^+$ and $CD4^-$) were pelleted by centrifugation and re-suspended in 10 mL cRPMI to count.

2.2.12 Isolation of T cells by negative selection MACS

$CD3^+$ T cells were isolated from mouse spleen and LNs by depletion of non-target cells using a mouse T cell enrichment kit (Thermo Fisher Scientific) according to the manufacturer's protocol.

Mononuclear cells were isolated from the spleen and LNs of either naïve or MOG-immunised C57BL/6J mice and pelleted by centrifugation (342g, 5 mins). The cell pellet was re-suspended in 1 mL RBC lysis buffer for 2 minutes to lyse the erythrocytes. Cells were washed in cRPMI and counted with EBAO. 1 x 10^7 cells were re-suspended in 100 µL of MACS buffer. 20 µL of Magnisort enrichment antibody cocktail was added to the cell suspension which was mixed well by pulse vortexing 5 times. Cells were incubated at room temperature for 10 minutes. Cells were washed by bringing the volume of the cell suspension up to 4 mL with MACS buffer followed by pelleting by centrifugation. Cells were re-suspended in 100 µL of MACS buffer and 20 µL of Magnisort negative selection beads were added. The cell suspension was mixed well by pulse vortexing 5 times and then incubated at room temperature for 5 minutes. The cell suspension volume was brought up to 2.5 mL with MACS buffer and mixed well by pipetting up and down 3 times with a P1000 set to 1 mL. The tube containing the cell suspension was inserted into the Magnisort magnet and incubated at room temperature for 5 minutes. The magnet containing the tube was picked up and the supernatant was poured into a clean tube in a quick continuous motion. Cells were pelleted by centrifugation and re-suspended in 10 mL cRPMI to count.

2.2.13 Isolation of CD4 T cells by negative selection MACS

CD4 T cells were isolated from mouse spleen and LN cells by depletion of non-target cells using a mouse CD4 T cell enrichment kit (Thermo Fisher Scientific) according to the manufacturer's protocol.

Mononuclear cells were isolated from the spleen and LNs of either naïve or MOG-immunised C57BL/6J mice and pelleted by centrifugation (342 g, 5 mins). The cell pellet was re-suspended in 1 mL RBC lysis buffer for 2 minutes to lyse the erythrocytes. Cells were washed in cRPMI and counted with EBAO. 1 x 10^7 cells were re-suspended in 100 µL of MACS buffer. 20 µL of Magnisort enrichment antibody cocktail was added to the cell suspension which was mixed well by pulse vortexing 5 times. Cells were incubated at room temperature for 10 minutes. Cells were washed by bringing the volume of the cell suspension up to 4 mL with MACS buffer followed by pelleting by centrifugation. Cells were re-suspended in 100 µL of MACS buffer and 20 µL of Magnisort negative selection beads were added. The cell suspension was mixed well by pulse vortexing 5 times and then incubated at room temperature for 5 minutes. The cell suspension volume was brought up to 2.5 mL with MACS buffer and mixed well by pipetting up and down 3 times with a P1000 set to 1 mL. The tube containing the cell suspension was inserted into the Magnisort magnet and incubated at room temperature for 5 minutes. The magnet containing the tube was picked up and the supernatant was poured into a clean tube in a quick continuous motion. Cells were pelleted by centrifugation and re-suspended in 10 mL cRPMI to count.

2.2.14 *in vitro* immune cell expansion

2.2.14.1 $CD27^-$ γδ T cell expansion

Mononuclear cells were isolated from mouse spleen and LNs and pelleted by centrifugation (342 g, 5 mins). The cell pellet was re-suspended in 1 mL RBC lysis buffer for 2 minutes to lyse the erythrocytes. Cells were washed in γδ cRPMI and counted with EBAO. Cell density was adjusted to 2 x 10^6 cells/mL.

100 µL cell suspension per well was added to anti-TCR-γδ-coated 96 well round bottom tissue culture plates (Greiner Bio-one). 100 µL of $CD27^-$ γδ expansion cytokine cocktail (IL-1β; 5 ng/mL, IL-23; 5 ng/mL and anti-IFN-γ; 10 µg/mL) was added to each well. Cells were incubated at 37°C for 3 days. After 3 days cells were harvested and washed with PBS. Cells were then counted and re-suspended at a density of 2 x 10^6 cells/mL. 100 µL cell suspension per well was added to fresh uncoated tissue culture plates and a further 100 µL of $CD27^-$ γδ expansion cytokine cocktail was added. Cells were incubated at 37°C for a further 4 days. On day 7, cells were harvested and washed before being used in experiment.

2.2.14.2 $CD27^+$ γδ T cell expansion

Mononuclear cells were isolated from mouse spleen and LNs and pelleted by centrifugation (342 g, 5 mins). The cell pellet was re-suspended in 1 mL RBC lysis buffer for 2 minutes to lyse the erythrocytes. Cells were washed in γδ cRPMI and counted with EBAO. Cell density was adjusted to 2 x 10^6 cells/mL.

100 µL cell suspension per well was added to anti-TCR-γδ-coated 96 well round bottom tissue culture plates. 100 µL of $CD27^+$ γδ expansion cytokine cocktail (IL-2, IL-7, and IL-15; 20 ng/mL) was added to each well. Cells were incubated at 37° for 3 days. After 3 days, cells were harvested and washed with PBS. Cells were then counted and re-suspended at a density of 2 x 10^6 cells/mL. 100 µL cell suspension per well was added to fresh uncoated tissue culture plates and a further 100 µL of $CD27^+$ γδ expansion cytokine cocktail was added. Cells were incubated at 37°C for a further 4 days. On day 7, cells were harvested and washed before being used in experiment.

2.2.14.3 MOG-specific Tr1 cell generation and expansion

MOG-specific Tr1 cells were generated and expanded according to a previously developed protocol [69]. MOG specific Tr1 cells were generated *in vivo* by s.c immunisation of C57BL/6J mice with MOG (100 µg/mouse), retinoic acid (RA; 400 µg/mouse) and IL-2 (500 ng/mouse) on day 0 and day 14. LN cells were isolated from immunised mice on day 21

and mononuclear cells were isolated. Cells were counted and re-suspended at a cell density of 2 x 10^6 cells/mL. Cells were cultured in 6 well plates (4 mL per well) in the presence of MOG (100 µg/mL), RA (10^{-6} M) and IL-2 (10 ng/mL) and incubated at 37°C for 4 days. After 4 days of culture, more IL-2 (10 ng/mL) was added, and the cells were cultured for a further 4 days. After 8 days of culture, cells were harvested and washed before being used in experiment.

2.2.15 MOG-specific suppression assay

CD4 or γδ T cells were isolated by MACS from the spleen and LN of MOG-immunised mice. Cells were counted and stimulated *in vitro* with MOG (100 µg/mL), IL-1β (2.5 ng/mL) and IL-23 (10 ng/mL) for 3 hours in the presence of 1 x 10^5 BMDCs per well. Cells were incubated at 37°C and after 3 hours expanded MOG-specific Tr1 cells were added to the culture. MOG-specific Tr1 cells were added in 100 µL/well at increasing densities starting at a density resulting in 1:1 co-culture of CD4/γδ effector T cell: Tr1 and increasing to a density of 1 effector T cell to 10 Tr1 cells. The activation conditions used for CD4 T cells and $CD27^-$ γδ T cells were MOG (100 µg/mL), IL-1β (2.5 ng/mL) and IL-23 (10 ng/mL).

2.2.16 Antigen-specific cytokine production

Spleen and LN cells from MOG-immunised mice were cultured at a 50:50 ratio at a density of 2 x 10^6 cells/mL in the presence of MOG (100 µg/mL) with or without IL-1β (10 ng/mL) and IL-23 (10 ng/mL). Neutralisation of IL-10, PD-1 or TGF-β was investigated using anti-IL-10, anti-PD-1, anti-TGF-β antibodies or the small molecule inhibitor SB431542. Cells were incubated at 37°C for 72 hours. Cells were pelleted by centrifugation (342 g, 5 mins) and supernatants were collected to determine concentrations of IL-17A and IFN-γ by ELISA. Cell pellets were re-suspended in brefeldin A and incubated for a further 4 hours before intracellular cytokine staining and analysis by flow cytometry.

2.2.17 Flow cytometry

2.2.17.1 Flow cytometry staining and analysis

Cells were isolated from their respective organs and processed into a lysed, single-cell suspension prior to staining. For intracellular cytokine staining, cells were isolated and stimulated for 4 hours at 37^{o} with PMA, ionomycin and brefeldin A or brefeldin A alone as indicated. Cells were washed with PBS and stained using an appropriate Live/Dead fixable stain kit diluted 1 in 1000 in PBS. 50 µL live/dead stain was added to each sample and samples were incubated in the dark for 20 minutes on ice. Cells were washed with FACS buffer, pelleted by centrifugation (342 g, 5 mins) and supernatants were discarded. Surface staining was carried out for 20 minutes on ice in the dark using fluor-conjugated antibodies diluted in FACS buffer in the presence of Fcγ receptor blocking antibody to prevent non-specific binding. The surface stain was made up by adding appropriate dilutions (1 in 100-500) of different fluor-conjugated antibodies to FACS buffer to make a master mix of which 50 µL was added to each sample. Cells were washed twice with FACS buffer followed by surface staining and the supernatants were discarded. For intracellular and intranuclear staining, cells were fixed using 100 µL of FoxP3 Fixation/Permeabilisation working solution and incubated for 30 minutes at room temperature or overnight at 4^{o}C. Cells were washed with 1X permeabilisation buffer before intracellular or intranuclear staining. The intracellular stain was made up by adding appropriate dilutions (1 in 100-500) of different fluor-conjugated antibodies to 1X permeabilisation buffer to make a master mix of which 50 µL was added to each sample. Cells were stained on ice in the dark for 1 hour. Cells were then washed twice with permeabilisation buffer and washed once finally with FACS buffer. Supernatants were discarded and cells were re-suspended in a final volume of 200 µL FACS buffer. Cells were stored at 4^{o}C in the dark before flow cytometric analysis.

Flow cytometric data was acquired using LSRFortessa (BD Biosciences) with FACS Diva software or Cytek Aurora with SpectroFlo software. For conventional cytometry, compensation was calculated using individually stained comp beads (BD Biosciences). For spectral flow cytometry, data was unmixed based on single-stained compensation beads (BD Biosciences). Live, single cells were identified using the gating strategies outlined in

section 2.3. FlowJo software (TreeStar Inc.) was used to analyse flow cytometric data. Percentage and absolute number of cells were calculated on the basis of live, single cells. Fluorescence minus one (FMO) controls were used as a guide for gating strategies.

2.2.17.2 Gating strategy for the identification of T cell subsets in the spleen and LN

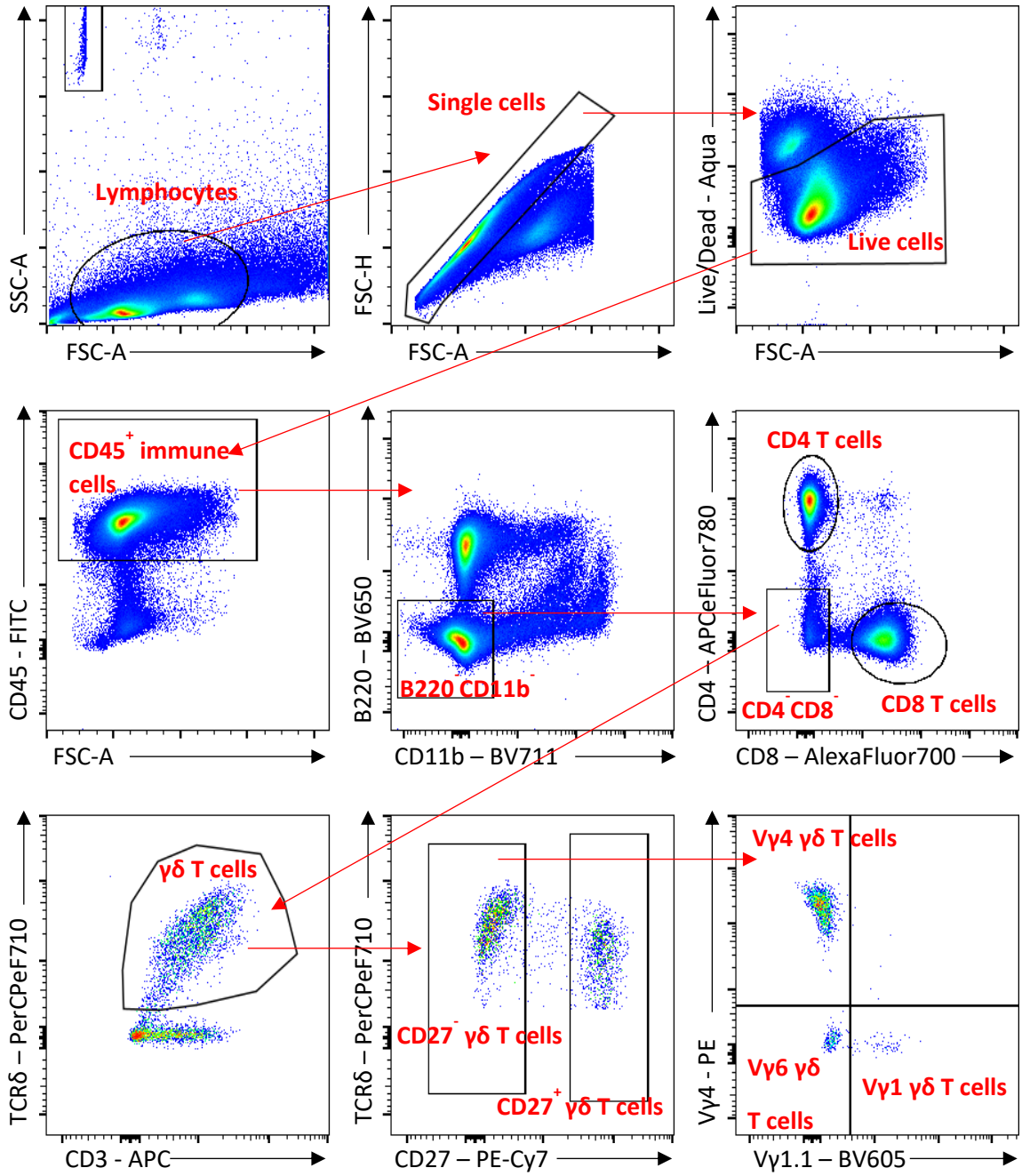

2.2.17.3 Gating strategy for the identification of innate immune cell subsets in the spleen

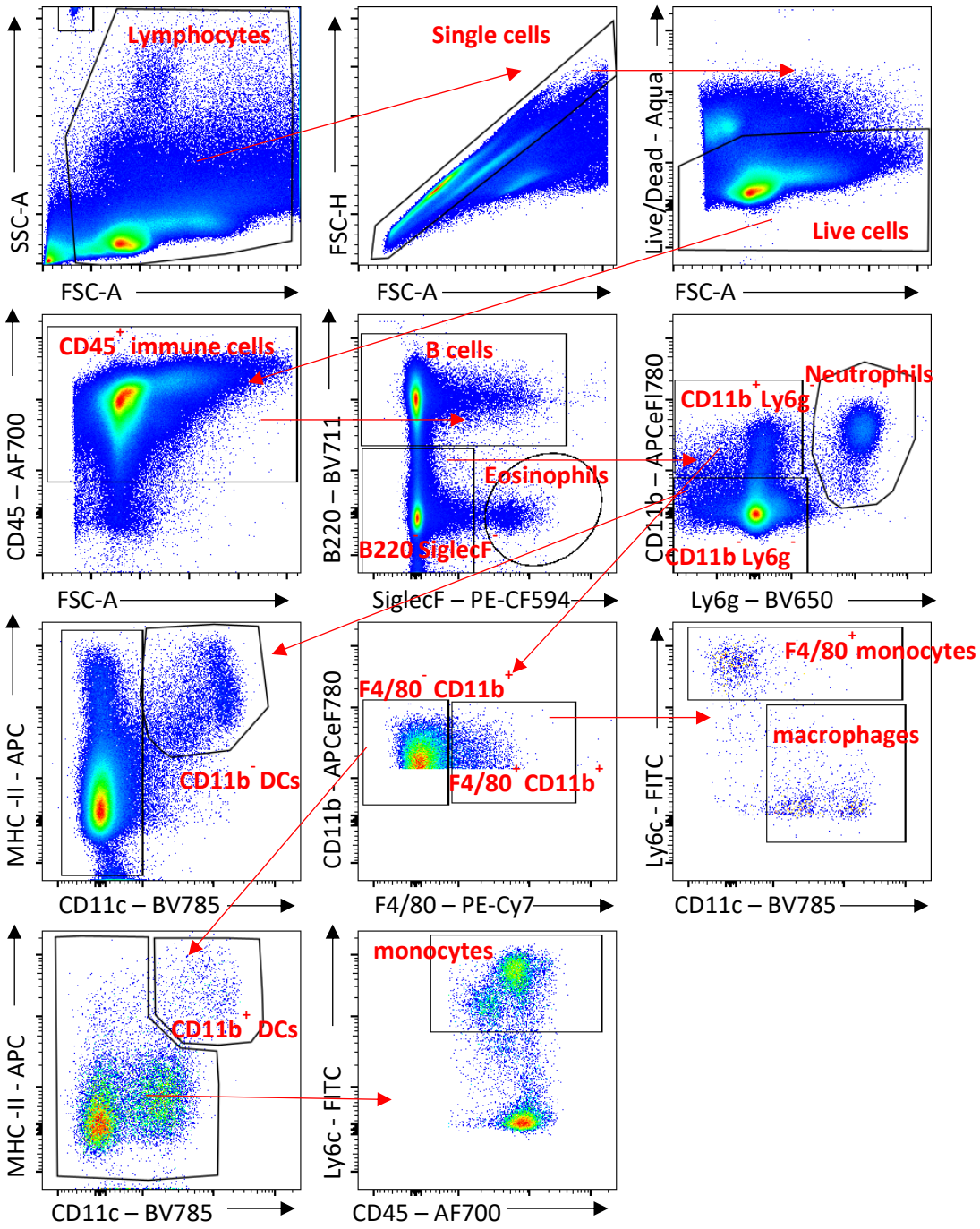

2.2.17.4 Gating strategy for the identification of infiltrating immune cells in the brain

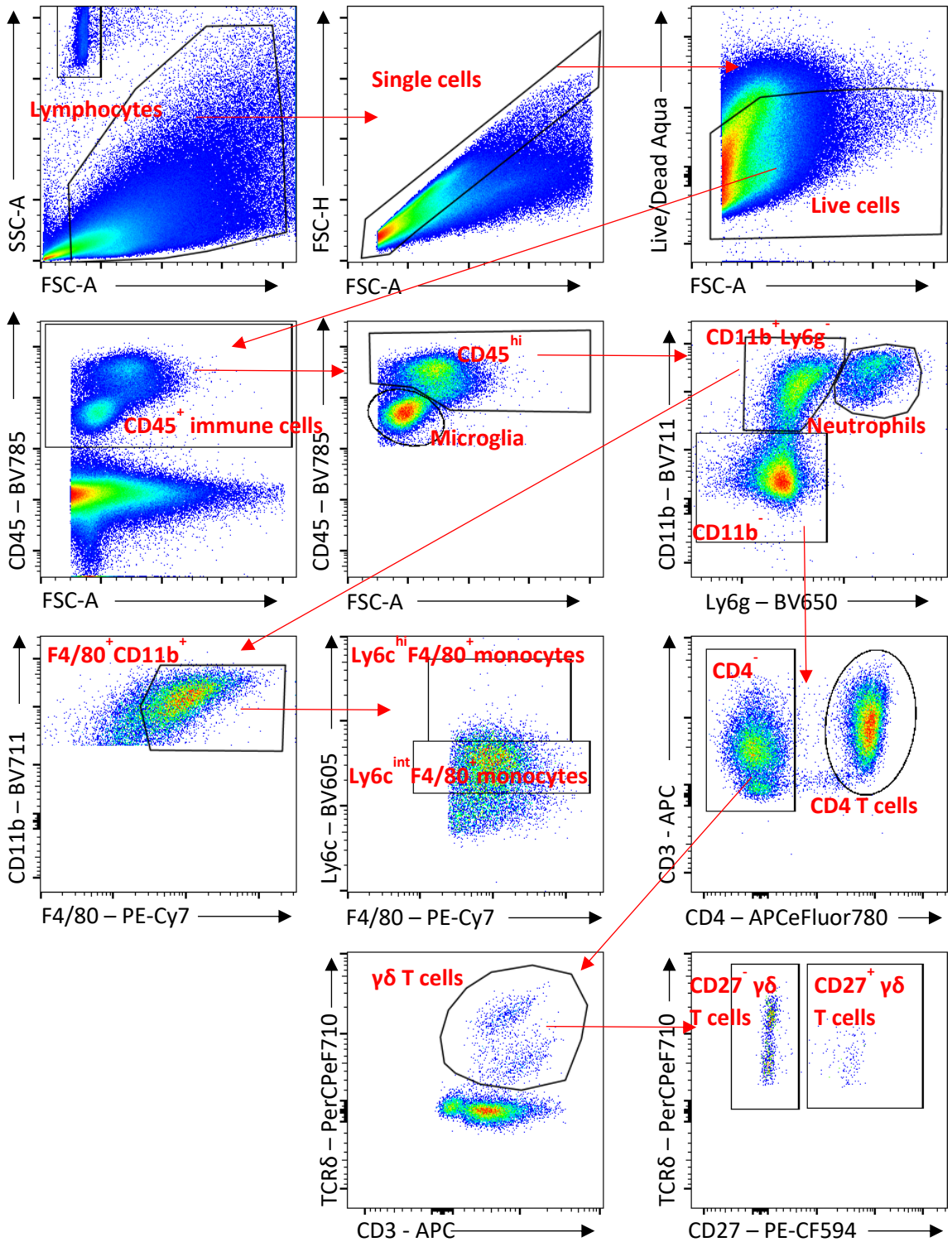

2.2.17.5 Fluorescence-activated cell sorting (FACS)

Mononuclear cells were isolated from the spleen and LN of naïve or MOG-immunised C57BL/6J mice as previously described. Cells were lysed with 1 mL of RBC lysis buffer for 2 minutes and then washed with FACS sort buffer. Cells were counted in EBAO and the cell pellet was re-suspended in surface stain to yield a desired cell density of 50 x 10^6 cells/mL. The surface stain was made up in FACS sort buffer by adding 1 in 200 dilution of each fluor-conjugated antibody in the presence of Fcγ receptor blocking antibody. Samples were stained in the dark for 30 minutes at 4°C. Cells were washed twice using FACS buffer prior to isolation of target populations using the FACSAria Fusion High Performance Cell Sorter (BD Biosciences). Propidium Iodide (PI) Ready Flow reagent was added to the cells prior to cell sorting to allow for discrimination of live from dead cells.

2.2.17.6 Phosphoflow staining

γδ T cells were expanded as described in 2.2.14 and serum-starved overnight to reduce background phosphorylation. Cells were centrifuged (342 g, 5 mins) and re-suspended in cRPMI containing their respective stimulations. $CD27^-$ γδ T cells were stimulated with IL-1β (2.5 ng/mL) and IL-23 (10 ng/mL) in the presence or absence of TGF-β (5 ng/mL) for 15, 30 and 60 minutes. $CD27^+$ γδ T cells were stimulated with IL-12 (2.5 ng/mL) and IL-18 (10 ng/mL) in the presence or absence of TGF-β (5 ng/mL) for 15, 30 and 60 minutes. After the cells were stimulated, they were stained using Live/dead Aqua as described in 2.2.17. 1X lyse/fix buffer was prepared in dH_2O and prewarmed to 37°C. Cells were fixed by adding 1mL 1X lyse/fix buffer to each sample followed by vigorous mixing and incubation at 37°C for 10 minutes. Cells were then washed twice with FACS buffer. Permeabilisation buffer III was cooled to -20°C. Following fixation, samples were pelleted by centrifugation and permeabilised with 200 µL pre-cooled perm buffer III per sample. Perm buffer III was added to samples following brief vortexing to loosen the cells and vortexing was continued while adding perm buffer III. Samples were incubated on ice for 30 minutes. Cells were then washed twice with FACS buffer before proceeding to staining for both surface markers and phospho-specific targets in the same step, as described in 2.2.17.

2.2.17.7 Primeflow RNA assay

MOG-specific Tr1 cells were generated as described in 2.2.14.3. Samples were fixed by mixing cell pellets well with fixation buffer 1 for 30 minutes on ice. Cells were washed and pelleted by centrifugation (342 g, 5 mins). Samples were then permeabilised using 1X Primeflow RNA perm buffer containing RNase inhibitors. 1 mL RNA perm buffer was added to each sample and mixed by inversion. Cells were then pelleted by centrifugation. Intracellular staining was carried out as described in 2.2.17.1 using Primeflow RNA perm buffer as the staining buffer. After 1 hour on ice, samples were washed with Primeflow RNA perm buffer and pelleted by centrifugation. Samples were then fixed using 1 mL Primeflow RNA fixation buffer 2 for 1 hour at room temperature. Cells were washed with 1 mL Primeflow RNA wash buffer and pelleted by centrifugation. Cell pellets were then resuspended in 100 µL RNA target probe diluent containing the target probes. Samples were incubated at 40^{o}C for 2 hours. Samples were then washed with 1 mL Primeflow RNA buffer. Cells were pelleted by centrifugation and pellets were resuspended in 100 µL Primeflow RNA PreAmp mix and incubated for 1.5 hours at 40^{o}C. Samples were then washed three times with 1 mL Primeflow RNA wash buffer each time. After washing, 100 µL RNA Amp mix was added to each tube followed by incubation for 1.5 hours at 40^{o}C. Samples were washed twice with 1 mL Primeflow RNA wash buffer. 100 µL Primeflow RNA label probe diluted in Primeflow RNA label probe diluent was added to each sample followed by incubation for 1.5 hours at 40^{o}C. Cells were washed with 1 mL Primeflow RNA wash buffer. Cells were pelleted by centrifugation and resuspended in 1 mL Primeflow RNA storage buffer before being analysed by flow cytometry.

2.2.18 Enzyme-linked immunosorbent assay (ELISA)

ELISA kits (R&D & BD Biosciences) were used to quantitatively analyse the concentrations of various cytokines in cell supernatants. High-binding certified 96-well microtiter plates (Greiner Bio-one) were coated with 50 µL/well capture antibody in PBS and incubated for 2 hours at room temperature or overnight at 4^{o}C. Capture antibody was removed from each well and 100 µL blocking buffer (1% BSA) was added to each well and incubated at

room temperature for 2 hours. Blocked plates were then washed 3 times each with ELISA wash buffer (PBS-tween). 50 µL/well cell supernatant in triplicate was added either undiluted or diluted in 1% BSA. Standards were prepared by serially diluting a specific top working standard (6 consecutive 1:2 dilutions) and added to the plate in triplicate. Each plate also had three blank wells which contained 50 µL 1% BSA alone. Plates were incubated either at room temperature for 2 hours or overnight at 4^{o}C. Plates were washed 3 times with ELISA wash buffer and 50 µL/well biotinylated anti-mouse detection antibody diluted in 1% BSA was added and incubated for 2 hours at room temperature. Plates were washed a further three times and 50 µL HRP-conjugated streptavidin diluted in 1% BSA was added to each well and incubated for 20 minutes in the dark at room temperature. Plates were washed five times with ELISA wash buffer and 50 µL substrate solution (TMB) was added to each well. Once the standard curve had developed sufficiently the enzyme reaction was stopped by adding 25 µL/well of stop solution (1M H_2SO_4). The absorbance was read at 450 nm using a Versamax Tunable Microplate Reader with SoftMax Pro software. Cytokine concentration in each unknown sample was determined by reference to the standard curve prepared using recombinant cytokine of a known concentration and following subtraction of the blank absorbance reading from each sample on the plate.

2.2.19 Real-time quantitative polymerase chain reaction (Rt-qPCR)

Spinal cords were isolated from mice with EAE and collected into 1 mL buffer RPE containing 10 µL β-me. Spinal cord tissue samples were homogenised using a tissue lyser (Qiagen) at 27.5 rpm/second for 5 minutes. For Rt-qPCR of FACS-purified cells, cells were stimulated for 2 hours and pelleted by centrifugation (342 g, 5 mins). Cell pellets were re-suspended in 350 µL buffer RPE containing 3.5 µL β-me. 350 µL 70% ethanol was added to each of the lysed samples and mixed well by pipetting. 700 µL of each sample was transferred to an individual RNeasy mini spin column placed in a 2 mL collection tube. Samples were centrifuged for 15 seconds at 8000 g. The flow-through was discarded. 700 µL buffer RW1 was added to the column followed by centrifugation for 15 seconds at 8000 g. The flow-through was discarded. 500 µL buffer RPE was applied to each column followed by centrifugation for 15 seconds at 8000 g. The flow-through was again

discarded. A further 500 µL buffer RPE was added to each column followed by centrifugation for 2 minutes at 8000 g. The RNeasy spin column was placed in a new collection tube and the RNA was eluted with 20 µL RNase-free dH_2O. Samples were centrifuged for 1 minute at 8000 g.

The RNA concentration in each sample was determined using a Nanodrop spectrophotometer and the concentrations were equalised across samples by dilution with RNase-free dH_2O. RNA samples were reverse transcribed into cDNA using the Applied Biosystems High-Capacity cDNA reverse transcription kit according to the manufacturer's protocol. Reverse-transcribed cDNA was diluted to the desired concentration using RNase-free dH_2O. Real-time PCR for the detection of mRNA was performed using pre-designed Taqman gene expression assays (Applied Biosystems). Eukaryotic 18S ribosomal RNA was used as an endogenous control. Samples were assayed on an Applied Biosystems 7500 Fast Real Time PCR machine.

2.2.20 Statistical analysis

Statistical analyses were performed using GraphPad Prism software. Differences were analysed by unpaired Student's *t* test (two conditions) or by one-way analysis of variance (ANOVA) with the Tukey's post test (3 or more conditions). Differences between groups for clinical scores and percentage weight change in EAE were analysed by two-way ANOVA with repeated measures followed by the Sidak's multiple comparisons test. Error bars indicate the mean ± standard error of the mean (SEM) or standard deviation (SD) as indicated in individual figure legends. *P* values of 0.05 or less were considered to be statistically significant.

Chapter 3
IL-17A-producing γδ T cells are regulated by PD-1 in a model of CNS autoimmunity

3.1 Introduction

Seminal research into the mechanism of action of PD-1 has revealed that PD-1 signalling suppresses T cell receptor-mediated activation, proliferation, and cytokine production by CD4 T cells [56]. However, the role that PD-1 plays in regulating γδ T cell function is relatively unexplored. IL-17A-producing γδ T cells are thought to be primarily cytokine-activated in EAE [169]. Studies have shown that PD-1 blockade at the beginning of EAE can increase the severity of EAE and MOG-specific IFN-γ production [125]. However, the ability of PD-1 signalling to regulate γδ T cells in autoimmunity has not been examined.

PD-1 is expressed by skin-resident Vγ6 γδ T cells [256]. IL-17A-producing Vγ6 γδ T cells and Vγ4 γδ T cells in the skin express Scart1 and Scart2, respectively. A comparison of transcriptional profiles between Vγ4 and Vγ6 γδ T cells showed that, *pdcd1*, the gene that encodes PD-1, was more highly expressed by the Scart1^{+} Vγ6-expressing population. PD-1-expressing Vγ6 γδ T cells have also been described in a murine model of metastatic breast cancer [177]. Edwards et al. reported that lung-resident Vγ6 γδ T cells expressed much higher PD-1 than Vγ4 γδ T cells both at steady-state and in the pre-metastatic lung. PD-1 engagement on IL-1β+IL-23-activated Vγ6 γδ T cells suppressed IL-17A production via activation of FOXO1. In the pre-metastatic lung, lung-resident Vγ4 γδ T cells expressed high levels of the checkpoint molecule Tim3.

Human γδ T cells can be activated via direct binding of PAgs to their TCR [257]. A further study elucidated the mechanism whereby γδ T cells can be activated via direct TCR binding to induce downstream TCR signalling cascades [258]. Vγ9Vδ2 γδ T cells are activated by BTN3A1 which induces TCR signalling events that lead to phosphorylation of Zap70, PLCγ, Akt, NF-κB, ERK, and MAPK [258]. Human Vγ4 γδ T cells can be activated in a similar manner via direct binding of BTN2A1 and BTN3A1 to the TCR [259].

The ability of human γδ T cells to be activated directly via their TCRs suggests that checkpoint expression by these cells can modulate their function. In the BM of multiple myeloma (MM) patients, γδ T cells can recognise malignant B cells in a TCR-dependent manner [260]. Vγ9Vδ2 γδ T cells present in the BM of MM patients have high PD-1 expression and are anergic [261]. PD-L1 expression is increased on most myeloma cells and anti-PD-1 treatment partly rescued reactivity of Vγ9Vδ2 γδ T cells to PAg [261].

Similarly, in a study that investigated the role of PD-1 in regulating γδ T cell activation in AML, it was demonstrated that anti-PD-1 treatment increased IFN-γ production and CD107a expression by PD-1 expressing Vγ9Vδ2 γδ T in response to the PAg zoledronate [262]. Anti-PD-1 treatment also improved adoptive cell therapy with Vγ9Vδ2 γδ T cells in a humanised mouse model of prostate cancer [263].

ICIs have shown excellent efficacy in the treatment of certain cancers and have been approved for the treatment of NSCLC and metastatic melanoma [264]. Clinical use of ICIs has greatly improved prognoses for these malignancies, but treatment with these antibodies commonly cause irAEs in patients. [265]. The most common manifestations of irAEs present in the skin, GI tract, and endocrine system [148] [266]. ICIs have also been reported to cause neurological side effects in patients with melanoma, glioblastoma, and Hodgkin's lymphoma [267]. Treatment with cancer immunotherapy drugs targeting either PD-1 or CTLA-4 has been associated with relapses in MS patients. In a 2019 review, Garcia et al., identified 14 cases of MS relapse following ICI treatment. These relapses were severe and included rapid neurologic progression and death [268]. In a further report, treatment of NSCLC with pembrolizumab, an ICI targeting PD-1, was shown to cause MS in a patient with prior history of white matter brain lesions, but no previous neurological symptoms [269]. Furthermore, a single nucleotide polymorphism (SNP) in the PD-1 gene (*pdcd1*) has been associated with disease progression in MS [270]. This SNP reduced the inhibitory function of PD-1 on CD4 T cell activation and cytokine production. PD-L1 expression has been identified in CNS tissue specimens from both healthy controls and MS patients [271].

Previous studies that have examined the role of PD-1 signalling during EAE have demonstrated that disease severity and the onset of clinical signs of EAE was enhanced in PD-L1$^{-/-}$ mice [271]. Ortler et al. demonstrated that PD-L1$^{-/-}$ mice with EAE had increased MOG-specific IFN-γ and IL-17A production by CD4 T cells. This phenotype was not observed in PD-L2$^{-/-}$ mice [272]. It has also been demonstrated that increasing PD-L1 expression by DCs is associated with decreased severity of EAE [273]. Macrophages have been implicated in the increased severity of EAE in PD-1$^{-/-}$ mice [274]. The mentioned study showed that increased IL-6 production by macrophages of PD-1$^{-/-}$RAG2$^{-/-}$ mice enhanced the differentiation of Th17 cells and exacerbated EAE.

The aim of this chapter was to investigate the role of PD-1 signalling in regulating γδ T cell function during EAE. Previous studies have explored how antigen-specific γδ T cells are regulated by PD-1 signalling and how PD-1 regulates the function of cytokine-activated Vγ6 γδ T cells. Vγ4 γδ T cells are the main early source of IL-17A in EAE [171]. The effect of PD-1 signalling on CD4 T cell function is well-documented but the effect of PD-1 signalling on Vγ4 γδ T cell function remains unexplored. In the present study we used a PD-1 neutralising antibody to explore how PD-1 signalling affects the development of EAE. We also used flow cytometry to examine, which immune cell types are responsive to anti-PD-1 treatment during CNS autoimmunity.

3.2 Results

3.2.1 CD27$^-$ Vγ4 γδ T cells express high levels of PD-1 in naïve mice and this is augmented during EAE.

To investigate immune cell populations that may be regulated via the PD-1 signalling pathway during EAE, expression of PD-1 by T cell subpopulations in the LN was assessed throughout the course of disease. LNs were isolated from naïve mice and mice 5 and 10 days post induction of EAE. At all time-points examined, the highest PD-1 expression, as determined by absolute number, was found on CD4 T cells (Fig 3.1 B). There were much fewer PD-1-expressing CD8 T cells and CD27$^+$ γδ T cells in the LN of mice throughout EAE. In naïve mice, the number of PD-1$^+$ CD27$^-$ γδ T cells was very low but this population expanded throughout EAE (Fig 3.1 B). There were significantly more PD-1-expressing CD27$^-$ γδ T cells in the LN at day 10 post induction of EAE when compared with PD-1-expressing CD8 and CD27$^+$ γδ T cells (Fig 3.1 B). Both the CD27$^+$ and CD27$^-$ γδ T cell compartment represented the T cell population expressing the highest frequency of PD-1 in the LN of naïve mice (Fig 3.1 A). However, throughout EAE the frequency of PD-1-expressing CD27$^-$ γδ T cells was significantly higher than CD4, CD8, and CD27$^+$ γδ T cells (Fig 3.1 C).

γδ T cells can be separated into subpopulations based on expression of different Vγ chains [161]. γδ T cells expressing different Vγ chain subsets are found in lymphoid and mucosal tissues [162]. To further examine the expression of PD-1 by CD27$^-$ γδ T cells during EAE, various tissues including the LN, PEC, lung, and nasal tissue were harvested, and PD-1 expression was measured on Vγ1, Vγ4, and Vγ6-expressing CD27$^-$ γδ T cells. There were significantly higher numbers of PD-1-expressing Vγ4 γδ T cells in the LN of naïve mice and on day 10 of EAE (Fig 3.2 A). In the naïve lung, there was a significantly greater number of PD-1$^+$ Vγ6 γδ T cells when compared to Vγ1 or Vγ4-expressing γδ T cells (Fig 3.2 C). A similar pattern was observed in the lung on day 5 post induction of EAE but by day 10 of EAE there is an expansion of PD-1$^+$ Vγ4 γδ T cells (Fig 3.2 C). In contrast to the LN, both the PEC and nasal tissue of naïve mice, had greater numbers of PD-1$^+$ Vγ6 γδ T cells when compared with the Vγ1 and Vγ4 γδ T cells (Fig 3.2 B, D). This phenotype was maintained on day 5 of EAE but by day 10 of EAE there was an expansion of PD-1$^+$ Vγ4 γδ T cells in the PEC and nasal tissue. On day 10 of EAE in both the PEC and nasal tissue there were equal

numbers of PD-1-expressing Vγ4 and Vγ6 γδ T cells (Fig 3.2 B, D). Across all timepoints and tissues examined there was very low expression of PD-1 by Vγ1 γδ T cells (Fig 3.2 A, B, C, D). These data demonstrate that $CD27^-$ Vγ4 γδ T cells express the highest amount of PD-1 in the LN both in naïve mice and throughout EAE.

3.2.2 Neutralisation of PD-1 signalling increases the severity of EAE by increasing IL-17A production by $CD27^-$ γδ T cells

Blockade of the PD-1 signalling pathway has previously been shown to exacerbate EAE [125, 271, 272]. Previous studies demonstrated that blocking PD-1-PD-L1 interactions resulted in increased MOG-specific IFN-γ production by CD4 T cells in EAE. IL-17A is a key cytokine in the development and pathogenesis of EAE [171]. To examine the role of PD-1 signalling in modulating IL-17A production by T cell subsets in EAE, an anti-PD-1 antibody was used to block PD-1 signalling *in vivo.*

Treatment with anti-PD-1 significantly increased the severity of EAE when compared with mice treated with an isotype control antibody (Fig 3.3 A). Anti-PD-1 treatment also enhanced the onset of EAE as isotype control-treated mice developed clinical symptoms of EAE later than anti-PD-1-treated mice (Fig 3.3 A). When compared with the control group, the anti-PD-1-treated group lost significantly more weight, beginning on day 10 of EAE (Fig 3.3 B).

An examination of the number of various T cell subsets in the LN on day 3 and day 6 post induction of EAE showed that there was no differences in the total number of γδ, CD4, or CD8 T cells in the LN on day 3 between anti-PD-1-treated mice and isotype control-treated mice (Fig 3.4 A, B, C). On day 6, there was a significant increase in the total number of γδ T cells, CD4 T cells, and CD8 T cells in the LN following treatment with anti-PD-1 (Fig 3.4 A, B, C).

Murine γδ T cells can be separated into two subpopulations based on expression of CD27 [168]. $CD27^+$ γδ T cells are predominantly IFN-γ producers, whereas $CD27^-$ γδ T cells secrete IL-17A. Both the frequency and total number of $CD27^-$ γδ T cells were significantly higher in the LN of anti-PD-1-treated mice when compared with isotype control-treated

mice (Fig 3.5 A, B). There was a significant increase in the frequency, total number, and mean fluorescence intensity (MFI) of IL-17A production by $CD27^-$ γδ T cells in the LN of anti-PD-1-treated mice (Fig 3.5 C, D).

The vast majority of IL-17A-producing $CD27^-$ γδ T cells express either the Vγ4 or Vγ6 γ chain [275]. There was a significant increase observed in the total number of $CD27^-$ Vγ4 γδ T cells between isotype control-treated and anti-PD-1-treated mice (Fig 3.6 A). Furthermore, there was also an increase in the frequency, number, and MFI of IL-17A produced by $CD27^-$ Vγ4 γδ T cells (Fig 3.6 B, C). Additionally, there was a significant increase in the frequency, number, and MFI of RORγt expressed by $CD27^-$ Vγ4 γδ T cells in the LN of anti-PD-1-treated mice (Fig 3.6 D, E).

In contrast to Vγ4 γδ T cells, there was no difference in the total number of $CD27^-$ Vγ6 γδ T cells in the LN between anti-PD-1-treated and isotype control-treated mice (Fig 3.7 A). Similarly, there were no differences in frequency, number, or MFI of either IL-17A or RORγt-expressing $CD27^-$ Vγ6 γδ T cells between anti-PD-1-treated and isotype control-treated mice with EAE (Fig 3.7 B, C, D, E).

These findings were validated *in vitro* using spleen and LN cells from naïve and MOG-immunised mice. IL-1β and IL-23 induces IL-17A production by γδ T cells [169]. Treatment of spleen and LN cells from MOG-immunised mice with IL-1β and IL-23 induced IL-17A, IFN-γ, and GM-CSF production, and this was significantly augmented upon addition of anti-PD-1 to the spleen and LN cells (Fig 3.8 A). Similarly, when spleen and LN cells from MOG-immunised mice were re-stimulated with MOG, IL-17A, IFN-γ, and GM-CSF was produced, and this was significantly enhanced following addition of anti-PD-1 to the spleen and LN cells (Fig 3.8 A, B, C). Stimulation of spleen and LN cells from MOG-immunised mice with MOG, IL-1β+IL-23 induced production of IL-17A, IFN-γ, and GM-CSF but addition of anti-PD-1 to the spleen and LN cells did not significantly impact cytokine production (Fig 3.8 A, B, C).

To validate that the IL-1β+IL-23-induced IL-17A production in the culture was not produced by bystander-activated CD4 T cells, the experiment was repeated using spleen and LN cells from naïve mice. In a similar manner, there was a significant increase in IL-17A and IFN-γ production by the IL-1β+IL-23-stimulated spleen and LN cells upon addition

of anti-PD-1 (Fig 3.8 A, B). There was a slight increase observed in IL-1β+IL-23-induced GM-CSF produced by the naïve spleen and LN cells, following addition of anti-PD-1, but this result was not significant (Fig 3.8 C). These data illustrate how anti-PD-1 treatment increases IL-17A production by $CD27^-$ γδ T cells during EAE.

3.2.3 Anti-PD-1 treatment enhances antigen-specific T cell responses during EAE

The clinical efficacy of ICI treatment of cancer is considered to reflect enhancement of the CD4 and CD8 T cell responses in the TME [276]. Therefore, we examined the effect of anti-PD-1 treatment on CD4 and CD8 T cell responses during EAE.

There was a significant increase in the number of CD4 T cells in the LN of anti-PD-1-treated mice when compared with isotype control-treated mice on day 9 of EAE (Fig 3.9 A). Furthermore, the frequency of IL-17A-producing CD4 T cells was enhanced, though not significantly, in the LN of anti-PD-1-treated mice (Fig 3.9 B). On day 9 of EAE, there was also a significant increase in the number of IL-17A-producing CD4 T cells in the LN of anti-PD-1-treated mice (Fig 3.9 B). There was an increase in the frequency and number of RORγt-expressing CD4 T cells following anti-PD-1 treatment, although this difference was not significant (Fig 3.9 C). There was a significant decrease in the frequency of $Tbet^+$ CD4 T cells following anti-PD-1 treatment (Fig 3.9 D). There were no differences observed in the number of Tbet-expressing CD4 T cells in the LN of anti-PD-1-treated mice (Fig 3.9 D).

Anti-PD-1 treatment has previously been shown to reduce CD4 Treg cell conversion in murine cancer models, thereby enhancing anti-tumour immunity [277]. The effect of anti-PD-1 treatment on Treg cell conversion during EAE was investigated. There was a significant increase in both the frequency and number of $CD25^{hi}$ $FoxP3^+$ CD4 T cells (Treg cells) in the LN of anti-PD-1-treated mice on day 9 of EAE (Fig 3.10 A, B, C).

Polyfunctional CD4 T cells are a hallmark of the pathogenesis of EAE and modulation of these cells impacts the severity of EAE [171]. Cytokine production by CD4 T cells in the LN was examined during EAE. There were no significant differences in the frequency or number of GM-CSF, IFN-γ, or TNF-producing CD4 T cells between anti-PD-1 or isotype control-treated mice in the LN on day 9 of EAE (Fig 3.11 A, C, D). There was a significant

increase in both the frequency and number of IL-17A$^+$ CD4 T cells in the LN on day 9 of EAE following anti-PD-1 treatment (Fig 3.11 B).

An examination of the MOG-specific T cell responses in anti-PD-1 and isotype control-treated mice with EAE, showed a significant increase in MOG-specific IL-17A production following re-stimulation of spleen cells from mice with EAE with 100 µg/mL MOG (Fig 3.12 A). There were no significant differences in MOG-specific IFN-γ, GM-CSF, or TNF production observed between treatment groups (Fig 3.12 B, C, D). These data indicate that anti-PD-1 treatment during EAE significantly enhances the antigen-specific Th17 cell response.

3.2.4 Anti-PD-1 treatment increases infiltration of IL-17A-producing T cells into the CNS during EAE

Inflammatory γδ and CD4 T cells infiltrate into the brain and spinal cord during EAE where they precipitate disease [278]. As anti-PD-1 treatment during EAE increases the severity of disease, the effect of anti-PD-1 treatment on T cell infiltration into the CNS was examined. mRNA expression of *il17a, rorc, ifng,* and *tbx21* were all significantly increased in the spinal cord of anti-PD-1-treated mice at the peak of EAE (Fig 3.13 A, B, C, D). There was a significant increase in the number of γδ T cells infiltrating the brains of anti-PD-1-treated mice at the peak of EAE (Fig 3.14 A). There were comparable numbers of CD27$^+$ γδ T cells in the brains of anti-PD-1 and isotype control-treated mice (Fig 3.14 B). Conversely, there was a significant increase in the frequency and number of CD27$^-$ γδ T cells in the brains of anti-PD-1-treated mice at the peak of EAE when compared with isotype control-treated mice (Fig 3.14 D, E). The phenotype of infiltrated CD27$^-$ γδ T cells was examined. There was no difference observed in the frequency of RORγt$^+$ CD27$^-$ γδ T cells (Fig 3.15 A). However, there was a significant increase in the number of RORγt-expressing CD27$^-$ γδ T cells in the brains of mice with EAE following anti-PD-1 treatment (Fig 3.15 B). Both the frequency and number of IL-17A$^+$ CD27$^-$ γδ T cells was significantly augmented in the brain at the peak of EAE following anti-PD-1 treatment (Fig 3.15 D, E).

There was a significant increase in the number of CD4 T cells infiltrating the brain at the peak of EAE in anti-PD-1-treated mice (Fig 3.16 A). Anti-PD-1 treatment did not significantly impact the frequency or number of RORγt-expressing CD4 T cells in the brains of mice with EAE (Fig 3.16 B). However, there was a significant increase in the number of Treg cells in the brain at the peak of EAE in anti-PD-1-treated mice (Fig 3.16 D). This difference was not reflected in the frequency of Treg cells in the brain following anti-PD-1 treatment (Fig 3.16 D). There was a significant increase in the absolute number but not the frequency of GM-CSF, IL-17A, IFN-γ, and TNF-producing CD4 T cells in the brains of anti-PD-1-treated mice (Fig 3.17 A, B, C, D). These data show that anti-PD-1 treatment during EAE enhances infiltration of inflammatory CD4 T cells into the brain where they increase the severity of disease.

3.2.5 γδ T cells are required for the increase in severity of EAE induced by anti-PD-1 treatment

A previous study from the lab has indicated that the severity of EAE is reduced in TCRδ$^{-/-}$ mice, which demonstrates a pathogenic role for γδ T cells in CNS autoimmunity [169]. Sutton et al. also demonstrated that IL-17A production by γδ T cells amplifies the MOG-specific CD4 T cell response. The results of the present study so far have revealed that anti-PD-1 treatment enhances IL-17A production by CD27^{-} γδ T cells. TCRδ$^{-/-}$ mice were used to examine the role of γδ T cells in mediating the exacerbation of EAE induced by anti-PD-1 treatment.

Treatment with anti-PD-1 significantly enhanced the severity of EAE in WT mice as determined by clinical score and percentage weight loss (Fig 3.18 A). There were no differences in clinical score or percentage weight loss between isotype control or anti-PD-1-treated TCRδ$^{-/-}$ mice with EAE (Fig 3.18 B).

There was an increase in the frequency and number of RORγt-expressing CD4 T cells in anti-PD-1-treated WT mice with EAE (Fig 3.19 A). This difference was not observed in TCRδ$^{-/-}$ mice (Fig 3.19 A). Similarly, the frequency and absolute number of IL-17A-producing CD4 T cells was increased in anti-PD-1 treated WT mice with EAE (Fig 3.19 C). This phenotype was not observed in TCRδ$^{-/-}$ mice treated with anti-PD-1 (Fig 3.19 C). These

findings suggest that anti-PD-1 treatment during EAE increases the severity of disease by modulating the function of γδ T cells that further impact CD4 T cell function.

3.2.6 PD-L1-expressing DCs suppress IL-17A production by γδ T cells in a PD-1-dependent manner

The present study has thus far demonstrated that PD-1 regulates IL-17A production by $CD27^-$ γδ T cells. Since innate cells direct T cell responses, this study examined the possible role of PD-L1 expression by innate immune cells in suppressing IL-17A-producing γδ T cells. PD-L1 expression by $F4/80^+$ monocytes, macrophages, neutrophils, $CD11b^+$, and $CD11b^-$ DCs was measured both in naïve mice and at the early stages of EAE. $F4/80^+$ monocytes and neutrophils from the spleen had low expression of PD-L1 (Fig 3.20 A, B). In contrast, up to 80% of macrophages in the spleen were $PD\text{-}L1^+$ 72 hours post-induction of EAE (Fig 3.20 A). Macrophages also had the highest MFI of PD-L1 expression in naïve mice and mice with EAE (Fig 3.20 B). Both $CD11b^+$ and $CD11b^-$ populations of DCs had moderate expression of PD-L1 (Fig 3.20 A, B).

EAE is induced using *Mtb*-containing CFA [279]. Stimulation of BMDCs with *Mtb* induced IL-1β and IL-23 production (Fig 3.21 A) as well as enhanced expression of PD-L1 and PD-L2 by BMDCs (Fig 3.21 B). Co-culture of *Mtb*-stimulated BMDCs with $CD27^-$ γδ T cells induced IL-17A production (Fig 3.22 A). $CD27^-$ γδ T cells were stimulated with IL-1β and IL-23 to induce IL-17A production. Co-culture of IL-1β+IL-23-activated $CD27^-$ γδ T cells with BMDCs, suppressed IL-17A production (Fig 3.22 B). Addition of anti-PD-1 to the co-cultured BMDCs and $CD27^-$ γδ T cells significantly increased IL-17A production (Fig 3.22 B). These findings demonstrate that *Mtb* activates $CD27^-$ γδ T cells to produce IL-17A via activation of innate immune cells and this is constrained by PD-1-PD-L1 interactions.

3.2.7 IL-1β+IL-23-activated Vγ6 γδ T cells are regulated by PD-1 signalling

IL-17A production by lung-resident Vγ6 γδ T cells is regulated by PD-1 signalling in a breast cancer metastasis model [177]. In the present study, a co-culture method was used to

measure the regulation of Vγ6 γδ T cells by PD-1. Vγ6 γδ T cells produced IL-17A *in vitro* in response to IL-1β+IL-23 which was supressed following co-culture with BMDCs (Fig 3.23 A). Further addition of anti-PD-1 to the co-cultured BMDCs and Vγ6 γδ T cells slightly reversed the suppression of IL-17A production (Fig 3.23 A). When Vγ6 γδ T cells were stimulated with anti-TCRδ rather than IL-1β+IL-23, addition of anti-PD-1 to the co-cultured BMDCs and Vγ6 γδ T cells did not affect IL-17A production (Fig 3.23 B).

Recombinant PD-L1 was used to assess the effect of PD-1 engagement on Vγ6 γδ T cell function *in vitro*. Activation of Vγ6 γδ T cells with IL-1β+IL-23-induced expression of *il17a, rorc,* and *ptpn11.* When IL-1β+IL-23-activated Vγ6 γδ T cells were cultured in the presence of plate-bound PD-L1, there was a significant decrease in the expression of *il17a, rorc,* and *ptpn11* (Fig 3.24 A, B, C). Stimulation of Vγ6 γδ T cells with anti-TCRδ did not induce any significant expression of *il17a, rorc,* or *ptpn11 in vitro* (Fig 3.24 A, B, C). Furthermore, addition of PD-L1 to anti-TCRδ-stimulated Vγ6 γδ T cells, did not suppress gene expression of *il17a, rorc,* or *ptpn11* (Fig 3.24 A, B, C). Stimulation with PD-L1 did not change the frequency or number of IL-17A-producing Vγ6 γδ T cells activated with IL-1β+IL-23 or anti-TCRδ (Fig 3.25 A, B). However, PD-L1 significantly decreased the MFI of IL-17A production by Vγ6 γδ T cells stimulated with IL-1β+IL-23 but not with anti-TCRδ (Fig 3.25 C).

To examine the regulation of Vγ6 γδ T cells *in vivo,* mice were immunised with MOG+CFA to induce EAE or with CFA alone and treated with either anti-PD-1 or isotype control antibody. All mice received PT on the day of induction of EAE. In mice immunised with MOG+CFA there was no difference in the number of Vγ6 γδ T cells in the LN following treatment with anti-PD-1 (Fig 3.26 A). However, when mice were immunised with CFA alone, anti-PD-1 treatment significantly enhanced the number of Vγ6 γδ T cells in the LN (Fig 3.26 A). Similarly, there were no differences in the frequency, number, or MFI of IL-17A production by Vγ6 γδ T cells following anti-PD-1 treatment in mice immunised with MOG+CFA (Fig 3.26 B). However, there was a significant increase in the number of IL-17A-producing Vγ6 γδ T cells following anti-PD-1 treatment when mice were immunised with CFA alone (Fig 3.26 B). There was a similar pattern observed in RORγt expression by Vγ6 γδ T cells in response to anti-PD-1 treatment. When mice were immunised with MOG+CFA there was no difference in the frequency, number, or MFI of RORγt expression by Vγ6 γδ T cells following anti-PD-1 treatment (Fig 3.26 D). However, following immunisation of

mice with CFA in the absence of MOG, there was a significant increase in the frequency and number of RORγt-expressing Vγ6 γδ T cells in the LN of anti-PD-1-treated mice (Fig 3.26 D). These findings suggest that Vγ6 γδ T cells are not regulated by PD-1 during EAE.

3.2.8 IL-17A-producing Vγ4 γδ T cells are regulated by PD-1 in a TCR-dependent manner

Vγ4 γδ T cells are a key early source of IL-17A during the induction of EAE [171] and the present study has shown that they express high levels of PD-1 in the LN at the onset of EAE. We examined how PD-1 regulates the function of Vγ4 γδ T cells. Co-culture of IL-1β +IL-23-stimulated Vγ4 γδ T cells with BMDCs, suppressed IL-17A production and this was not modified by addition of PD-1 neutralising antibody (Fig 3.27 A). However, when TCRδ-stimulated Vγ4 γδ T cells were co-cultured with BMDCs, addition of anti-PD-1 enhanced IL-17A production (Fig 3.27 B).

Activation of Vγ4 γδ T cells with IL-1β and IL-23 enhanced expression of *il17a* and *rorc* (Fig 3.28 A, B) but this was not affected by PD-1 engagement (Fig 3.28 A, B). Conversely, anti-TCRδ-induced expression of *il17a* and *rorc* by Vγ4 γδ T cells was significantly suppressed upon PD-1 engagement (Fig 3.28 A, B). Anti-TCRδ stimulation induced expression of *ptpn11* by Vγ4 γδ T cells, which is a gene associated with downstream TCR signalling events [280]. Anti-TCRδ-induced *ptpn11* gene expression by Vγ4 γδ T cells was suppressed by PD-L1 (Fig 3.28 C).

IL-17A production by IL-1β+IL-23-stimulated Vγ4 γδ T cells was not impacted by PD-1 engagement (Fig 3.29 A, B, C). However, the frequency and number of anti-TCRδ-stimulated IL-17A-producing Vγ4 γδ T cells was significantly reduced by adding PD-L1-Fc (Fig 3.29 A, B).

In order to examine the regulation of IL-17A production by Vγ4 γδ T cells during EAE mice were immunised with MOG+CFA to induce EAE or with CFA alone and treated with either anti-PD-1 or isotype control antibody. All mice received PT on the day of induction of EAE. There was a significant increase in the number of Vγ4 γδ T cells in the LN following anti-PD-1 treatment in mice immunised with either MOG+CFA or CFA alone (Fig 3.30 A). The frequency, number, and MFI of IL-17A expression by Vγ4 γδ T cells was significantly

increased following anti-PD-1 treatment of mice immunised with MOG+CFA (Fig 3.30 B). Interestingly, when mice were immunised with CFA alone there were no differences in the frequency, number, or MFI of IL-17A production by Vγ4 γδ T cells between isotype control-treated and anti-PD-1-treated mice (Fig 3.30 B). Similarly, there was a significant increase in the frequency, number, and MFI of RORγt expression by Vγ4 γδ T cells in the LN of anti-PD-1-treated mice immunised with MOG+CFA. This anti-PD-1-induced increase in the number of RORγt-expressing Vγ4 γδ T cells was also observed in mice immunised with CFA alone (Fig 3.30 D). However, anti-PD-1 treatment of mice immunised with CFA alone did not affect the frequency or MFI of RORγt expression by Vγ4γδ T cells when compared with isotype control-treated mice immunised with CFA. These data suggest that anti-PD-1 increases IL-17A production by Vγ4 γδ T cells in a MOG-dependent manner.

3.3 Discussion

The present study has uncovered a novel mechanism whereby IL-17A-producing CD27$^-$ γδ T cells are regulated *in vivo* in an autoimmune disease model. CD27$^-$ γδ T cells expressed the highest frequency of PD-1 in the LN of naïve mice and this was further augmented during EAE. Enhanced PD-1 expression is considered to be a sign of activation or exhaustion during chronic viral infections [281]. PD-1 inhibits conventional T cell responses via inhibition of TCR signalling [115].Since γδ T cells, especially IL-17A-secreting CD27$^-$ γδ T cells, are activated with IL-1β+IL-23 without TCR stimulation this suggests that PD-1 may regulate γδ T cell function via a distinct mechanism to αβ T cells. PD-1 expression is regulated by the transcription factors NFAT, AP-1, Notch, and Tbet [282]. These transcription factors are generally associated with TCR signalling which is consistent with the demonstration that TCR-stimulated antigen-specific T cells express higher levels of PD-1 than naïve T cells to regulate signalling via their TCR. STAT3 enhances expression of PD-1 by CD8 T cells [283]. STAT3 is also associated with regulation of IL-17A production and RORγt expression by T cells [284]. Taken together these data suggest that STAT3 regulation of IL-17A production by γδ T cells could influence PD-1 expression by these cells as a regulatory mechanism in the absence of TCR signalling. This hypothesis is consistent with the increased expression of PD-1 by CD27$^-$ γδ T cells during the early stages of EAE.

The ability of PD-1 to regulate IL-17A production by CD27$^-$ γδ T cells in this study opens the question as to how γδ T cells are activated *in vivo* and whether γδ T cells are autoantigen-specific in EAE. IL-17A-producing Vγ6 γδ T cells are fetally-derived and require the transcription factor promyelocytic leukaemia zinc finger (PLZF) for their development [285]. PLZF is a specific transcriptional regulator of NKT cell development and is associated with innate lymphocyte populations that can acquire T helper cell phenotypes [286]. Vγ6 γδ T cells can have innate-like functions. In a model of *B. pertussis* infection, Vγ6 γδ T cells were identified as the main source of IL-17A in the lungs at the early stages of infection [172]. IL-17A-producing Vγ6 γδ T cells also accumulated rapidly in the kidney at the early stages of *S. aureus* infection [287]. In addition to their role in protection against infection, Vγ6 γδ T cells can play a pathogenic role in cancer. In a murine model of ovarian cancer, IL-17A-producing Vγ6 γδ T cells promoted tumour

growth [288]. Furthermore, IL-17A production by Vγ6 γδ T cells was regulated by PD-1 in the lung in a breast cancer metastasis model [177]. This particular study showed that PD-1 regulated Vγ6 γδ T cells activated by IL-1β and IL-23. Similarly, results from the present study have shown that IL-1β+IL-23-activated Vγ6 γδ T cells were regulated by PD-1 signalling. Interestingly, anti-PD-1 treatment did not enhance IL-17A production by Vγ6 γδ T cells in mice immunised with MOG+CFA but did enhance IL-17A production by Vγ6 γδ T cells immunised with CFA alone. These data suggest that Vγ6 γδ T cells are not regulated by PD-1 during EAE. Additionally, the study mentioned above by Edwards et al. showed that PD-1 engagement increased FOXO1 expression by Vγ6 γδ T cells in order to suppress IL-17A production [177]. FOXO1 expression has also been associated with sustained expression of PD-1 by CD8 T cells [289]. These data suggest that when IL-1β and IL-23 activate Vγ6 γδ T cells to produce IL-17A via STAT3, PD-1 expression is upregulated. Engagement of PD-1 can suppress cytokine-activated Vγ6 γδ T cells via FOXO1. The findings of the present study suggest that IL-17A-producing Vγ6 γδ T cells are not regulated by PD-1 during EAE as Vγ6 γδ T cells are not activated by IL-1β+IL-23 alone in this context. CFA immunisation alone appears to primarily activate Vγ6 γδ T cells via IL-1β+IL-23 explaining why PD-1 regulates Vγ6 γδ T cell in the absence of MOG.

The present study has demonstrated that unlike Vγ6 γδ T cells, Vγ4 γδ T cell function is regulated by PD-1 in EAE. Vγ4 γδ T cells function similarly to Vγ6 γδ T cells but have more adaptive characteristics. Following re-infection with the respiratory pathogen *B. pertussis*, IL-17A-producing memory Vγ4 γδ T cells expanded in the lungs and contributed to rapid bacterial clearance [172]. IL-17A-producing memory Vγ4 γδ T cells have also been shown to expand in a model of hypersensitivity pneumonitis upon re-challenge [290]. In the present study, anti-PD-1 treatment enhanced IL-17A production by Vγ4 γδ T cells in mice immunised with MOG+CFA but did not enhance IL-17A production by Vγ4 γδ T cells in mice immunised with CFA alone. These data suggest that antigen-specific Vγ4 γδ T cells are induced in response to MOG during EAE. This could explain how Vγ4 γδ T cells purified from MOG-immunised mice that are activated via their TCR *in vitro* are regulated by PD-1 signalling. PD-1 suppresses T cell responses via blocking TCR signalling. In EAE, antigen-specific Vγ4 γδ T cells appear to develop and expand and these cells are regulated by PD-1. Although γδ T cells are not traditionally considered as TCR-MHC activated cells,

evidence does exist to support the idea that γδ T cells can recognise antigen in the context of MHC-II [291]. As Vγ4 γδ T cells from mice immunised with CFA alone were not regulated by PD-1 during EAE and IL-1β+IL-23-activated Vγ4 γδ T cells are not suppressed by recombinant PD-L1 *in vitro* this suggests that PD-1 does not regulate IL-1β+IL-23-activated Vγ4 γδ T cells during EAE.

The impact of immune checkpoint inhibition on γδ T cell function has recently come under more scrutiny due to the pro-tumour role of IL-17A in murine cancer models. [288, 292, 293]. Anti-PD-1 treatment does not reduce tumour growth in certain murine cancer models where IL-17A is produced by γδ T cells [294]. In lung tumour biopsies from patients treated with pembrolizumab, response to treatment was associated with decreased expression of *rorc* [295]. Furthermore, blockade of IL-17A improved the response to anti-PD-1 treatment in a murine model of CRC by increasing infiltration of CD8 T cells into the tumour [296]. In the present study, anti-PD-1 treatment enhanced IL-17A production by γδ T cells. This suggests that increased IL-17A production by γδ T cells in the TME could prevent ICIs from effectively reducing tumour growth. These data could explain why certain cancer types are resistant to treatment with ICIs. However, in autoimmune diseases this modulation of IL-17A production by PD-1 could be exploited for therapeutic benefit. PD-1 agonistic monoclonal antibodies that can induce PD-1 signalling can specifically suppress T cell activation via the TCR [297]. Peresolimab is a humanised monoclonal antibody that stimulates PD-1 signalling *in vivo* and has shown efficacy in a phase II clinical trial in patients with RhA [298]. Findings from the present study in EAE together with the demonstration that MS disease pathogenesis is associated with *rorc* expression [299] suggest that a PD-1 agonistic monoclonal antibody may have efficacy for the treatment of MS and other autoimmune diseases.

The effect of ICIs on Treg cell function and expansion appears to be context-dependent. In a murine colon cancer model, the efficacy of a DC vaccine was improved by addition of anti-PD-1 [277]. Dyck et al. demonstrated that anti-PD-1 treatment inhibited the induction of FoxP3-expressing Treg cells which allowed for expansion of IFN-γ- and TNF-producing CD8 T cells in response to a therapeutic cancer vaccine. Vaccine-induced anti-tumour CD8 T cells were able to kill tumour cells in the absence of Treg cells. PD-1 has also been shown to sustain FoxP3 stability in induced Treg cells and were protective in a murine model of

graft versus host disease (GvHD) [300]. However, in other contexts, anti-PD-1 treatment expands Treg cells. In a subset of gastric cancer patients, anti-PD-1 treatment rapidly expanded Treg cells, which were highly immunosuppressive and overwhelmed tumour-reactive effector T cells that rendered PD-1 blockade ineffective [301]. An association between PD-1 expression by effector T cells and Treg cells has been identified as a predictor of the clinical efficacy of PD-1 blockade therapies [302]. Responders to PD-1 blockade had high infiltration of PD-1-expressing CD8 T cells into the tumour, whereas non-responders had increased PD-1 expression by Treg cells in the TME. Resistance to ICI treatment has also been linked with high Treg cell activity in tumours [303]. The study mentioned above demonstrated that depletion of Treg cells was able to sensitise tumours to ICI therapy. The present study demonstrated that treatment with anti-PD-1 significantly increased the number and frequency of FoxP3-expressing Treg cells in the periphery and CNS during EAE. These data are consistent with the literature although increased numbers of Treg cells did not decrease the severity of EAE in anti-PD-1-treated mice. Depletion of Treg cells during EAE has previously been shown to increase the severity of EAE by enhancing the expansion and motility of effector T cells [247]. However, data from the present study demonstrates that as well as enhancing the number of Treg cells, anti-PD-1 treatment also increases the differentiation and expansion of polyfunctional T cells that are pathogenic in EAE. These data suggest that an increase in the number of Treg cells alone does not reduce the severity of EAE as there is also an increase in the number of polyfunctional encephalitogenic T cells. Furthermore, exTh17 cells from RhA patients have been shown to resist Treg cell-mediated suppression, providing a possible explanation as to how increased Treg cell numbers during EAE did not suppress the severity of disease [304].

γδ T cells can function as a bridge between the innate and adaptive immune responses. As γδ T cells do not have the same activation requirements as conventional T cells, they can be activated rapidly, and their activity can influence antigen-specific CD4 and CD8 T cell responses. In EAE, IL-1β and IL-23-activated γδ T cells provide an early source of IL-17A, which amplifies autoantigen-specific Th17 responses [169]. IFN-γ-producing γδ T cells also influence the anti-tumour immune response in the B16 murine melanoma model [305]. Infiltration of IFN-γ-producing γδ T cells promoted tumour antigen-induced CD8 T

cell responses. IFN-γ produced by both γδ T cells and NK cells increased expression of MHC-I on tumour cells which increased their immunogenicity [306]. Human Vγ9Vδ2 γδ T cells activated DCs, which in turn increased the magnitude of the antigen-specific response [307]. In the present study, IL-17A production by CD4 T cells was increased in response to treatment with anti-PD-1 during EAE. However, the effect of anti-PD-1 was reversed in TCRδ$^{-/-}$ mice. These data suggest that γδ T cells are a major target for the modulation of EAE by anti-PD-1. Previous work from the lab has demonstrated that early IL-17A plays a priming role in EAE by recruiting IL-1β-producing neutrophils and Ly6c^{hi} monocytes that induce Th17 cells [171]. Taken together, these data suggest that increasing IL-17A production by γδ T cells alone can orchestrate increased antigen-specific T cell responses that in turn enhance the severity of EAE.

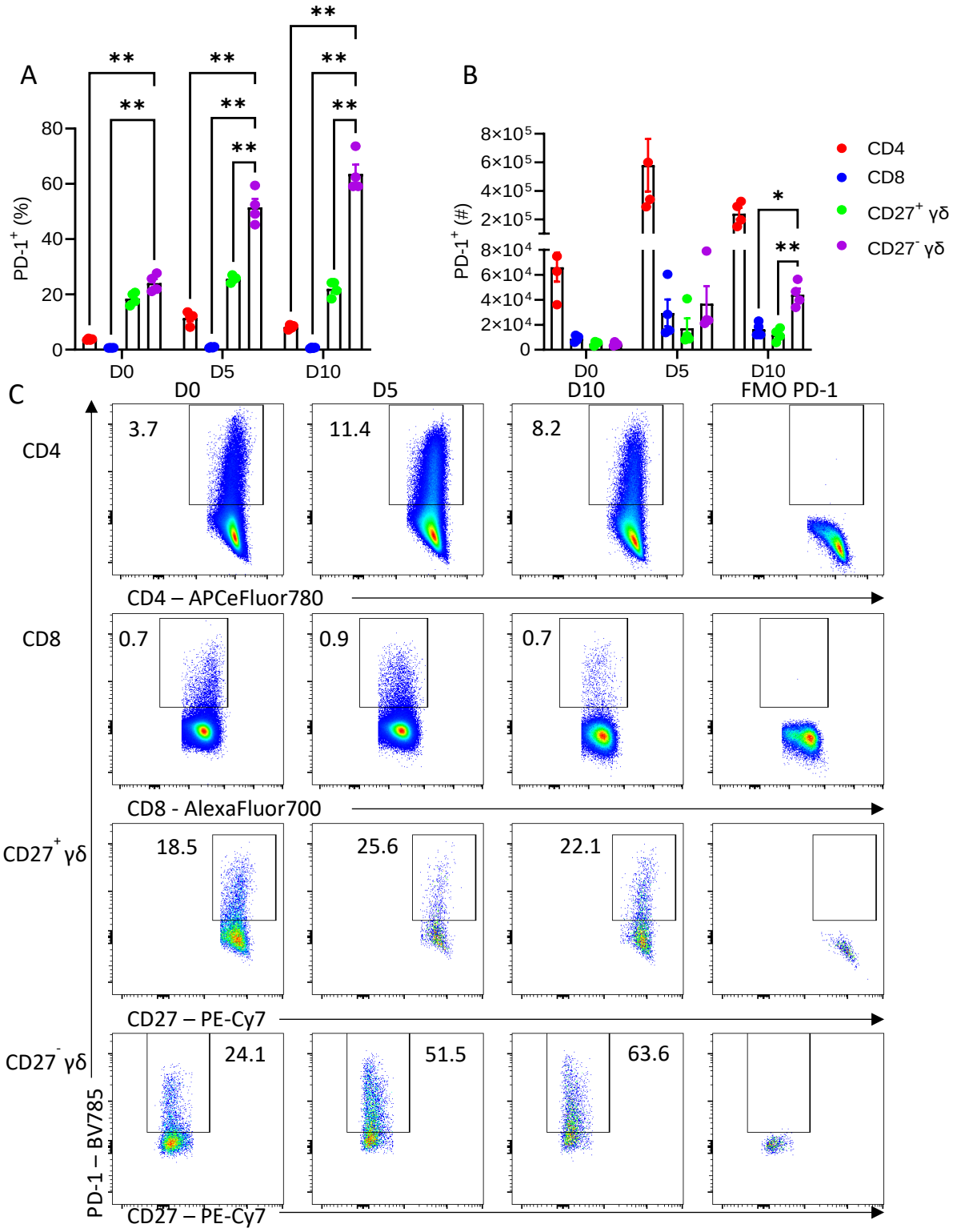

Figure 3.1 CD27$^-$ γδ T cells express the highest frequency of PD-1 in the LN throughout EAE. EAE was induced in C57BL/6J mice by s.c injection of MOG (100 µg) emulsified in CFA. Mice were injected i.p with 250 ng PT on days 0 and 2. Naïve C57BL/6J mice, or mice 5 days and 10 days post induction of EAE were sacrificed. Axillary and brachial LNs were isolated, and cells were stained for surface CD3, CD4, CD8, CD27, TCRδ, and PD-1 and analysed by flow cytometry. Cells were gated according to the gating strategy in figure 2.2.17.2. Results are (A) frequency and (B) absolute number of PD-1-expressing CD4, CD8, CD27$^+$ γδ, and CD27$^-$ γδ T cells with (C) representative FACS plots. Results are representative of two independent experiments. Data are mean ± SEM (n=4 per group). $^{**}p < 0.005$ by two-way ANOVA with Tukey's multiple comparisons test.

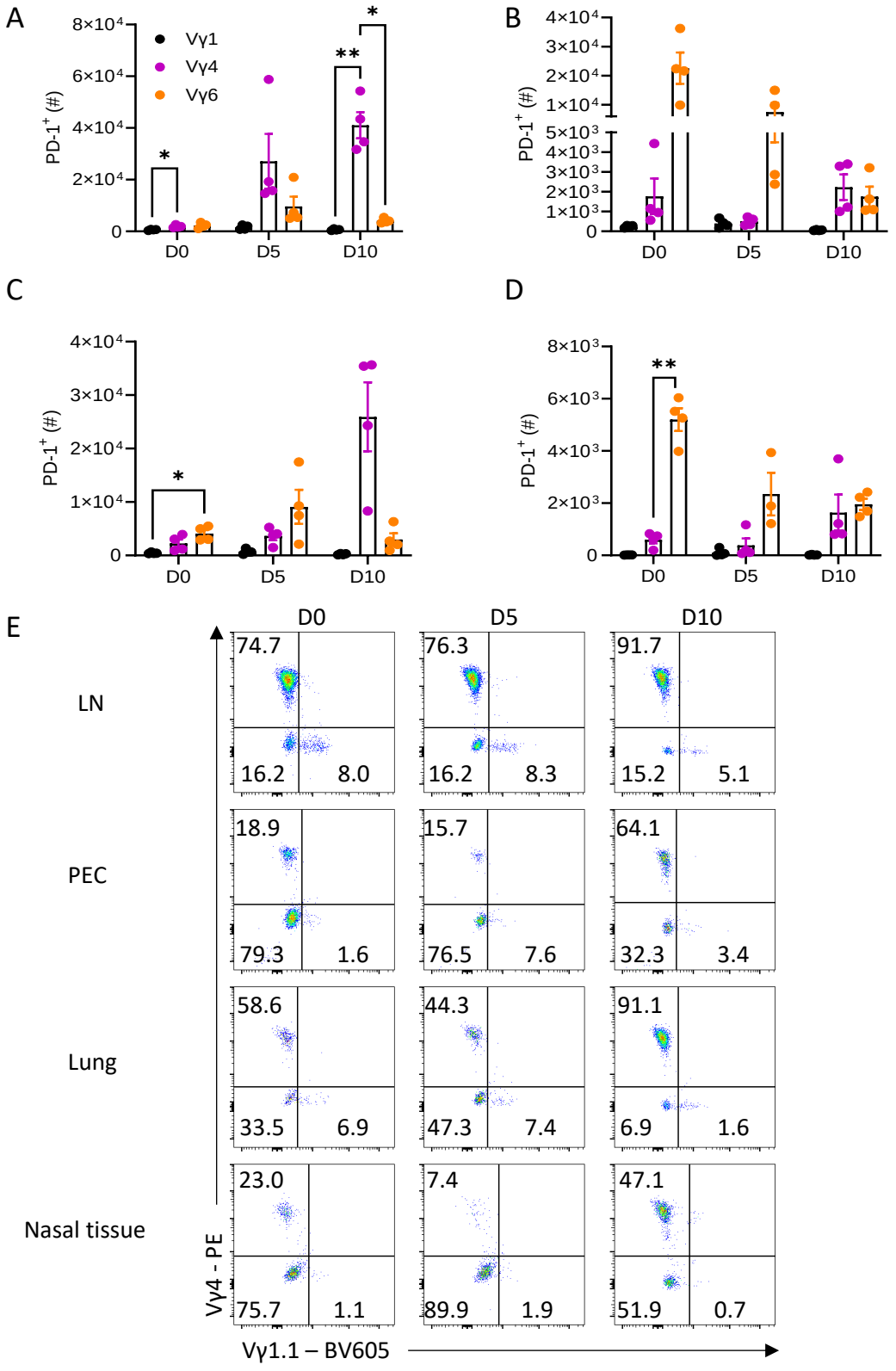

Figure 3.2 CD27$^-$ γδ T cells expressing the Vγ4 chain expand in the LN and lung during EAE. Naïve C57BL/6J mice, or mice 5 days and 10 days post induction of EAE were sacrificed. LN, PEC, lung, and nasal tissue was isolated and cell suspensions were prepared. Cell suspensions were stained for surface CD3, CD27, TCRδ, Vγ1.1, Vγ4, and PD-1 and analysed by flow cytometry. Cells were gated according to the gating strategy in figure 2.2.17.2. Results are absolute number of PD-1$^+$ CD27$^-$ γδ T cells expressing either the Vγ1.1, Vγ4 or Vγ6 (Vγ1.1$^-$Vγ4$^-$) TCR γ chain in the (A) LN, (B) PEC, (C) lung and (D) nasal tissue throughout EAE with (E) representative FACS plots. Results are representative of two independent experiments. Data are mean ± SEM (n=4 per group). * $p < 0.05$, ** $p < 0.01$ by two-way ANOVA with Tukey's multiple comparisons test.

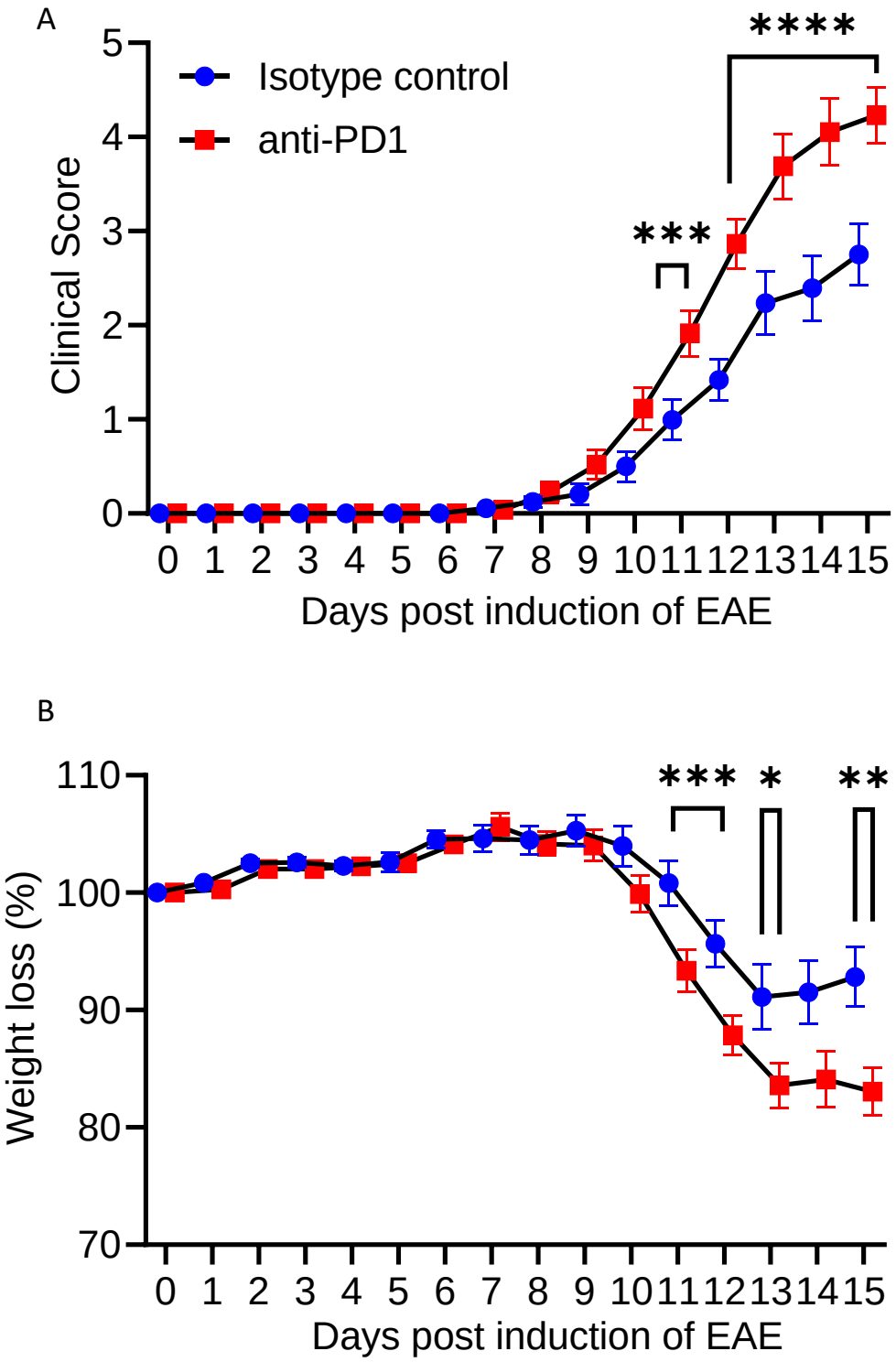

Figure 3.3 Treatment with anti-PD1 significantly increases the severity of EAE. EAE was induced in C57BL/6J mice. Mice were injected i.p with 200 µg of PD-1 neutralising antibody or IgG2a isotype control antibody on the day prior to induction of EAE and on days 2 and 5 of EAE. Mice were assessed daily for the development of EAE by (A) clinical score and (B) % weight loss. Data are mean ± SEM for n=40 mice per group combined from 6 independent experiments. *p < 0.05, **p < 0.01, ***p < 0.001, ****p < 0.0001 by two-way ANOVA with Sidak's multiple comparisons test.

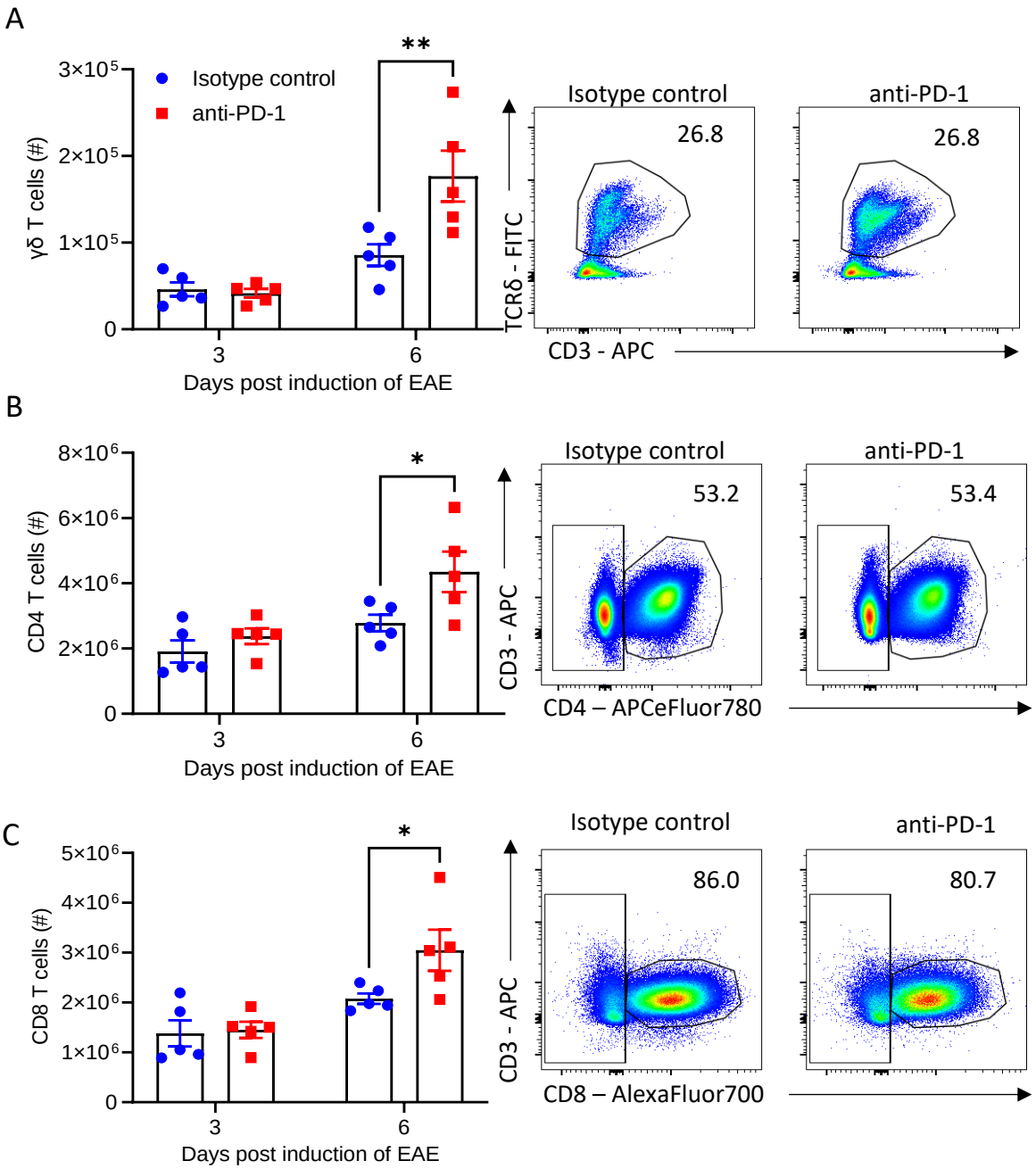

Figure 3.4 Treatment with anti-PD-1 increases the number of γδ T cells in the LN at the onset of EAE. EAE was induced in C57BL/6J mice. Mice were injected i.p with 200 µg of PD-1 neutralising antibody or IgG2a isotype control antibody on the day prior to induction of EAE and on days 2 and 5 of EAE. On days 3 and 6 post induction of EAE, mice were sacrificed, and cells were isolated from axillary and brachial LNs. Cells were stained for surface CD3, CD4, CD8, and TCRδ and analysed by flow cytometry. Results are absolute number of (A) γδ T cells, (B) CD4 T cells, and (C) CD8 T cells in the LN on days 3 and 6 post induction of EAE in isotype control versus anti-PD-1-treated mice with representative FACS plots on day 6. Results are representative of three independent experiments. Data are mean ± SEM (n=5 per group). $^{*}p < 0.05$, $^{**}p < 0.01$ by two-way ANOVA with Sidak's multiple comparisons test.

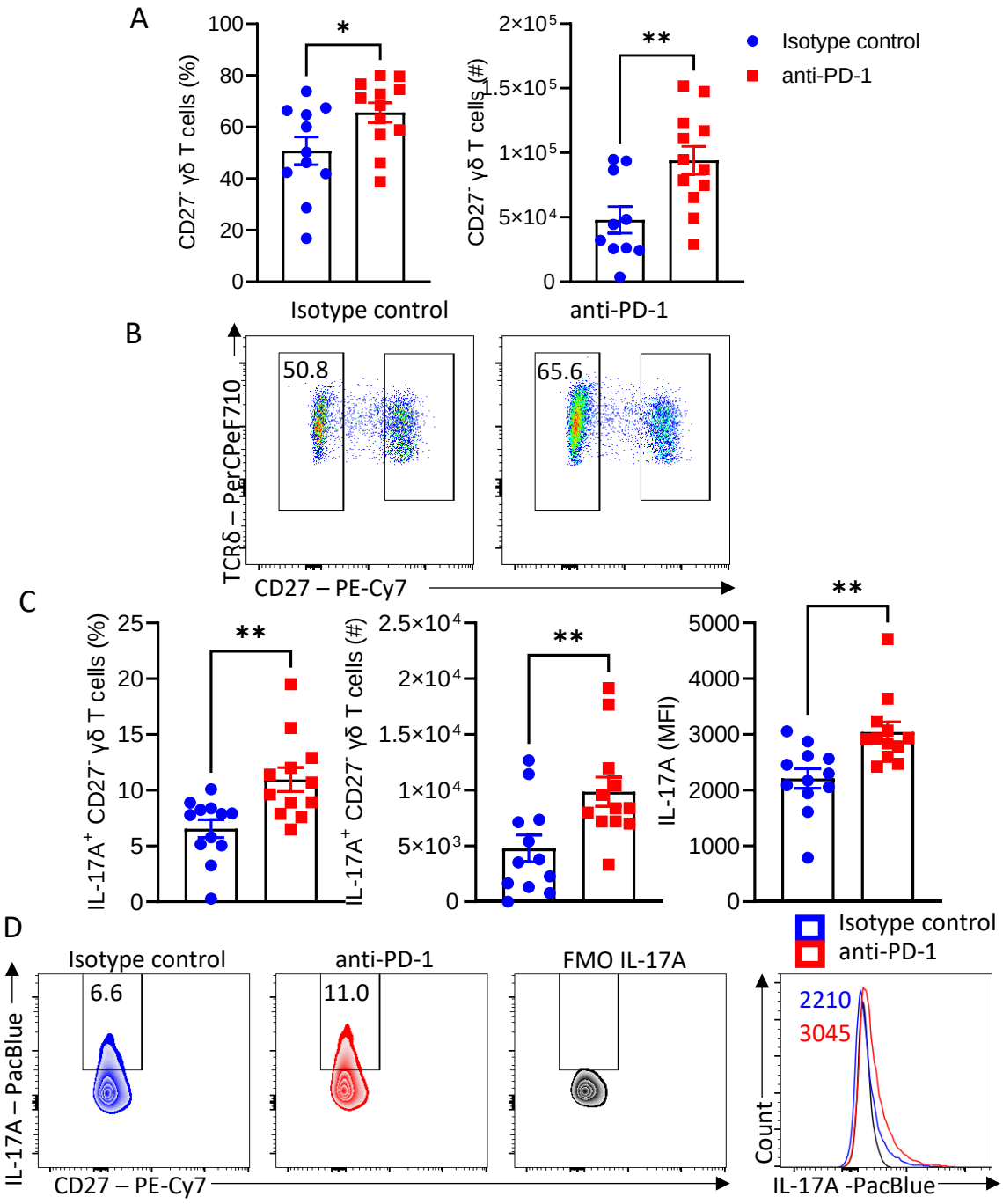

Figure 3.5 Treatment with anti-PD1 increases the number of IL-17A-producing CD27⁻ γδ T cells in the LN at the onset of EAE. EAE was induced in C57BL/6J mice. Mice were injected i.p with 200 µg of PD-1 neutralising antibody or IgG2a isotype control antibody on the day prior to induction of EAE and on days 2 and 5 of EAE. On day 6 post induction of EAE, mice were sacrificed, and cells were isolated from axillary and brachial LNs. Cells were incubated with brefeldin A for 4 hours followed by staining for surface CD3, CD27, TCRδ, and intracellular IL-17A and analysed by flow cytometry. Results are (A) frequency and absolute number of CD27⁻ γδ T cells with (B) representative FACS plots. (C) Frequency, absolute number, and MFI of IL-17A-producing CD27⁻ γδ T cells in the LN on day 6 post induction of EAE in isotype control versus anti-PD-1-treated mice with (D) representative FACS plots. Results are representative of three independent experiments. Data are mean ± SEM (n=12 per group). $^{*}p < 0.05$, $^{**}p < 0.01$ by unpaired Student's *t* test.

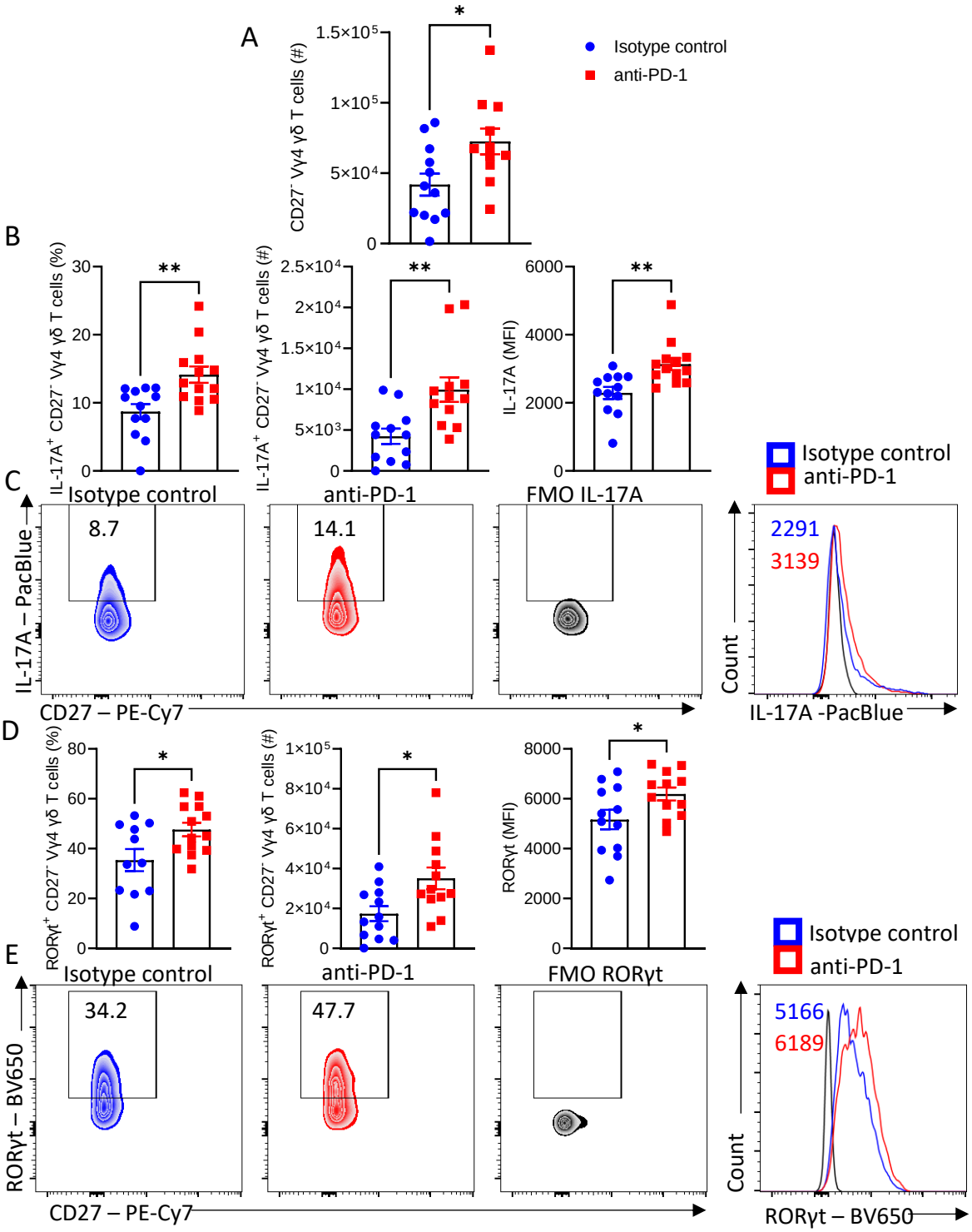

Figure 3.6 Treatment with anti-PD1 increases the number of IL-17A-producing CD27$^-$ Vγ4 γδ T cells in the LN at the onset of EAE. EAE was induced in C57BL/6J mice. Mice were injected i.p with 200 µg of PD-1 neutralising antibody or IgG2a isotype control antibody on the day prior to induction of EAE and on days 2 and 5 of EAE. On day 6 post induction of EAE, mice were sacrificed, and cells were isolated from axillary and brachial LNs. Cells were incubated with brefeldin A for 4 hours followed by staining for surface CD3, CD27, TCRδ, Vγ4, and intracellular IL-17A and analysed by flow cytometry. Results are (A) absolute number of CD27$^-$ Vγ4 γδ T cells, (B) frequency, absolute number, and MFI of IL-17A-producing CD27$^-$ Vγ4 γδ T cells with (C) representative FACS plots. (D) Frequency, absolute number, and MFI of RORγt-expressing CD27$^-$ Vγ4 γδ T cells in the LN in isotype control versus anti-PD-1-treated mice with (E) representative FACS plots. Results are representative of three independent experiments. Data are mean ± SEM (n=12 per group). $^*p < 0.05$, $^{**}p < 0.01$ by unpaired Student's *t* test.

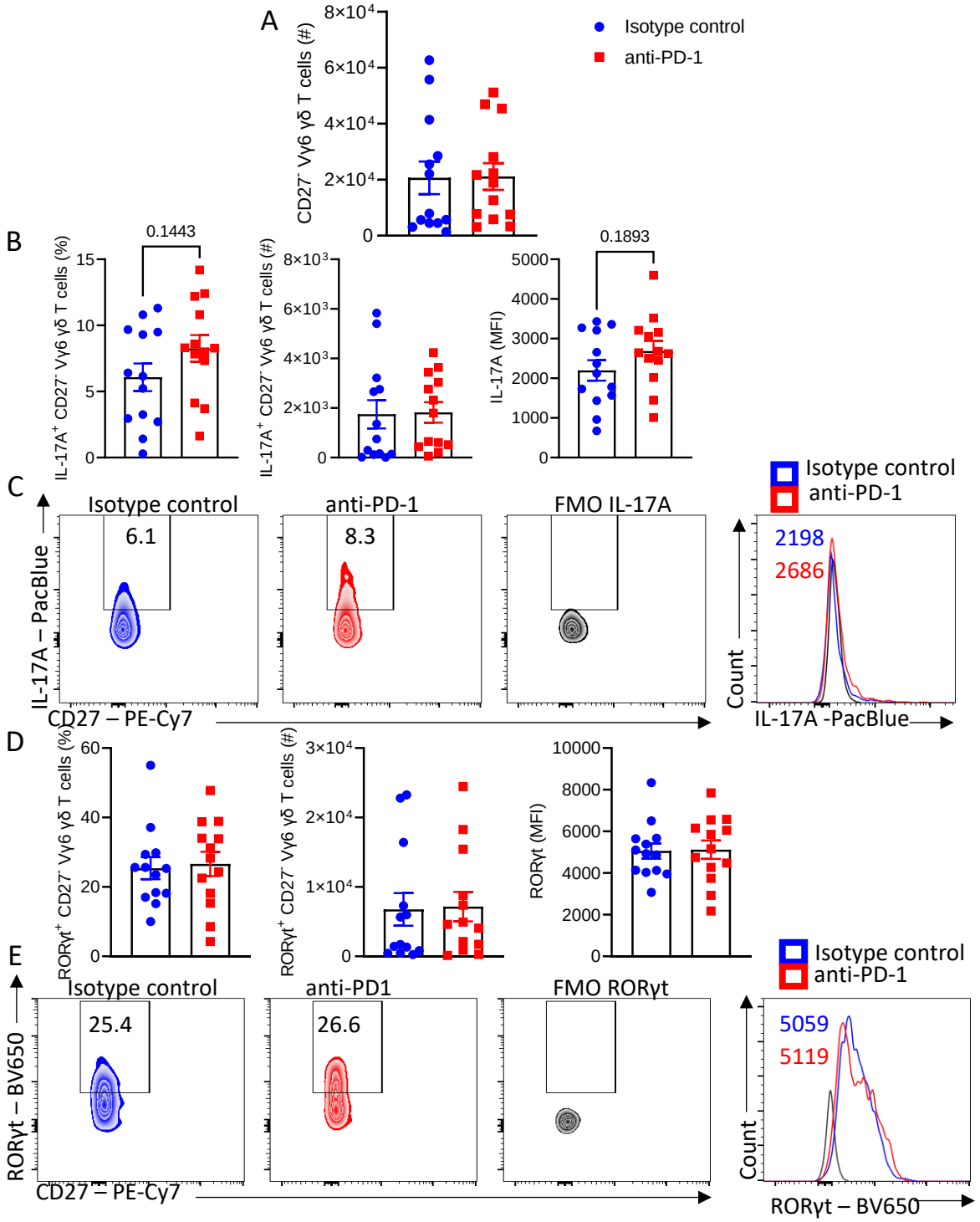

Figure 3.7 Blocking PD-1 signalling does not affect CD27⁻ Vγ6 γδ T cells in the LN at the onset of EAE. EAE was induced in C57BL/6J mice. Mice were injected i.p with 200 µg of PD-1 neutralising antibody or IgG2a isotype control antibody on the day prior to induction of EAE and on days 2 and 5 of EAE. On day 6 post induction of EAE, mice were sacrificed, and cells were isolated from axillary and brachial LNs. Cells were incubated with brefeldin A for 4 hours followed by staining for surface CD3, CD27, TCRδ, Vγ1.1, Vγ4, and intracellular IL-17A and analysed by flow cytometry. Results are (A) absolute number of CD27⁻ Vγ6 γδ T cells, (B) frequency, absolute number, and MFI of IL-17A-producing CD27⁻ Vγ6 γδ T cells with (C) representative FACS plots. (D) Frequency, absolute number, and MFI of RORγt-expressing CD27⁻ Vγ6 γδ T cells in the LN in isotype control versus anti-PD-1-treated mice with (E) representative FACS plots. Results are representative of three independent experiments. Data are mean ± SEM (n=12 per group). $p > 0.05$ was considered not significant by unpaired Student's *t* test.

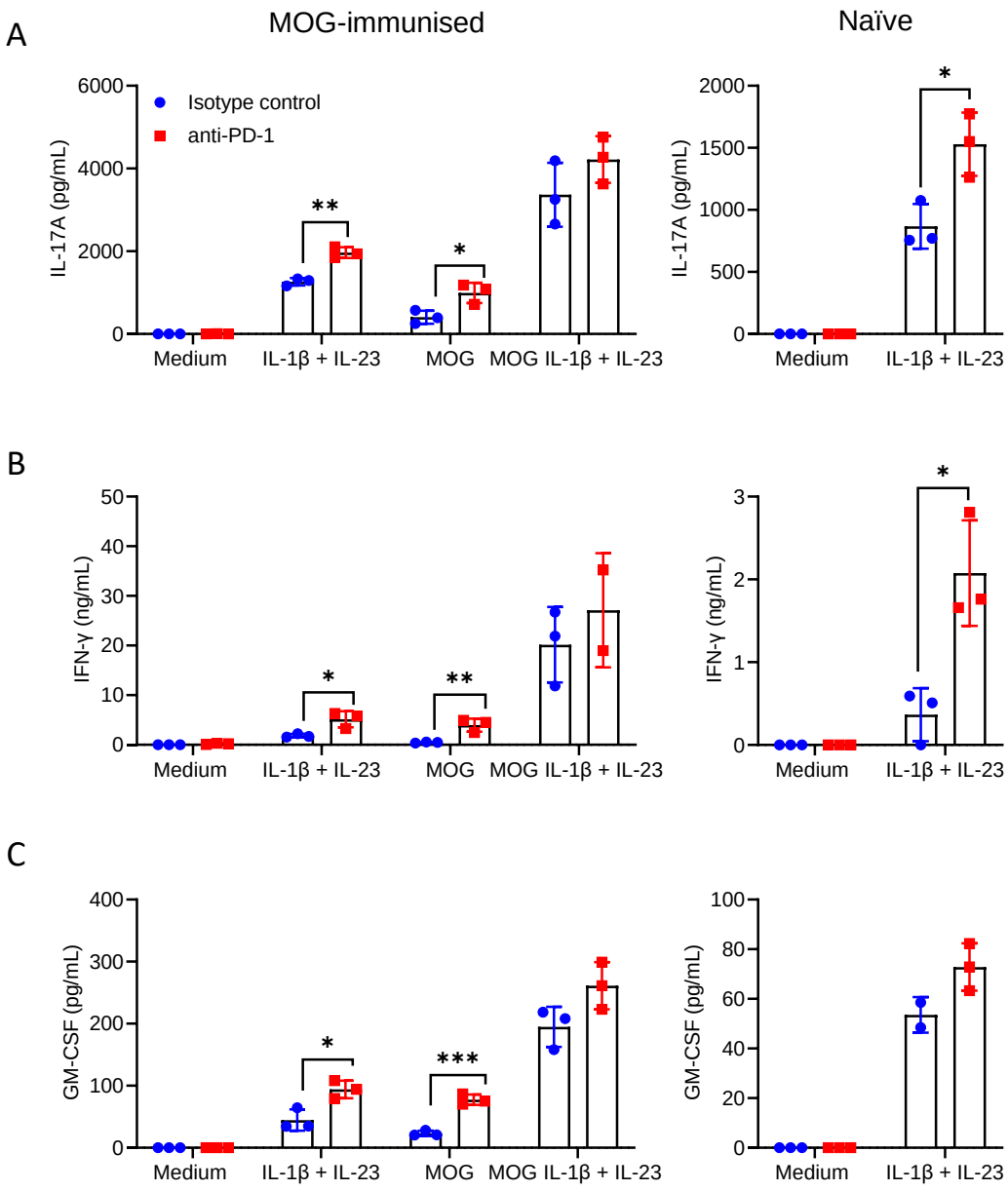

Figure 3.8 Anti-PD-1 treatment increases IL-1β+IL-23-induced IL-17A. C57BL/6J mice were immunised with MOG emulsified in CFA. Axillary, brachial, inguinal LNs and spleens were harvested either from naïve mice or 10 days after immunisation and cultured with MOG (100 µg/mL), IL-1β and IL-23 (10 ng/mL) in the presence or absence of anti-PD-1 or isotype control antibody (10 µg/mL). Supernatants were collected after 72 hours and concentrations of (A) IL-17A, (B) IFN-γ and (C) GM-CSF were quantified by ELISA. Data are shown as mean ± SD. $^{*}p < 0.05$, $^{**}p < 0.01$ $^{***}p < 0.001$ by unpaired Student's *t* test isotype control versus anti-PD-1.

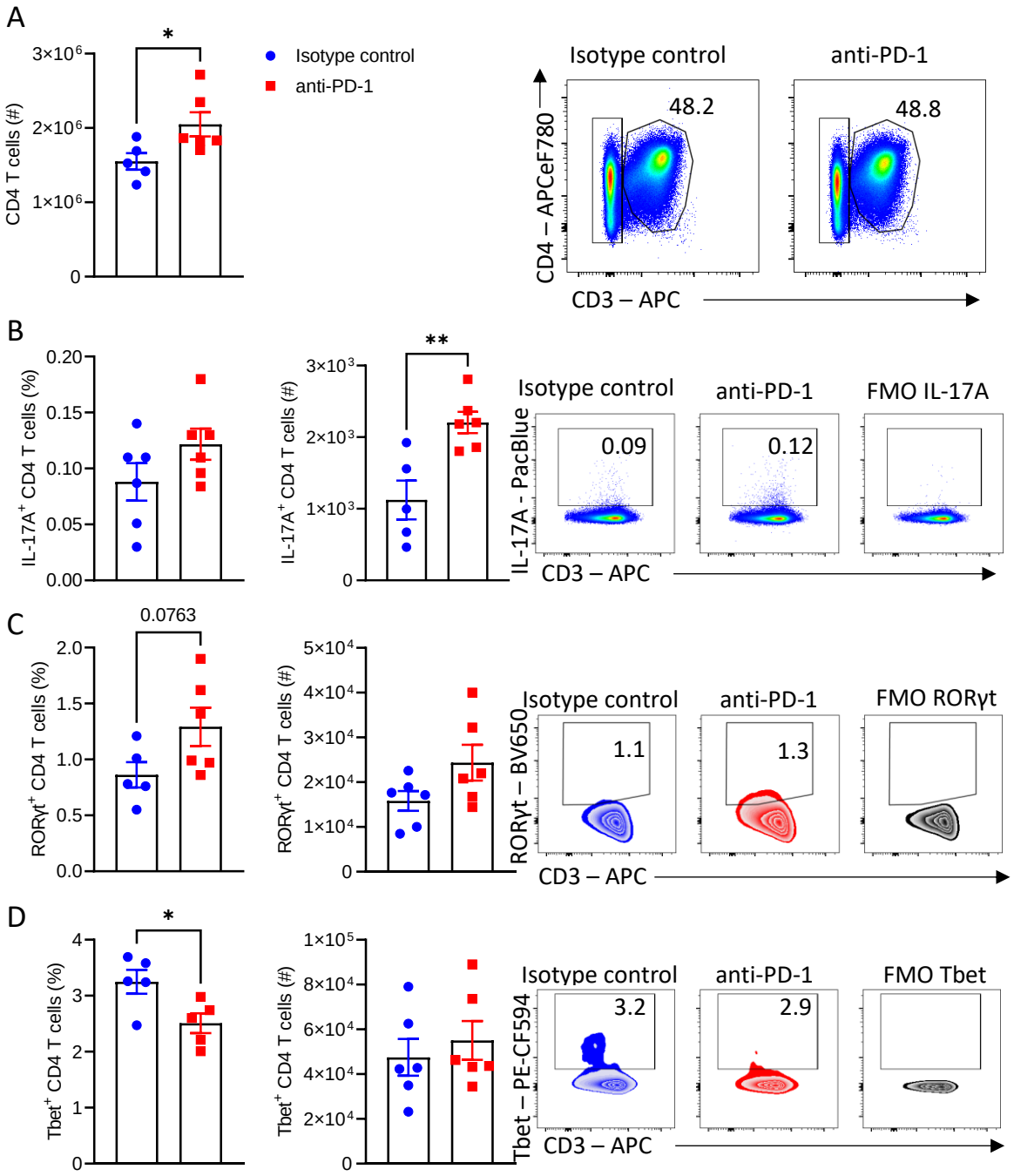

Figure 3.9 Treatment with PD1 neutralising antibody increases the absolute number of IL-17A-producing CD4 T cells in the LN during EAE. EAE was induced in C57BL/6J mice. Mice were injected i.p with 200 µg of PD-1 neutralising antibody or IgG2a isotype control antibody on the day prior to induction of EAE and on days 2 and 5 of EAE. On day 9 post induction of EAE, mice were sacrificed, and cells were isolated from the LN. Cells were incubated with brefeldin A for 4 hours followed by staining for surface CD3, CD4, and intracellular IL-17A, RORγ,t and Tbet and analysed by flow cytometry. Results are (A) absolute number of CD4 T cells in the LN on day 9 of EAE. Frequency and absolute number of (B) IL-17A-producing (C) RORγt-expressing and (D) Tbet-expressing CD4 T cells with representative FACS plots. Results are representative of three independent experiments. Data are mean ± SEM (n=6 per group). $^{*}p < 0.05$, $^{**}p < 0.01$ by unpaired Student's *t* test.

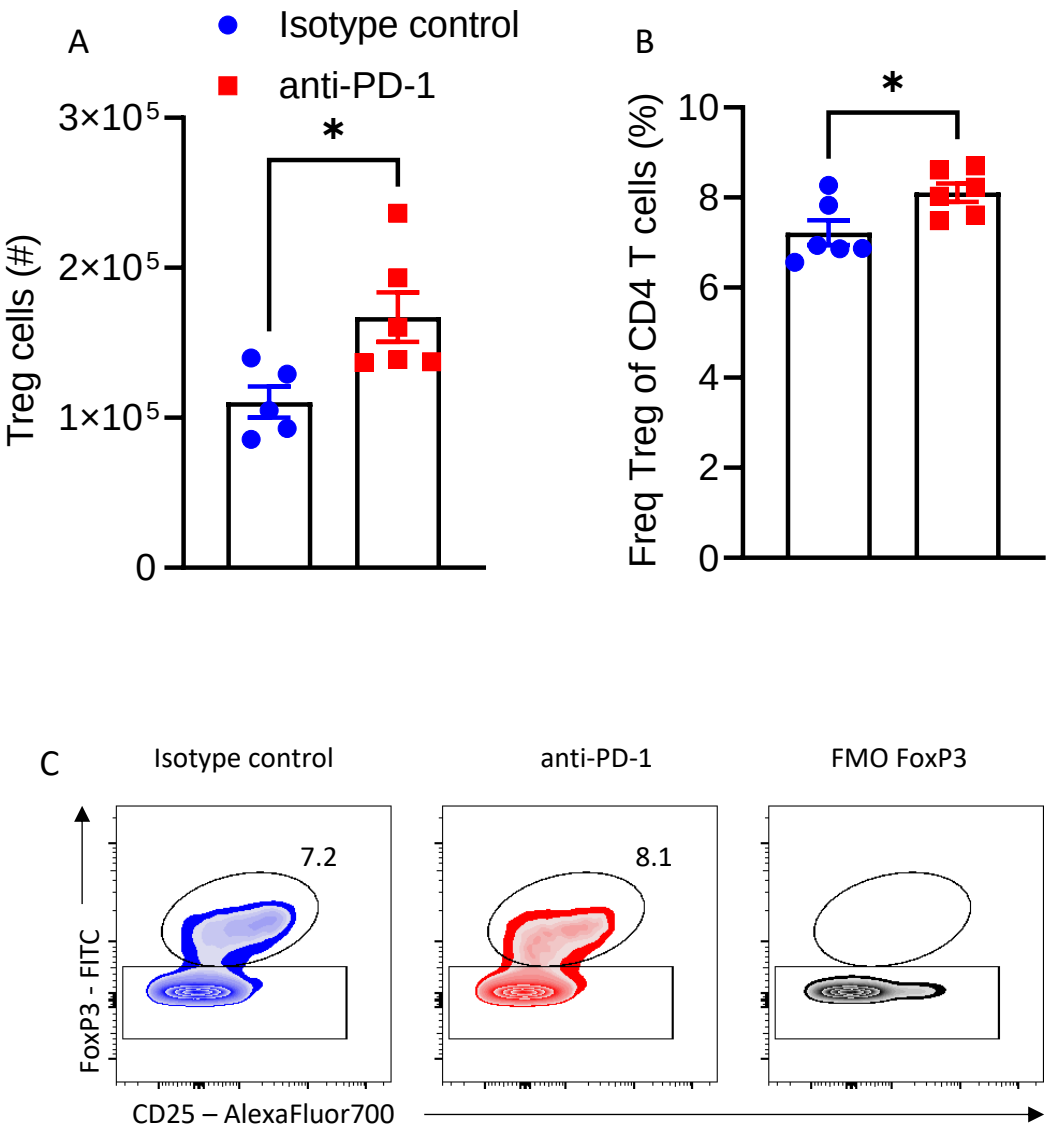

Figure 3.10 Anti-PD-1 increases the absolute number of Treg cells in the LN at the onset of EAE. EAE was induced in C57BL/6J mice. Mice were injected i.p with 200 µg of PD-1 neutralising antibody or IgG2a isotype control antibody on the day prior to induction of EAE and on days 2 and 5 of EAE. On day 9 post induction of EAE, mice were sacrificed, and axillary and brachial LNs were isolated. Cells were incubated with brefeldin A for 4 hours followed by staining for surface CD3, CD4, CD25, and intracellular FoxP3 and analysed by flow cytometry. Results are (A) frequency and (B) absolute number of Treg cells in the LN on day 9 of EAE with (C) representative FACS plots. Results are representative of three independent experiments. Data are mean ± SEM (n=6 per group). $^{*}p < 0.05$ by unpaired Student's *t* test.

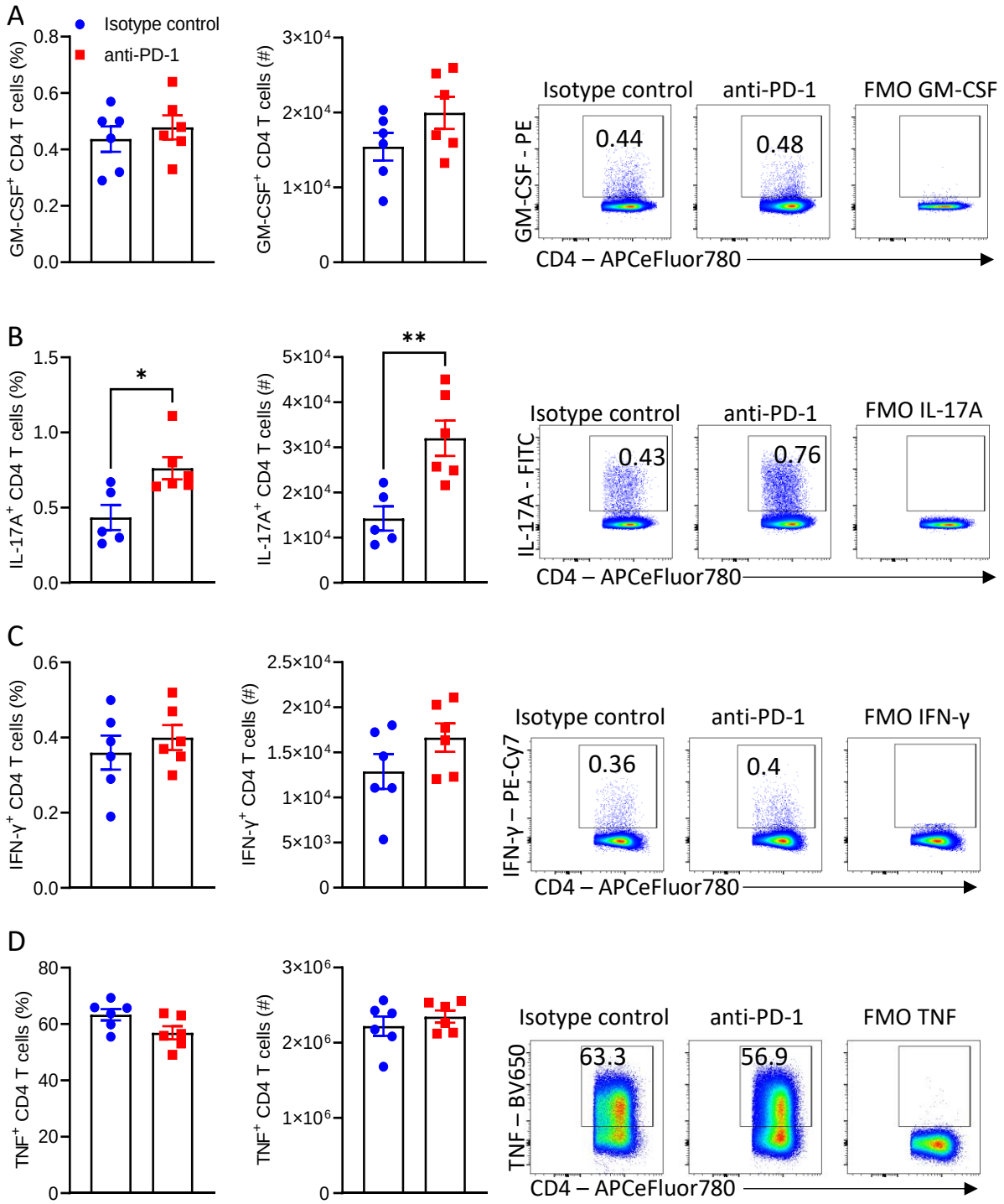

Figure 3.11 Treatment with anti-PD1 increases the absolute number of IL-17A-producing CD4 T cells in the LN during EAE. EAE was induced in C57BL/6J mice. Mice were injected i.p with 200 µg of PD-1 neutralising antibody or IgG2a isotype control antibody on the day prior to induction of EAE and on days 2 and 5 of EAE. On day 9 post induction of EAE, mice were sacrificed, and cells were isolated from the axillary and brachial LNs. Cells were incubated with PMA, ionomycin and brefeldin A for 4 hours followed by staining for surface CD3, CD4, and intracellular GM-CSF, IL-17A, IFN-γ, and TNF and analysed by flow cytometry. Results are the frequency and absolute number of (A) GM-CSF-producing, (B) IL-17A-producing, (C) IFN-γ-producing, and (D) TNF-producing CD4 T cells with representative FACS plots. Results are representative of three independent experiments. Data are mean ± SEM (n=6 per group). $^{*}p < 0.05$, $^{**}p < 0.01$ by unpaired Student's *t* test.

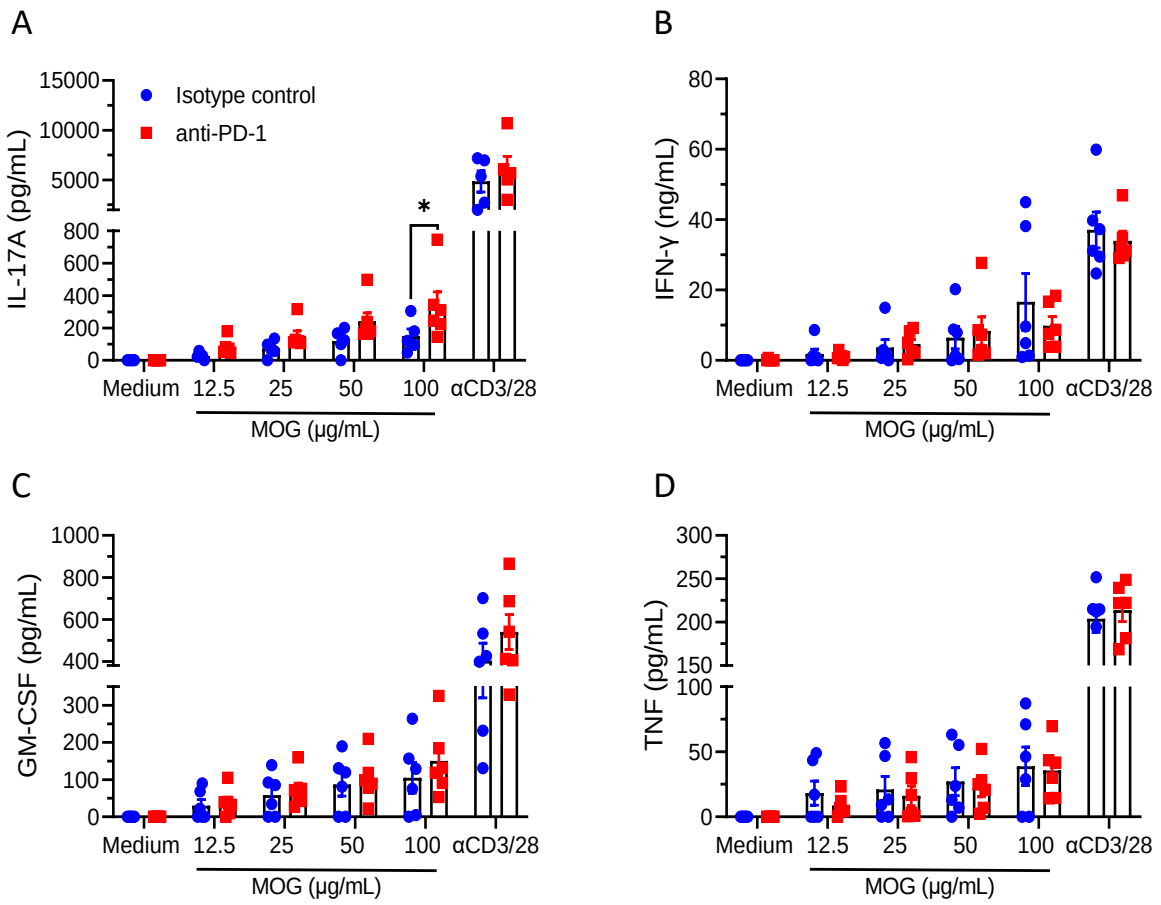

Figure 3.12 MOG-specific IL-17A production from spleen and LN is increased in anti-PD-1-treated mice. EAE was induced in C57BL/6J mice. Mice were injected i.p with 200 μg of PD-1 neutralising antibody or IgG2a isotype control antibody on the day prior to induction of EAE and on days 2 and 5 of EAE. On day 9, mice were sacrificed, and spleen and LN cells were harvested. Cells were re-stimulated *in vitro* with MOG at increasing concentrations (12.5, 25, 50, 100 μg/mL) or with anti-CD3 and anti-CD28 (1 μg/mL). After 72 hours, supernatants were collected and (A) IL-17A, (B) IFN-γ, (C) GM-CSF, and (D) TNF production was measured by ELISA. Data are representative of two independent experiments. Data are mean ± SEM (n=6 per group). $^{*}p < 0.05$ by two-way ANOVA with Sidak's multiple comparisons test.

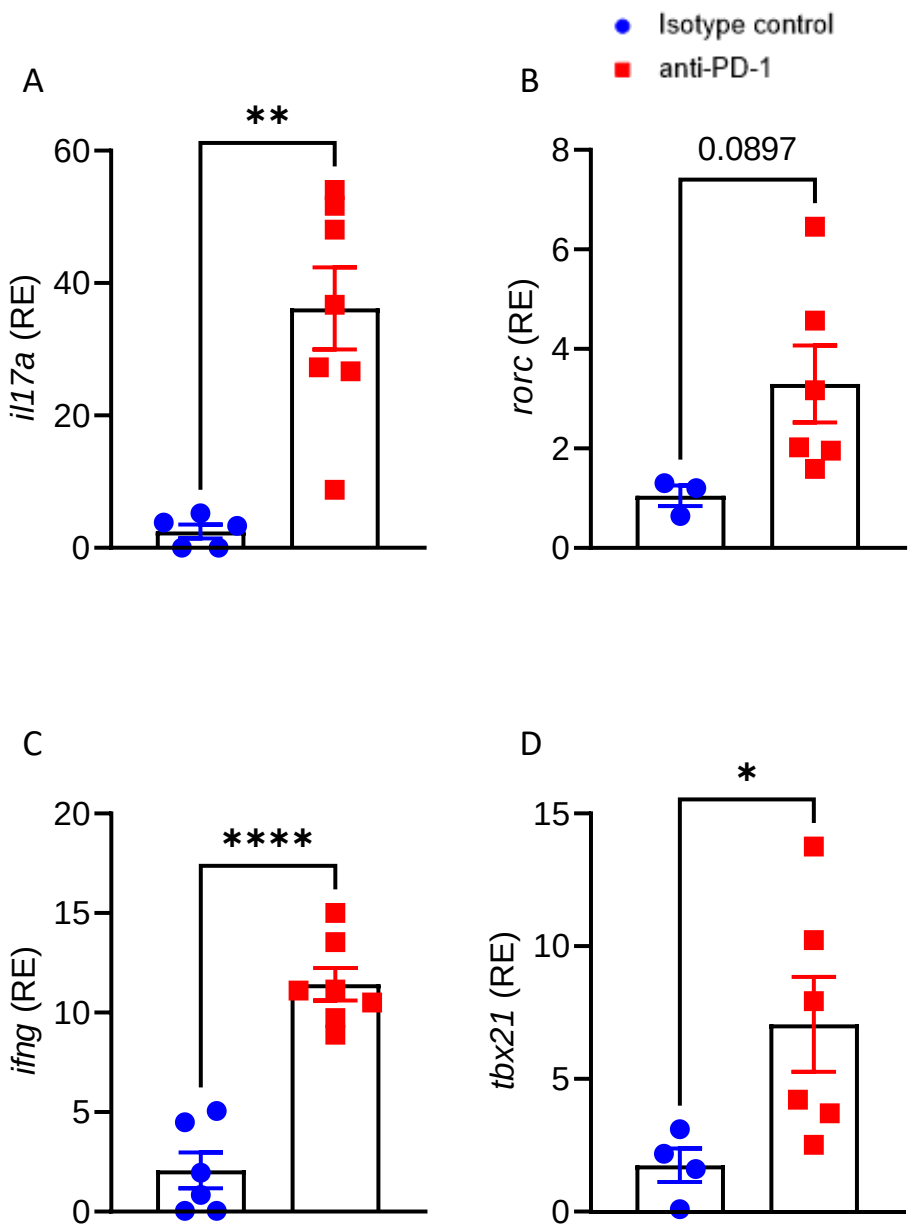

Figure 3.13 Treatment with anti-PD-1 significantly increases *il17a* and *ifng* gene expression in the spinal cord at the peak of EAE. EAE was induced in C57BL/6J mice. Mice were injected i.p with 200 µg of PD-1 neutralising antibody or IgG2a isotype control antibody on the day prior to induction of EAE and on days 2 and 5 of EAE. On day 12 post induction of EAE, mice were sacrificed, and perfused with PBS prior to harvesting of the spinal cord. (A) i*l17a*, (B) *rorc*, (C) *ifng* and (D) *tbx21* mRNA expression was measured by Rt-PCR normalized to 18S rRNA and relative to isotype control-treated mice. Results are representative of two independent experiments. Data are mean ± SEM (n=7 per group). $^{*}p < 0.05$, $^{**}p < 0.01$, $^{****}p < 0.0001$ by unpaired Student's *t* test.

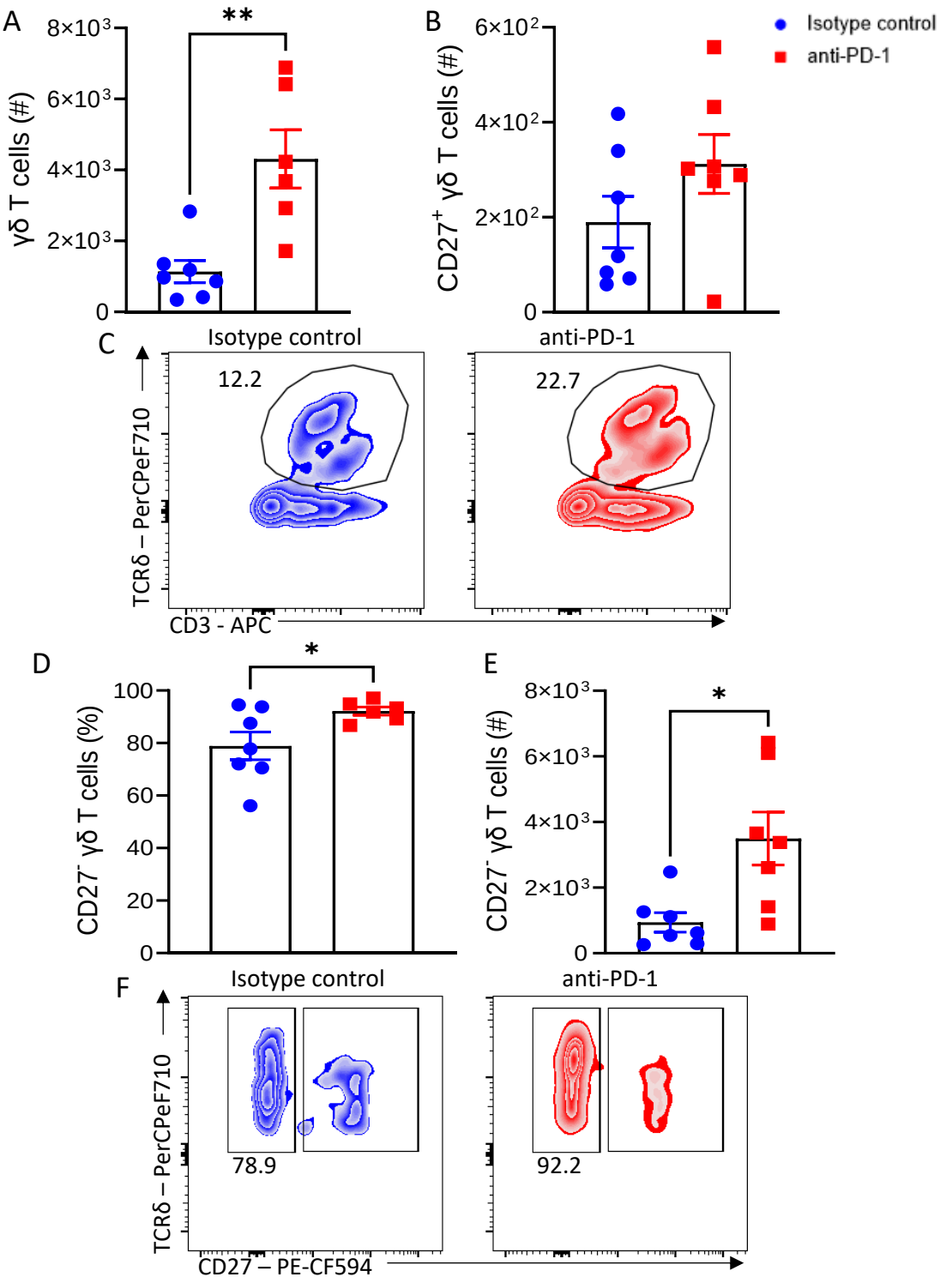

Figure 3.14 Treatment with anti-PD1 significantly increases expansion of CD27⁻ γδ T cells in the brain at the peak of EAE. EAE was induced in C57BL/6J mice. Mice were injected i.p with 200 µg of PD-1 neutralising antibody or IgG2a isotype control antibody on the day prior to induction of EAE and on days 2 and 5 of EAE. On day 12 post induction of EAE, mice were sacrificed and perfused with PBS prior to harvesting the brain. Mononuclear cells were isolated from the brain and stained for surface CD3, CD27, and TCRδ followed by analysis by flow cytometry. Immune populations were gated according to the gating strategy outlined in figure 2.2.17.4. Results are absolute number of (A) γδ T cells and (B) CD27⁺ γδ T cells with (C) representative FACS plots. (D) Frequency of γδ T cells that are CD27⁻ and (E) absolute number of CD27⁻ γδ T cells with (F) representative FACS plots. Results are representative of two independent experiments. Data are mean ± SEM (n=7 per group). *p < 0.05, **p < 0.01, by unpaired Student's *t* test.

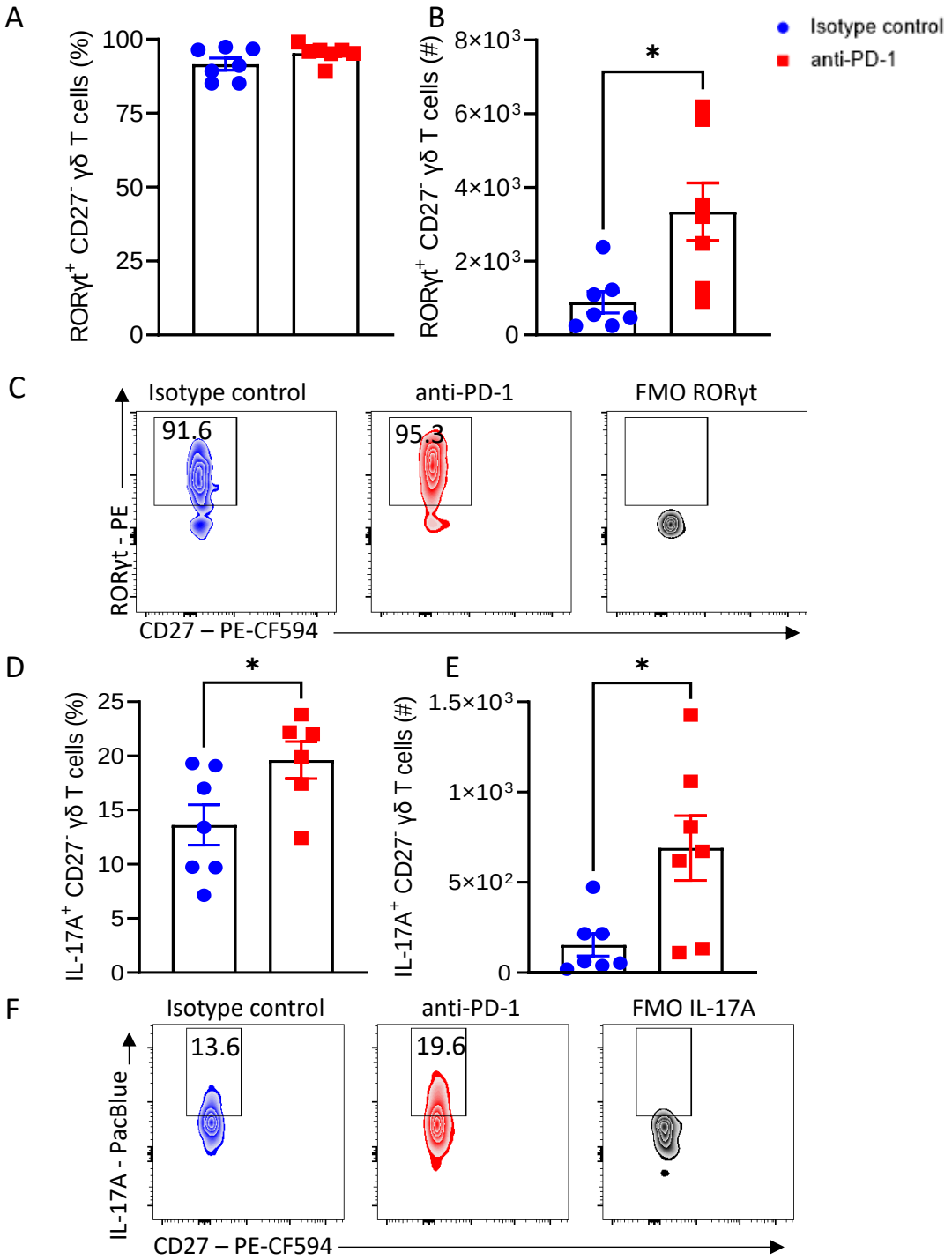

Figure 3.15 Treatment with anti-PD1 significantly increases expansion of RORγt-expressing and IL-17A-producing CD27⁻ γδ T cells in the brain at the peak of EAE. EAE was induced in C57BL/6J mice. Mice were injected i.p with 200 µg of PD-1 neutralising antibody or IgG2a isotype control antibody on the day prior to induction of EAE and on days 2 and 5 of EAE. On day 12 post induction of EAE, mice were sacrificed and perfused with PBS prior to harvesting the brain. Mononuclear cells were isolated from the brain and incubated with brefeldin A for 4 hours. Cells were stained for surface CD3, CD27, TCRδ and intracellular RORγt and IL-17A followed by analysis by flow cytometry. Results are (A) frequency and (B) absolute number of RORγt-expressing γδ T cells with (C) representative FACS plots. (D) Frequency and (E) absolute number of IL-17A-producing CD27⁻ γδ T cells with (F) representative FACS plots. Results are representative of two independent experiments. Data are mean ± SEM (n=7 per group). *p < 0.05, by unpaired Student's *t* test.

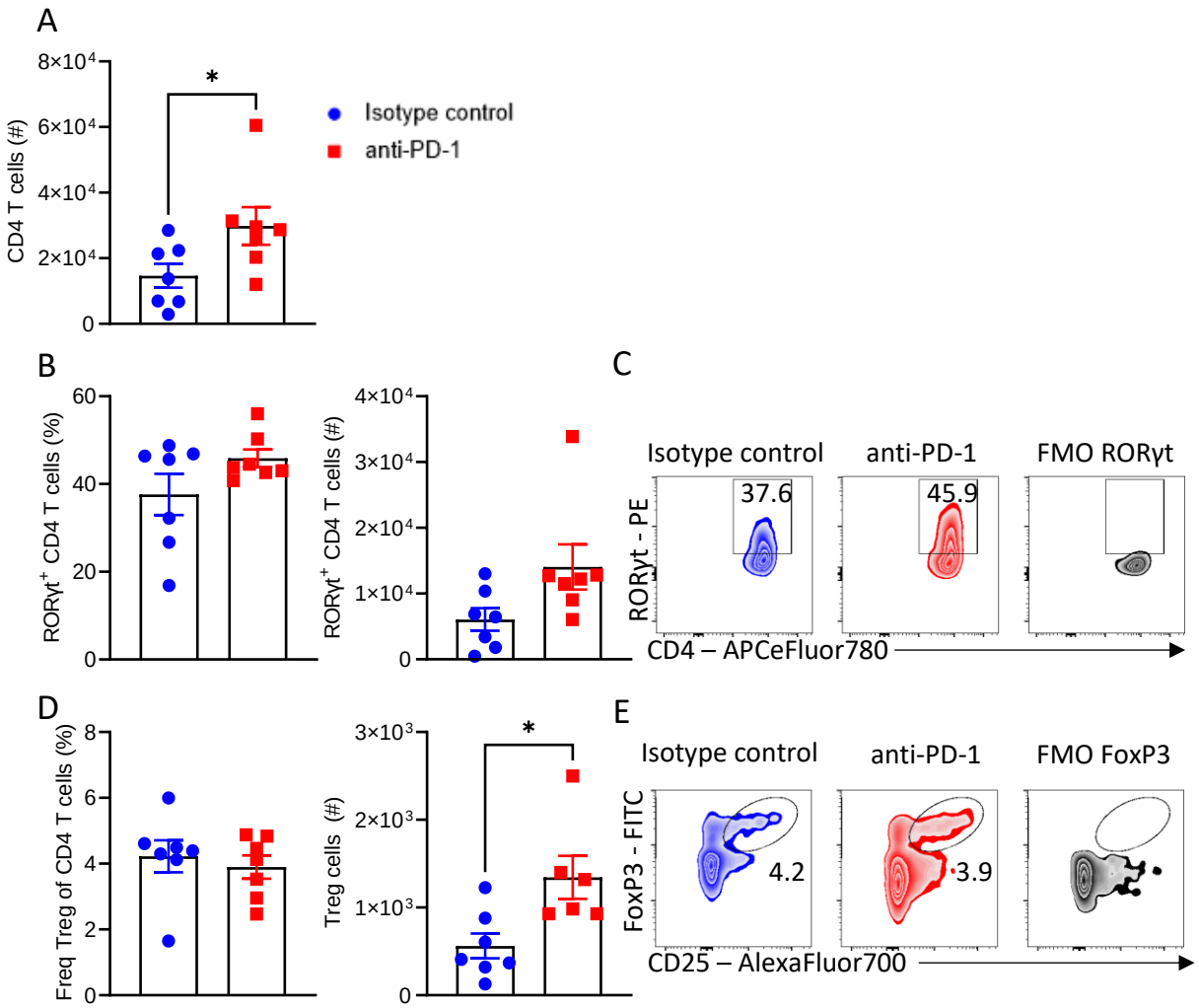

Figure 3.16 Treatment with anti-PD1 significantly increases the number of CD4 T cells and CD4 Treg cells in the brain at the peak of EAE. EAE was induced in C57BL/6J mice. Mice were injected i.p with 200 µg of PD-1 neutralising antibody or IgG2a isotype control antibody on the day prior to induction of EAE and on days 2 and 5 of EAE. On day 12 post induction of EAE, mice were sacrificed and perfused with PBS prior to harvesting the brain. Mononuclear cells were isolated from the brain and incubated with brefeldin A for 4 hours. Cells were stained for surface CD3, CD4, CD25, and intracellular RORγt, and FoxP3 followed by analysis by flow cytometry. Results are (A) absolute number of CD4 T cells and (B) frequency, and absolute number of RORγt-expressing CD4 T cells with (C) representative FACS plots. (D) Frequency and absolute number of Treg cells with (E) representative FACS plots. Results are representative of two independent experiments. Data are mean ± SEM (n=7 per group). *p < 0.05, by unpaired Student's *t* test.

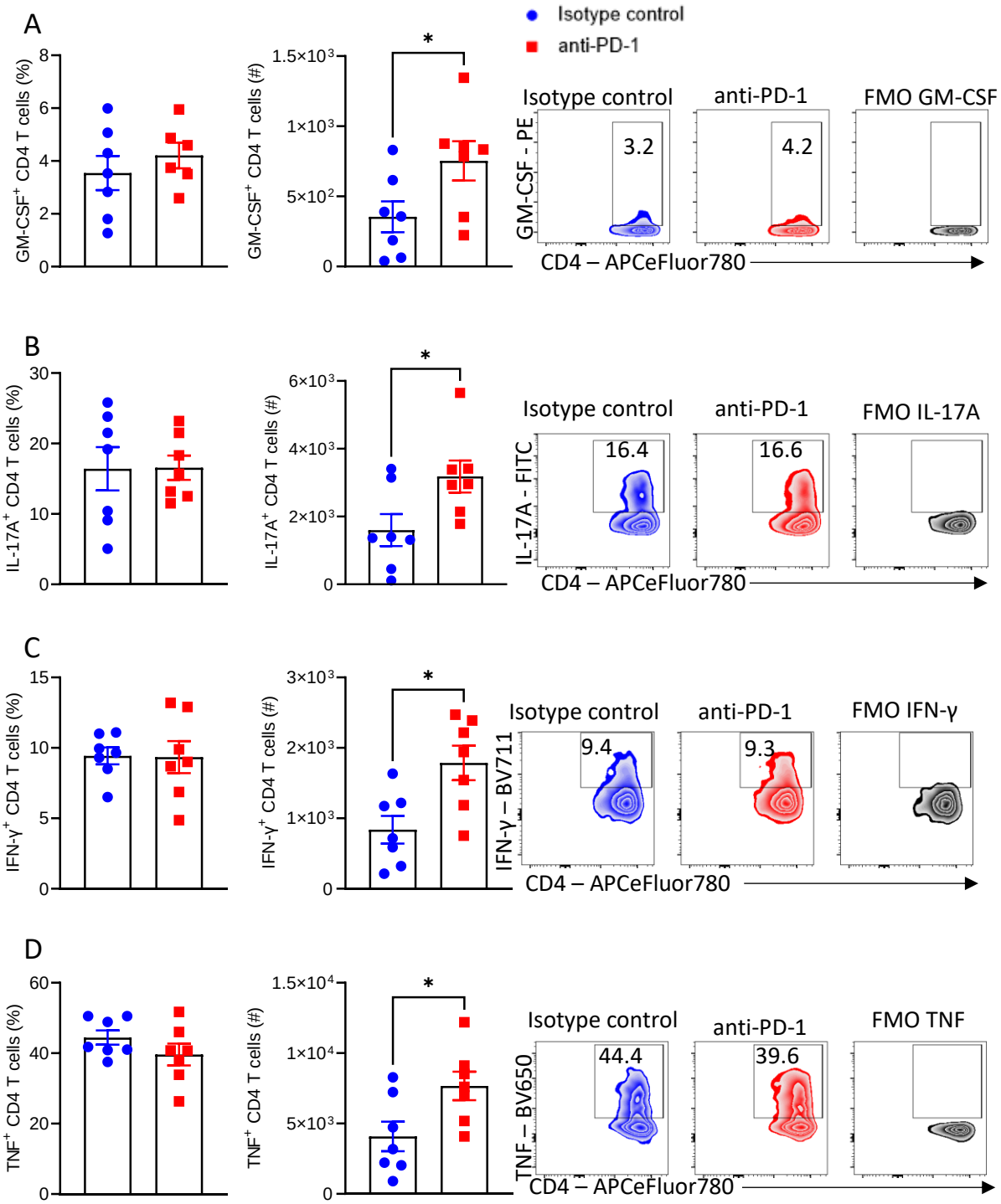

Figure 3.17 Treatment with anti-PD1 increases the absolute number of cytokine producing CD4 T cells in the brain at the peak of EAE. EAE was induced in C57BL/6J mice. Mice were injected i.p with 200 µg of PD-1 neutralising antibody or IgG2a isotype control antibody on the day prior to the induction of EAE and on days 2 and 5 of EAE. On day 12 post induction of EAE, mice were sacrificed, and perfused with PBS prior to harvesting the brain. Mononuclear cells were isolated from the brain and incubated with PMA, ionomycin, and brefeldin A for 4 hours followed by staining for surface CD3, CD4, and intracellular GM-CSF, IL-17A, IFN-γ, and TNF and analysed by flow cytometry. Results are frequency and absolute number of (A) GM-CSF-producing, (B) IL-17A-producing, (C) IFN-γ-producing, and (D) TNF-producing CD4 T cells with representative FACS plots. Results are representative of three independent experiments. Data are mean ± SEM (n=7 per group) $^{*}p < 0.05$ by unpaired Student's *t* test.

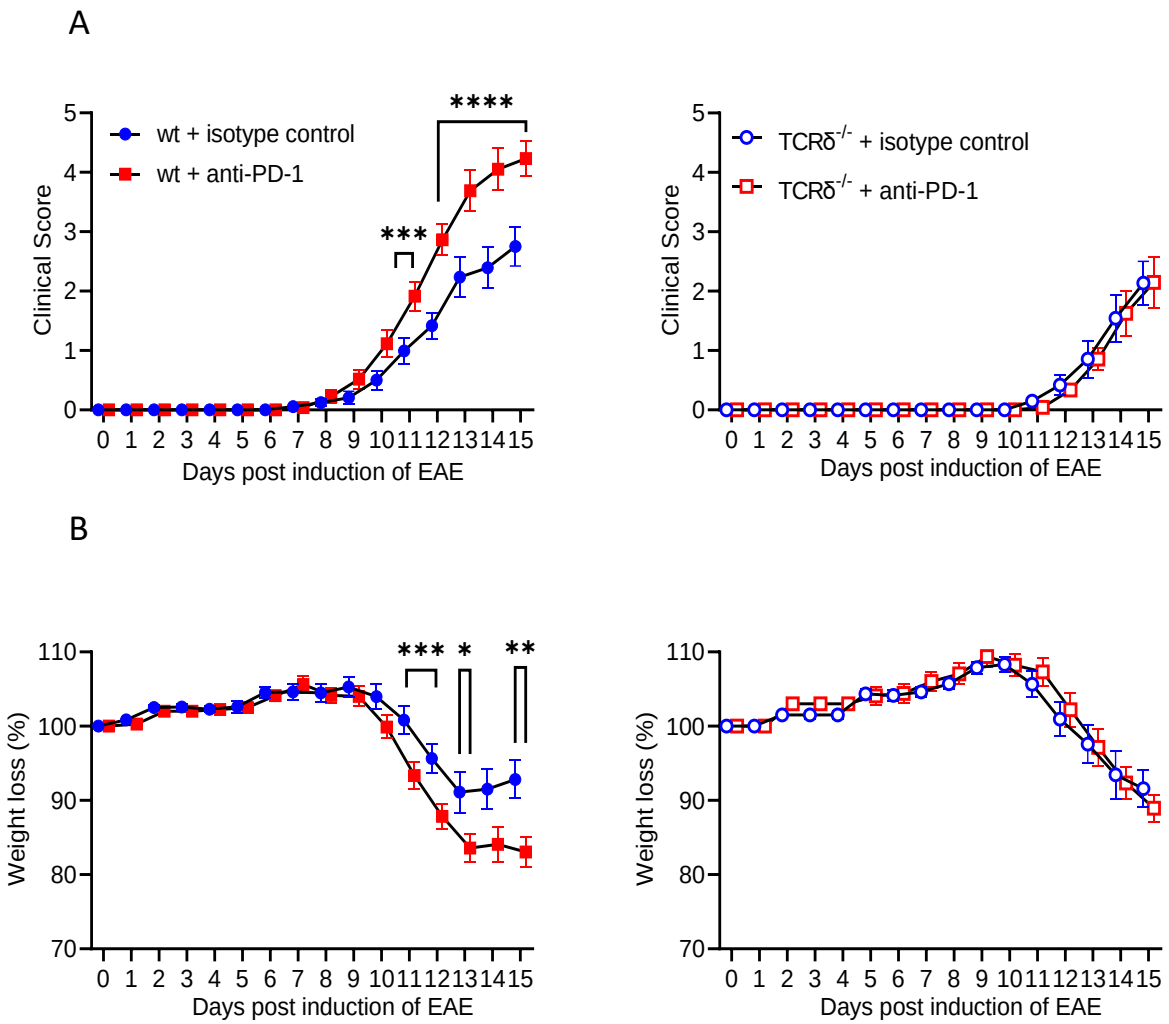

Figure 3.18 Treatment with anti-PD1 fails to increase EAE disease severity in mice that lack γδ T cells. EAE was induced in WT and TCRδ$^{-/-}$ mice by s.c injection with MOG emulsified in CFA. Mice were injected i.p with 250 ng PT on day 0. Mice were injected i.p with 200 µg of PD-1 neutralising antibody or IgG2a isotype control antibody on the day prior to induction of EAE and on days 2 and 5 of EAE. Mice were assessed daily for the development of EAE by clinical score and % weight loss. Results are (A) clinical score and (B) % weight loss of WT and TCRδ$^{-/-}$ mice treated with either isotype control or anti-PD-1 antibody during EAE. Data are mean ± SEM for n=12 mice per group combined from 2 independent experiments. *p < 0.05, **p < 0.005, ***p < 0.001, ****p < 0.0001 by two-way ANOVA with Sidak's multiple comparisons test.

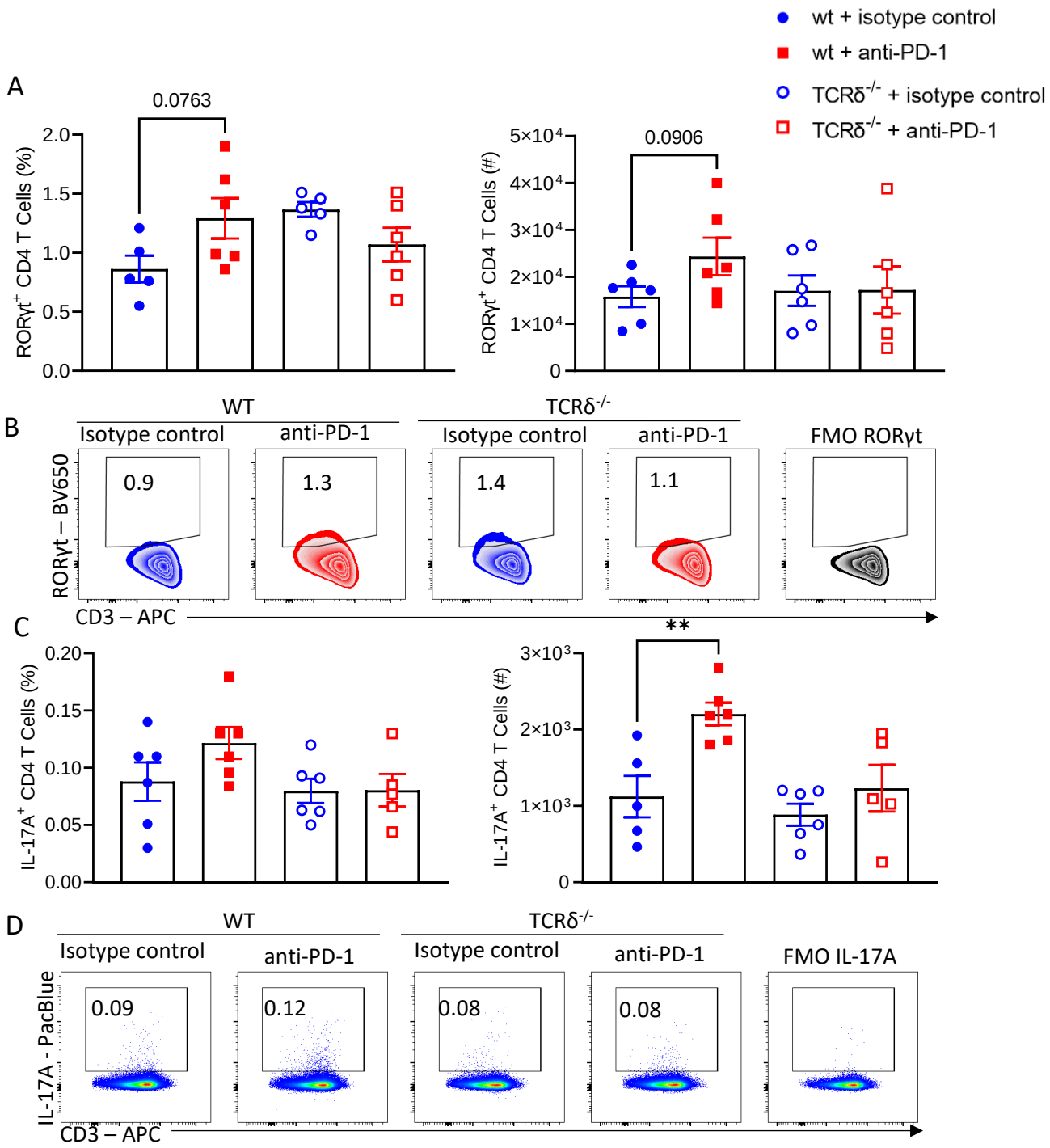

Figure 3.19 Treatment with anti-PD1 increases the absolute number of IL-17A-producing CD4 T cells in the LN of WT mice but not in TCRδ$^{-/-}$ mice during EAE. EAE was induced in C57BL/6J mice and TCRδ$^{-/-}$ mice. Mice were injected i.p with 200 µg of PD-1 neutralising antibody or IgG2a isotype control antibody on the day prior to induction of EAE and on days 2 and 5 of EAE. On day 9 post induction of EAE, mice were sacrificed, and cells were isolated from the axillary and brachial LNs. Cells were incubated with brefeldin A for 4 hours followed by staining for surface CD3, CD4, and intracellular RORγt, and IL-17A and analysed by flow cytometry. Results are (A) frequency and absolute number of RORγt-expressing CD4 T cells in the LN on day 9 of EAE with (B) representative FACS plots. (C) Frequency and absolute number of IL-17A-producing CD4 T cells with (D) representative FACS plots. Results are representative of two independent experiments. Data are mean ± SEM (n=6 per group). $^{**}p < 0.01$ by one-way ANOVA with Tukey's post test.

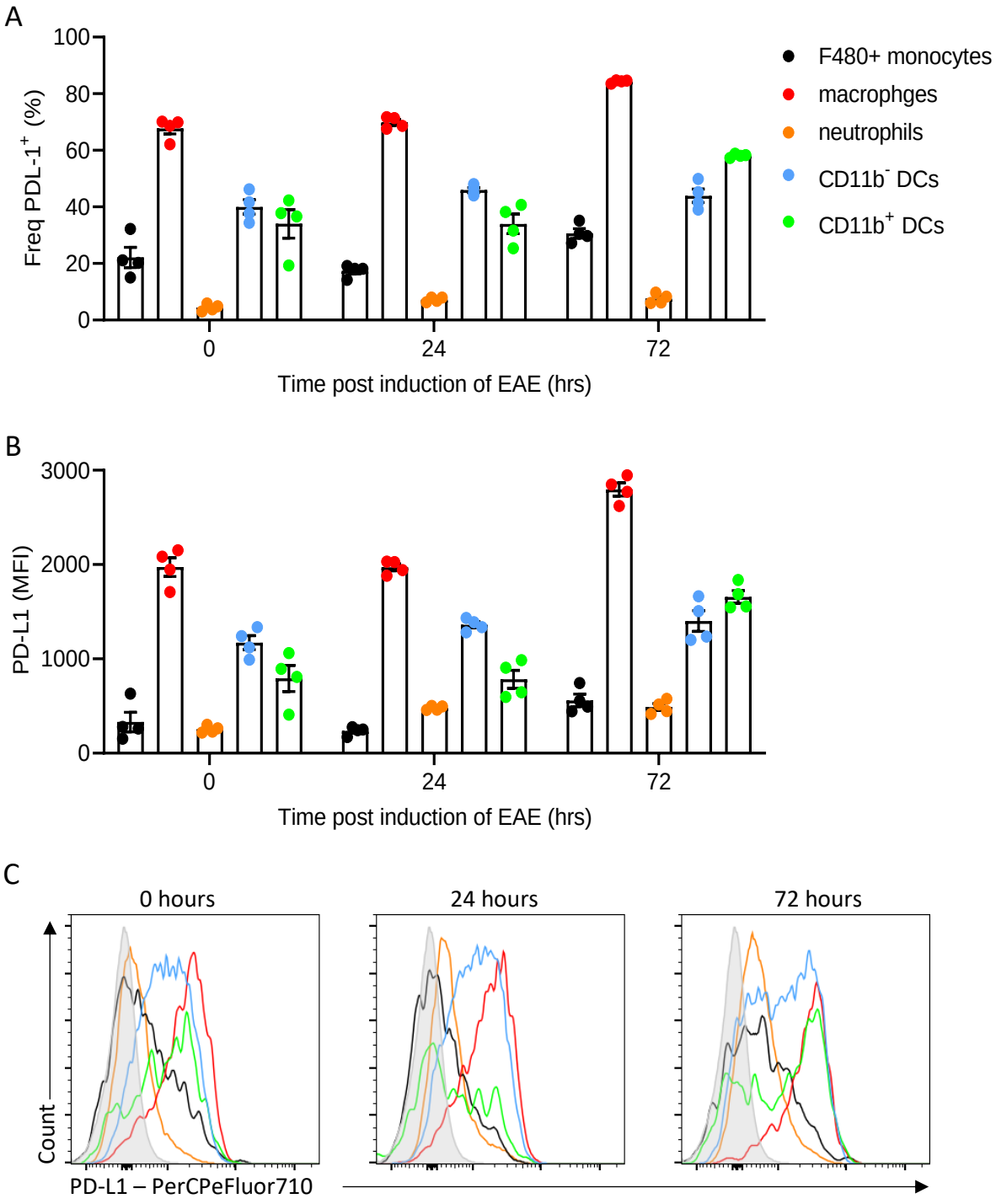

Figure 3.20 Macrophages and DCs express the highest levels of PD-L1 in the spleen up to 72 hours post induction of EAE. Naïve C57BL/6J mice, or mice 24 hours and 72 hours post induction of EAE were sacrificed. Spleen cells were isolated and stained for viability, surface B220, CD45, CD11b, CD11c, F4/80, Ly6c, Ly6g, MHC-II, SiglecF, and PD-L1 in the presence of an Fc receptor blocking antibody. Cells were analysed by flow cytometry and innate immune cell populations were defined according to the gating strategy in figure 2.2.17.3. Results are (A) frequency and (B) MFI of PD-L1 expression by innate immune cell populations in the spleen with (C) representative FACS plots. Data are mean ± SEM (n=4 per group).

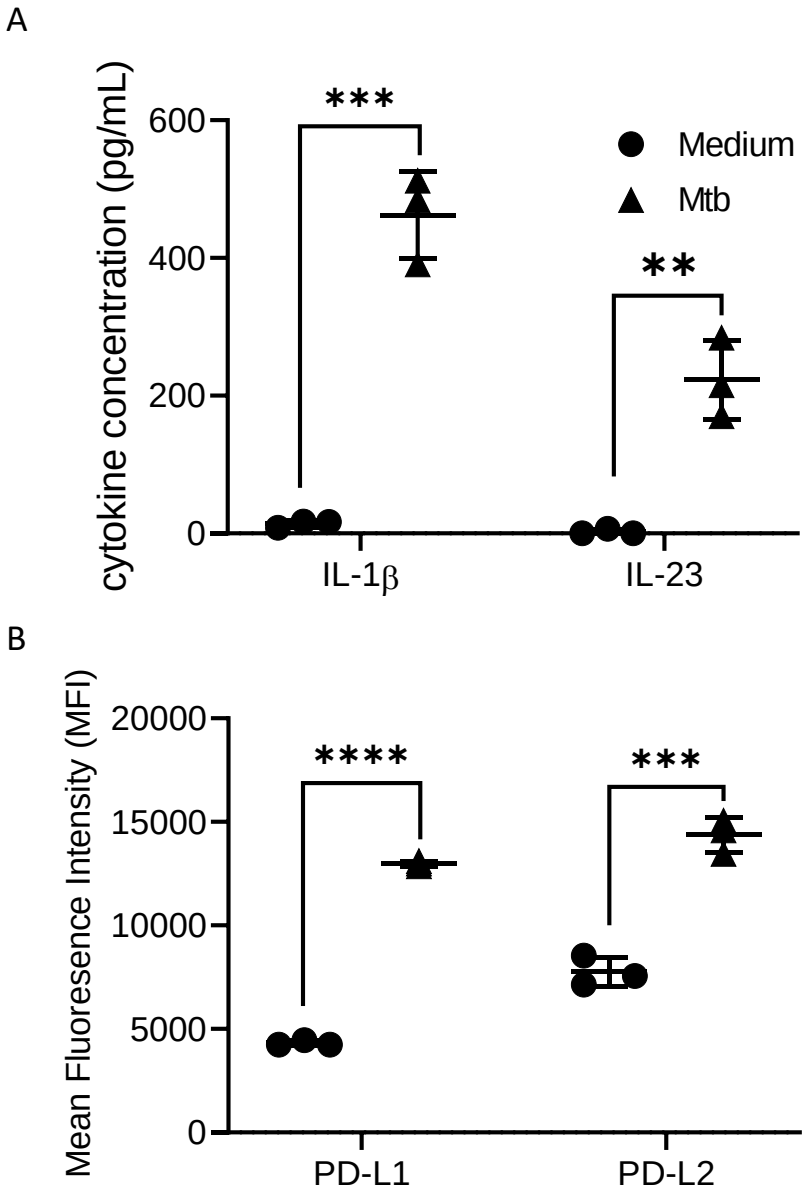

Figure 3.21 *Mtb*-stimulation increases PD-L1 and PD-L2 expression by BMDCs. BMDCs from naïve C57BL/6J mice were stimulated with *Mtb* (10 μg/mL) or medium alone. After 24 hours supernatants were harvested and cells were stained for viability and surface CD11b, CD11c, PD-L1, and PD-L2. Results are (A) concentration of IL-1β and IL-23 in culture supernatants as determined by ELISA and (B) MFI of PD-L1 and PD-L2 expression by BMDCs as determined by flow cytometry. Results are representative of three independent experiments. Data are mean ± SD (n=3). $^{**}p < 0.01$, $^{***}p < 0.001$, $^{****}p < 0.0001$ by unpaired Student's *t* test.

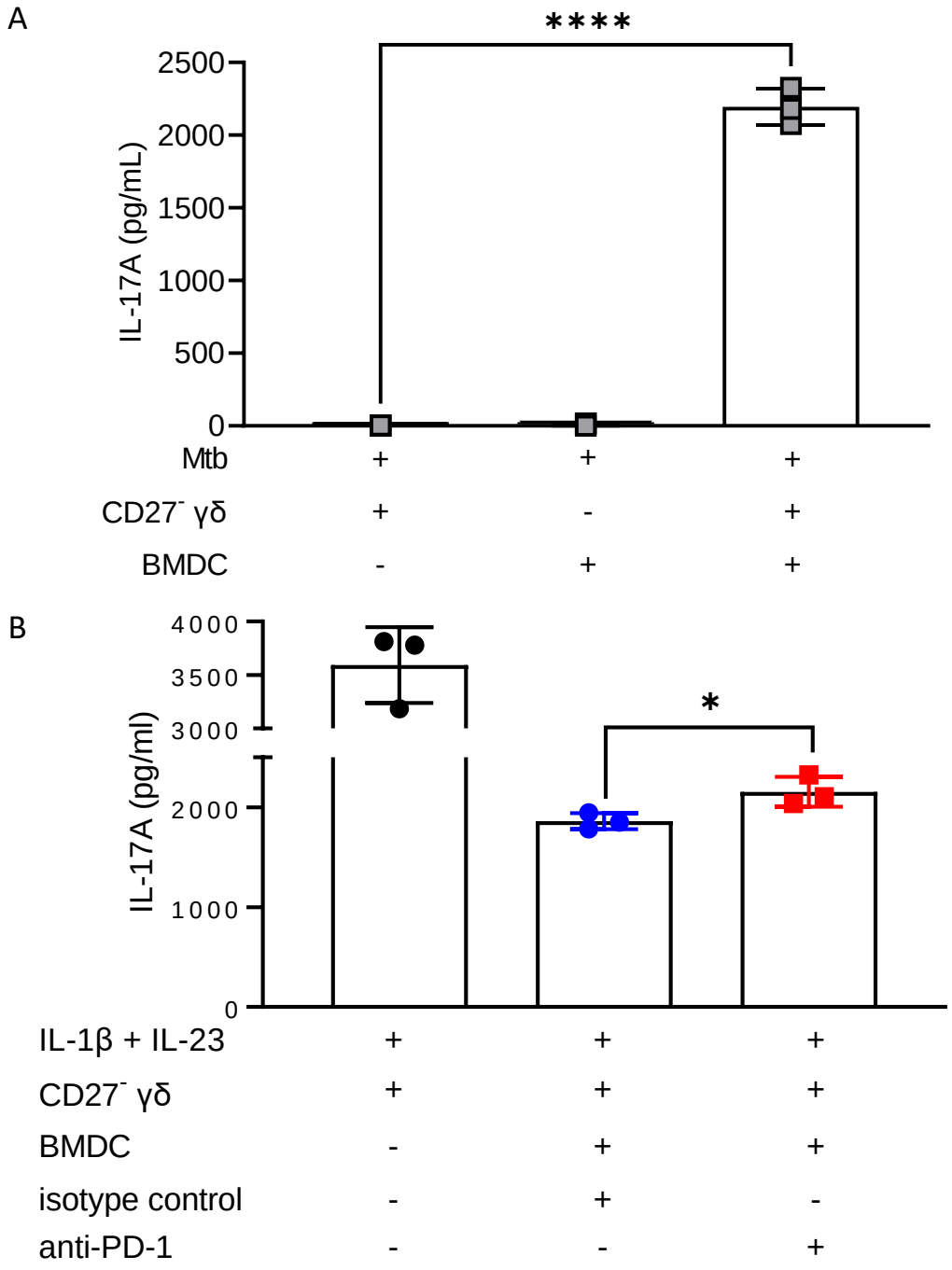

Figure 3.22 IL-17A production by CD27$^-$ γδ T cells is regulated by PD-1. BMDCs were expanded from naïve C57BL/6J mice and stimulated with either *Mtb* (10 μg/mL) or IL-1β (2.5 ng/mL) and IL-23 (10 ng/mL) and co-cultured with CD27$^-$ γδ T cells FACS-purified from the LNs of mice with EAE in the presence or absence of PD-1 neutralising antibody or isotype control antibody (10 μg/mL). Culture supernatants were collected after 24 hours and IL-17A concentrations were quantified by ELISA. Results are IL-17A concentration in culture supernatants of (A) CD27$^-$ γδ T cells co-cultured with *Mtb*-stimulated BMDCs and (B) CD27$^-$ γδ T cells activated with IL-1β and IL-23 and co-cultured with BMDCs in the presence of PD-1 neutralising antibody or isotype control antibody. Results are representative of two independent experiments. Data are mean ± SD (n=3). $^*p < 0.05$, $^{****}p < 0.0001$ by one-way ANOVA with Tukey's multiple comparisons test.

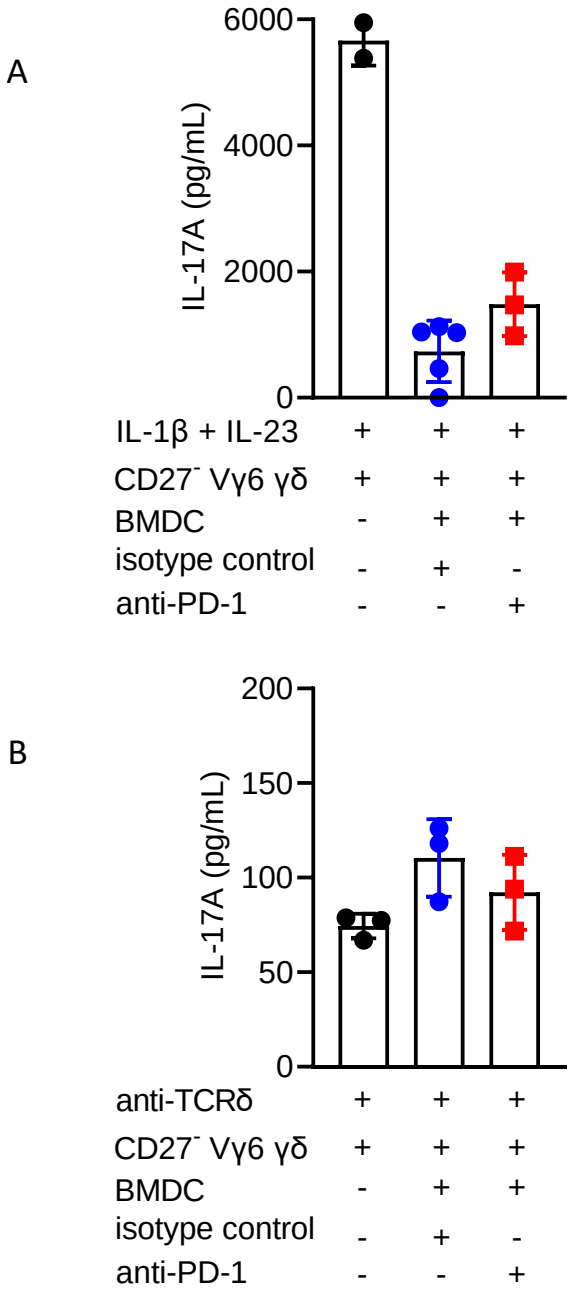

Figure 3.23 The effect of anti-PD-1 treatment on IL-1β+IL-23-induced IL-17A production by Vγ6 γδ T cells. EAE was induced in C57BL/6J mice. On day 7, LN and spleen cells were isolated and stained for surface CD3, CD27, TCRδ, Vγ1.1, and Vγ4. CD27$^-$ Vγ6 γδ T cells were FACS-purified. Purified cells were co-cultured with BMDCs and activated *in vitro* with either IL-1β (2.5 ng/mL) and IL-23 (10 ng/mL) or anti-TCRδ (1 µg/mL) in the presence or absence of either isotype control or anti-PD-1 antibody (10 µg/mL). Supernatants were harvested after 48 hours and IL-17A concentrations were quantified by ELISA. Results are concentrations of IL-17A in culture supernatants of CD27$^-$ Vγ6 γδ T cells activated *in vitro* with (A) IL-1β+IL-23 or (B) anti-TCRδ. Results are representative of three independent experiments. Data are mean ± SD (n=3), statistics by unpaired Student's *t* test.

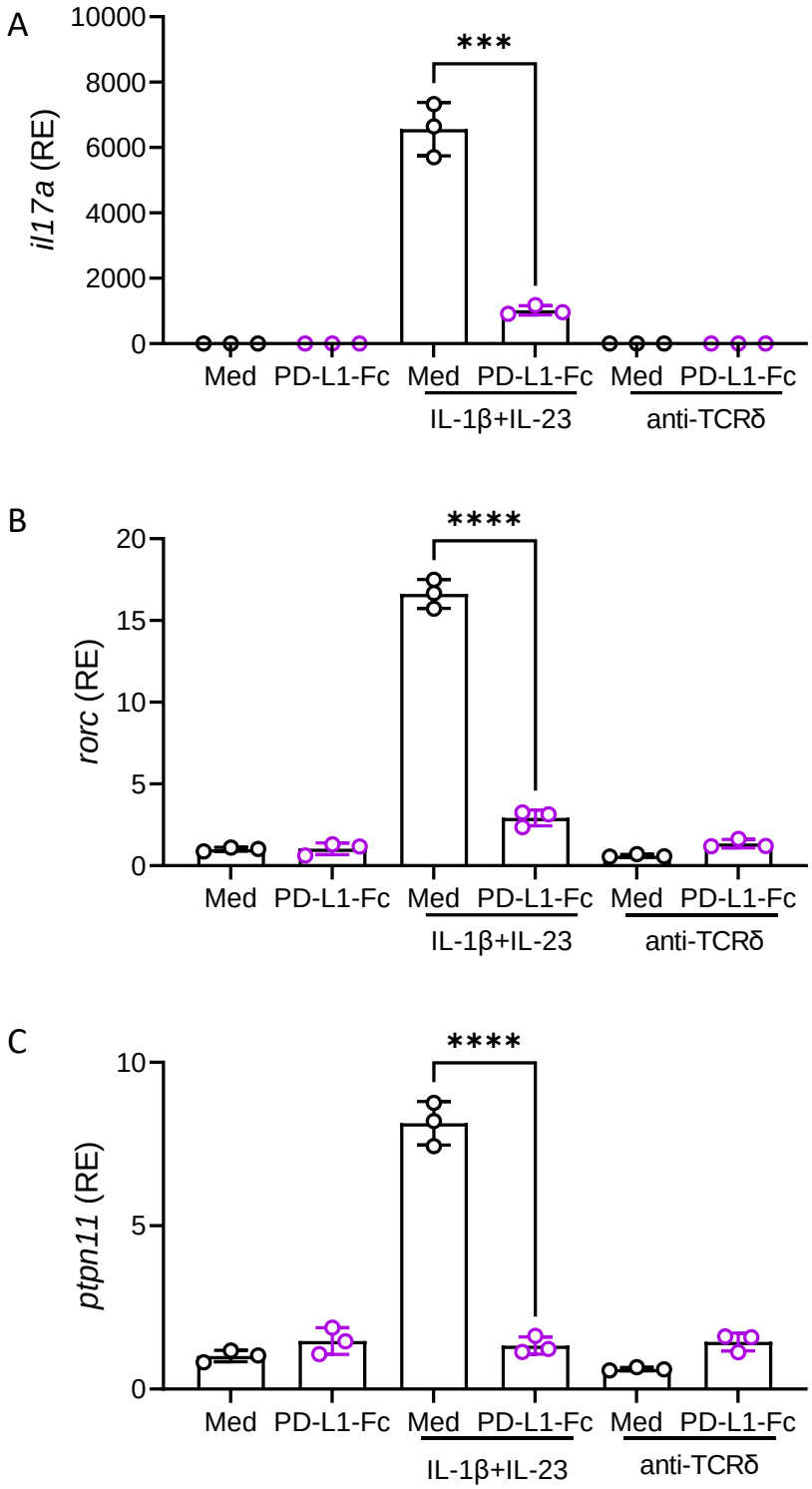

Figure 3.24 PD-1 engagement suppresses IL-1β+IL-23-activated Vγ6 γδ T cells. EAE was induced in C57BL/6J mice. On day 7, LN and spleen cells were isolated and stained for surface CD3, CD27, TCRδ, Vγ1.1, and Vγ4. $CD27^-$ Vγ6 γδ T cells were FACS-purified. Purified cells were co-cultured with BMDCs and activated *in vitro* with either IL-1β (2.5 ng/mL) and IL-23 (10 ng/mL) or anti-TCRδ (1 μg/mL) in the presence or absence of plate-bound PD-L1-Fc (25 μg/mL) for 2 hours. Results are mRNA expression of (A) *il17a*, (B) *rorc,* and (C) *ptpn11* as measured by Rt-PCR normalized to 18S rRNA and relative to medium only. Results are representative of three independent experiments. Data are mean ± SD (n=3). $^{***}p < 0.001$, $^{****}p < 0.0001$ by unpaired Student's *t* test.

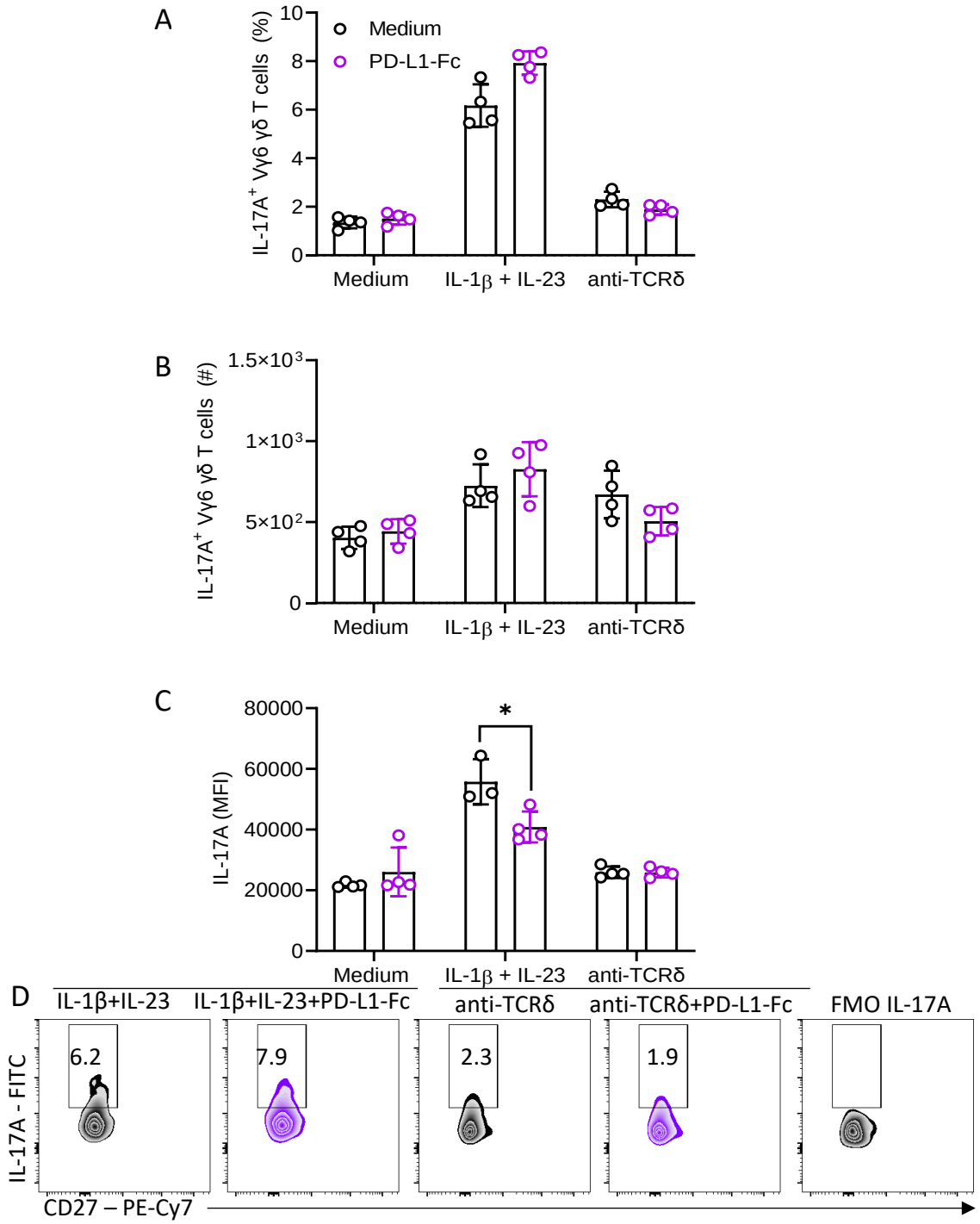

Figure 3.25 PD-1 engagement suppresses IL-17A production by IL-1β+IL-23-activated CD27⁻ Vγ6 γδ T cells. CD27⁻ γδ T cells were expanded from the spleen and LNs of naïve C57BL/6J mice. Cells were harvested after 3 days in culture and re-stimulated with either IL-1β (2.5 ng/mL) and IL-23 (10 ng/mL) or anti-TCRδ (1 µg/mL) in the presence or absence of plate-bound PD-L1-Fc (25 µg/mL) for 4 days. Cells were incubated with brefeldin A for 4 hours and stained for surface CD3, CD27, TCRδ, Vγ1.1, Vγ4, and intracellular IL-17A and analysed by flow cytometry. Results are (A) frequency, (B) absolute number and (C) MFI of IL-17A production by CD27⁻ Vγ6 γδ T cells with (D) representative FACS plots. Results are representative of three independent experiments. Data are mean ± SD (n=4). $^{*}p < 0.05$ by unpaired Student's *t* test.

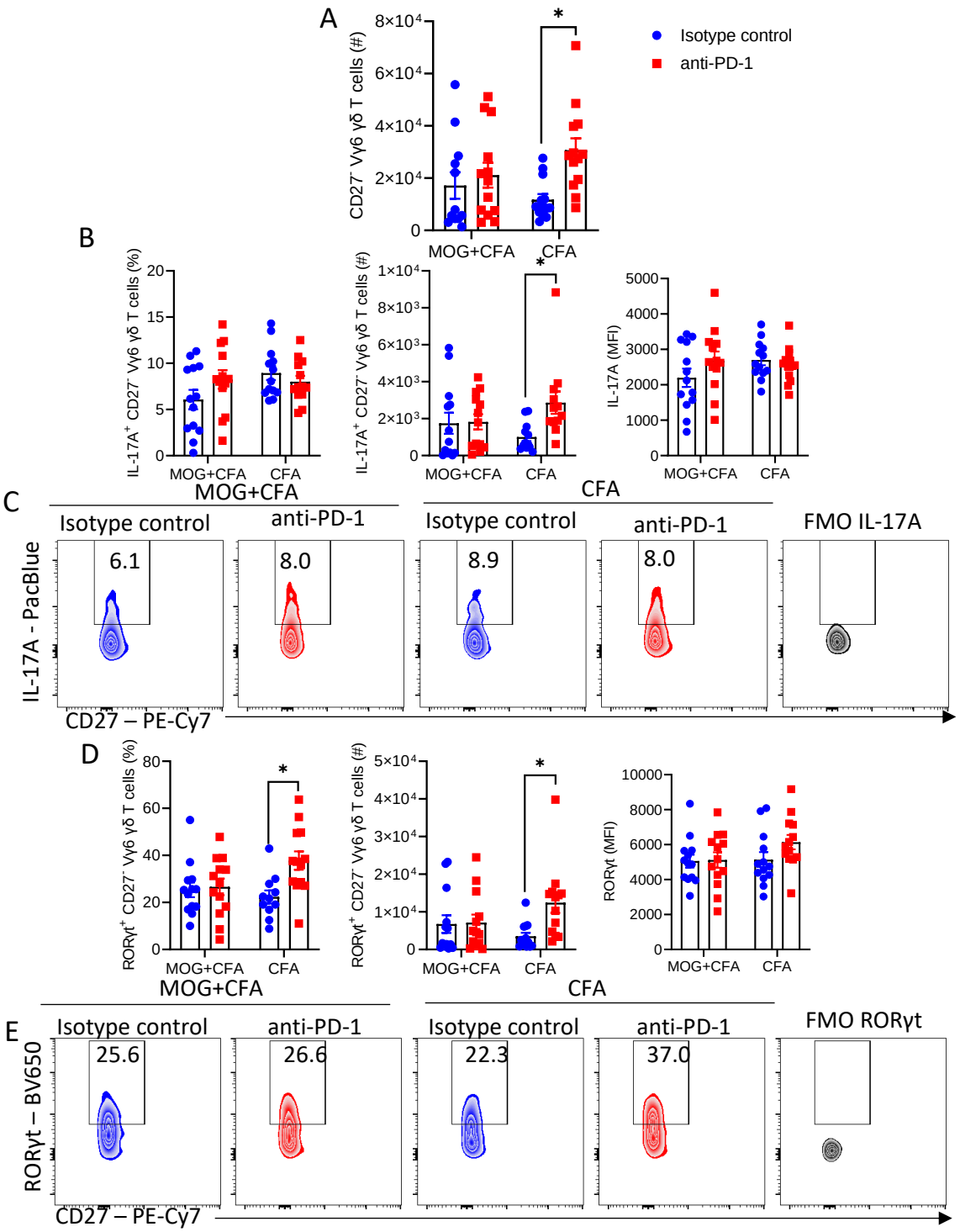

Figure 3.26 CD27⁻ Vγ6 γδ T cells in mice immunised with CFA in the absence of MOG are regulated by PD-1. C57BL/6J mice were treated i.p with either anti-PD-1 (200 µg) or IgG2a isotype control antibody. The next day, mice were immunised s.c with MOG peptide emulsified in CFA or CFA alone in addition to i.p immunisation with PT (250 ng). Mice were treated with either anti-PD-1 or isotype control antibody on days 2 and 5 of EAE. On day 6, axillary and brachial LNs were harvested followed by incubation with brefeldin A for 4 hours and staining for surface CD3, CD27, TCRδ, Vγ1.1, Vγ4, and intracellular IL-17A, and RORγt. Results are (A) absolute number of CD27⁻ Vγ6 γδ T cells in the LN on day 6 of EAE. (B) Frequency, absolute number, and MFI of IL-17A-producing CD27⁻ Vγ6 γδ T cells with (C) representative FACS plots and (D) frequency, absolute number, and MFI of RORγt-expressing CD27⁻ Vγ6 γδ T cells with (E) representative FACS plots. Results are representative of three independent experiments. Data are mean ± SEM (n=12), $^{*}p < 0.05$ by one-way ANOVA with Tukey's multiple comparisons test.

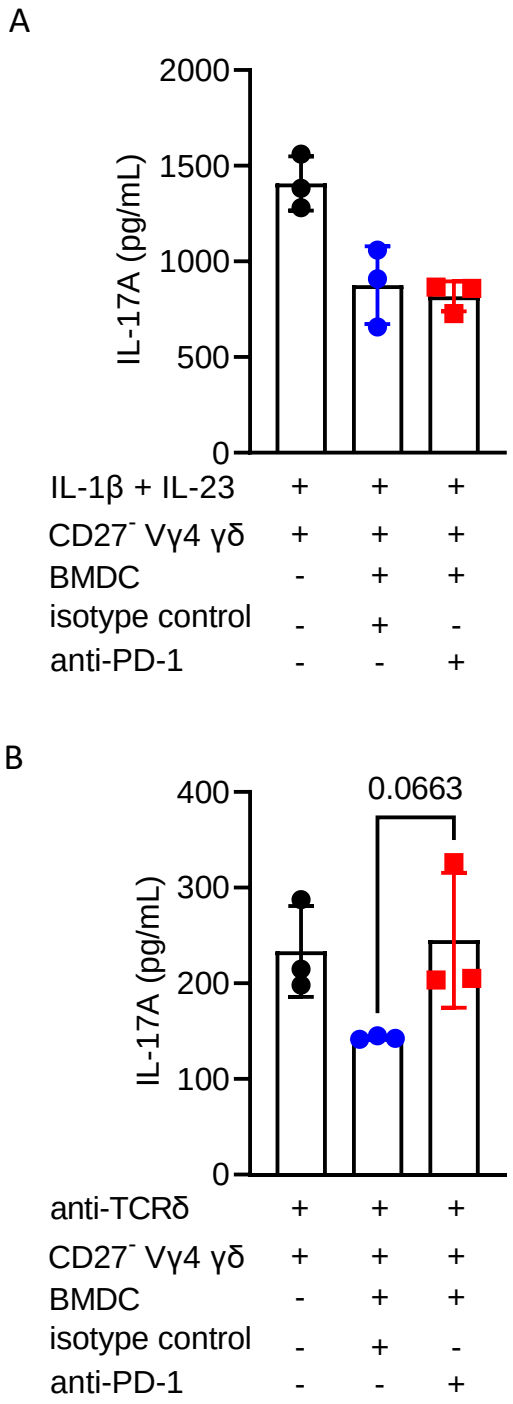

Figure 3.27 The effect of anti-PD-1 treatment on TCR-induced IL-17A production by Vγ4 γδ T cells. EAE was induced in C57BL/6J mice. On day 7, LN and spleen cells were isolated and stained for surface CD3, CD27, TCRδ, and Vγ4. CD27$^-$ Vγ4 γδ T cells were FACS-purified. Purified cells were co-cultured with BMDCs and activated *in vitro* with either IL-1 β (2.5 ng/mL) and IL-23 (10 ng/mL) or anti-TCRδ (1 µg/mL) in the presence or absence of either isotype control or anti-PD-1 antibody (10 µg/mL). Supernatants were harvested after 48 hours and IL-17A concentrations were quantified by ELISA. Results are concentrations of IL-17A in culture supernatants of CD27$^-$ Vγ4 γδ T cells activated *in vitro* with (A) IL-1β+IL-23 or (B) anti-TCRδ. Results are representative of three independent experiments. Data are mean ± SD (n=3), statistics by unpaired Student's *t* test.

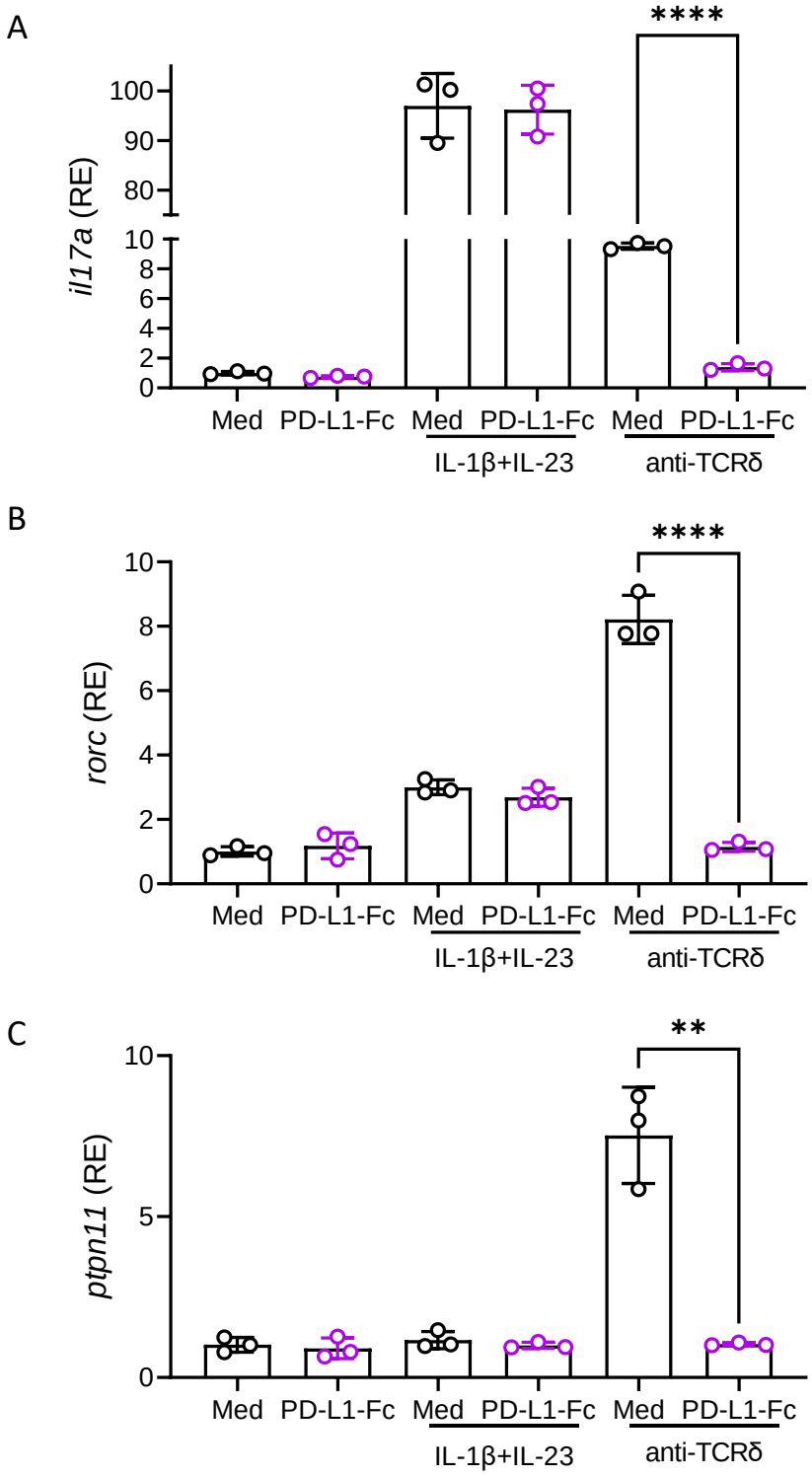

Figure 3.28 PD-1 engagement suppresses TCR-activated Vγ4 γδ T cells. EAE was induced in C57BL/6J mice. On day 7, LN and spleen cells were isolated and stained for surface CD3, CD27, TCRδ. and Vγ4. CD27$^-$ Vγ4 γδ T cells were FACS-purified. Purified cells were activated *in vitro* with either IL-1β (2.5 ng/mL) and IL-23 (10 ng/mL) or anti-TCRδ (1 μg/mL) in the presence or absence of plate-bound PD-L1-Fc (25 μg/mL) for 2 hours. Results are mRNA expression of (A) *il17a*, (B) *rorc,* and (C) *ptpn11* as measured by Rt-PCR normalized to 18S rRNA and relative to medium only. Results are representative of three independent experiments. Data are mean ± SD (n=3). $^{**}p < 0.01$, $^{****}p < 0.0001$ by unpaired Student's *t* test.

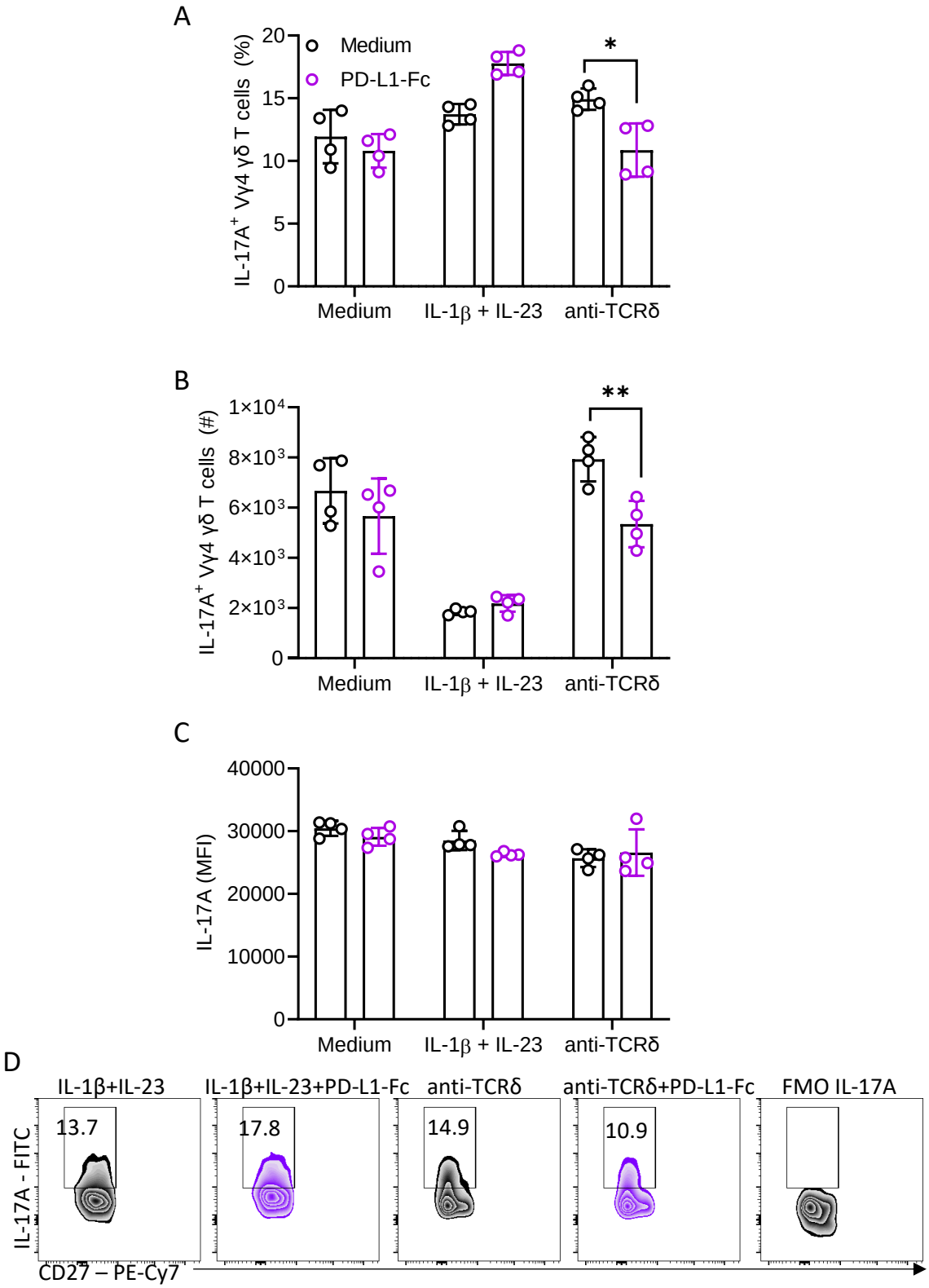

Figure 3.29 PD-1 engagement suppresses IL-17A production by TCR-activated CD27⁻ Vγ4 γδ T cells. CD27⁻ γδ T cells were expanded from the spleen and LN of naïve C57BL/6J mice. Cells were harvested after 3 days and re-stimulated with either IL-1β (2.5 ng/mL) and IL-23 (10 ng/mL) or anti-TCRδ (1 µg/mL) in the presence or absence of plate-bound PD-L1-Fc (25 µg/mL) for 4 days. Cells were incubated with brefeldin A for 4 hours and stained for surface CD3, CD27, TCRδ, Vγ4, and intracellular IL-17A and analysed by flow cytometry. Results are (A) frequency, (B) absolute number, and (C) MFI of IL-17A production by CD27⁻ Vγ4 γδ T cells with (D) representative FACS plots. Results are representative of three independent experiments. Data are mean ± SD (n=4). $^{*}p < 0.05$, $^{**}p < 0.01$ by unpaired Student's *t* test.

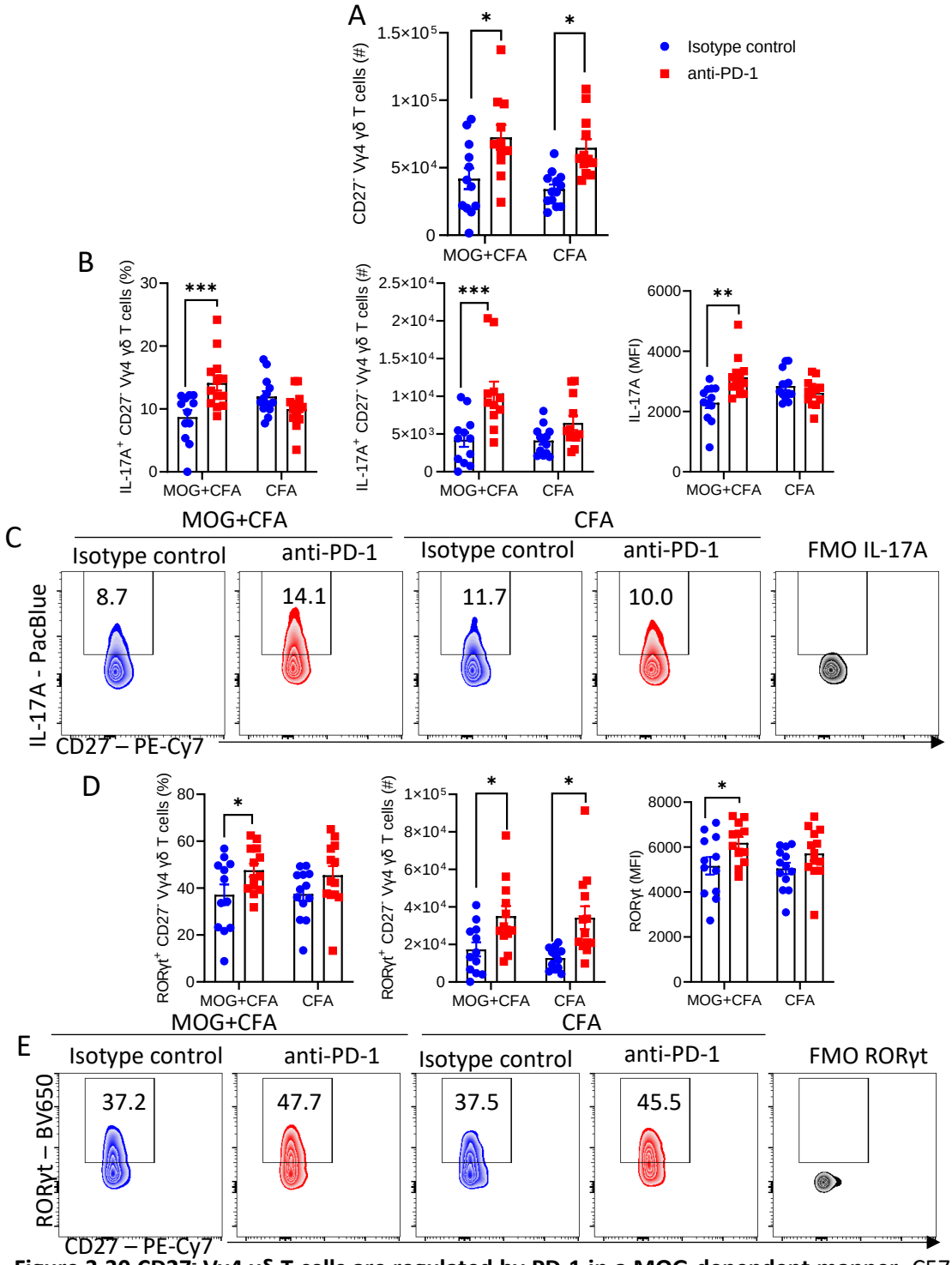

Figure 3.30 CD27⁻ Vγ4 γδ T cells are regulated by PD-1 in a MOG-dependent manner. C57BL/6J mice were treated i.p with either anti-PD-1 (200 µg) or isotype control antibody. The next day, mice were immunised s.c with MOG peptide emulsified in CFA or CFA alone in addition to i.p immunisation with Pertussis toxin (250 ng). Mice were treated with either anti-PD-1 or isotype control antibody on days 2 and 5 of EAE. On day 6, axillary and brachial LNs were harvested followed by incubation with brefeldin A for 4 hours and staining for surface CD3, CD27, TCRδ, Vγ4, and intracellular IL-17A, and RORγt. Results are (A) absolute number of CD27⁻ Vγ4 γδ T cells in the LN on day 6 of EAE. (B) Frequency, absolute number, and MFI of IL-17A-producing CD27⁻ Vγ4 γδ T cells with (C) representative FACS plots and (D) frequency, absolute number, and MFI of RORγt-expressing CD27⁻ Vγ4 γδ T cells with (E) representative FACS plots. Results are representative of three independent experiments. Data are mean ± SEM (n=12), $^{*}p < 0.05$, $^{**}p < 0.01$, $^{***}p < 0.001$ by one-way ANOVA with Tukey's multiple comparisons test.

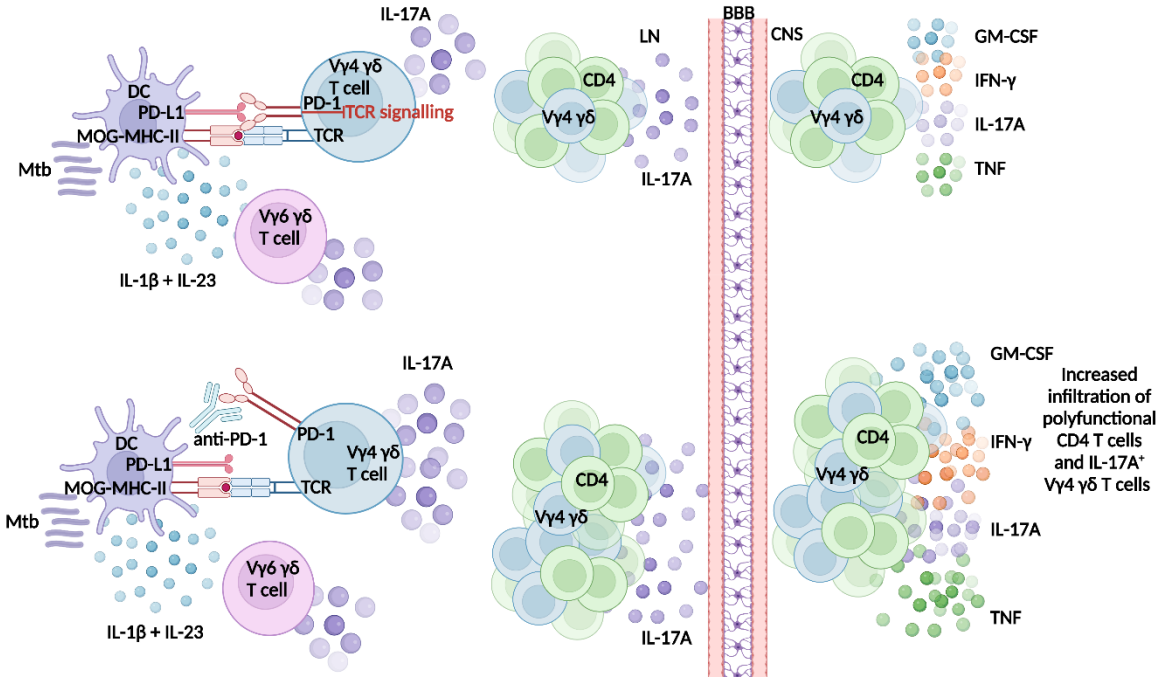

Figure 3.31 Proposed mechanism for the PD-1-mediated regulation of IL-17A-producing Vγ4 γδ T cells during EAE. Vγ4 γδ T cells are activated in the LN via their TCR. PD-1 engagement by PD-L1-expressing DCs negatively regulates IL-17A production by MOG-specific Vγ4 γδ T cells. Vγ6 γδ T cells are activated to produce IL-17A by IL-1β and IL-23 in the LN but they are not regulated by PD-1 during EAE. IL-17A-producing Vγ4 γδ T cells recruit innate immune cells that orchestrate the induction of autoantigen-specific IL-17A-producing CD4 T cells in the periphery. Pathogenic Vγ4 γδ T cells and CD4 T cells migrate into the CNS where they precipitate autoimmunity. When mice are treated with anti-PD-1 during the induction of EAE, IL-17A production by Vγ4 γδ T cells is enhanced. Increased IL-17A leads to enhanced recruitment of innate immune cells and increased induction of pathogenic CD4 T cells. Anti-PD-1 treatment enhances IL-17A production by Vγ4 γδ T cells which leads to increased expansion and CNS infiltration of polyfunctional Vγ4 γδ T cells and CD4 T cells where they worsen autoimmunity.

Chapter 4
IL-10 regulates T cell migration into the CNS during EAE

4.1 Introduction

The protective role of IL-10 in regulating the pathogenesis of autoimmune diseases including EAE is well established [308]. IL-$10^{-/-}$ mice develop more severe EAE than WT mice, and IL-$10^{-/-}$ mice produce higher levels of antigen-specific IFN-γ and TNF. Furthermore, over-expression of IL-10 protects mice from the development of clinical signs of EAE. The protective effect of IL-10 was dependent on its expression in the CNS [309]. In EAE, IL-10 was initially studied in the context of Th2 cells but more recent studies have identified IL-10-producing CD4 T cells (Treg cells) or Tr1 cells as critical sources of IL-10 in EAE [310]. Previous studies from the Mills lab have shown that respiratory infection with the bacterial pathogen *B. pertussis* one day prior to the induction of EAE protects mice from development of the disease [311]. Mice were protected from EAE by induction of IL-10-producing CD4 T cells that suppressed integrin expression by pathogenic T cells and subsequent entry into the CNS. Decreased *il10* mRNA expression has been associated with increased severity of MS [312]. Reduced IL-10 is also associated with relapse in RRMS [313].

Tr1 cells do not express FoxP3 and differ from naturally occurring Treg cells in that they can be generated in the periphery in response to antigen stimulation under tolerogenic conditions [63]. Tr1 cells are identified by expression of the surface markers CD49b and LAG-3 in both mice and humans [60]. Development of protocols to generate or enhance autoantigen specific Tr1 cells remain a promising strategy to treat autoimmune diseases. Previous work by Raverdeau et al. has used RA as an adjuvant in combination with IL-2 and MOG to induce and expand MOG-specific IL-10-producing Tr1 cells *in vivo* [69]. Adoptive transfer of MOG-specific Tr1 cells significantly reduced the severity of EAE.

IL-10-producing T cells play a central role in protection against autoimmune diseases by inhibition of autoreactive immune cells in the periphery [314-316]. B cells have also been identified as an important source of IL-10 and these cells function in regulating immune responses. IL-10-producing Breg cells suppress effector T cell responses and induce Tr1 cells in CIA [317]. IL-10-producing Breg cells accumulate in the CNS of mice with EAE where they have a protective effect via suppression of T cell responses [318]. In MS, patients display defects in Breg cells particularly during relapse, rather than during remission, in

RRMS [319]. Alemtuzumab is an immunotherapy that provides sustained suppression of disease in MS and has been shown to restore the MS-related deficiency in Breg cells [320]. The mentioned study has provided a possible mechanistic basis for the efficacy of alemtuzumab in the treatment of RRMS. Additionally, B cell deficient mice failed to recover from MOG-induced EAE [321]. IL-10 production by B cells was required for remission from EAE providing further evidence for a protective role for B cell-derived IL-10 in the pathogenesis of EAE.

The suppressive effect of IL-10 on T cell responses is coordinated by APCs. IL-10 signalling modulates the function of APCs, leading to suppression of the induction of T cell responses [65]. Loss of IL-10 signalling promoted the differentiation of pro-inflammatory microglia [322]. Studies have also linked the clinical benefit of IFN-β treatment in MS with IL-10 production by microglia [323]. IFN-β treatment increased IL-10 production by microglial cells. Furthermore, a longitudinal study demonstrated that after 12 months of IFN-β treatment, MS patients had significantly increased numbers of IL-10-producing cells in the circulation [324]. IFN-β treatment also significantly reduced IL-17A production by patient lymphocytes following PHA stimulation, suggesting that IFN-β increases IL-10 production by innate immune cells, which suppresses antigen-specific T cell responses in MS.

In addition to evidence from the EAE model, the direct effect of IL-10 on IL-17A production by CD4 T cells has been explored in multiple contexts. In a model of Influenza virus infection, IL-$10^{-/-}$ mice had increased expression of Th17-associated cytokines, which exacerbated inflammation that is protective against a high-dose influenza virus challenge [325]. CD4 T cells can co-express IL-10 and IL-17. IL-6 and TGF-β signalling *in vivo* induces IL-10 production by Th17 cells, which limits their pathogenicity during EAE. IL-$10^{-/-}$ had increased numbers of IL-17A-producing γδ, CD4, and CD8 T cells following colonisation with *S. aureus* [83].

While the effect of IL-10 on CD4 and CD8 T cell function is well established, little is known about the effects of IL-10 on γδ T cell function. Many studies that have examined immune suppression by T cell-derived IL-10 have focused on APCs that modulate antigen-specific T cell responses. As γδ T cells do not require interaction with APCs to become activated, it is possible that IL-10 or IL-10-producing CD4 T cells may suppress γδ T cell function independent of APCs. MOG-specific Tr1 cells were used to investigate the ability of IL-10

to regulate IL-17A-producing T cell subsets. An IL-10R neutralising antibody was used to block IL-10 signalling throughout EAE. Trafficking of pathogenic T cells into the CNS was examined as well as priming of these cells in the periphery.

4.2 Results

4.2.1 Innate immune cells express IL-10R (CD210) during EAE

In order to examine which cell types may possibly mediate the effect of IL-10 signalling during EAE, the expression of IL-10R (CD210) by various immune cell types was investigated in the spleens of mice with EAE. Over 90% of both $CD11b^+$ and $CD11b^-$ DCs expressed CD210 and expression levels on DC populations were significantly higher than that of other innate immune cell populations analysed (Fig 4.1 A). A significant number of monocytes expressed CD210 in the spleen during EAE (Fig 4.1 B). Neutrophils also expressed CD210 in the spleen during EAE but had the lowest frequency of CD210 expression of the populations examined (Fig 4.1 A, B). Lower numbers of macrophages, $CD11b^+$, and $CD11b^-$ DCs expressed CD210 (Fig 4.1 B). $CD11b^-$ DCs had the highest MFI of CD210 expression (Fig 4.1 C). The MFI of CD210 expression by $CD11b^+$ DCs was significantly higher than that of the monocyte population (Fig 4.1 C).

A comparison of CD210 expression by innate immune cells and CD4, CD8, and γδ T cells, revealed that the MFI of CD210 expression by $CD11b^-$ DCs was significantly higher than the MFI of CD210 expressed by all T cell subsets examined (Fig 4.2 A). The MFI overlay of CD210 expression by T cell populations closely mirrors that of the FMO control showing that T cells do not express significant amounts of CD210 in the spleen during EAE, suggesting that treatment with anti-CD210 primarily affects innate immune cell populations (Fig 4.2 B). These data demonstrate that the effect of IL-10 on the development of EAE is mediated by innate immune cell populations.

4.2.2 Neutralisation of IL-10R enhances T cell responses and the severity of EAE

An IL-10R neutralising antibody was used to examine the effect of IL-10 signalling on the development of clinical signs of EAE. Disease severity was enhanced in the anti-CD210-treated group with EAE; this was significant on day 12 of disease (Fig 4.3 A). Weight loss was also enhanced in anti-CD210-treated mice when compared with isotype control-treated mice (Fig 4.3 B). These data demonstrate that neutralisation of IL-10R signalling during EAE enhances the severity of disease.

There was no difference in the total number of CD4 T cells in the LN of anti-CD210-treated when compared with isotype control-treated mice (Fig 4.4 A). There was a significant increase in the frequency, number, and MFI of IL-17A expression by CD4 T cells in the LN of anti-CD210-treated mice when compared with isotype control-treated mice on day 6 of EAE (Fig 4.4 B). There was a significant increase in the frequency and absolute number of IFN-γ-producing CD4 T cells in the LN of anti-CD210-treated mice on day 6 of EAE (Fig 4.4 C). Similarly, there was no difference in the total number of CD8 T cells in the LN following anti-CD210 treatment (Fig 4.5 A). However, there was a significant increase in the frequency and number of IFN-γ-producing CD8 T cells in the LN of anti-CD210-treated mice on day 6 of EAE (Fig 4.5 B, C).

An examination of γδ T cells during EAE revealed that there was no difference in the number of $CD27^+$ γδ T cells in the LN of mice with EAE following anti-CD210 treatment (Fig 4.6 A). Anti-CD210 treatment induced a significant increase in the total number of $CD27^-$ γδ T cells in the LN of mice with EAE (Fig 4.6 B). Investigating further, there was a significant increase observed in the frequency, number, and MFI of IL-17A expression by $CD27^-$ γδ T cells in the LN of mice treated with anti-CD210 when compared with isotype control-treated mice on day 6 of EAE (Fig 4.6 C).

During EAE, there was a significant increase in the number of IFN-γ-producing $CD27^+$ γδ T cells in the LN of anti-CD210-treated mice (Fig 4.6 D). There was a slight increase, although not significant, in the frequency of IFN-γ-producing $CD27^+$ γδ T cells in the LN of anti-CD210-treated mice during EAE (Fig 4.6 D). There was no significant difference in the MFI of IFN-γ expression by $CD27^+$ γδ T cells between groups (Fig 4.6 D).

The effect of anti-CD210 treatment on MOG-specific T cell responses was also examined. There were no significant differences in either MOG-specific IL-17A or IFN-γ production in the spleens of mice treated with anti-CD210 or isotype control antibody (Fig 4.7 A, B). There was a significant increase in anti-CD3/28-stimulated IFN-γ production by spleen cells from anti-CD210-treated mice with EAE (Fig 4.7 B)

4.2.3 Neutralisation of IL-10R signalling enhances the expression of integrins by T cells during EAE

As anti-CD210 treatment significantly enhanced the onset of EAE, the ability of IL-10R neutralisation to modulate integrin expression in the periphery, and possibly migration of T cells into the CNS, was examined. The frequency and number of CD49d-expressing CD4 T cells in the LN on day 6 of EAE was significantly higher in anti-CD210-treated mice when compared with isotype control-treated mice (Fig 4.8 A). Similarly, there was a significant increase in both the frequency and number of CD49d-expressing CD8 T cells in the LN of mice treated with anti-CD210 during EAE (Fig 4.8 B). Whilst there were no differences observed in either the frequency or number of $CD49d^{+}$ $CD27^{+}$ γδ T cells following anti-CD210 treatment, there was a significant increase in the frequency and number of CD49d-expressing $CD27^{-}$ γδ T cells in the LN of mice with EAE following treatment with anti-CD210 (Fig 4.8 C, D).

The frequency, number, and MFI of CD11a expression by $CD11a^{hi}$ CD4 T cells in the LN of mice with EAE was significantly increased in anti-CD210-treated mice when compared with isotype control-treated mice (Fig 4.9 A). Neutralisation of CD210 did not change either the frequency or number of CD11a expressing CD8 T cells (Fig 4.9 B). However, there was a significant increase in the MFI of CD11a expression by CD8 T cells following anti-CD210 treatment (Fig 4.9 B). The frequency, number, and MFI of CD11a expression by $CD27^{+}$ γδ T cells remained unchanged in response to anti-CD210 treatment during EAE (Fig 4.9 C). Although there was no change in the frequency of $CD27^{-}$ γδ T cells expressing CD11a in response to treatment with anti-CD210, there was a significant increase in the number of CD11a-expressing $CD27^{-}$ γδ T cells and MFI of CD11a expression by these cells on day 6 of EAE (Fig 4.9 D). These findings demonstrate that blocking IL-10 signalling increases integrin expression by T cells in the LN during the induction of EAE.

4.2.4 Neutralisation of IL-10R signalling increases migration of T cells into the CNS during EAE

Results from the present study have demonstrated that neutralisation of IL-10R signalling enhances the severity of EAE and integrin expression by T cells in the periphery. Therefore,

the infiltration of T cells and other immune cells into the CNS and the phenotype of CNS-infiltrating immune cells was examined in anti-CD210-treated and isotype control-treated mice during EAE. There was no difference in the total number of $CD45^{hi}$ immune cells, B cells, neutrophils, or $Ly6c^{hi}$ monocytes infiltrating the brain at the peak of EAE in anti-CD210-treated mice (Fig 4.10 A, C, D, E). However, there was a significant decrease in the number of microglia in the brains of mice following anti-CD210 treatment when compared with isotype control-treated mice at the peak of EAE (Fig 4.10 B).

There was no difference observed in the total number of CD4 T cells or in the in the frequency or number of $CD11a^{hi}$ CD4 T cells infiltrating the brain during EAE following anti-CD210 treatment (Fig 4.11 A, B). Additionally, the MFI of CD11a expression by $CD11a^{hi}$ CD4 T cells was also unchanged in response to anti-CD210 treatment during EAE (Fig 4.11 B). Conversely, there was a significant increase in the frequency and number of CD49d-expressing CD4 T cells in the brains of mice during EAE following anti-CD210 treatment (Fig 4.11 D). An examination of cytokine production by brain-infiltrated CD4 T cells revealed that anti-CD210 treatment did not affect the frequency, number, or MFI of either IFN-γ or IL-17A production by CD4 T cells during EAE (Fig 4.12 A, C).

Anti-CD210 treatment did not alter the number of γδ T cells, $CD27^{+}$ γδ T cells, or $CD27^{-}$ γδ T cells in the brain at the peak of EAE (Fig 4.13 A). However, there was an increase in the number of CD49d-expressing $CD27^{-}$ γδ T cells in the brain following treatment with anti-CD210 during EAE (Fig 4.13 B). There was also a significant increase in the frequency of $CD49d^{+}$ $CD27^{-}$ γδ T cells in the brain at the peak of EAE in mice treated with anti-CD210 (Fig 4.13 B). Anti-CD210 treatment did not affect IL-17A production by $CD27^{-}$ γδ T cells in the brain at the peak of EAE (Fig 4.13 D).

There was a significant increase in the total number of brain-infiltrating CD8 T cells during EAE in response to treatment with anti-CD210 (Fig 4.14 A). Additionally, anti-CD210 treatment resulted in a significant increase in the frequency, number, and MFI of CD49d expression by CD8 T cells infiltrating the brain during EAE (Fig 4.14 B). These data show that blocking IL-10R signalling increases T cell migration into the brain during EAE.

4.2.5 IL-10-producing MOG-specific Tr1 cells suppress autoantigen-specific CD4 T cells

In order to examine the possible role of IL-10-producing Tr1-type Treg cells in the modulation of EAE, a protocol to expand MOG-specific Tr1 cells [69] by immunisation with MOG, RA and IL-2 and *in vitro* expansion with MOG and IL-2 was used (Fig 4.15 A). As IL-10 is difficult to detect by traditional intracellular cytokine staining methods, Primeflow was used to detect IL-10 mRNA expression by this population (Fig 4.15 B). Expanded Tr1 cells produced IL-10 *in vitro* in response to stimulation with MOG in the presence of APCs (Fig 4.16 A). Stimulation with PMA in combination with anti-CD3 induced significantly increased IL-10 production by MOG-specific Tr1 cells (Fig 4.16 A). Co-culture of MOG-specific CD4 T cells isolated from MOG-immunised mice with increasing ratios of Tr1 cells significantly suppressed IL-17A production (Fig 4.16 B). Addition of anti-IL-10 to the co-culture of CD4 T cells from MOG-immunised mice with MOG-specific Tr1 cells significantly increased IL-17A production, suggesting that MOG-specific Tr1 cells suppress IL-17A production by MOG-specific CD4 T cells in an IL-10-dependent manner (Fig 4.16 B).

Treg cells conventionally suppress effector T cell responses in a contact-dependent manner, which requires the presence of an APC to effectively mediate suppression. As γδ T cells do not necessarily require TCR engagement to become activated [169] the ability of MOG-specific Tr1 cells to suppress IL-17A-producing $CD27^-$ γδ T cells activated with IL-1β+IL-23 was examined. There were no differences in the frequency of $IL\text{-}17A^+$ $CD27^-$ γδ T cells following co-culture with MOG-specific Tr1 cells in the presence of APCs (Fig 4.17 A). Only co-culture of IL-1β+IL-23-activated $CD27^-$ γδ T cells with the highest ratio of Tr1 cells (1:10) significantly decreased the number of IL-17A-producing $CD27^-$ γδ T cells (Fig 4.17 B). There were no differences observed in the MFI of IL-17A expression by $CD27^-$ γδ T cells in response to co-culture with Tr1 cells (Fig 4.17 C). Co-culture of IL-17A-producing $CD27^-$ γδ T cells with increasing ratios of MOG-specific Tr1 cells in the presence of APCs did not significantly affect IL-17A production as measured by ELISA (Fig 4.17 E).

MOG-specific CD4 T cells from MOG-immunised mice were purified and activated with MOG, IL-1β+IL-23 *in vitro,* and co-cultured with increasing ratios of MOG-specific Tr1 cells. Co-culture of MOG, IL-1β+IL-23-stimulated CD4 T cells from MOG-immunised mice with MOG-specific Tr1 cells significantly decreased the frequency of $IL\text{-}17A^+$ CD4 T cells at both

the 1:5 and 1:10 ratios of CD4:Tr1 (Fig 4.18 A). Following co-culture of MOG, IL-1β+IL-23-activated CD4 T cells with increasing ratios of Tr1 cells there was a significant dose-dependent decrease in the number of IL-17A-producing CD4 T cells observed (Fig 4.18 B). The MFI of IL-17A expression by CD4 T cells was only significantly decreased at the highest ratio of CD4:Tr1 (1:10) (Fig 4.18 C). Similarly, the concentration of IL-17A in the supernatant of co-cultured MOG-specific CD4 T cells and Tr1 cells was significantly decreased at higher ratios of CD4:Tr1 (Fig 4.18 E). Similarly, addition of Tr1 cells induced a significant dose-dependent decrease in the frequency and number of IFN-γ-producing CD4 T cells (Fig 4.19 A, B). There was also a significant, dose-dependent decrease in the MFI of IFN-γ expression by MOG, IL-1β+IL-23-activated CD4 T cells upon co-culture with MOG-specific Tr1 cells (Fig 4.19 D). These data were further validated by measuring the concentration of IFN-γ in the culture supernatant, which was also significantly reduced in response to co-culture of MOG-specific CD4 T cells with increasing ratios of MOG-specific Tr1 cells (Fig 4.19 E).

These data have demonstrated that IL-10-producing Tr1 cells, in the presence of APCs, suppress MOG-specific IL-17A and IFN-γ production by CD4 T cells but do not regulate IL-17A production by IL-1β+IL-23-stimulated $CD27^-$ γδ T cells.

4.3 Discussion

Several studies have investigated the mechanism of IL-10-mediated suppression with regards to the induction of inflammation. IL-10 suppresses antigen-specific IFN-γ and TNF production in EAE [308]. In the present study, neutralisation of IL-10R signalling enhanced TCR-induced IFN-γ production. Furthermore, blocking IL-10-mediated signalling in mice with EAE did not enhance MOG-specific IFN-γ or IL-17A production by CD4 T cells in the spleen. The fact that IL-10 expression is required in the CNS in order to suppress the severity of EAE suggests that IL-10 does not exert its suppressive effects during the induction phase of the autoimmune response [309].

The findings from the current study suggest that IL-10 regulates T cell activity during EAE by regulating integrin expression by T cells during the induction phase of EAE. CD11a is the α chain of the $\alpha_L\beta_2$ integrin, also known as leukocyte function-associated antigen 1 (LFA-1) [326]. CD11a expression has previously been associated with increased infiltration of Treg cells into the CNS during EAE, particularly in the absence of the α_4 integrin [327]. In the current study, neutralisation of IL-10R signalling was associated with significantly enhanced expression of CD11a by CD4 T cells and $CD27^-$ γδ T cells in the LN, but not in the CNS during active EAE. These data suggest that IL-10 suppresses integrin expression by T cells in the periphery as a regulatory mechanism to prevent them from entering into the CNS and causing damage.

CD49d expression was also assessed in both the periphery and CNS during EAE. CD49d is the α chain of the $\alpha_4\beta_1$ integrin, also known as VLA-4. CD49d has an established role in T cell migration into the CNS during EAE [328]. Targeting VLA-4 inhibits vascular cellular adhesion molecule-1 (VCAM-1)-mediated binding of immune cells to inflamed brain vessels and subsequent entry into the CNS. VLA-4 is also a therapeutic target for the treatment of MS. Natalizumab is an anti-VLA-4 monoclonal antibody, which prevents leukocyte entry into the CNS [329]. The immunosuppressive effect of anti-VLA-4 treatment specifically on the CNS is supported by the adverse effects caused by this treatment. Natalizumab can cause progressive multifocal leukoencephalopathy (PML), resulting from a re-activation of the opportunistic John Cunningham (JC) virus that infects oligodendrocytes. The efficacy of IFN-β in the treatment of MS has been linked to reduced

VLA-4 expression levels by peripheral blood leukocytes [330]. In the present study, CD49d expression by CD4, CD8, and $CD27^-$ γδ T cells was significantly elevated in both the LNs and brains of mice with EAE following treatment with anti-CD210. These data suggest that IL-10 can suppress CD49d expression by T cells, thereby preventing their entry into the CNS. Anti-CD210 treatment during EAE significantly increased the severity of EAE which is consistent with the demonstration that IL-10 suppresses integrin expression by T cells in the periphery and prevents them from entering into the CNS, where they precipitate the clinical signs of EAE.

IL-10 can regulate immune cell migration, including T cell recruitment to the spinal cord during EAE [331]. Expansion of MOG-specific Th17 cells in the presence of IL-10 decreased expression levels of both CD11a and CD49d by T h17 cells. *In vivo* transfer of IL-10-treated Th17 cells suppressed their migration to the lung following infection with the respiratory pathogen *B. pertussis* [311]. In a murine tumour model, infiltration of IL-10 producing T cells into the TME suppressed infiltration of anti-tumour IFN-γ-producing CD8 T cells [332]. Furthermore, in a model of *Mtb* infection, IL-10 overexpression was associated with a decrease in CXCR3 expression by CD4 T cells, which were not able to migrate into the lung, increasing infection mortality [333].

The suppressive effect of IL-10 on T cell responses is not thought to be mediated by a direct effect of IL-10 on T cells. In humans, IL-10 can suppress antigen-specific T cell responses by down-regulating expression of MHC-II by monocytes thereby inhibiting T cell activation [65]. The findings of the present study suggest that IL-10 does not regulate EAE through a direct effect on T cells. Innate immune cells including monocytes, macrophages, $CD11b^-$, and $CD11b^+$ DCs in the spleens of mice with EAE expressed IL-10R, whereas T cells did not express significant levels of IL-10R. These data suggest that IL-10 may act directly on innate immune cells to modulate T cell activation or migration into the CNS during EAE. In the current study, anti-CD210 treatment significantly reduced the number of microglia in the brains of mice with EAE, suggesting that IL-10 may play a homeostatic role in maintaining microglia in the CNS. This is consistent with an *in vitro* study, which showed that IL-10 treatment promoted the expansion and phagocytic activity of microglia [334].

In addition to the increased expression of integrins by T cells during EAE, neutralisation of IL-10R enhanced cytokine production by T cells in the LN. Blocking IL-10R signalling

enhanced IFN-γ and IL-17A production by CD4 T cells, CD8 T cells, and $CD27^-$ γδ T cells in the LN of mice with EAE. These findings are consistent with the hypothesis that IL-10 neutralisation enhances APC-mediated activation of T cells in the LN during the induction phase of EAE. However, anti-CD210 treatment did not modify the number of cytokine-producing CD4 T cells or $CD27^-$ γδ T cells in the brains of mice at the peak of EAE. The disparity between cytokine production and integrin expression by T cells in the CNS is difficult to rationalise. Increased integrin expression by T cells suggests that there is increased T cell priming in the LN which leads to increased infiltration into the CNS. However, the increased expression of integrins by T cells did not lead to increased numbers of CD4 T cells or $CD27^-$ γδ T cells infiltrating the CNS. One explanation for this could be the tissue-specific role for IL-10 in regulating T cell responses. IL-10-producing CD4 T cells in the CNS have previously been shown to promote inflammation by supporting effector T cell responses [335]. The mentioned study showed that ablation of IL-10 production by CD4 T cells decreased the severity of EAE. Furthermore, CD4 T cells were identified as the target of T cell-derived IL-10. Taken together, these findings suggest that neutralisation of IL-10R in the periphery enhances T cell activation by acting on APCs but once these T cells migrate into the CNS their capacity to make cytokines is not enhanced because IL-10 is required in the CNS to support pathogenic T cell responses during EAE. Although the number of CD4 or $CD27^-$ γδ T cells was not impacted by anti-CD210 treatment during EAE, there was a significant increase in the number of CD8 T cells infiltrating the CNS in anti-CD210-treated mice. CD8 T cells are also pathogenic in EAE and are clonally expanded in the brains of MS patients [336].

Studies using IL-10-producing Tr1 cells showed that autoantigen-specific Th1 and Th17 cells can be suppressed by Tr1 cells *in vitro*. In the present study, co-culture of MOG-specific Tr1 cells with CD4 effector T cells purified from MOG-immunised mice significantly reduced MOG, IL-1β+IL-23-induced IL-17A and IFN-γ production by CD4 T cells. The suppressive effect of expanded Tr1 cells on MOG-specific IL-17A production was partially dependent on IL-10, suggesting that Tr1 cells may act by both contact-dependent and contact-independent methods. The requirement for APCs is crucial to the suppression of antigen-specific CD4 T cell function by Treg cells, regardless of their production of anti-inflammatory cytokines [337]. The ability of IL-17A-producing γδ T cells to escape

regulation by Tr1 cells in the present study is potentially due to their capacity to become activated by the cytokines IL-1β and IL-23 in the absence of TCR engagement [169]. γδ T cells are a critical early source of IL-17A which is required to mobilise innate immune cells that kickstart the inflammatory autoimmune cascade in EAE [171]. The findings of the current study unveil a novel mechanism whereby IL-17A-producing γδ T cells can escape regulation which allows them to precipitate autoimmunity.

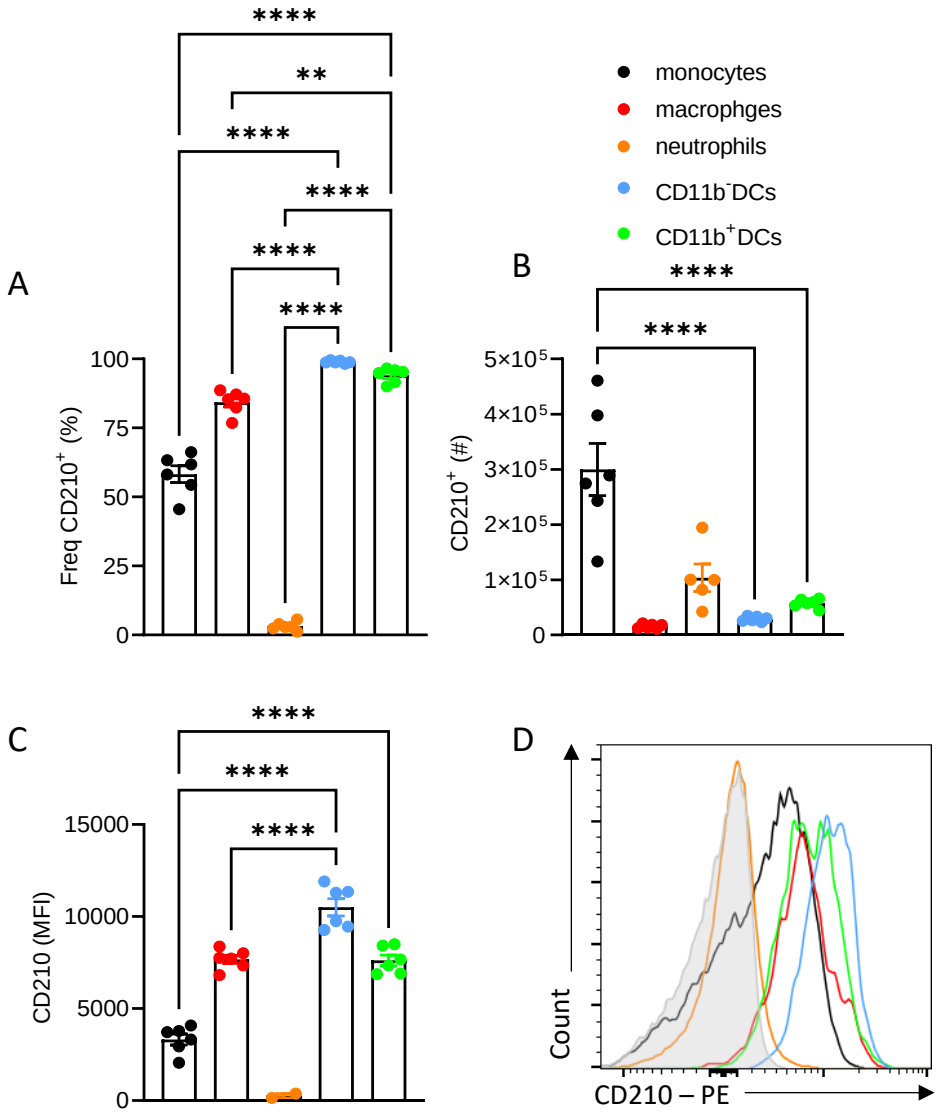

Figure 4.1 DCs express high levels of CD210 in the spleen during EAE. EAE was induced in C57BL/6J mice. On day 6 of EAE, mice were sacrificed, and spleens were harvested. Spleen cells were stained for surface CD11b, CD11c, F4/80, Ly6c, Ly6g, and MHC-II and analysed by flow cytometry. Innate immune cells were gated according to the gating strategy in figure 2.2.17.3. Results are (A) frequency, (B) absolute number, and (C) MFI of CD210-expressing innate immune cell subsets in the spleen on day 6 of EAE with (D) representative FACS plots. Data are mean ± SEM for n=6 mice per group and are representative of two independent experiments. $^{**}p < 0.01$, $^{****}p < 0.0001$ by one-way ANOVA with Tukey's multiple comparisons test.

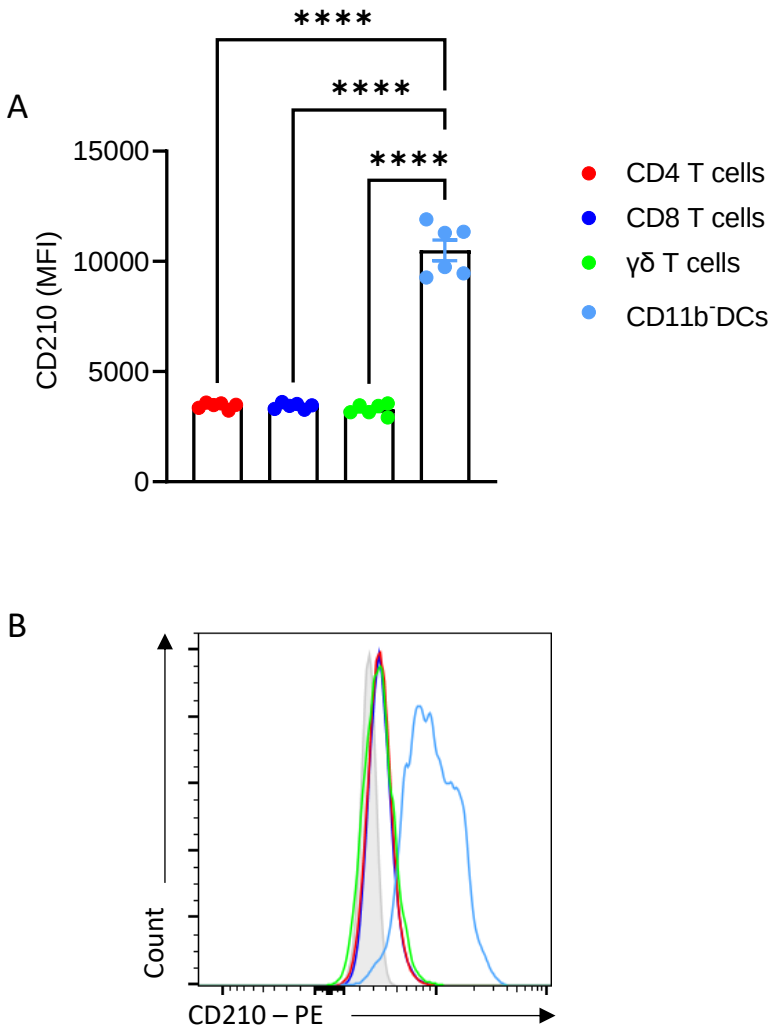

Figure 4.2 T cells express low levels of CD210 in the spleen during EAE when compared with DCs. EAE was induced in C57BL/6J mice. On day 6 of EAE, mice were sacrificed, and spleens were harvested. Spleen cells were stained for surface CD11b, CD11c, CD3, CD4, CD8, F4/80, Ly6c, MHC-II, and TCRδ and analysed by flow cytometry. Innate immune cells were gated according to the gating strategy in figure 2.2.17.3. Results are (A) MFI of CD210-expressing T cell subsets in the spleen on day 6 of EAE with (B) representative FACS plots. Data are mean ± SEM for n=6 mice per group and are representative of two independent experiments. $^{****}p < 0.0001$ by one-way ANOVA with Tukey's multiple comparisons test.

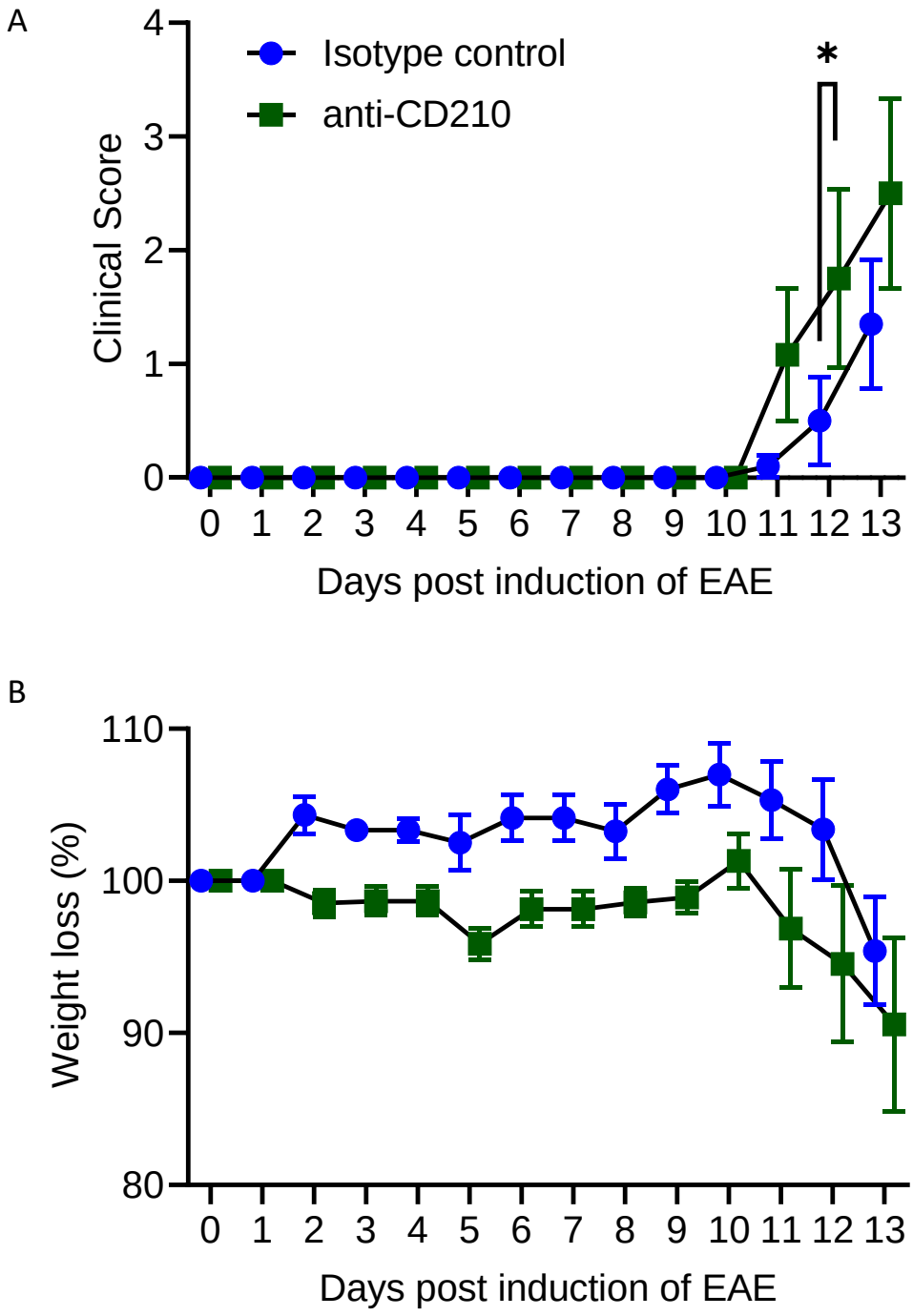

Figure 4.3 Treatment with IL-10R neutralising antibody (anti-CD210) increases the severity of EAE. EAE was induced in C57BL/6J mice by s.c injection of MOG emulsified in CFA. Mice were injected i.p with 250 ng PT on day 0. Mice were injected i.p with 200 µg of CD210 neutralising antibody or IgG2a isotype control antibody on the day prior to induction of EAE and on days 2 and 5 of EAE. Mice were assessed daily for the development of EAE by (A) clinical score and (B) % weight loss. Data are mean ± SEM for n=6 mice per group and are representative of two independent experiments. $^{*}p < 0.05$ by two-way ANOVA with Sidak's multiple comparisons test.

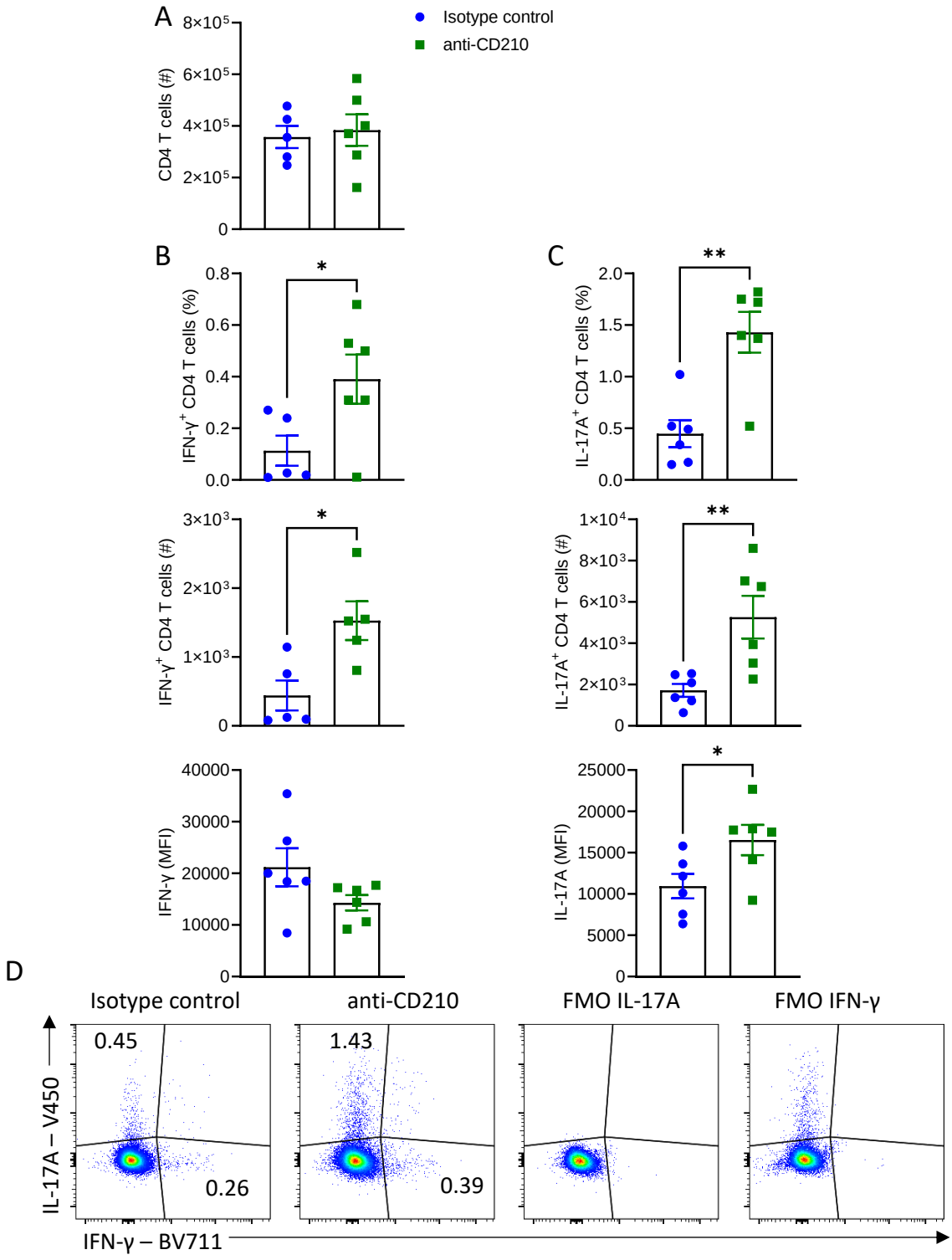

Figure 4.4 Treatment with anti-CD210 during EAE increases IFN-γ and IL-17A production by CD4 T cells in the LN. EAE was induced in C57BL/6J mice. Mice were injected i.p with 200 µg of CD210 neutralising antibody or IgG2a isotype control antibody on the day prior to induction of EAE and on days 2 and 5 of EAE. On day 6 of EAE, LNs were harvested and incubated with PMA, ionomycin, and brefeldin A for 4 hours followed by staining for surface CD3, CD4, and intracellular IFN-γ, and IL-17A and flow cytometric analysis. Results are (A) absolute number of CD4 T cells in the LN on day 6 of EAE. Frequency, absolute number, and MFI of (B) IFN-γ and (C) IL-17A-producing CD4 T cells with (D) representative FACS plots. Data are mean ± SEM for n=6 mice per group and are representative of two independent experiments. $^{*}p < 0.05$, $^{**}p < 0.01$ by unpaired Student's *t* test.

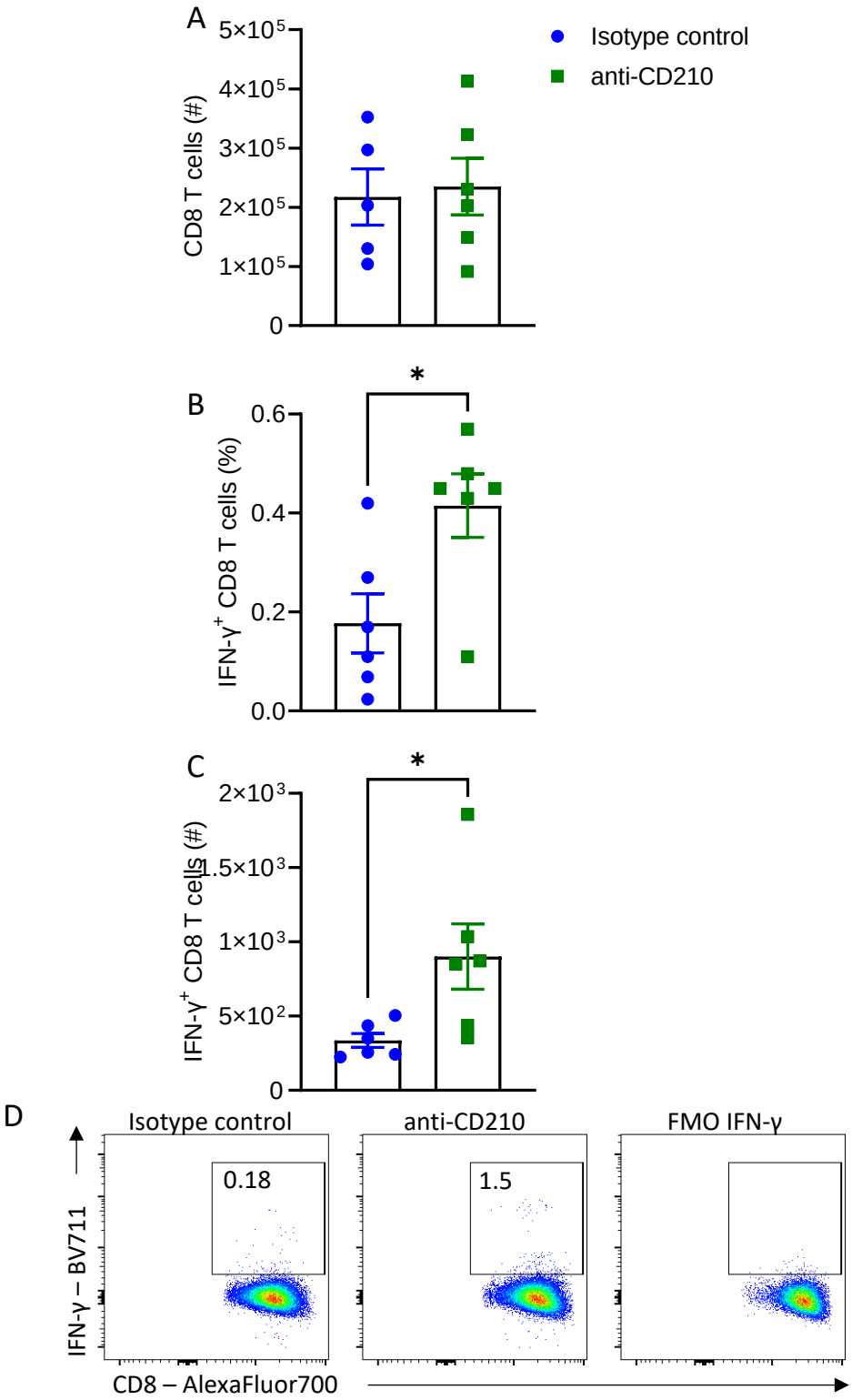

Figure 4.5 Treatment with anti-CD210 during EAE increases IFN-γ production by CD8 T cells in the LN. EAE was induced in C57BL/6J mice. Mice were injected i.p with 200 µg of CD210 neutralising antibody or IgG2a isotype control antibody on the day prior to induction of EAE and on days 2 and 5 of EAE. On day 6 of EAE, LNs were harvested and incubated with PMA, ionomycin, and brefeldin A for 4 hours followed by staining for surface CD3, CD8, and intracellular IFN-γ and flow cytometric analysis. Results are (A) absolute number of CD8 T cells in the LN on day 6 of EAE. (B) Frequency and (C) absolute number of IFN-γ-producing CD8 T cells with (D) representative FACS plots. Data are mean ± SEM for n=6 mice per group and are representative of two independent experiments. $^{*}p < 0.05$, by unpaired Student's *t* test.

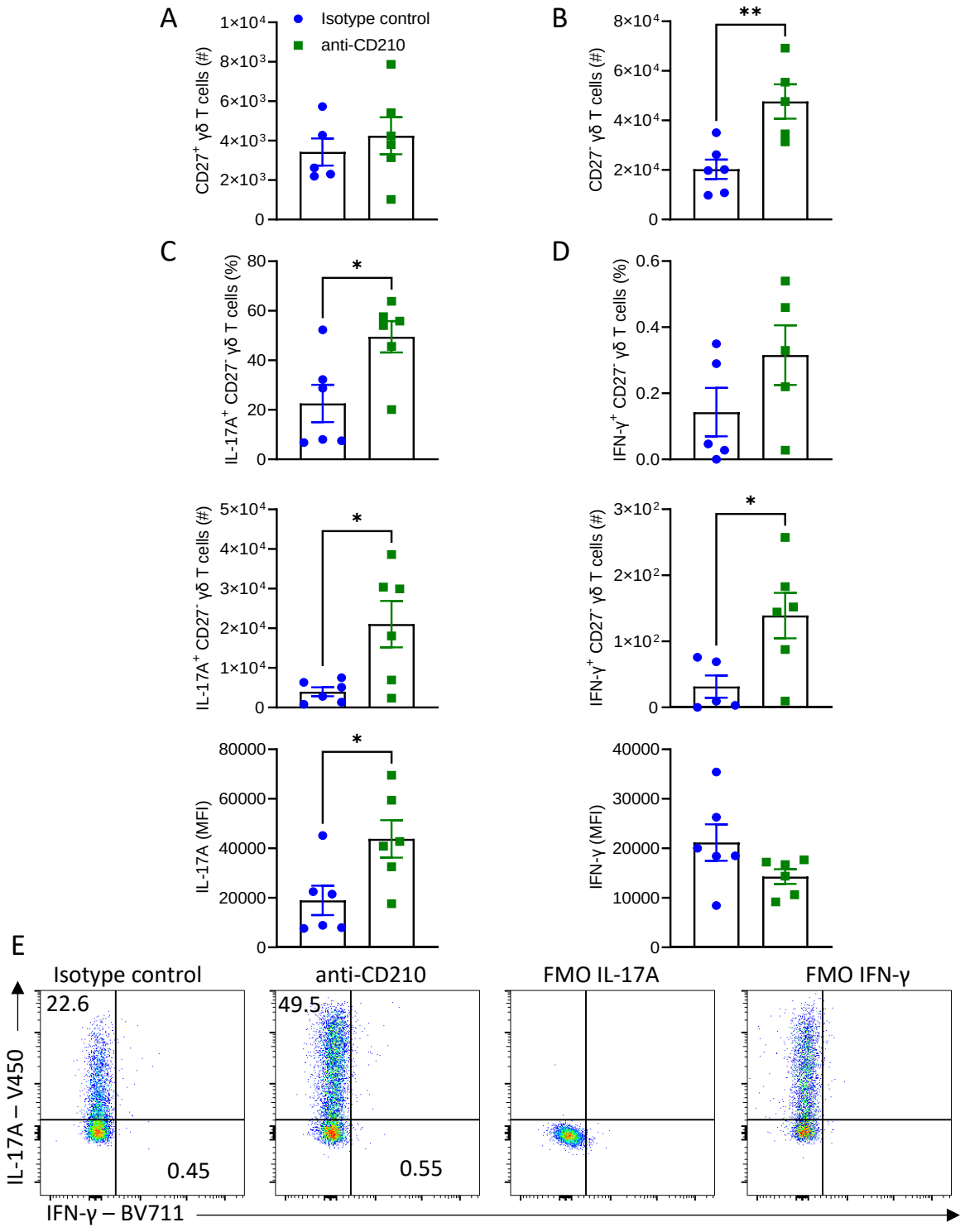

Figure 4.6 Treatment with anti-CD210 during EAE increases IFN-γ and IL-17A production by CD27⁻ γδ T cells in the LN. EAE was induced in C57BL/6J mice. Mice were injected i.p with 200 µg of CD210 neutralising antibody or IgG2a isotype control antibody on the day prior to induction of EAE and on days 2 and 5 of EAE. On day 6 of EAE, LNs were harvested and incubated with PMA, ionomycin, and brefeldin A for 4 hours followed by staining for surface CD3, CD27, TCRδ, and intracellular IFN-γ, and IL-17A and flow cytometric analysis. Results are absolute number of (A) CD27⁺ γδ T cells and (B) CD27⁻ γδ T cells in the LN on day 6 of EAE. Frequency, absolute number, and MFI of (C) IFN-γ and (D) IL-17A-producing CD27⁻ γδ T cells with (E) representative FACS plots. Data are mean ± SEM for n=6 mice per group and are representative of two independent experiments. $^{*}p < 0.05$, $^{**}p < 0.01$ by unpaired Student's *t* test.

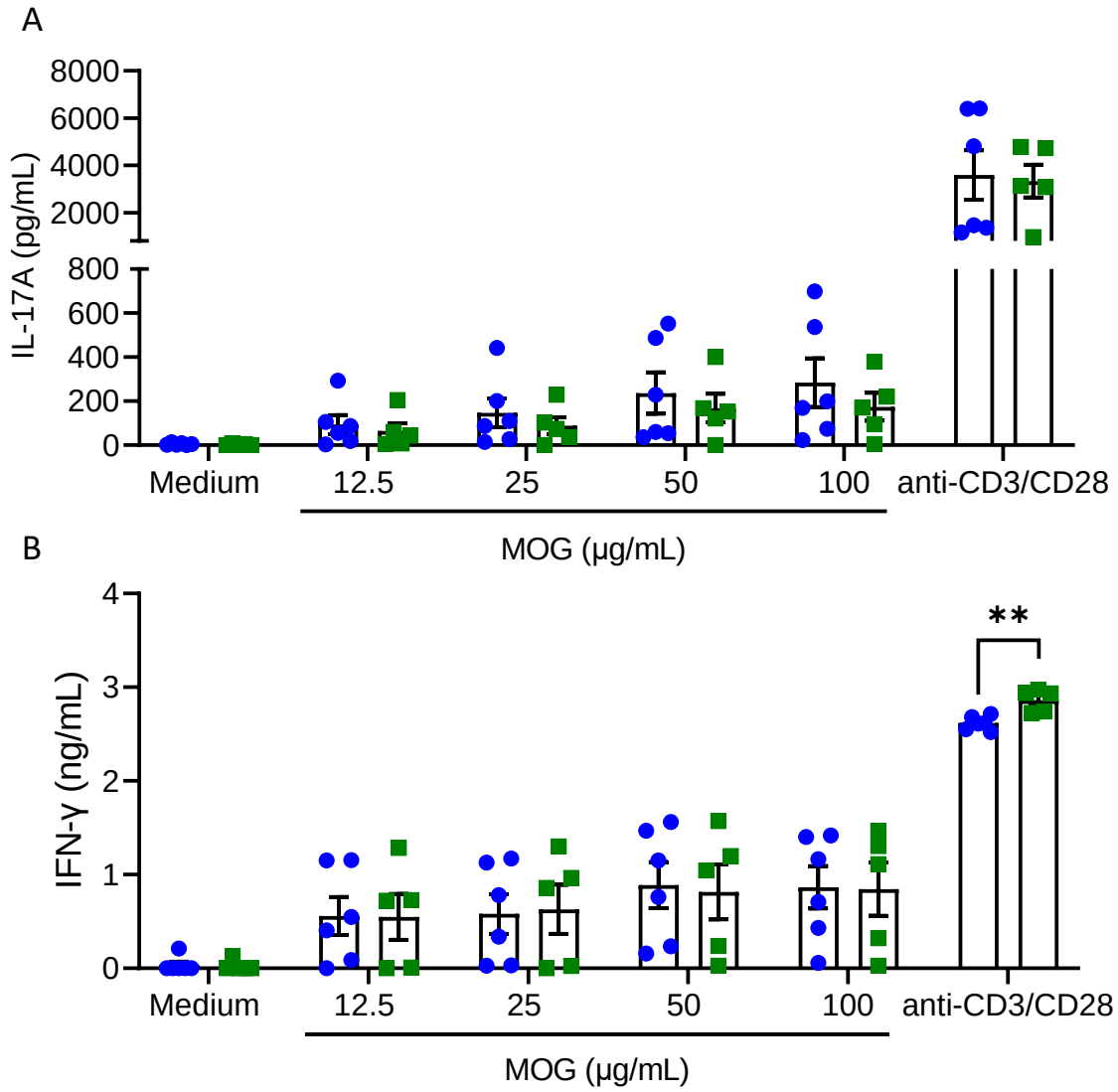

Figure 4.7 Treatment with anti-CD210 does not increase MOG-specific T cell responses in the spleen and LN during EAE. EAE was induced in C57BL/6J mice. Mice were injected i.p with 200 µg of CD210 neutralising antibody or IgG2a isotype control antibody on the day prior to induction of EAE and on days 2 and 5 of EAE. On day 10 of EAE, LNs and spleens were harvested and cultured *in vitro* for 72 hours with increasing concentrations of MOG (12.5, 25, 50, and 100 µg/mL). Supernatants were collected and concentrations of cytokines were quantified by ELISA. Results are MOG-specific (A) IL-17A and (B) IFN-γ production by LN and spleen culture of isotype control-treated versus anti-CD210-treated mice. Data are mean ± SEM for n=6 mice per group and are representative of two independent experiments. $^{**}p < 0.01$ by unpaired Student's *t* test.

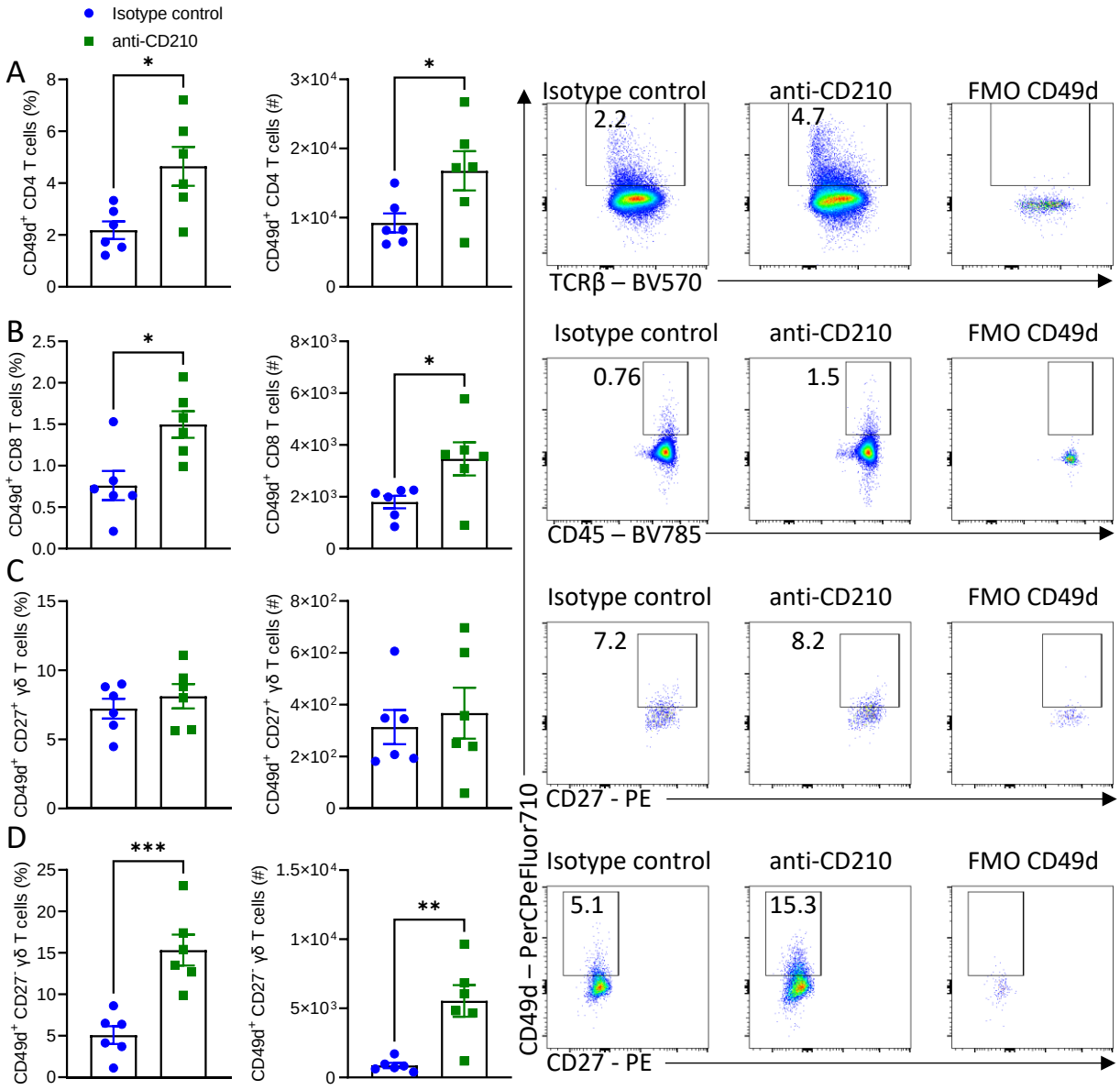

Figure 4.8 Treatment with anti-CD210 during EAE significantly increases CD49d expression by T cell subsets in the LN. EAE was induced in C57BL/6J mice. Mice were injected i.p with 200 µg of CD210 neutralising antibody or IgG2a isotype control antibody on the day prior to induction of EAE and on days 2 and 5 of EAE. On day 6 of EAE, LNs were harvested and stained for surface CD3, CD4, CD8, CD27, TCRδ, and CD49d followed by flow cytometric analysis. Results are frequency, absolute number, and representative FACS plots of CD49d expression by (A) CD4, (B) CD8, (C) $CD27^+$ γδ, and (D) $CD27^-$ γδ T cells in the LN on day 6 of EAE. Data are mean ± SEM for n=6 mice per group and are representative of two independent experiments. $^*p < 0.05$, $^{**}p < 0.01$, $^{***}p < 0.001$ by unpaired Student's *t* test.

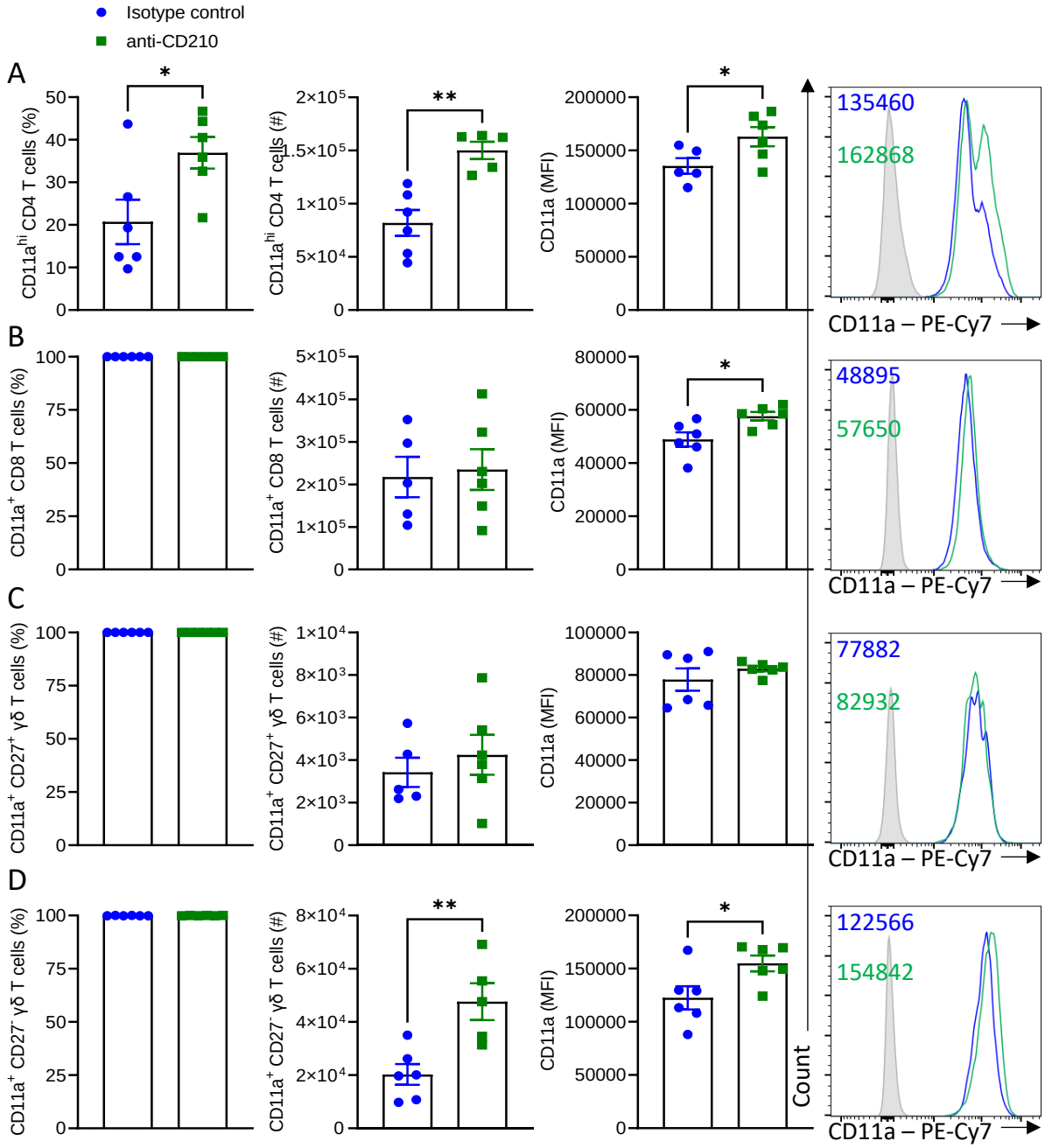

Figure 4.9 Treatment with anti-CD210 during EAE significantly increases CD11a expression by T cell subsets in the LN. EAE was induced in C57BL/6J mice. Mice were injected i.p with 200 µg of CD210 neutralising antibody or IgG2a isotype control antibody on the day prior to induction of EAE and on days 2 and 5 of EAE. On day 6 of EAE, LNs were harvested and stained for surface CD3, CD4, CD8, CD27, TCRδ, and CD11a followed by flow cytometric analysis. Results are frequency, absolute number, MFI, and representative FACS plots of CD11a expression by (A) CD4 (B) CD8, (C) $CD27^+$ γδ, and (D) $CD27^-$ γδ T cells in the LN on day 6 of EAE. Data are mean ± SEM for n=6 mice per group and are representative of two independent experiments. $^*p < 0.05$, $^{**}p < 0.01$ by unpaired Student's *t* test.

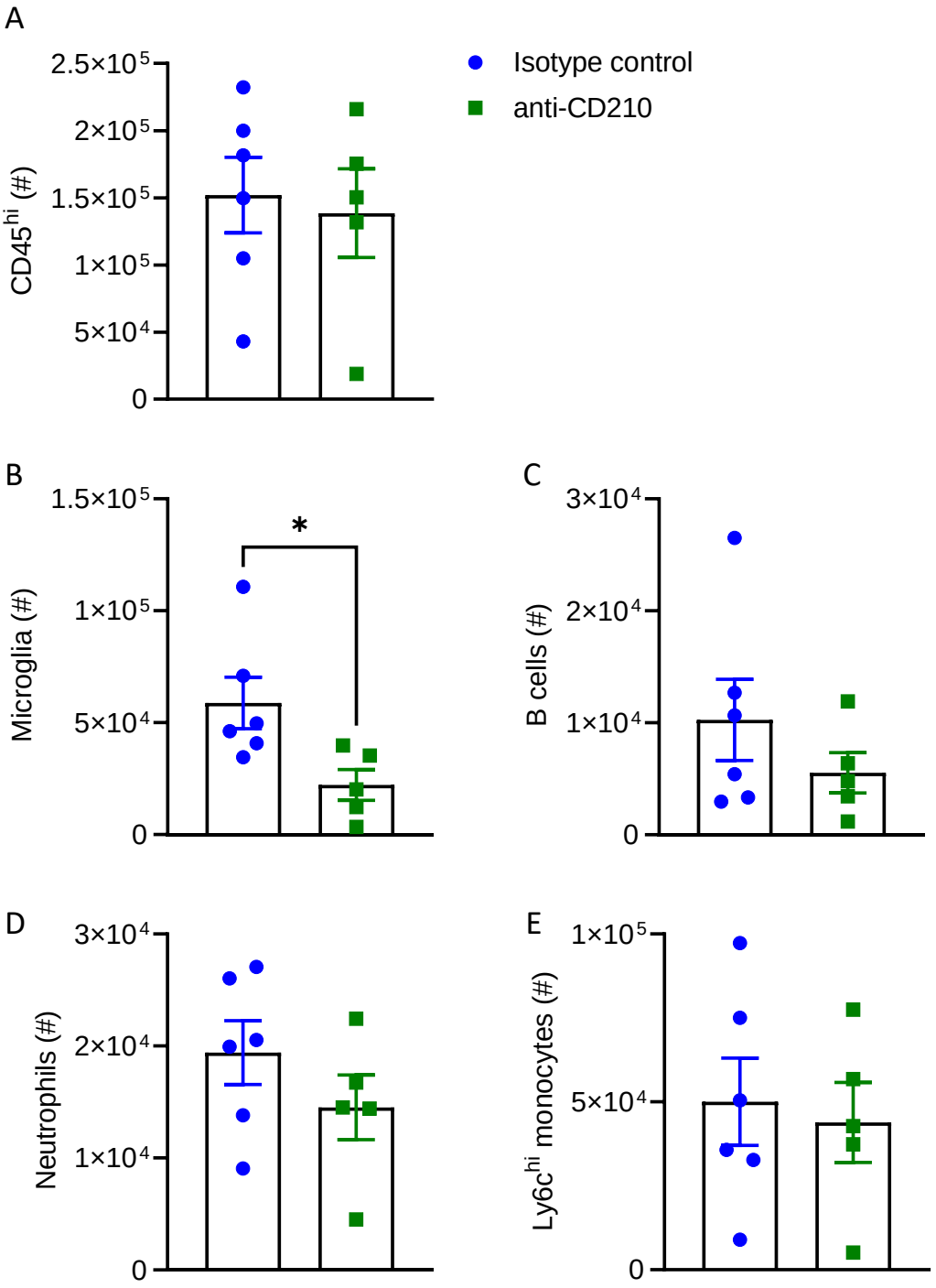

Figure 4.10 Neutralisation of IL-10R-mediated signalling during EAE significantly reduces the number of microglia in the brain at the peak of disease. EAE was induced in C57BL/6J mice. Mice were injected i.p with 200 µg of CD210 neutralising antibody or IgG2a isotype control antibody on the day prior to induction of EAE and on days 2 and 5 of EAE. On day 13 of EAE, mice were sacrificed and perfused with PBS. Brains of mice were harvested and processed into single cell suspensions followed by staining for B220, CD11b, CD45, Ly6cs and Ly6g and analysis by flow cytometry. Immune cells were gated according to the gating strategy in figure 2.2.17.4. Results are absolute number of (A) $CD45^{hi}$, (B) microglia, (C) B cells, (D) neutrophils, and (E) $Ly6c^{hi}$ monocytes in the brain on day 13 of EAE. Data are mean ± SEM for n=6 mice per group and are representative of two independent experiments. $^{*}p < 0.05$ by unpaired Student's *t* test.

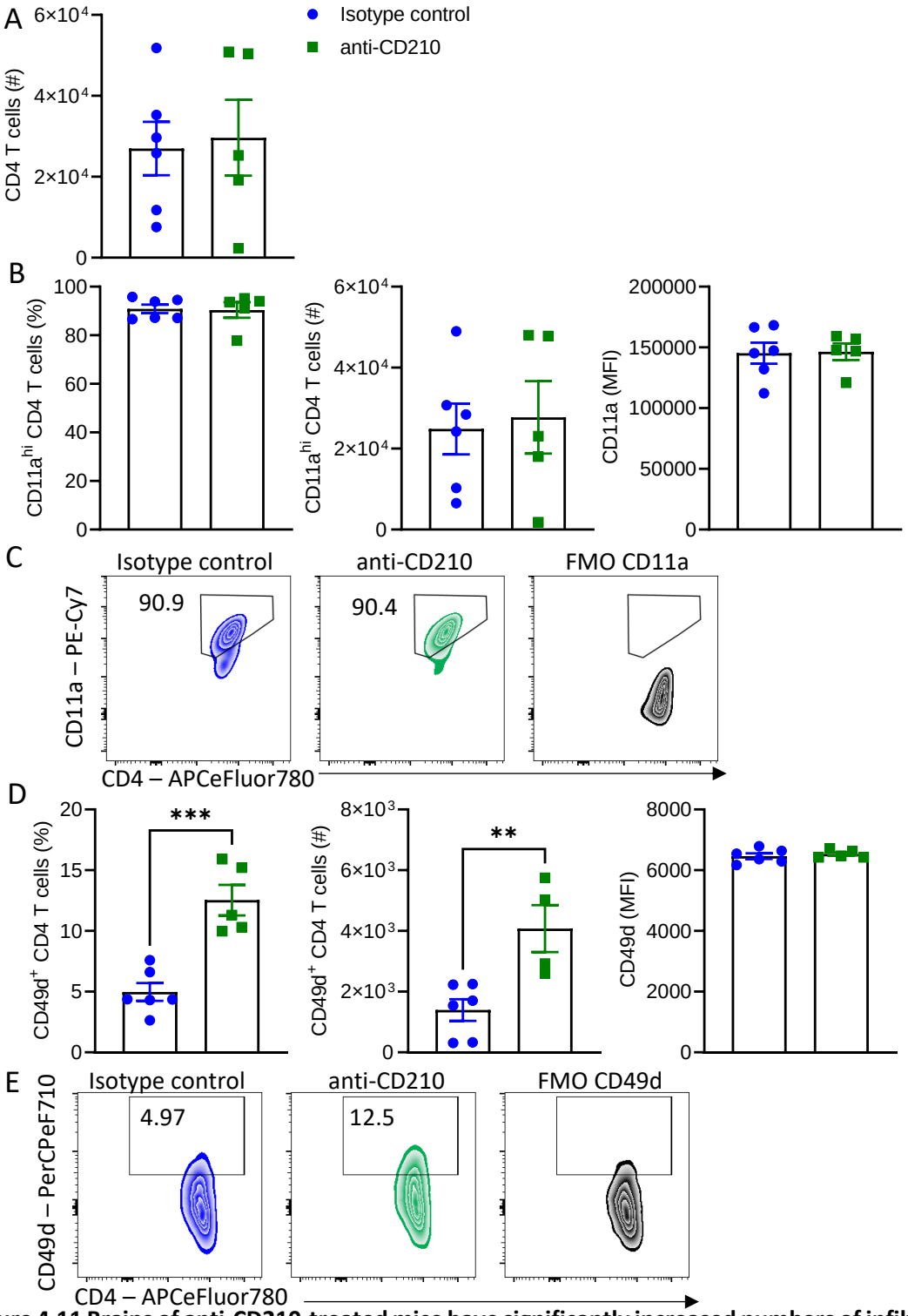

Figure 4.11 Brains of anti-CD210-treated mice have significantly increased numbers of infiltrated CD49d-expressing CD4 T cells at the peak of EAE. EAE was induced in C57BL/6J mice. Mice were injected i.p with 200 µg of CD210 neutralising antibody or IgG2a isotype control antibody on the day prior to induction of EAE and on days 2 and 5 of EAE. On day 13 of EAE, mice were sacrificed and perfused with PBS. Brains of mice were harvested and processed into single cell suspensions followed by staining for CD3, CD11a, CD4, and CD49d and analysis by flow cytometry. Results are absolute number of (A) CD4 T cells, frequency, absolute number, and MFI of (B) CD11a expression by CD4 T cells with (C) representative FACS plots and (D) CD49d expression by CD4 T cells with (E) representative FACS plots in the brain on day 13 of EAE. Data are mean ± SEM for n=6 mice per group and are representative of two independent experiments. $^{**}p < 0.01$, $^{***}p < 0.001$ by unpaired Student's *t* test.

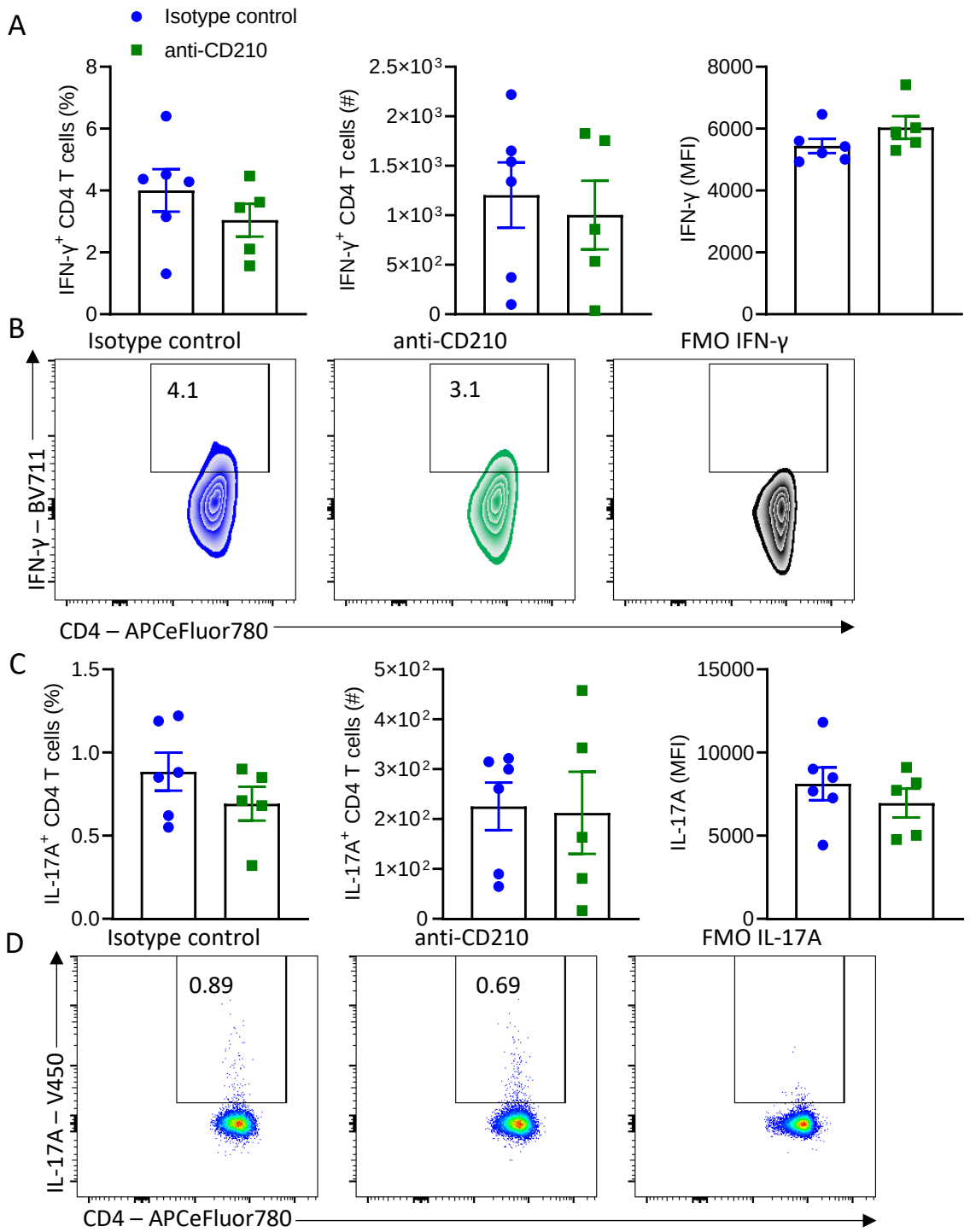

Figure 4.12 Neutralisation of IL-10R signalling does not affect cytokine production by brain-infiltrating CD4 T cells at the peak of EAE. EAE was induced in C57BL/6J mice. Mice were injected i.p with 200 µg of CD210 neutralising antibody or IgG2a isotype control antibody on the day prior to induction of EAE and on days 2 and 5 of EAE. On day 13 of EAE, mice were sacrificed and perfused with PBS. Brains of mice were harvested and processed into single cell suspensions followed by incubation with PMA, ionomycin, and brefeldin A for 4 hours, staining for surface CD3, CD4, and intracellular IFN-γ, and IL-17A and analysis by flow cytometry. Results are frequency, absolute number, and MFI of (A) IFN-γ expression by CD4 T cells with (B) representative FACS plots and frequency, absolute number, and MFI of (C) IL-17A expression by CD4 T cells with (D) representative FACS plots. Data are mean ± SEM for n=6 mice per group and are representative of two independent experiments.

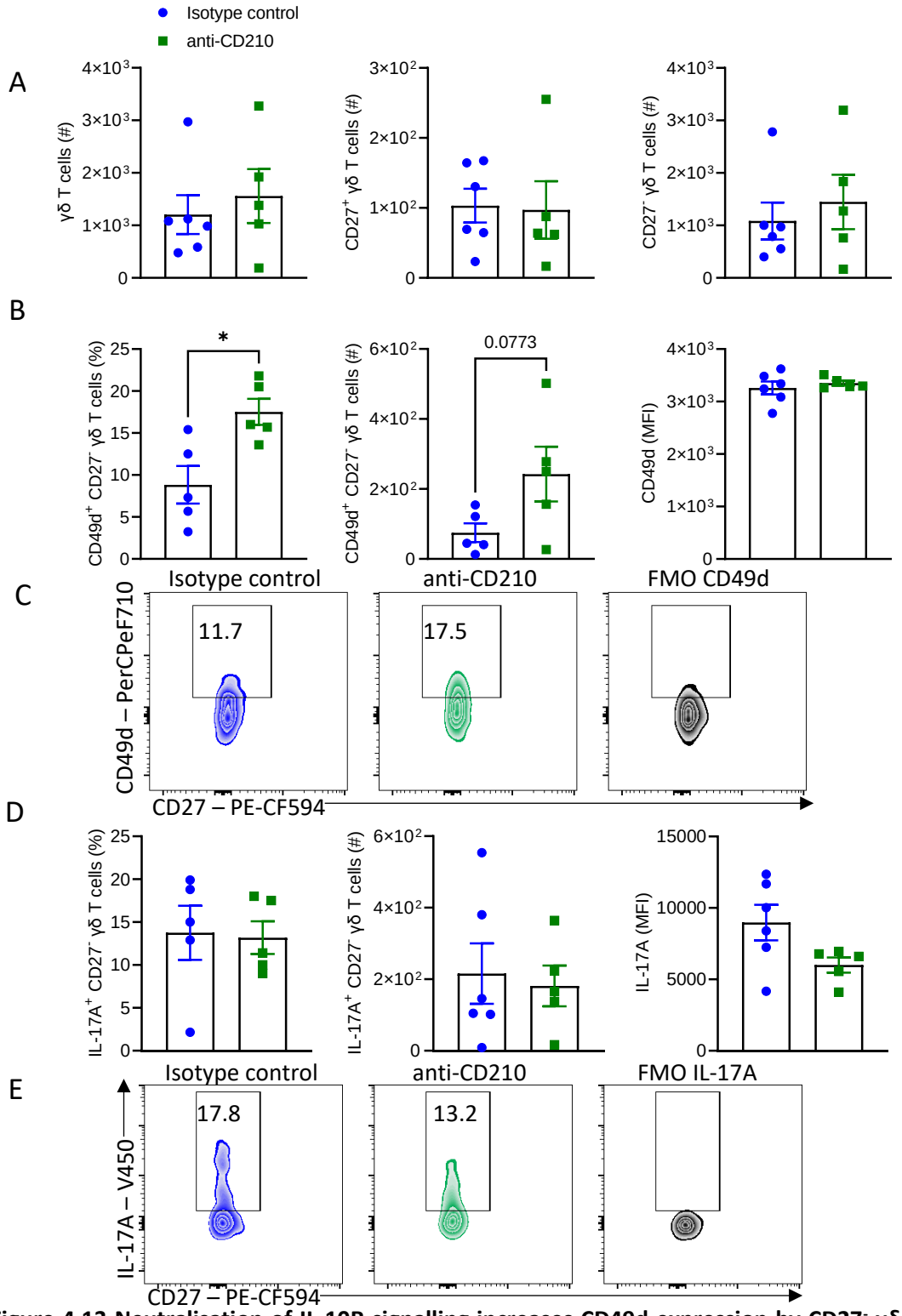

Figure 4.13 Neutralisation of IL-10R signalling increases CD49d expression by CD27$^-$ γδ T cells infiltrating the brain at the peak of EAE. EAE was induced in C57BL/6J mice. Mice were injected i.p with 200 µg of CD210 neutralising antibody or IgG2a isotype control antibody on the day prior to induction of EAE and on days 2 and 5 of EAE. On day 13 of EAE, mice were sacrificed and perfused with PBS. Brains of mice were harvested and processed into single cell suspensions followed by incubation with PMA, ionomycin, and brefeldin A for 4 hours, staining for surface CD3, CD27, CD49d, TCRδ, and intracellular IL-17A and analysis by flow cytometry. Results are (A) absolute number of γδ T cell populations. (B) Frequency, absolute number, and MFI of CD49d expression by CD27$^-$ γδ T cells with (C) representative FACS plots and (D) frequency, absolute number, and MFI of IL-17A expression by CD27$^-$ γδ T cells with (E) representative FACS plots. Data are mean ± SEM for n=6 mice per group and are representative of two independent experiments. $^*p < 0.05$ by unpaired Student's *t* test.

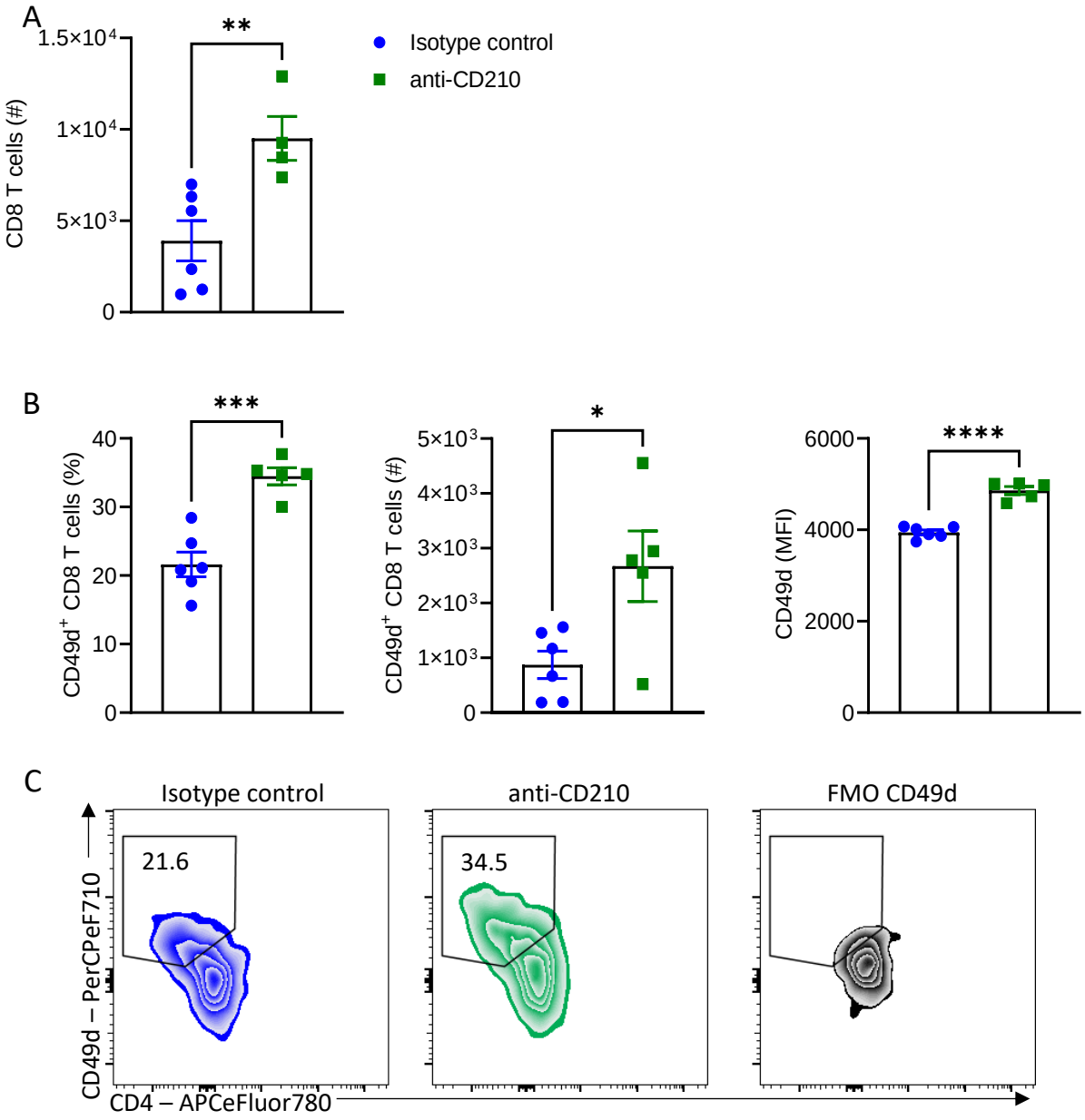

Figure 4.14 Neutralisation of IL-10R signalling increases CD49d expression by CD8 T cells infiltrating the brain at the peak of EAE. EAE was induced in C57BL/6J mice. Mice were injected i.p with 200 µg of CD210 neutralising antibody or IgG2a isotype control antibody on the day prior to induction of EAE and on days 2 and 5 of EAE. On day 13 of EAE, mice were sacrificed and perfused with PBS. Brains of mice were harvested and processed into single cell suspensions followed by staining for surface CD3, CD8, CD49d and analysis by flow cytometry. Results are (A) absolute number of CD8 T cells in the brain. (B) Frequency, absolute number, and MFI of CD49d expression by CD8 T cells with (C) representative FACS plots. Data are mean ± SEM for n=6 mice per group and are representative of two independent experiments. $^{*}p < 0.05$, $^{**}p < 0.01$, $^{***}p < 0.001$, $^{****}p < 0.0001$ by unpaired Student's *t* test.

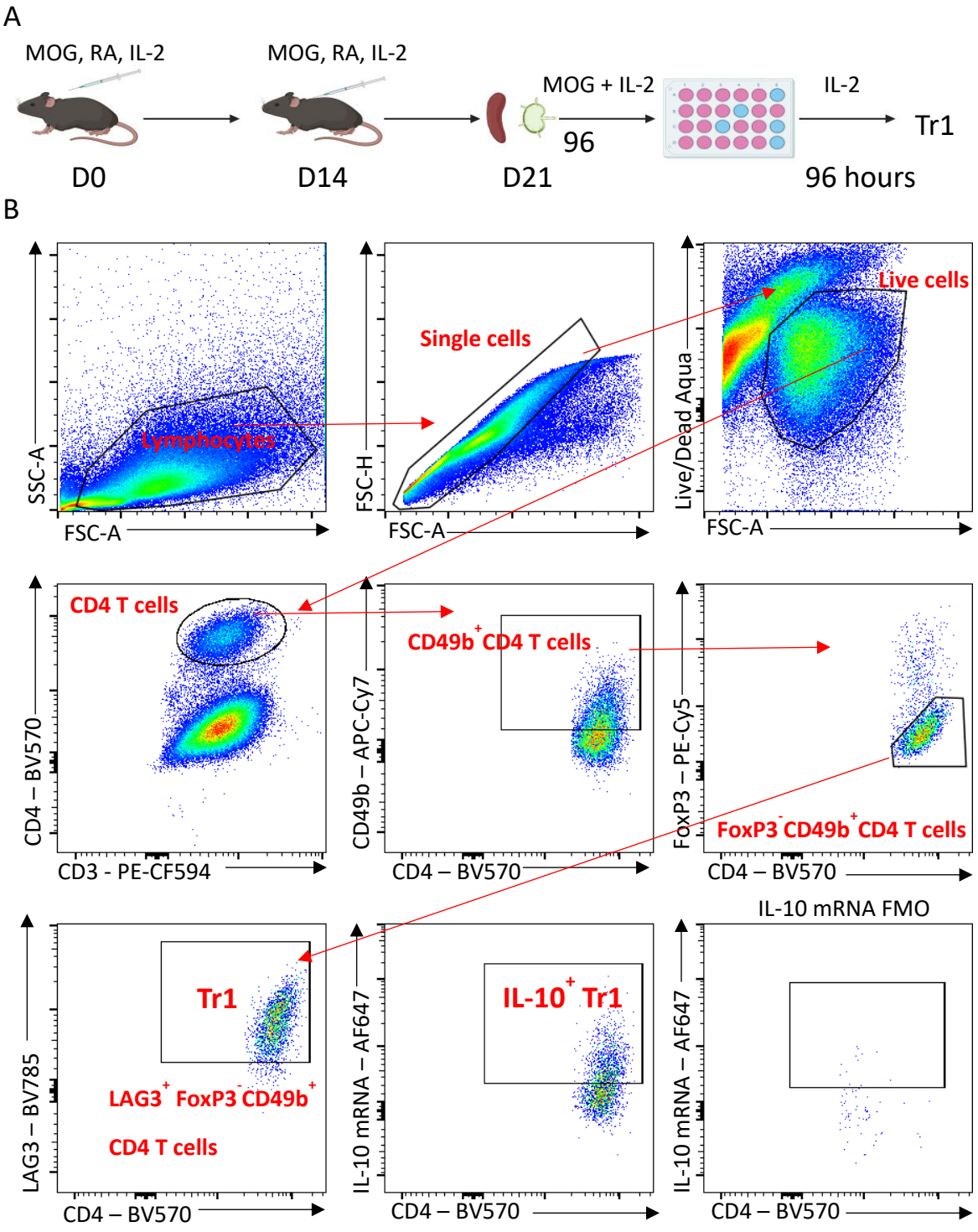

Figure 4.15 Experimental method and gating strategy for identifying Tr1 cells from expansion culture. (A) C57BL/6J mice were immunised s.c with MOG (100 µg), IL-2 (500 ng) and retinoic acid (400 µg) on days 0 and 14. On day 21, mice were sacrificed, and spleen and LN cells were harvested. Cells were cultured *in vitro* for 8 days with MOG (100 µg/mL), IL-2 (10 ng/mL), and retinoic acid (1 µM). Cells were stained for surface CD3, CD4, CD49b, LAG3, intracellular FoxP3, and IL-10 mRNA by Primeflow RNA assay. (B) MOG-specific Tr1 cells were identified according to the gating strategy shown above; CD4 T cells expressing CD49b and LAG3 that lack FoxP3 expression.

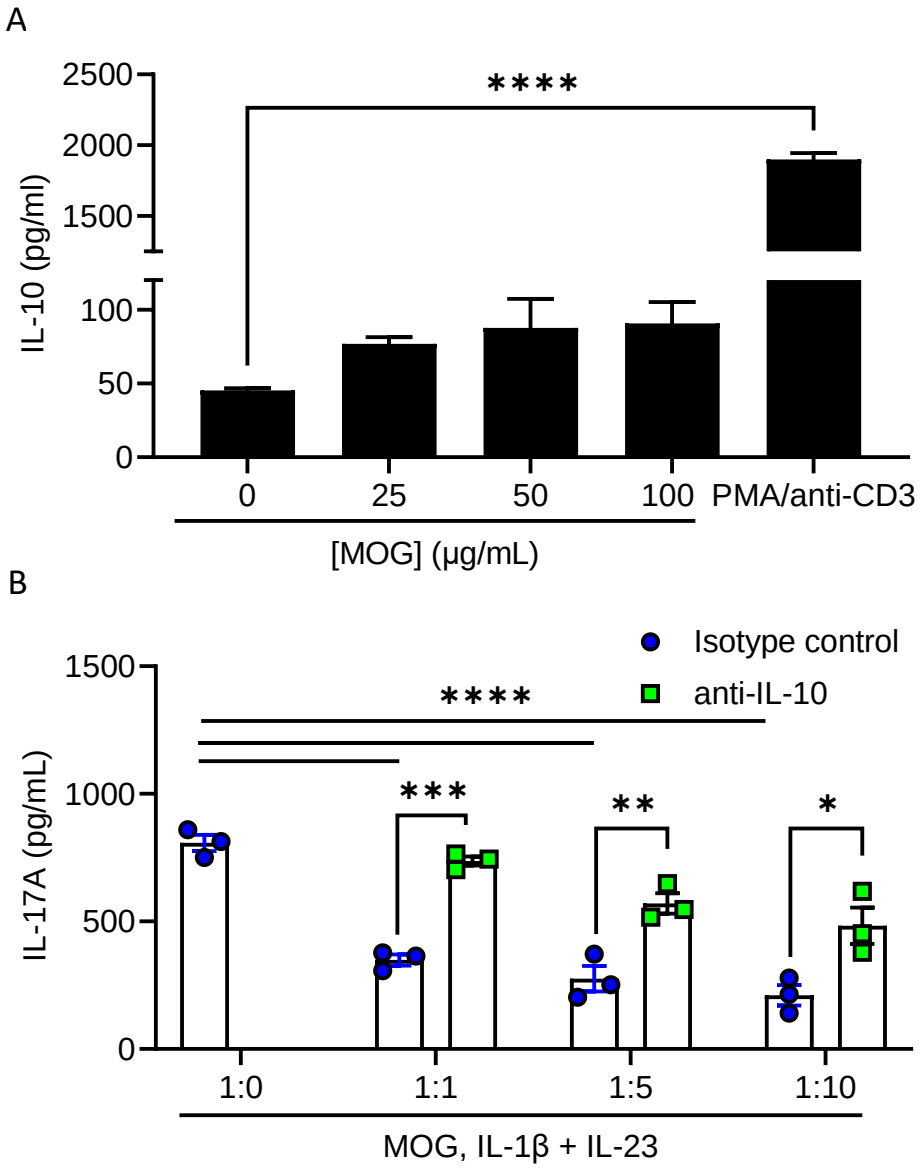

Figure 4.16 Suppression of IL-17A-producing MOG-specific CD4 T cells by MOG-specific Tr1 cells is IL-10 dependent. MOG-specific Tr1 cells were expanded according to the schematic shown in figure 4.15 A. Cells were harvested and stimulated *in vitro* with increasing concentrations of MOG or PMA and anti-CD3 in the presence of APCs. MOG-specific Tr1 cells were co-cultured at increasing ratios with CD4 T cells FACS-purified from the LN of mice with EAE in the presence of APCs and re-stimulated with MOG, IL-1β and IL-23 in addition to IL-10 neutralising antibody or isotype control antibody. Culture supernatants were collected after 72 hours. Results are (A) IL-10 concentration in the supernatants of MOG-specific Tr1 cells re-stimulated with increasing concentrations of MOG and (B) IL-17A concentration in the supernatants of MOG-specific CD4 T cells co-cultured with APCs and Tr1 cells in the presence of IL-10 neutralising antibody or isotype control antibody. Data are mean ± SD and are representative of two independent experiments. $^{*}p < 0.05$, $^{**}p < 0.01$, $^{***}p < 0.001$, $^{****}p < 0.0001$ isotype control versus anti-IL-10 by unpaired Student's *t* test or $^{****}p < 0.0001$ 1:0 versus increasing ratios of Tr1 cells by one-way ANOVA with Dunnett's multiple comparisons test.

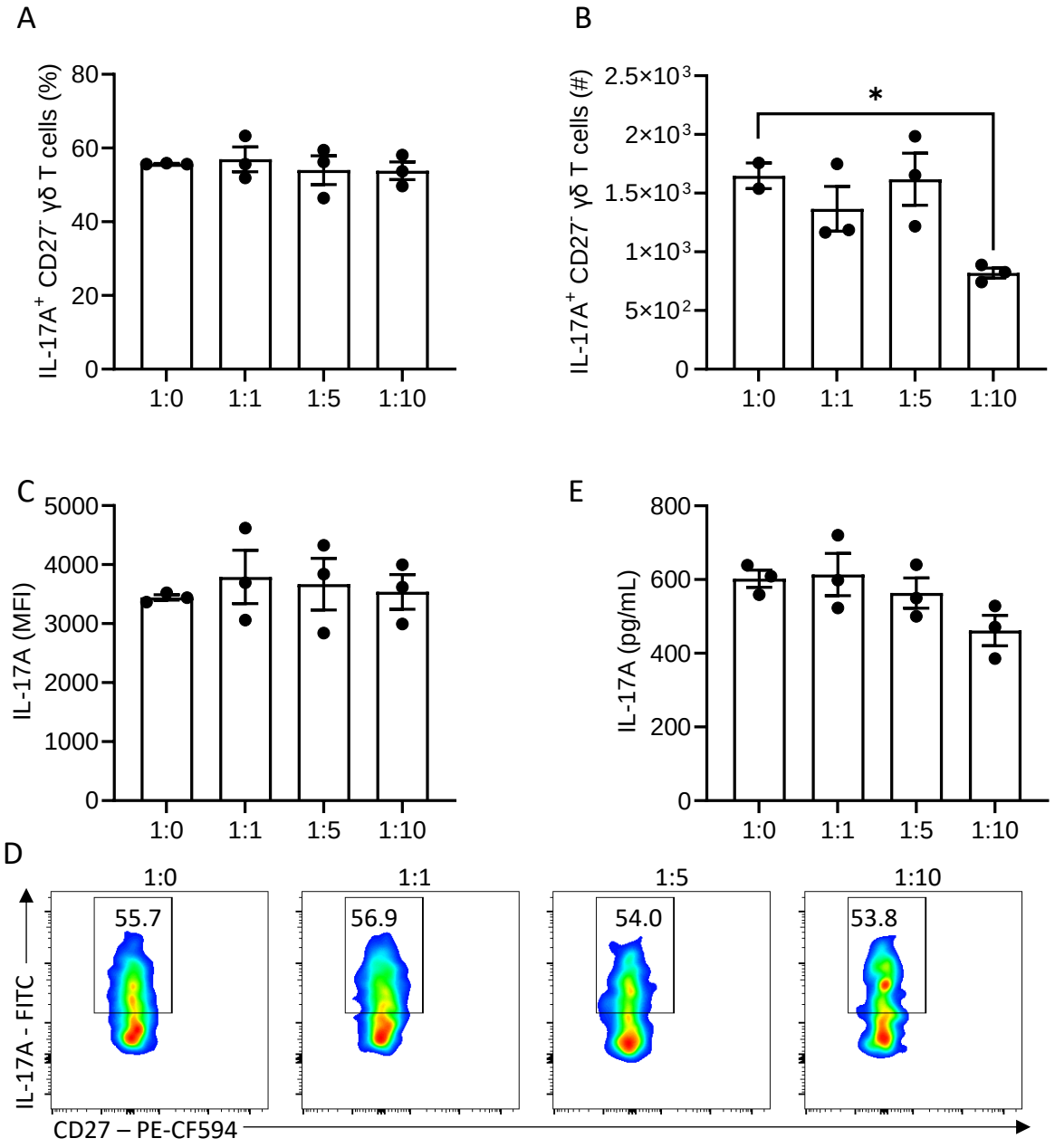

Figure 4.17 Higher ratios of MOG-specific Tr1 cells co-cultured with CD27⁻ γδ T cells isolated from MOG-immunised mice suppress IL-17A production. C57BL/6J mice were immunised with MOG emulsified in CFA. After 10 days, spleen and LNs were harvested and CD27⁻ γδ T cells were purified by FACS sorting. CD27⁻ γδ T cells were cultured in the presence of MOG (100 µg/mL), IL-1β (10 ng/mL) and IL-23 (10 ng/mL) for 3 days in the presence or absence of increasing ratios of MOG-specific Tr1 cells and APCs. MOG-specific Tr1 cells were generated according to the schematic shown in figure 4.15 A. After 72 hours, supernatants were collected for cytokine quantification by ELISA and cells were harvested and incubated with PMA, ionomycin, and brefeldin A, stained for surface CD3, CD27, TCRδ, and intracellular IL-17A and analysed by flow cytometry. Results are (A) frequency, (B) absolute number, and (C) MFI of IL-17A-producing CD27⁻ γδ T cells co-cultured with increasing ratios of MOG-specific Tr1 cells with (D) representative FACS plots. (E) IL-17A concentrations in supernatants as determined by ELISA. Data are mean ± SD and are representative of three independent experiments. $^{*}p < 0.05$, 1:0 versus increasing ratios of Tr1 cells by one-way ANOVA with Dunnett's multiple comparisons test.

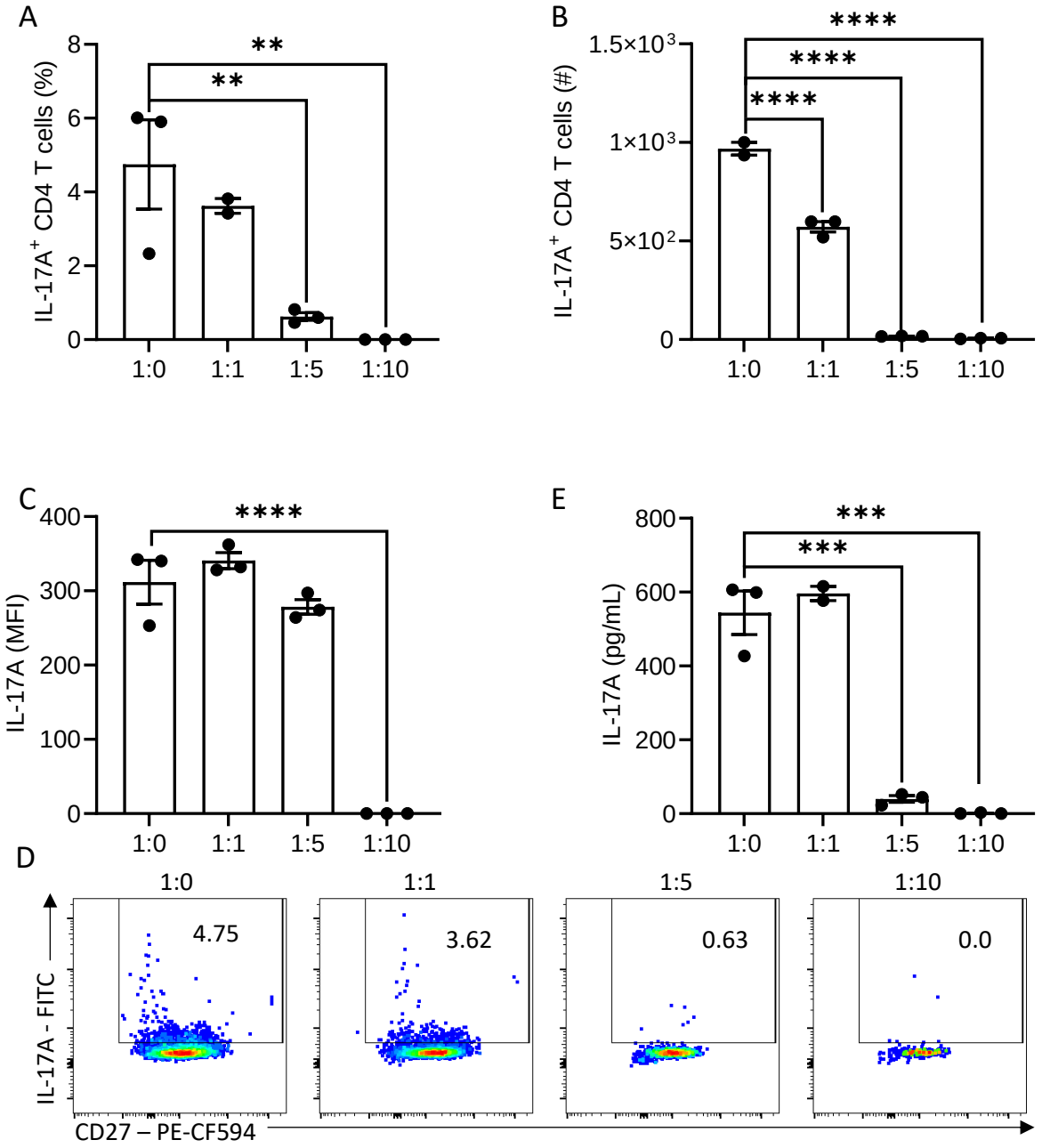

Figure 4.18 MOG-specific Tr1 cells suppress IL-17A production by CD4 T cells isolated from MOG-immunised mice. C57BL/6J mice were immunised with MOG emulsified in CFA. After 10 days, spleen and LNs were harvested and CD4 T cells were purified by FACS sorting. CD4 T cells were cultured in the presence of MOG (100 µg/mL), IL-1β (10 ng/mL) and IL-23 (10 ng/mL) for 3 days in the presence or absence of increasing ratios of MOG-specific Tr1 cells and APCs. MOG-specific Tr1 cells were generated according to the schematic shown in figure 4.15 A. After 72 hours, supernatants were collected for cytokine quantification by ELISA and cells were harvested and incubated with PMA, ionomycin, and brefeldin A and stained for surface CD3, CD4, and intracellular IL-17A and analysed by flow cytometry. Results are (A) frequency, (B) absolute number, and (C) MFI of IL-17A-producing CD4 T cells co-cultured with increasing ratios of MOG-specific Tr1 cells with (D) representative FACS plots. (E) IL-17A concentrations in supernatants as determined by ELISA. Data are mean ± SD and are representative of three independent experiments. $^{**}p < 0.01$, $^{***}p < 0.001$, $^{***}p < 0.0001$ 1:0 versus increasing ratios of Tr1 cells by one-way ANOVA with Dunnett's multiple comparisons test.

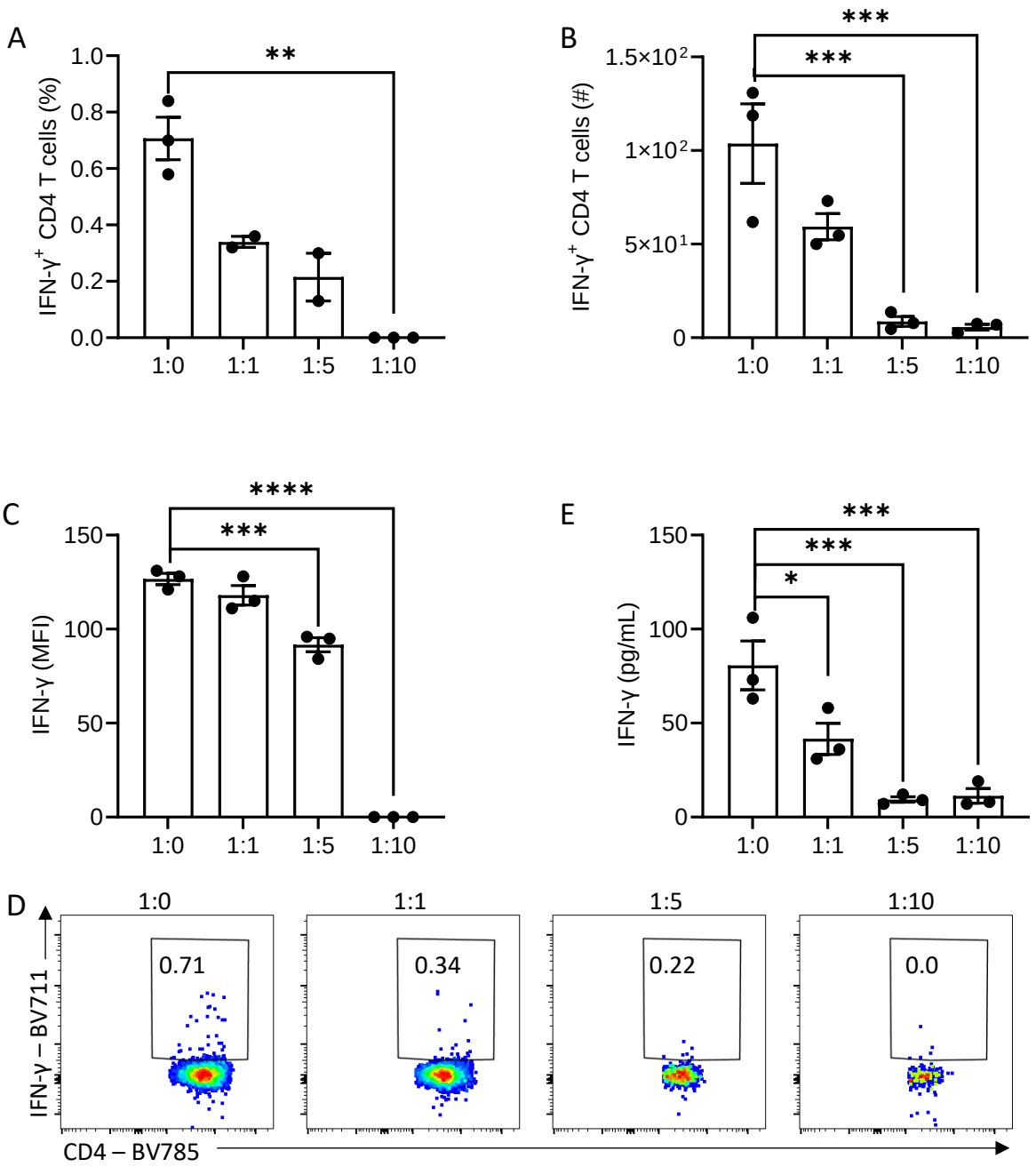

Figure 4.19 MOG-specific Tr1 cells suppress IFN-γ production by CD4 T cells isolated from MOG-immunised mice. C57BL/6J mice were immunised with MOG emulsified in CFA. After 10 days, spleen and LNs were harvested and CD4 T cells were purified by FACS sorting. CD4 T cells were cultured in the presence of MOG (100 µg/mL), IL-1β (10 ng/mL) and IL-23 (10 ng/mL) for 3 days in the presence or absence of increasing ratios of MOG-specific Tr1 cells and APCs. MOG-specific Tr1 cells were generated according to the schematic shown in figure 4.15 A. After 72 hours, supernatants were collected for cytokine quantification by ELISA and cells were harvested and incubated with PMA, ionomycin, and brefeldin A, stained for surface CD3, CD4, and intracellular IFN-γ and analysed by flow cytometry. Results are (A) frequency, (B) absolute number, and (C) MFI of IFN-γ-producing CD4 T cells co-cultured with increasing ratios of MOG-specific Tr1 cells with (D) representative FACS plots. (E) IFN-γ concentrations in supernatants as determined by ELISA. Data are mean ± SD and are representative of three independent experiments. $^{*}p < 0.05$, $^{**}p < 0.01$, $^{***}p < 0.001$ 1:0 versus increasing ratios of Tr1 cells by one-way ANOVA with Dunnett's multiple comparisons test.

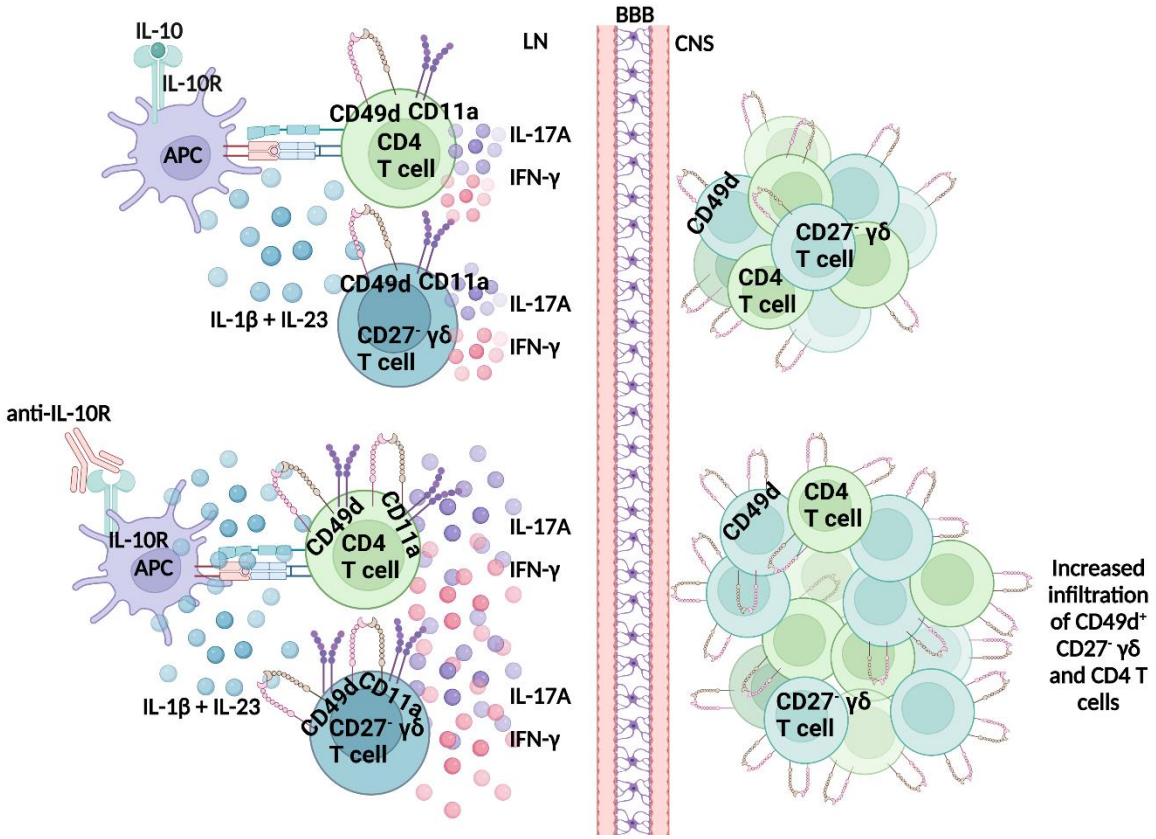

Figure 4.20 Proposed mechanism for the IL-10-mediated suppression of T cell infiltration into the CNS during EAE. IL-10 acts on APCs in the LN to regulate the induction of MOG-specific CD4 T cells and IL-17A-producing CD27$^-$ γδ T cells by production of IL-1β and IL-23. IL-17A and IFN-γ-producing CD27$^-$ γδ T cells and CD4 T cells in the periphery express CD11a and CD49d, which are components of the LFA-1 and VLA-4 integrins, respectively. CD49d expression facilitates entry of pathogenic CD27$^-$ γδ T cells and CD4 T cells into the CNS where they precipitate autoimmunity. When IL-10R signalling is blocked, priming of CD4 T cells and IL-1β+IL-23-mediated activation of CD27$^-$ γδ T cells is enhanced in the LN during the induction of EAE. Expression of LFA-1 and VLA-4 is enhanced which leads to increased infiltration of pathogenic CD27$^-$ γδ T cells and CD4 T cells into the CNS where they worsen EAE.

Chapter 5
TGF-β regulates IL-17A production by γδ T cells in an IFN-γ-dependent manner

5.1 Introduction

TGF-β is an anti-inflammatory cytokine that regulates the immune response. However, TGF-β plays a convoluted role in regulating the development and function of IL-17A-producing T cells. Treg cells regulate effector T cell responses via IL-2 over-consumption, which deprives responder T cells of IL-2 and induces their apoptosis [54]. Treg cells are also a potent source of TGF-β, which directly suppress T cell responses. CTLA-$4^{-/-}$ Treg cells can still suppress responder T cells and this is partially dependent on TGF-β [338]. Although TGF-β has broad immunosuppressive functions, it also plays a role in the development of Th17 cells. IL-6 in combination with TGF-β were initially described as key differentiation factors for Th17 cells that that co-produce IL-17A and IL-10, but these cells are not pathogenic in autoimmune diseases [34, 37]. Further studies identified IL-23 as an important cytokine for promoting the expansion and development of pathogenic Th17 cells [236]. Th17 cells that developed under the influence of IL-1β and IL-23 did not secrete IL-10 and were pathogenic in EAE. IL-1β has an established role in the induction of pathogenic Th17 cell responses in EAE [238]. More recent studies have identified an autocrine signalling mechanism that promotes the stability and pathogenicity of Th17 cells [339]. Deletion of TGF-β production by Th17 cells allowed them to become exTh17 cells that co-produced IFN-γ and IL-17A. Autocrine TGF-β signalling in Th17 cells prevented the development of pathogenic Th17 populations in EAE. The main role of TGF-β in the development of Th17 cells has been linked to suppression of IFN-γ production [45]. TGF-β is not required for the development of Th17 cells in mice that lack Tbet and STAT6 and these mice fail to develop Th1 and Th2 cells, respectively. These data suggest that TGF-β supports development of Th17 cells by suppressing Th1 cells.

As well as its role in the development of Th17 cells, TGF-β can also regulate T cell responses. Hepatitis C virus-specific Th17 cells are suppressed by TGF-β [340]. The HCV-derived protein NS4 induced TGF-β production by monocytes from HCV-infected patients. Neutralisation of TGF-β enhanced virus-specific IL-17A production by T cells from HCV-infected patients. Furthermore, helminth-induced suppression of Th17-mediated autoimmunity is partially mediated by TGF-β [341]. Infection with the helminth parasite *Fasciola hepatica* attenuated EAE, which was partially reversed by treatment with anti-

TGF-β. Furthermore, chronic *Leishmania donovani* infection has been associated with suppressed Th17 cell responses, which was reversed by anti-TGF-β [342]. TGF-β has also been shown to enhance the number of IL-17A-producing T cells in a model of colitis-associated colon cancer. Additionally, in the mentioned study, TGF-β signalling also increased IL-22 production by Th17 cells, which led to increased tumour growth in mice [343].

A study on the cytokine requirements for the induction of IL-17A production by γδ T cells demonstrated that *in vitro* stimulation with IL-1β and IL-23 in combination with TGF-β suppressed IFN-γ production and enhanced IL-17A production by $CD27^-$ γδ T cells [168]. The effect of TGF-β on IL-17A production by γδ T cells was lost following neutralisation of IFN-γ. TGF-β and IL-6 failed to induce IL-17A production by γδ T cells [169]. However, IL-1β, IL-6, and TGF-β induced IL-17A production by human Vγ2Vδ2 γδ T cells. IL-23 was required for the expansion of IL-17A-producing Vγ2Vδ2 γδ T cells [344].

TGF-β induces FoxP3 expression by human γδ T cells [345]. Although Treg cells suppress γδ T cells, this suppression is not mediated by TGF-β. Studies in a murine model of malaria infection have demonstrated that Treg cell-mediated suppression of both IFN-γ and IL-17A-producing γδ T cells was partially dependent on GITR-mediated contact [176]. Furthermore, $ST2^+$ Treg cells suppressed IL-17A production by γδ T cells in the lungs of mice following aeroallergen exposure in an IL-33-dependent manner [175]. TGF-β does not appear to directly inhibit IL-17A production by γδ T cells, but in a manner similar to CD4 T cells, TGF-β can suppress IFN-γ production by $CD27^+$ γδ T cells [168].

TGF-β binds to TGF-βRII and signals via SMAD2 and SMAD3 [346]. TGF-β type-I receptors specifically phosphorylate SMAD2 and SMAD3. SMAD2 and SMAD3 form complexes with SMAD4, which translocate to the nucleus where they regulate gene expression [347]. SMAD6 and SMAD7 are inhibitory SMADs that form a negative feedback loop in the TGF-β signalling pathway [348].

The possible role for TGF-β in modulating pathogenic IL-17A-producing T cells in EAE has not been fully elucidated. Treatment with recombinant TGF-β during EAE moderately decreased the severity of disease [349]. TGF-β treatment enhanced proliferation of NK cells *in vivo,* which in turn decreased IL-17A production by CD4 T cells. As discussed above,

TGF-β, in combination with IL-6, has a role in the development of Th17 cells. Specific deletion of TGF-β produced by Th17 cells resulted in a significant reduction in the induction of Th17 cells and the severity of EAE [350]. In MS patients, differential expression of microRNAs involved in TGF-β-mediated signalling have been associated with defects in Treg cells [351].

TGF-β has pleiotropic roles in regulating the development of IFN-γ- and IL-17A-producing T cells. The aim of the present study was to investigate the role of TGF-β in regulating the activation of γδ T cells. We used a small molecule inhibitor of TGF-β signalling, SB431542, to examine how TGF-β regulates both CD4 T cells and γδ T cells to influence the induction and severity of EAE.

5.2 Results

5.2.1 TGF-β regulates IFN-γ production by CD27$^+$ γδ T cells

While the ability of the anti-inflammatory cytokine TGF-β to regulate antigen-specific T cell responses is well established, the influence that this cytokine has on γδ T cell function is less clear. The present study examined the capacity of TGF-β to suppress cytokine-activated γδ T cells.

CD27$^+$ γδ T cells produced IFN-γ following *in vitro* activation with IL-12+IL-18, but not following stimulation with IL-1β+IL-23 (Fig 5.1 A, B). The frequency, number, and MFI of IFN-γ expression by IL-12+IL-18-stimulated CD27$^+$ γδ T cells was significantly suppressed by addition of TGF-β in a dose-dependent manner (Fig 5.1 A, B, D). However, IL-1β+IL-23 did not induce IFN-γ production by CD27$^+$ γδ T cells (Fig 5.1 A, B, D). Furthermore, TGF-β significantly suppressed proliferation of CD27$^+$ γδ T cells. CD27$^+$ γδ T cells were stimulated to proliferate with IL-2, IL-7, and IL-15 in the presence or absence of anti-TCRδ. Addition of TGF-β to the culture significantly decreased the frequency of proliferating CD27$^+$ γδ T cells following stimulation with IL-2+IL-7+IL-15 (Fig 5.2 A). The MFI of CellTraceViolet expression was also increased upon addition of TGF-β, confirming the suppression of proliferation of CD27$^+$ γδ T cells (Fig 5.2 B, C).

Conventional TGF-β signalling is coordinated intracellularly via SMAD phosphorylation and downstream signalling. Here, the ability of TGF-β to induce SMAD2/3 phosphorylation in IL-12+IL-18-activated CD27$^+$ γδ T cells was examined. TGF-β significantly enhanced pSMAD2/3 expression by IL-12+IL-18-stimulated CD27$^+$ γδ T cells (Fig 5.3 A, B). An examination of mRNA expression of TGF-β-responsive genes by CD27$^+$ γδ T cells showed that TGF-β significantly increased the expression of both *smad2* and *tgfbr2* both at rest and following stimulation with IL-12+IL-18 (Fig 5.4 A, D). TGF-β stimulation also significantly enhanced *smad7* expression by unstimulated CD27$^+$ γδ T cells (Fig 5.4 C). TGF-β promoted a non-significant increase in *smad3* expression by IL-12+IL-18-activated CD27$^+$ γδ T cells (Fig 5.4 B).

The effect of TGF-β on IFN-γ production by CD27$^-$ γδ T cells stimulated with either IL-12+IL-18 or IL-1β+IL-23 was examined. Stimulation of CD27$^-$ γδ T cells with IL-12+IL-18 induced IFN-γ production in a similar manner to that observed by CD27$^+$ γδ T cells (Fig 5.5 A, B, D).

Addition of TGF-β to IL-12+IL-18-stimulated CD27$^-$ γδ T cells significantly decreased the frequency, number, and MFI of IFN-γ producing CD27$^-$ γδ T cells (Fig 5.5 A, B, D). However, addition of TGF-β did not affect IFN-γ production by IL-1β+IL-23-activated CD27$^-$ γδ T cells (Fig 5.5 A, B, D). CD27$^-$ γδ T cells produced IL-17A following stimulation with IL-1β and IL-23, which was not affected by addition of TGF-β (Fig 5.6 A, B, D). TGF-β did not affect the frequency, number, or MFI of IL-17A expression by CD27$^-$ γδ T cells (Fig 5.6 A, B, D). In contrast, TGF-β significantly suppressed the proliferation of CD27$^-$ γδ T cells following stimulation with anti-TCRδ in the presence of IL-1β+IL-7+IL-23 (Fig 5.7 A). There was a significant increase in the MFI of CellTraceViolet expression by CD27$^-$ γδ T cells in response to stimulation with TGF-β, confirming the suppression of proliferation of CD27$^-$ γδ T cells (Fig 5.7 B, C).

Phosphorylation of SMAD2/3 in CD27$^-$ γδ T cells stimulated with TGF-β was then examined. Addition of TGF-β to IL-1β+IL-23-stimulated CD27$^-$ γδ T cells enhanced expression of pSMAD2/3, as assessed by flow cytometric analysis, after both 15 and 30 minutes of stimulation (Fig 5.8 A). In contrast to the data on CD27$^+$ γδ T cells, TGF-β stimulation of CD27$^-$ γδ T cells did not increase mRNA expression of *smad2, smad3, smad7,* or *tgfbr2* (Fig 5.9 A, B, C, D). On the contrary, there was a significant decrease in gene expression of *smad3* and *smad7* following stimulation of CD27$^-$ γδ T cells with TGF-β (Fig 5.9 B, C). IL-1β+IL-23 stimulation of CD27$^-$ γδ T cells significantly decreased expression of both *smad3* and *tgfbr2* when compared with unstimulated cells (Fig 5.9 B, D). Stimulation with IL-1β+IL-23 also resulted in decreased expression of *smad2* and *smad7 by* CD27$^-$ γδ T cells although this reduction was not significant (Fig 5.9 A, C). TGF-β stimulation did not significantly impact *smad* gene expression by IL-1β+IL-23-stimulated CD27$^-$ γδ T cells (Fig 5.9 A, B, C, D).

Phosphorylation of STAT3 plays a critical role in IL-17A production by CD27$^-$ γδ T cells [352]. Stimulation of CD27$^-$ γδ T cells with IL-1β and IL-23 induced phosphorylation of STAT3, which was increased upon addition of TGF-β (Fig 5.10 A). TGF-β significantly enhanced pSTAT3 expression by IL-1β+IL-23-stimulated CD27$^-$ γδ T cells after 60 minutes (Fig 5.10 A, B). In addition to enhanced phosphorylation of STAT3, *stat3* mRNA expression was significantly increased following addition of TGF-β to IL-1β+IL-23-stimulated CD27$^-$ γδ T cells (Fig 5.11 C). Interestingly, in the absence of IL-1β and IL-23, TGF-β significantly

decreased expression of *stat3* by CD27$^-$ γδ T cells (Fig 5.11 C). There was a significant reduction in the expression of *ifng* following addition of TGF-β to unstimulated CD27$^-$ γδ T cells but activation with IL-1β+IL-23 reversed this suppressive effect (Fig 5.11 B). Similarly, TGF-β significantly suppressed *rorc* expression by unstimulated CD27$^-$ γδ T cells but addition of TGF-β to IL-1β+IL-23-activated CD27$^-$ γδ T cells significantly increased *rorc* expression (Fig 5.11 D).

These data demonstrate that TGF-β suppresses the function of CD27$^+$ γδ T cells but not of CD27$^-$ γδ T cells. Although both cell types responded to TGF-β stimulation, IFN-γ production by CD27$^+$ γδ T cells was inhibited, whereas IL-17A production by CD27$^-$ γδ T cells was not significantly impacted.

5.2.2 Neutralisation of TGF-β significantly suppresses the induction of antigen-specific IL-17A production by CD4 T cells

The role that TGF-β plays in regulating the development of Th17 cells is still unclear. Certain studies have suggested that TGF-β is required to induce Th17 cells during the development of EAE, but other studies have shown that the role for TGF-β in the polarisation of Th17 cells is to suppress the development of Th1 cells, thereby increasing the proportion of Th17 cells [37, 45].

A TGF-β neutralising antibody was used to investigate the role of TGF-β in the development of MOG-specific T cell responses that are pathogenic in EAE. Stimulation of spleen and LN cells from MOG-immunised mice with IL-1β+IL-23, MOG, or MOG in combination with IL-1β+IL-23 promoted IFN-γ and IL-17A production by CD4 T cells (Fig 5.12 A, B). Addition of anti-TGF-β to IL-1β+IL-23, MOG, or MOG and IL-1β+IL-23-stimulated spleen and LN cells from MOG-immunised mice significantly increased the frequency and number of IFN-γ-producing CD4 T cells (Fig 5.12 A). Addition of anti-TGF-β did not affect IL-17A production by CD4 T cells stimulated with IL-1β+IL-23 but significantly suppressed the frequency of IL-17A$^+$ CD4 T cells following stimulation of spleen and LN cells from MOG-immunised mice with MOG alone (Fig 5.12 B). Addition of anti-TGFβ to MOG, IL-1β+IL-23-stimulated spleen and LN cells from MOG-immunised significantly decreased the frequency and number of IL-17A$^+$ CD4 T cells (Fig 5.12 B). There was also a significant

decrease in the frequency of MOG-stimulated IL-17A$^+$ CD4 T cells following addition of anti-TGF-β to spleen and LN cells from MOG-immunised mice (Fig 5.12 B). IL-1β+IL-23 stimulation of spleen and LN cells from MOG-immunised mice induced IL-17A and IFN-γ co-producing CD4 T cells (Fig 5.12 C). Upon addition of anti-TGF-β, the frequency and number of IL-17A$^+$IFN-γ$^+$ CD4 T cells was increased, but this effect was not significant (Fig 5.12 C). Addition of anti-TGF-β to MOG, IL-1β+IL-23-stimulated spleen and LN cells from MOG-immunised mice significantly decreased both the frequency and number of IL-17A$^+$IFN-γ$^+$ CD4 T cells (Fig 5.12 C).

The effect of anti-TGF-β treatment on γδ T cell activation was also examined. Stimulation of spleen and LN cells from MOG-immunised mice with IL-1β+IL-23 induced IFN-γ production by CD27$^-$ γδ T cells (Fig 5.13 A, B, C). Addition of anti-TGF-β to IL-1β+IL-23-stimulated spleen and LN cells from MOG-immunised mice significantly increased the absolute number and MFI of IFN-γ-producing CD27$^-$ γδ T cells (Fig 5.13 B, C). Similarly, addition of anti-TGF-β to MOG, IL-1β and IL-23-stimulated spleen and LN cells from MOG-immunised mice significantly increased the frequency and MFI of IFN-γ$^+$ CD27$^-$ γδ T cells (Fig 5.13 A, C). Conversely, neutralisation of TGF-β in the IL-1β+IL-23-stimulated spleen and LN cells from MOG-immunised mice significantly decreased the frequency and MFI of IL-17A production by CD27$^-$ γδ T cells (Fig 5.14 A, C). In a similar manner, anti-TGF-β treatment of MOG, IL-1β+IL-23-stimulated spleen and LN cells from MOG-immunised mice significantly reduced the frequency, number, and MFI of IL-17A-producing CD27$^-$ γδ T cells (Fig 5.14 A, B, C). These data demonstrate that TGF-β differentially regulates the induction of IL-17A and IFN-γ production by T cell subsets.

5.2.3 The effect of a TGF-β signalling inhibitor on T cells that mediate EAE

EAE is mediated by IL-17A-secreting CD4 and γδ T cells and these cells can transfer EAE to naïve mice. A small molecule inhibitor of TGF-β signalling, SB431542, was used to investigate the effect of TGF-β on T cells that mediate pathology in EAE. Spleen and LN cells from MOG-immunised mice were stimulated with IL-1β+IL-23, MOG, or MOG in combination with IL-1β and IL-23 in the presence or absence of SB431542. SB431542 treatment significantly increased IFN-γ production by spleen and LN cells from MOG-

immunised mice following stimulation with IL-1β+IL-23, MOG, or MOG in combination with IL-1β+IL-23 (Fig 5.15 A). SB431542 did not have any significant impact on IL-17A production by spleen and LN cells from MOG-immunised mice when stimulated with either IL-1β+IL-23 or MOG alone. However, addition of SB431542 to MOG, IL-1β+IL-23-stimulated-spleen and LN cells from MOG-immunised mice significantly decreased IL-17A production (Fig 5.15 B).

To adoptively transfer EAE, LN and spleen cells from MOG-immunised mice are cultured in the presence of MOG, IL-1β+IL-23 for 72 hours before being injected into naïve recipient mice. Previous results have demonstrated that SB431542 increased IFN-γ and decreased IL-17A production by MOG, IL-1β+IL-23-stimulated spleen and LN cells from MOG-immunised mice (Fig 5.15 A, B). Therefore, the effect of SB431542 treatment on the ability of MOG, IL-1β+IL-23-stimulated spleen and LN cells from MOG-immunised mice to transfer EAE was examined. The SB431542-treated spleen and LN cells transferred less severe disease than the vehicle control-treated spleen and LN cells as measured by clinical score (Fig 5.16 A). The mice that received SB431542-treated spleen and LN cells lost significantly less weight than mice that received vehicle control-treated spleen and LN cells by day 11 of EAE (Fig 5.16 B). These data demonstrate that SB431542 treatment has a protective effect in the adoptive transfer model of EAE.

Treatment of the whole adoptive transfer culture does not distinguish between the cell types that are responding to TGF-β inhibition in the culture. Therefore, CD4 T cells were separated and treated with either SB431542 or vehicle control for 6 hours before being washed and cultured for a further 72 hours with the remaining $CD4^-$ fraction of the spleen and LN cells from MOG-immunised mice. There was a significant decrease in the severity of EAE when CD4 T cells were pretreated with SB431542 when compared with CD4 T cells pretreated with the vehicle control (Fig 5.17 A). Mice that received the adoptive transfer culture with SB431542-pretreated CD4 T cells did not lose weight in contrast to mice that received the adoptive transfer culture with vehicle control-pretreated CD4 T cells (Fig 5.17 B).

This experiment was repeated separating γδ T cells instead of CD4 T cells and treating them with SB431542 before adoptive transfer to naïve mice. Similarly, γδ T cells were separated from the spleen and LN cells from MOG-immunised mice and treated with

either SB431542 or vehicle control for 6 hours before being washed and cultured for a further 72 hours with the remaining TCRγδ$^-$ fraction of the spleen and LN cells. After 72 hours of culture, the MOG, IL-1β+IL-23-stimulated spleen and LN cells from MOG-immunised mice that contained γδ T cells that had been pretreated with SB431542 transferred less severe EAE than the spleen and LN cells that contained vehicle control-pretreated γδ T cells (Fig 5.18 A). However, this protective effect was not as potent as that observed when CD4 T cells were pretreated with SB431542 (Fig 5.17 A). Mice that received MOG, IL-1β+IL-23-stimulated spleen and LN cells with SB431542-pretreated γδ T cells lost less weight than mice that received the spleen and LN cells containing vehicle control-pretreated γδ T cells (Fig 5.18 B). These experiments have shown that SB431542 treatment suppresses the pathogenic capacity of IL-17A-producing γδ and CD4 T cells.

5.2.4 Treatment with a small molecule inhibitor of TGF-β, SB431542, throughout EAE reduces the severity of disease

The experiments described previously have focused on the adoptive transfer model of EAE and how neutralisation of TGF-β signalling affects the ability of MOG-specific T cells to transfer disease. Here the effect of blocking TGF-β *in vivo* in the active model of EAE was examined. Treatment with SB431542 throughout actively induced EAE reduced the severity of EAE when compared with vehicle control-treated mice (Fig 5.19 A). Mice treated with SB431542 lost significantly less weight than the vehicle control-treated group on days 14, 15, and 16 of EAE (Fig 5.19 B).

An examination of T cell responses in the LN during the induction phase of EAE revealed that there was a significant decrease in the number of total CD27$^-$ γδ T cells in the LN of SB431542-treated mice on day 7 of EAE when compared with vehicle control-treated mice (Fig 5.20 A). SB431542 treatment significantly increased the frequency of GM-CSF$^+$ CD27$^-$ γδ T cells in the LN of mice with EAE (Fig 5.20 B). However, SB431542 treatment did not significantly change the number of GM-CSF-producing CD27$^-$ γδ T cells at the induction phase of EAE (Fig 5.20 B). SB431542 treatment increased, albeit not significantly, the number of IFN-γ$^+$ CD27$^-$ γδ T cells, but there were no differences in the frequency of IFN-γ-producing CD27$^-$ γδ T cells between treatment groups (Fig 5.20 C). Conversely, SB431542

treatment significantly decreased the number of IL-17A-producing CD27$^-$ γδ T cells in the LN of mice with EAE (Fig 5.20 D). Treatment with SB431542 moderately decreased both the frequency and number of TNF-producing CD27$^-$ γδ T cells in the LNs of mice with EAE but this difference was not significant (Fig 5.20 E).

The number of CD27$^+$ γδ T cells in the LN of mice with EAE was not significantly different following treatment with SB431542 (Fig 5.21 A). SB431542 treatment increased, although not significantly, the frequency of both GM-CSF$^+$ and IFN-γ$^+$ CD27$^+$ γδ T cells in the LN of mice with EAE (Fig 5.21 B, C). SB431542 treatment significantly decreased the number of TNF-producing CD27$^+$ γδ T cells in the LN of mice with EAE (Fig 5.21 D).

Treatment with SB431542 significantly decreased the total number of CD4 T cells in the LN of mice on day 7 of EAE (Fig 5.22 A). SB431542-treated mice had an increased frequency of GM-CSF-secreting CD4 T cells in the LN when compared with vehicle control-treated mice (Fig 5.22 B). There were no significant changes to either the frequency or number of IFN-γ-producing CD4 T cells during EAE between treatment groups (Fig 5.22 C). There was a significant decrease in the number of IL-17A- and TNF-producing CD4 T cells in the LN of mice treated with SB431542 during EAE (Fig 5.22 D, E).

The phenotype of CNS-infiltrated T cells was examined following treatment with SB431542. The frequency and MFI of GM-CSF-secreting CD27$^-$ γδ T cells was significantly enhanced in the brains of SB431542-treated mice at the peak of EAE (Fig 5.23 A). There was a slight increase in the frequency of IFN-γ-producing CD27$^-$ γδ T cells in the brains of mice with EAE following treatment with SB431542 (Fig 5.23 B). There was also an increase in the MFI of IFN-γ expression by CD27$^-$ γδ T cells in the brains of SB431542-treated mice when compared with vehicle control-treated mice (Fig 5.23 B). There was no difference in either the frequency or MFI of IL-17A expression by CD27$^-$ γδ T cells in the brains of mice with EAE following SB431542 treatment (Fig 5.23 C). There was a significant decrease in the frequency and MFI of RORγt-expressing CD27$^-$ γδ T cells in the brains of mice treated with SB431542 during EAE (Fig 5.23 D).

The effect of treatment with SB431542 on γδ T cells during EAE was similar to the effect of SB431542 observed in CD4 T cells. SB431542 treatment significantly increased the frequency of GM-CSF-secreting CD4 T cells in the brains of mice during EAE (Fig 5.24 A).

SB431542 also significantly enhanced the MFI of GM-CSF expression by CD4 T cells in the brain during EAE (Fig 5.24 A). Additionally, SB431542 treatment increased the frequency of IFN-γ-producing CD4 T cells in the brain during EAE (Fig 5.24 B). Similarly, there was an increase in the MFI of IFN-γ expression by CD4 T cells in the brains of SB431542-treated mice at the peak of EAE, although this difference was not significant (Fig 5.24 B). There was a slight decrease in the frequency of both IL-17A-producing and RORγt-expressing CD4 T cells in the brains of mice treated with SB431542 during EAE (Fig 5.24 C, D). Additionally, SB431542 treatment significantly decreased the MFI of RORγt expression by CD4 T cells in the brains of mice at the peak of EAE (Fig 5.24 D).

The antigen-specific response in the LN and spleen at the peak of EAE in SB431542-treated and vehicle control-treated mice was also examined. There was a significant decrease in MOG-specific IL-17A production in the SB431542-treated mice (Fig 5.25 A). There was also a significant decrease in anti-CD3/28-induced IL-17A production in the spleens of SB431542-treated mice with EAE (Fig 5.25 A). There was no significant effect of SB431542 treatment observed with respect to the induction of MOG-specific IFN-γ production in the spleens of mice with EAE (Fig 5.25 B). Collectively these findings demonstrate that blocking TGF-β signalling with SB431542 during EAE appears to suppress the induction of IL-17A- and TNF-producing γδ and CD4 T cells and enhances the induction of IFN-γ- and GM-CSF-producing γδ and CD4 T cells.

5.2.5 Neutralisation of IFN-γ reverses the suppressive effect of SB431542 on IL-17A-producing CD27$^-$ γδ T cells

Data from the EAE model suggests that there is an inverse relationship between IFN-γ and IL-17A production by T cells. Therefore, IFN-γ was neutralised *in vitro* to assess whether the suppressive effect of SB431542 on IL-17A production by CD27$^-$ γδ T cells was mediated by increased production of IFN-γ.

Treatment of IL-1β+IL-23-activated CD27$^-$ γδ T cells with SB431542 had a moderately suppressive effect on the frequency of IL-17A-producing CD27$^-$ γδ T cells (Fig 5.26 A). However, when IFN-γ was neutralised in this culture system, SB431542 treatment increased the frequency of IL-1β+IL-23-activated IL-17A-producing CD27$^-$ γδ T cells (Fig

5.26 A). Additionally, neutralisation of IFN-γ during SB431542 treatment of IL-1β+IL-23-activated $CD27^-$ γδ T cells enhanced the MFI of IL-17A expression when compared with SB431542 treatment alone (Fig 5.26 A).

Similarly, SB431542 treatment moderately suppressed the frequency of IL-1β+IL-23-activated $CD27^-$ γδ T cells expressing RORγt (Fig 5.26 C). Furthermore, following neutralisation of IFN-γ, SB431542 treatment increased RORγt expression by IL-1β+IL-23-activated $CD27^-$ γδ T cells (Fig 5.26 C). There was a significant increase in both the frequency and MFI of RORγt expression by IL-1β+IL-23-activated $CD27^-$ γδ T cells when IFN-γ was neutralised during SB431542 treatment (Fig 5.26 C). These data show that blocking TGF-β-mediated signalling in the absence of IFN-γ increases IL-17A production by IL-1β+IL-23-activated $CD27^-$ γδ T cells.

5.3 Discussion

The role that TGF-β plays in activating or regulating pathogenic T cells is controversial. TGF-β, in combination with IL-6, was originally identified as an important differentiation factor for Th17 cells [353]. EAE cannot be induced in mice that have CD4 T cells that lack expression of TGF-βRII. Furthermore, treatment of mice with anti-TGF-β protected mice from the clinical signs of EAE. IL-23 was identified as a crucial mediator of autoimmunity in combination with TGF-β. Similarly, the present study demonstrated that treatment with SB431542, a small molecule inhibitor of TGF-β signalling, reduced the severity of EAE. Additionally, treatment with SB431542 decreased IL-17A production and RORγt expression by γδ and CD4 T cells both in the LNs and brains of mice with EAE. The effect of TGF-β on RORγt is not thought to be mediated by traditional TGF-β-mediated signalling mechanisms. SMAD2 and SMAD3 are not required for TGF-β-mediated induction of RORγt expression by CD4 T cells [354]. It has also been revealed that the induction of Th17 cells occurred in the absence of SMAD signalling, via suppression of Eomesodermin (EOMES) expression, which in turn promoted induction of RORγt [355]. Similarly, the present study showed that while IL-17A and RORγt expression by γδ and CD4 T cells was decreased in the LNs and brains of mice during EAE in response to treatment with SB431542, IFN-γ production was increased.

Other studies have suggested that TGF-β is not required for the differentiation of Th17 cells [45]. In the absence of Tbet and STAT6, which are responsible for driving the differentiation of Th1 and Th2 cells respectively, Th17 cells were induced in the presence of IL-6 alone. Das et al. demonstrated that TGF-β suppressed the development of Th1 and Th2 cells rather than directly promoting the development of Th17 cells. In the present study, ablation of TGF-β-mediated signalling significantly increased IFN-γ production by γδ and CD4 T cells. IFN-γ-producing Th17 cells do not necessarily require Tbet to be pathogenic in EAE [356]. These data suggest that in the absence of TGF-β, IL-17A production by Th17 cells is suppressed and IFN-γ production is enhanced. Previous studies have demonstrated that IFN-$\gamma^{-/-}$ mice develop less severe EAE, thus explaining how SB431542 treatment suppressed the severity of EAE [357]. Neutralisation of IFN-γ during EAE delayed the onset of disease but increased the overall severity of disease [357]. These

findings suggest that IFN-γ influences the pathogenicity of Th17 cells throughout disease. Future work could include treatment with SB431542 later on during EAE to investigate whether this would worsen disease. Neutralisation of TGF-β during EAE in IFN-$\gamma^{-/-}$ mice would also provide insight into how TGF-β regulates IL-17A production in the absence of IFN-γ.

The impact of TGF-β on the pathogenicity of T cell subsets was also investigated by separating either CD4 T cells or γδ T cells and pretreating these cell types with SB431542 before adoptive transfer to naïve recipient mice. The results from these experiments showed that TGF-β signalling promoted pathogenicity of both CD4 T cells and γδ T cells in the adoptive transfer model of EAE. TGF-β-mediated regulation of γδ T cell function is poorly understood. Results from the present study suggest that TGF-β regulates $CD27^{+}$ γδ T cells and $CD27^{-}$ γδ T cells. Proliferation of $CD27^{+}$ γδ T cells and IFN-γ production by these cells was suppressed in response to TGF-β stimulation. This suppression was associated with increased expression of SMAD proteins, TGF-βRII, and phosphorylation of SMAD2/3. The demonstration that IFN-γ-producing $CD27^{+}$ γδ T cells are regulated by TGF-β in a conventional manner is consistent with a previous report which showed that TGF-β did not significantly suppress IFN-γ production by T cells that lacked expression of SMAD2 and SMAD3 [354]. While TGF-β suppressed proliferation of $CD27^{-}$ γδ T cells and increased phosphorylation of SMAD2/3, this did not translate to suppression of IL-17A production. Stimulation of $CD27^{-}$ γδ T cells with IL-1β and IL-23 decreased expression of SMAD proteins and TGF-βRII, and addition of TGF-β increased phosphorylation of STAT3. Treatment of IL-1β+IL23-activated $CD27^{-}$ γδ T cells with TGF-β increased mRNA expression of both *rorc* and *stat3*. TGF-β hyper-activated STAT3-activated fibroblasts in mice challenged with bleomycin [358]. These data suggest that TGF-β supports IL-1β+IL-23-mediated activation of $CD27^{-}$ γδ T cells to produce IL-17A via STAT3. It has previously been demonstrated that TGF-β can increase IL-1β+IL-23-induced IL-17A production by $CD27^{-}$ γδ T cells, but the mechanism of activation was not explored [168].

The findings of the present study demonstrate that neutralisation of TGF-β decreases IL-17A production by $CD27^{-}$ γδ T cells and that TGF-β can activate $CD27^{-}$ γδ T cells via STAT3. Previous studies have investigated the cross-regulation of IL-17A and IFN-γ production in the context of Th cell polarisation. IL-$17A^{-/-}$IL-$17F^{-/-}$ mice have higher IFN-γ production in

the bronchoalveolar lavage fluid (BALF) after intranasal allergen challenge [359]. Ablation of IL-17 in this model suppressed Th2 cell polarisation as a consequence of increased IFN-γ production. Furthermore, in a murine model of *Nippostrongylus brasiliensis* infection, IL-17A was identified as a major suppressor of IFN-γ [360]. In the mentioned study by Ajendra et al., γδ T cell-derived IL-17A suppressed IFN-γ production during infection. Neutralisation of IFN-γ in IL-17A$^{-/-}$ mice restored the Th2 response during the parasitic infection. Both studies demonstrated that IL-17A can regulate the Th2 response indirectly by suppressing Th1 responses. In the present study, blocking TGF-β-mediated signalling suppressed IL-17A production by CD27^{-} γδ T cells. Conversely, when IFN-γ was neutralised in the presence of a TGF-β inhibitor IL-17A production by CD27^{-} γδ T cells was enhanced. The findings of the present study suggest that TGF-β increases IL-17A production by CD27^{-} γδ T cells in an IFN-γ-dependent manner.

Inhibition of TGF-β signalling in mice with EAE enhanced GM-CSF and suppressed TNF production by both γδ and CD4 T cells. IL-17A and GM-CSF production by T cells during EAE is promoted by IL-1β [251]. In the present study, the increase of GM-CSF production in mice treated with the TGF-β inhibitor SB431542 could be dependent on increased IL-1β production. However, increased IL-1β induced by TGF-β inhibition may not increase IL-17A production by T cells in this context as TGF-β is also required to support the pathogenicity of IL-17A-producing T cells. These data unveil an interesting regulation of T cell cytokines by TGF-β during EAE. IL-17A and GM-CSCF production have previously been shown to be reciprocally regulated in human T cells [361]. Furthermore, reduced TGF-β is associated with increased GM-CSF production by T cells from MS patients [362]. In the present study, treatment with SB431542 during EAE also suppressed TNF production by T cells. Blockade of TNF during EAE reduced the severity of disease [363]. Furthermore, TNF promoted recruitment of lymphocytes to the CNS during EAE [364]. In the current study it is possible that SB431542 treatment of mice with EAE suppressed the severity of disease by suppressing TNF production by T cells which decreased infiltration of encephalitogenic immune cells into the CNS.

The findings from the present study have demonstrated that TGF-β regulates cytokine production by T cells during EAE. IL-17A was suppressed and IFN-γ production was enhanced in mice treated with SB431542. In the absence of IFN-γ, TGF-β appears to be

able to suppress IL-17A production by $CD27^-$ γδ T cells. Additionally, TGF-β regulates the development of Th17 cells in EAE and this appeared to also be dependent on IFN-γ. These findings provide an interesting insight into possible strategies that could be exploited to regulate pathogenic T cells in CNS autoimmunity.

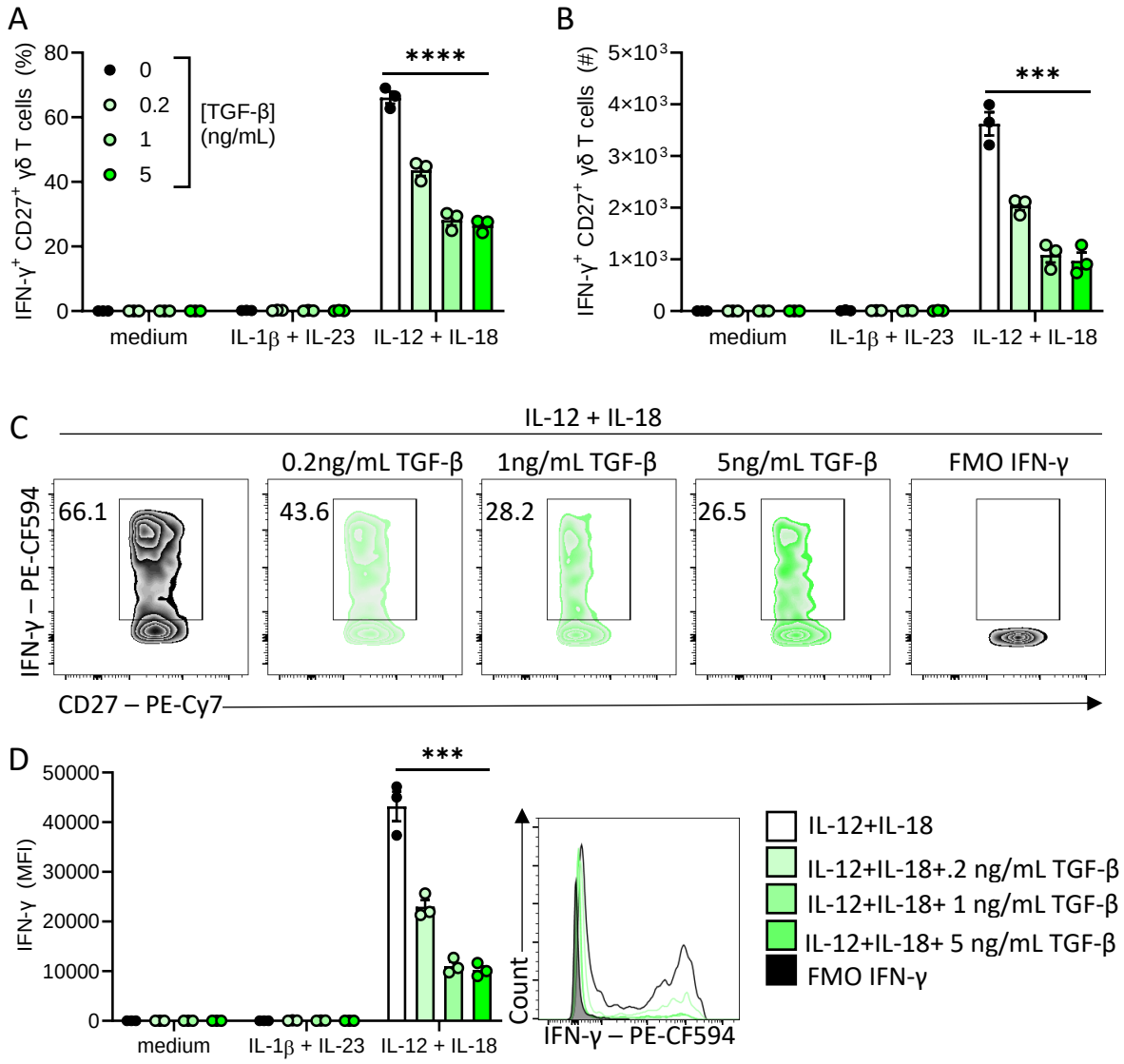

Figure 5.1 TGF-β suppresses IFN-γ production by IL-12+IL-18-stimulated CD27⁺ γδ T cells. LN and spleen cells were isolated from naïve C57BL/6J mice. CD3⁺ cells were enriched using a negative selection T cell enrichment kit. Cells were stimulated *in vitro* with either IL-1β (2.5 ng/mL) and IL-23 (10 ng/mL) or IL-12 (2.5 ng/mL) and IL-18 (10 ng/mL) in the presence or absence of increasing concentrations of TGF-β (0.2, 1, and 5 ng/mL). After 48 hours, cells were incubated with brefeldin A for 4 hours and stained for surface CD3, CD27, TCRδ, and intracellular IFN-γ followed by analysis by flow cytometry. Results are (A) frequency and (B) absolute number of IFN-γ-producing CD27⁺ γδ T cells with (C) representative FACS plots. (D) Mean fluorescence intensity (MFI) of IFN-γ expression by CD27⁺ γδ T cells with (E) representative FACS plots. Data are mean ± SD (n=3) and are representative of three independent experiments. ***$p < 0.001$, ****$p < 0.0001$ by one-way ANOVA with Dunnett's multiple comparisons test.

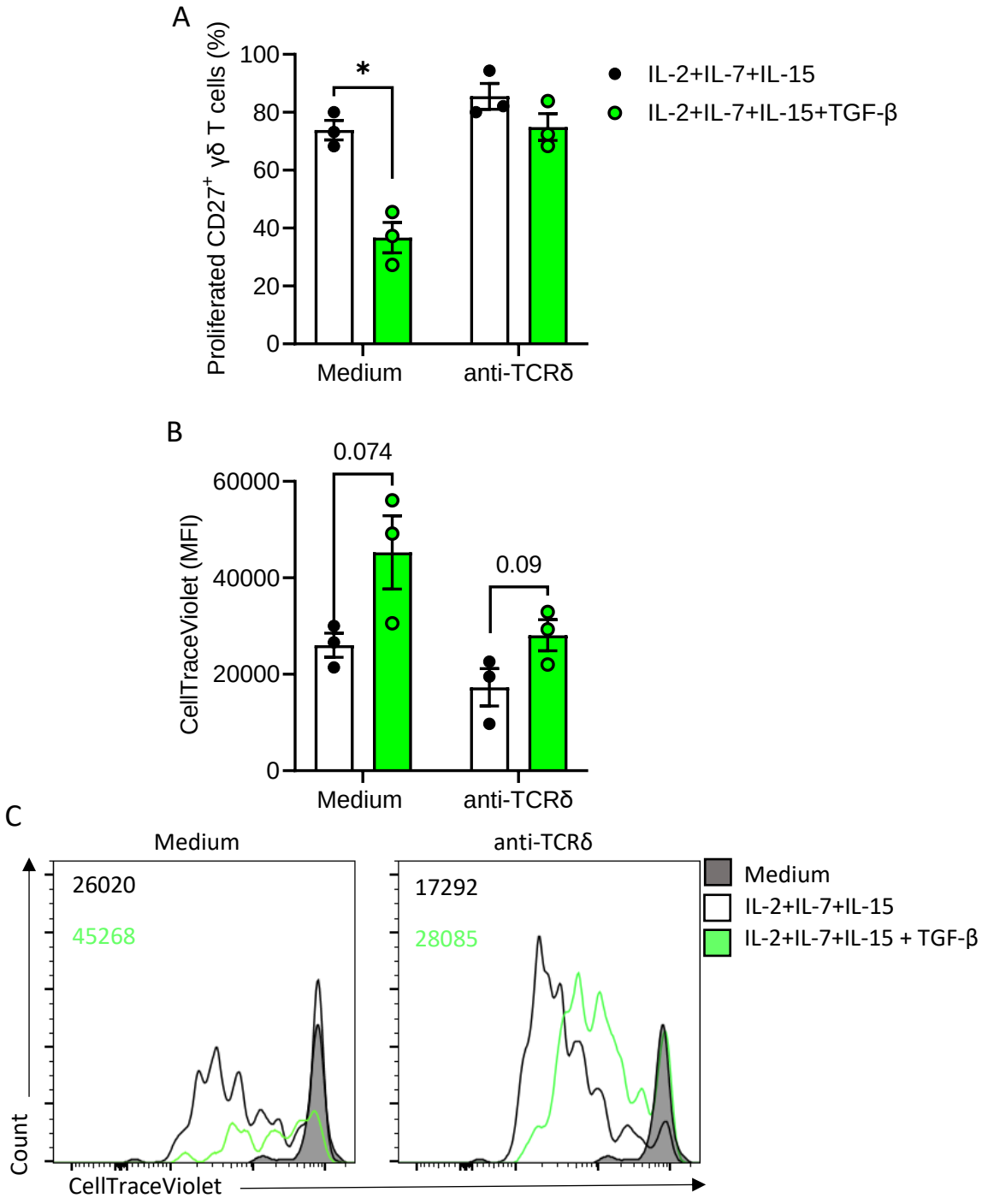

Figure 5.2 TGF-β suppresses proliferation of CD27⁺ γδ T cells. LN and spleen cells were isolated from naïve C57BL/6J mice. CD3⁺ cells were enriched using a negative selection T cell enrichment kit and stained with CellTraceViolet cell proliferation dye. Cells were stimulated with IL-2 (10 ng/mL), IL-7 (10 ng/mL), and IL-15 (10 ng/mL) in the presence or absence of anti-TCRδ with and without TGF-β (5 ng/mL). After 72 hours, cells stained for surface CD3, CD27, and TCRδ followed by analysis by flow cytometry. Results are (A) frequency and (B) MFI of CellTraceViolet expressed by proliferated CD27⁺ γδ T cells with (C) representative FACS plots. Data are mean ± SD (n=3) and are representative of two independent experiments. $^{*}p < 0.05$, by unpaired Student's *t* test.

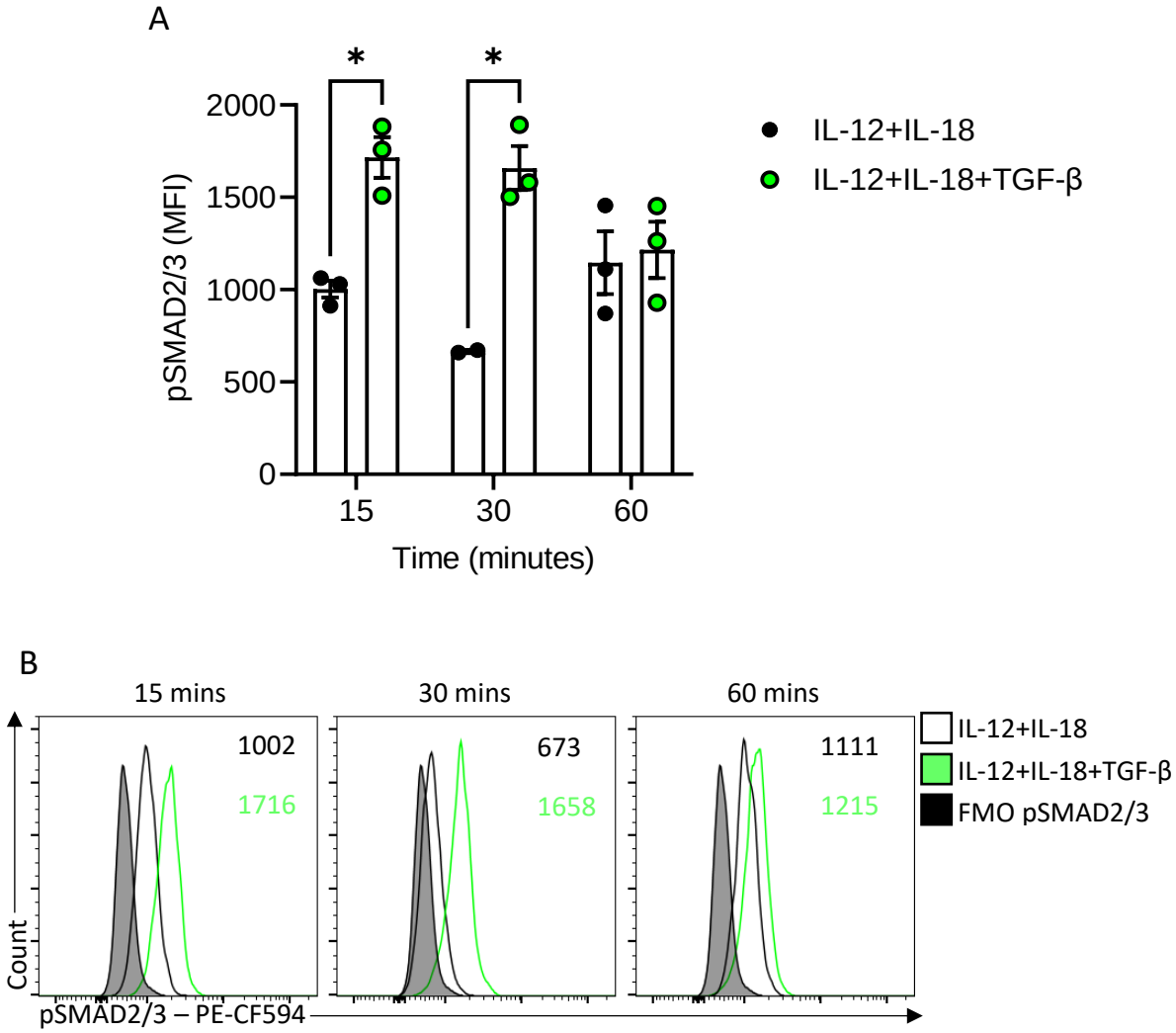

Figure 5.3 TGF-β induces SMAD2/3 phosphorylation in CD27⁺ γδ T cells. CD27⁺ γδ T cells were FACS-purified from the spleen and LN of naïve C57BL/6J mice. Sorted cells were serum-starved overnight to decrease background phosphorylation. The next day, cells were stimulated with IL-12 (10 ng/mL), and IL-18 (10 ng/mL) in the presence or absence of TGF-β (5 ng/mL) for 15, 30, and 60 minutes. Cells were stained for viability followed by methanol fixation and permeabilisation steps. Cells were stained for phosphorylated SMAD2/3 and analysed by flow cytometry. Results are (A) MFI of pSMAD2/3 expression by CD27⁺ γδ T cells with (B) representative FACS plots. Data are mean ± SD (n=3) and are representative of three independent experiments. $^{*}p < 0.05$ by two-way ANOVA with Sidak's multiple comparisons test.

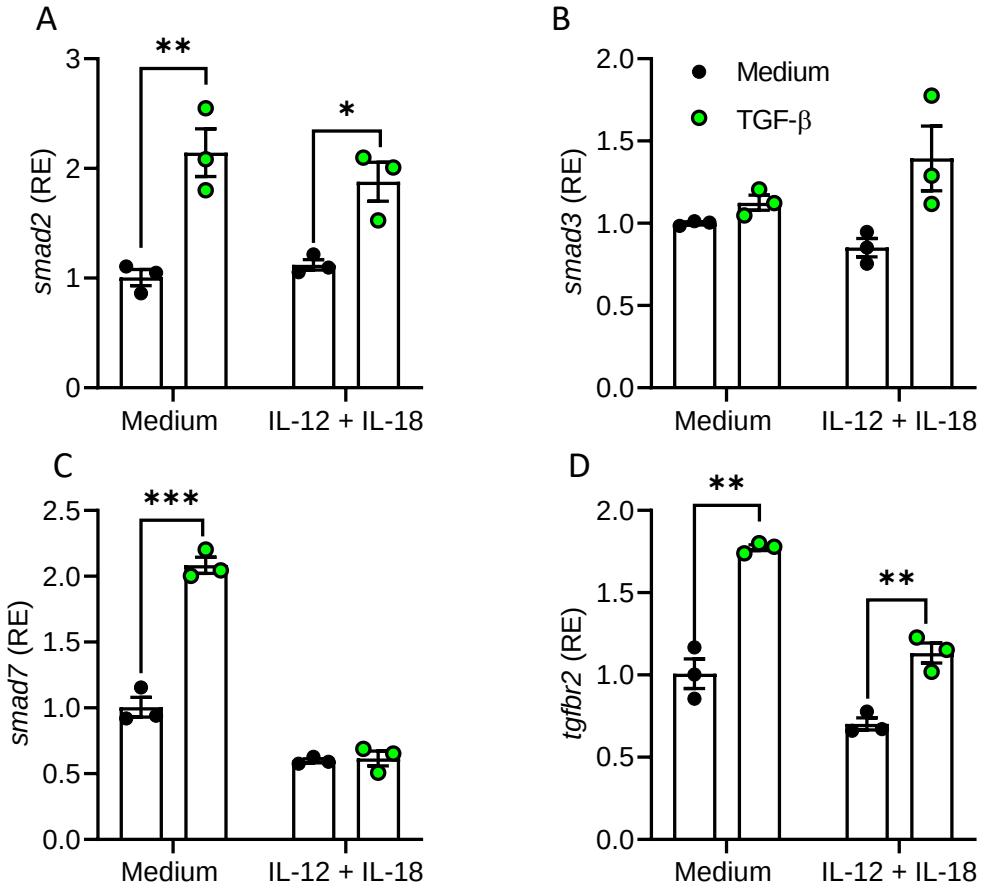

Figure 5.4 TGF-β increases mRNA expression of *smad* proteins in CD27⁺ γδ T cells. CD27⁺ γδ T cells were FACS-purified from the spleen and LN of naïve C57BL/6J mice. Cells were stimulated with IL-12 (10 ng/mL), and IL-18 (10 ng/mL) in the presence or absence of TGF-β (5 ng/mL) for 2 hours. mRNA expression was evaluated by Rt-PCR normalised to 18S rRNA and relative to the medium control. Results are mRNA expression of (A) *smad2*, (B) *smad3*, (C) *smad7,* and (D) *tgfbr2* by CD27⁺ γδ T cells. Data are mean ± SD (n=3) and are representative of three independent experiments. $^{**}p < 0.01$, $^{***}p < 0.001$ by unpaired Student's *t* test medium control versus TGF-β.

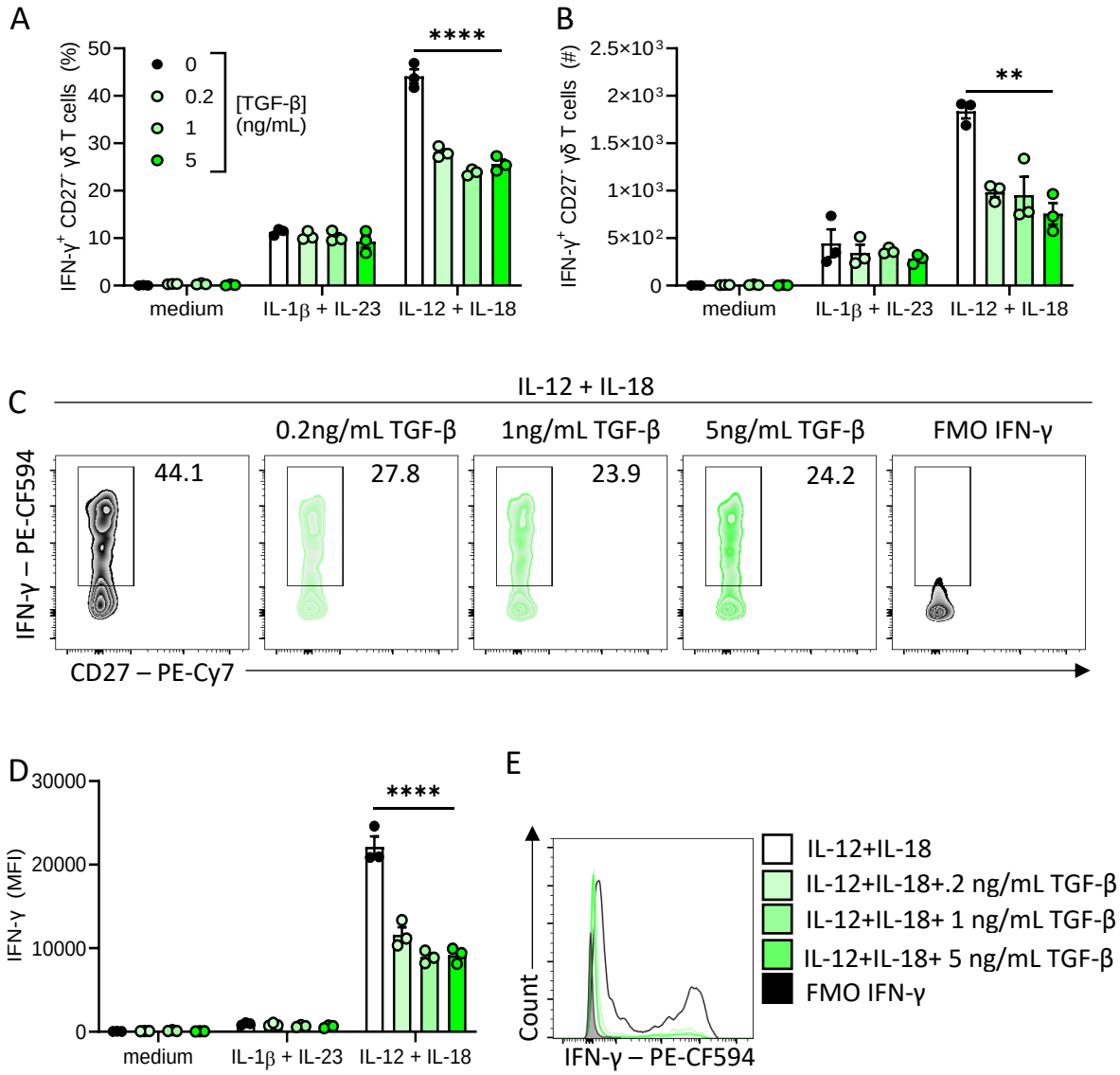

Figure 5.5 TGF-β does not suppress IFN-γ production by IL-1β+IL-23-stimulated CD27⁻ γδ T cells. LN and spleen cells were isolated from naïve C57BL/6J mice. CD3⁺ cells were enriched using a negative selection T cell enrichment kit. Cells were stimulated with either IL-1β (2.5 ng/mL) and IL-23 (10 ng/mL) or IL-12 (2.5 ng/mL) and IL-18 (10 ng/mL) in the presence or absence of increasing concentrations of TGF-β (0.2, 1, and 5 ng/mL). After 48 hours, cells were incubated with brefeldin A for 4 hours and stained for surface CD3, CD27, TCRδ, and intracellular IFN-γ followed by analysis by flow cytometry. Results are (A) frequency and (B) absolute number of IFN-γ-producing CD27⁻ γδ T cells with (C) representative FACS plots. (D) MFI of IFN-γ expression by CD27⁻ γδ T cells with (E) representative FACS plots. Data are mean ± SD (n=3) and are representative of three independent experiments. $^{**}p < 0.01$, $^{****}p < 0.0001$ by one-way ANOVA with Dunnett's multiple comparisons test.

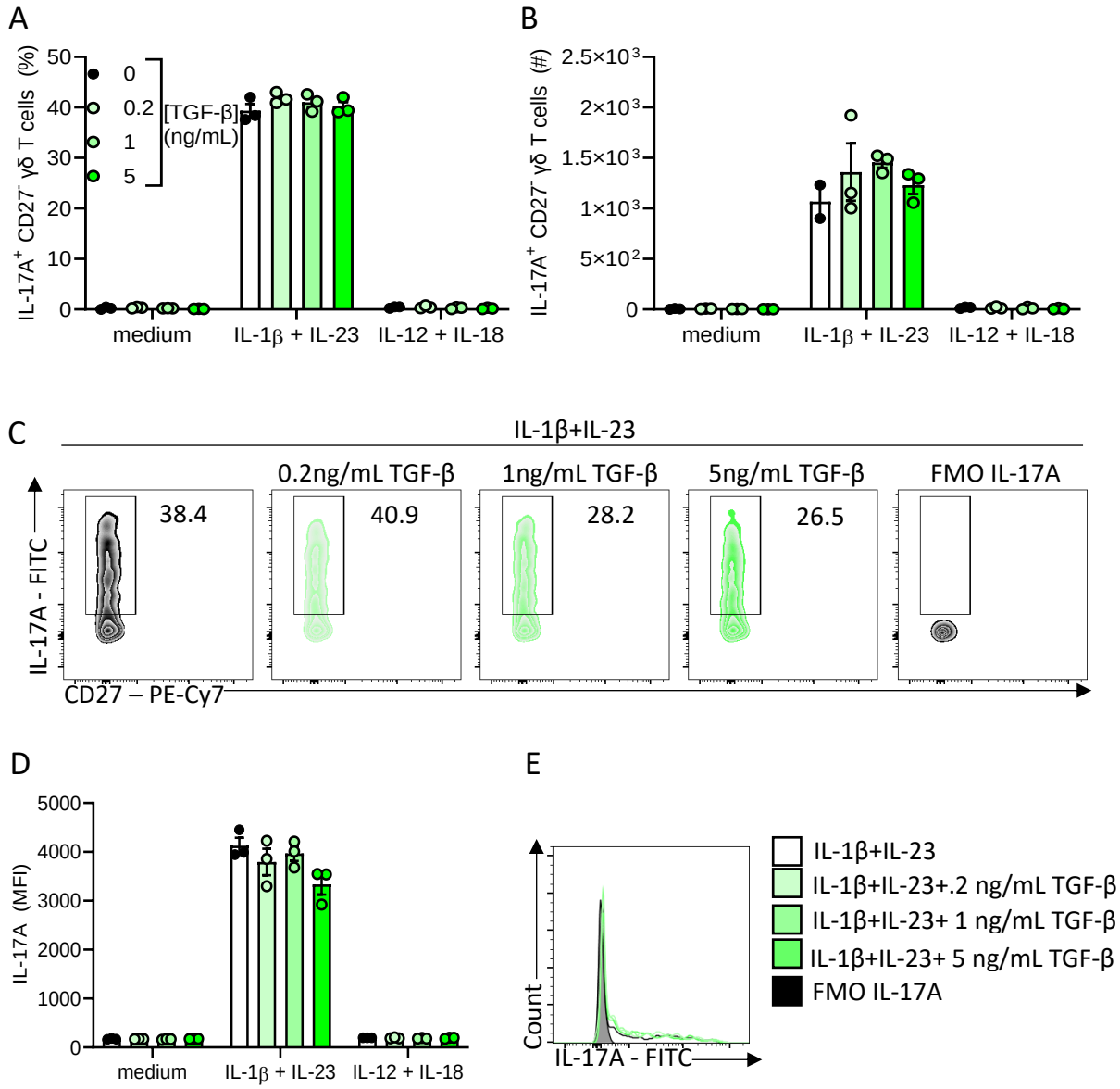

Figure 5.6 TGF-β does not suppress IL-17A production by IL-1β+IL-23-stimulated CD27⁻ γδ T cells. LN and spleen cells were isolated from naïve C57BL/6J mice. CD3⁺ cells were enriched using a negative selection T cell enrichment kit. Cells were stimulated with either IL-1β (2.5 ng/mL) and IL-23 (10 ng/mL) or IL-12 (2.5 ng/mL) and IL-18 (10 ng/mL) in the presence or absence of increasing concentrations of TGF-β (0.2, 1, and 5 ng/mL). After 48 hours, cells were incubated with brefeldin A for 4 hours and stained for surface CD3, CD27, TCRδ, and intracellular IL-17A followed by analysis by flow cytometry. Results are (A) frequency and (B) absolute number of IL-17A-producing CD27⁻ γδ T cells with (C) representative FACS plots. (D) MFI of IL-17A expression by CD27⁻ γδ T cells with (E) representative FACS plot. Data are mean ± SD (n=3) and are representative of three independent experiments.

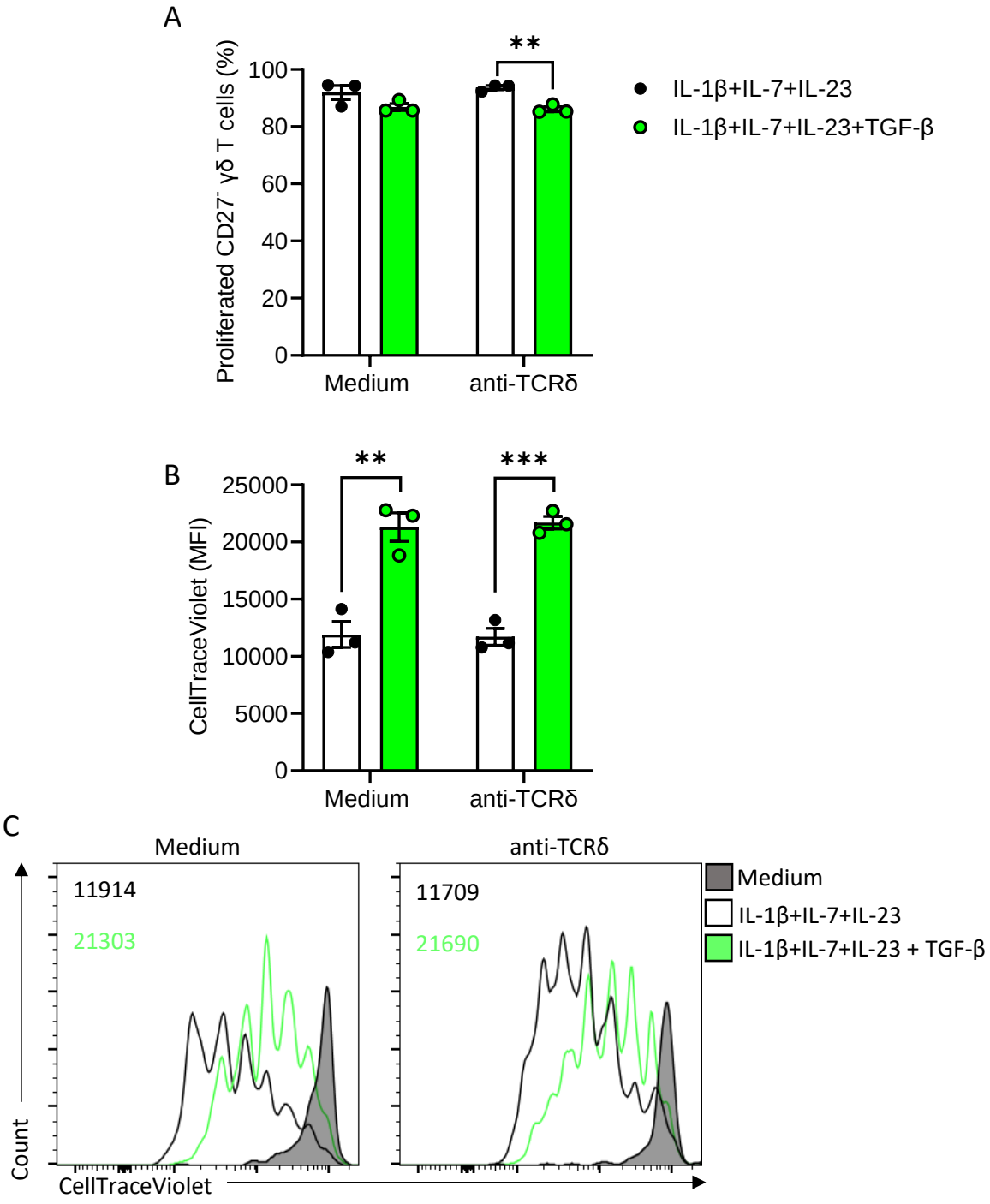

Figure 5.7 TGF-β suppresses proliferation of CD27$^-$ γδ T cells. LN and spleen cells were isolated from naïve C57BL/6J mice. CD3$^+$ cells were enriched using a negative selection T cell enrichment kit and stained with CellTraceViolet cell proliferation dye. Cells were stimulated with IL-1β (2.5 ng/mL), IL-7 (10 ng/mL), and IL-23 (10 ng/mL) in the presence or absence of anti-TCRδ and TGF-β (5 ng/mL). After 72 hours, cells were stained for surface CD3, CD27, and TCRδ followed by analysis by flow cytometry. Results are (A) frequency and (B) MFI of CellTraceViolet expressed by proliferated CD27$^-$ γδ T cells with (C) representative FACS plots. Data are mean ± SD (n=3) and are representative of two independent experiments. $^{**}p < 0.01$, $^{***}p < 0.001$ by unpaired Student's *t* test.

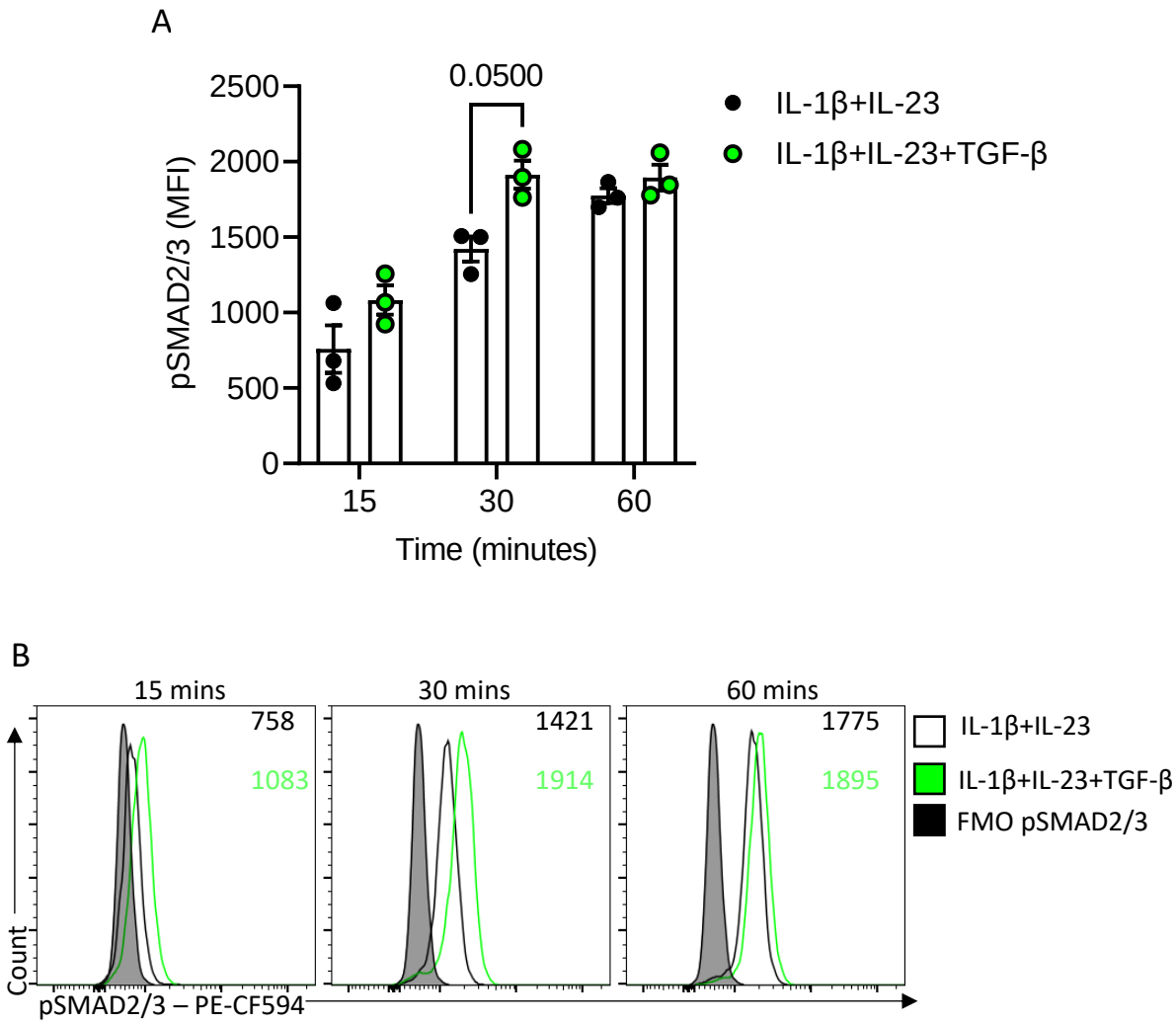

Figure 5.8 TGF-β induces SMAD2/3 phosphorylation in CD27$^-$ γδ T cells. CD27$^-$ γδ T cells were FACS-purified from the spleen and LN of naïve C57BL/6J mice. Sorted cells were serum-starved overnight to decrease background phosphorylation. The next day, cells were stimulated with IL-1β (2.5 ng/mL), and IL-23 (10 ng/mL) in the presence or absence of TGF-β (5 ng/mL) for 15, 30, and 60 minutes. Cells were stained for viability followed by methanol fixation and permeabilisation steps. Cells were stained for phosphorylated SMAD2/3 and analysed by flow cytometry. Results are (A) MFI of pSMAD2/3 expression by CD27$^-$ γδ T cells with (B) representative FACS plots. Data are mean ± SD (n=3) and are representative of three independent experiments. $^*p < 0.05$ by two-way ANOVA with Sidak's multiple comparisons test.

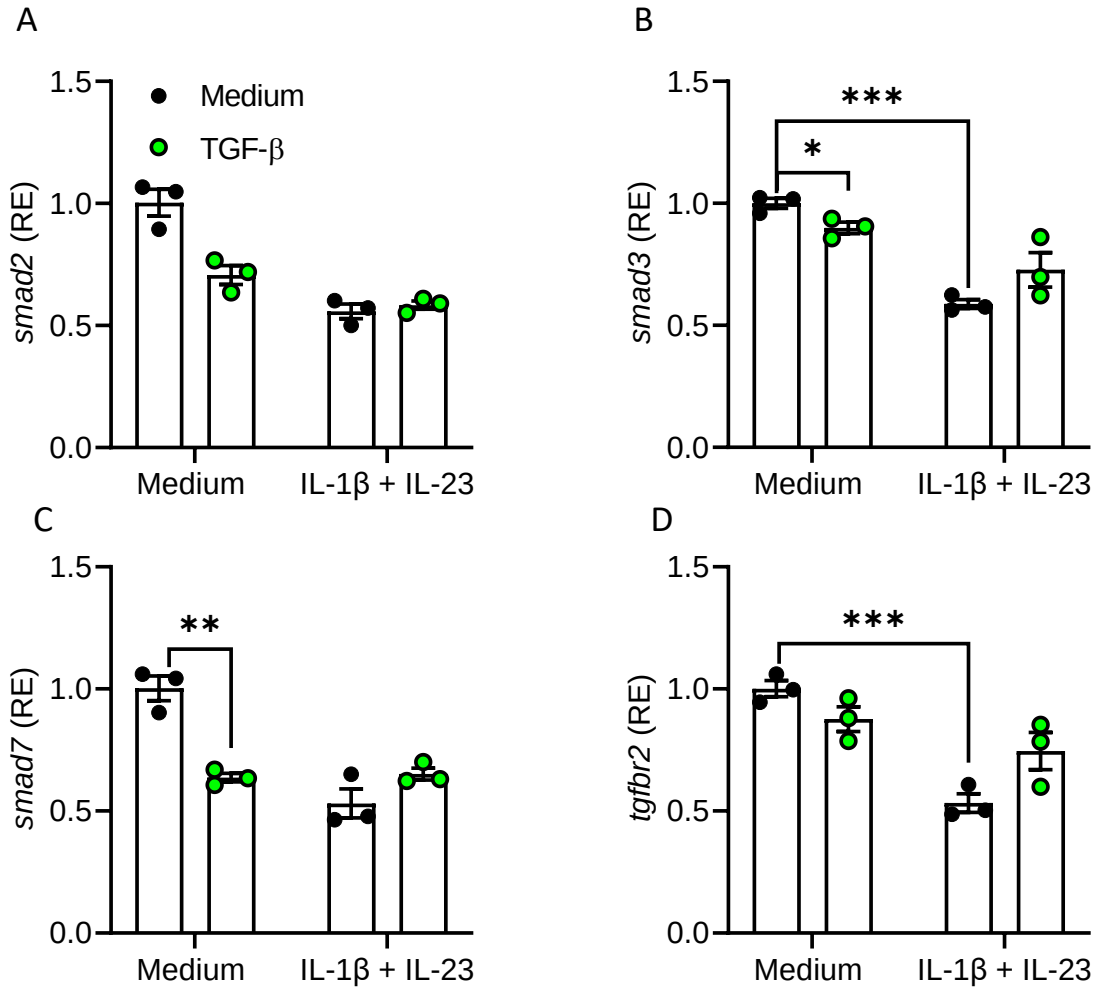

Figure 5.9 TGF-β does not increase mRNA expression of *smad* proteins in CD27$^-$ γδ T cells. CD27$^-$ γδ T cells were FACS-purified from the spleen and LN of naïve C57BL/6J mice. Cells were stimulated with IL-1β (2.5 ng/mL), and IL-23 (10 ng/mL) in the presence or absence of TGF-β (5 ng/mL) for 2 hours. mRNA expression was evaluated by Rt-PCR normalised to 18S rRNA and relative to the medium control. Results are mRNA expression of (A) *smad2*, (B) *smad3*, (C) *smad7,* and (D) *tgfbr2* by CD27$^-$ γδ T cells. Data are mean ± SD (n=3) and are representative of three independent experiments. $^*p < 0.05$, $^{**}p < 0.01$, $^{***}p < 0.001$ by unpaired Student's *t* test medium control versus TGF-β.

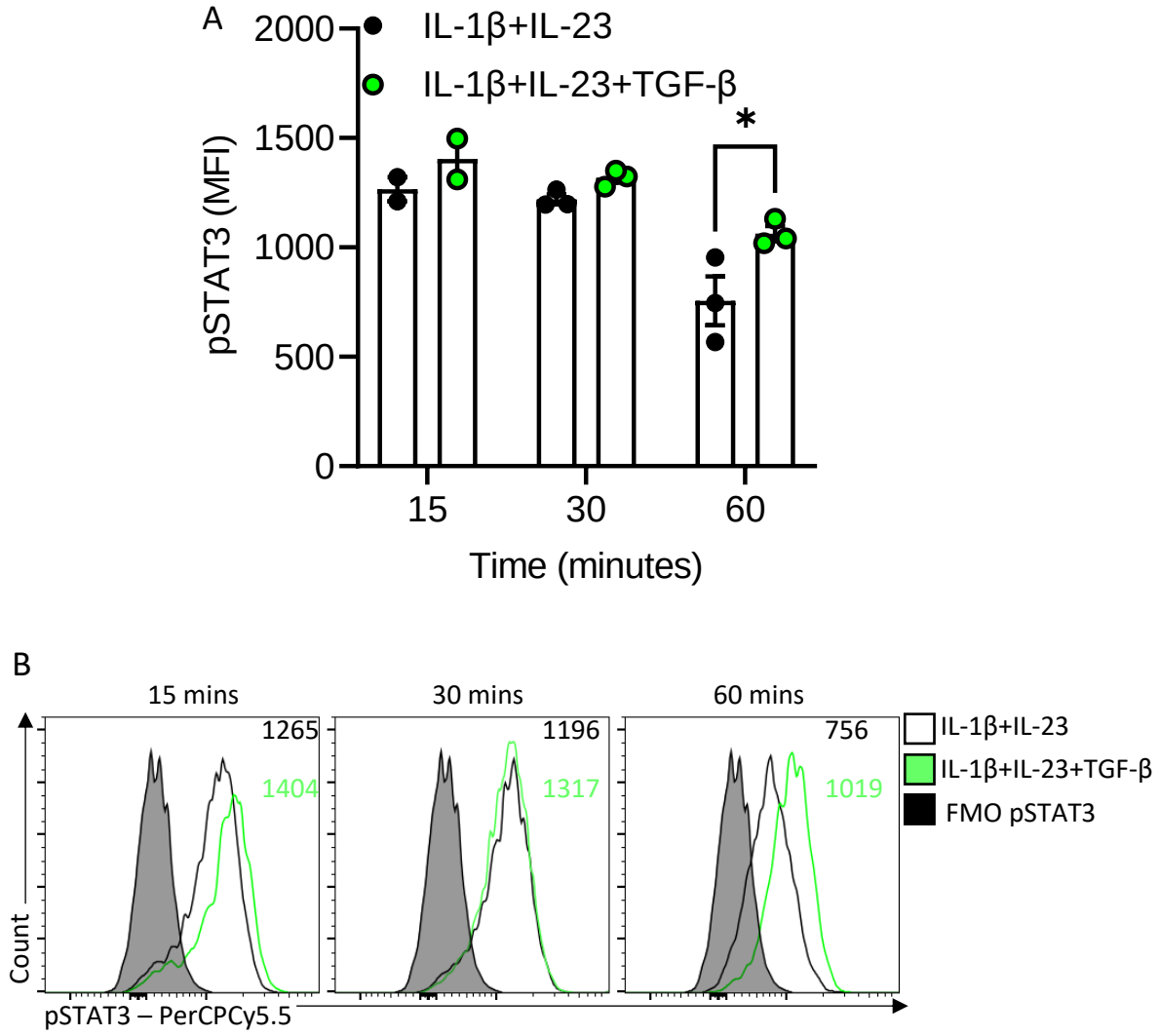

Figure 5.10 TGF-β increases STAT3 phosphorylation in CD27$^-$ γδ T cells. CD27$^-$ γδ T cells were FACS-purified from the spleen and LN of naïve C57BL/6J mice. Sorted cells were serum-starved overnight to decrease background phosphorylation. The next day, cells were stimulated with IL-1β (2.5 ng/mL), and IL-23 (10 ng/mL) in the presence or absence of TGF-β (5 ng/mL) for 15, 30, and 60 minutes. Cells were stained for viability followed by methanol fixation and permeabilisation steps. Cells were stained for phosphorylated STAT3 and analysed by flow cytometry. Results are (A) MFI of pSTAT3 expression by CD27$^-$ γδ T cells with (B) representative FACS plots. Data are mean ± SD (n=3) and are representative of three independent experiments. $^*p < 0.05$ by two-way ANOVA with Sidak's multiple comparisons test.

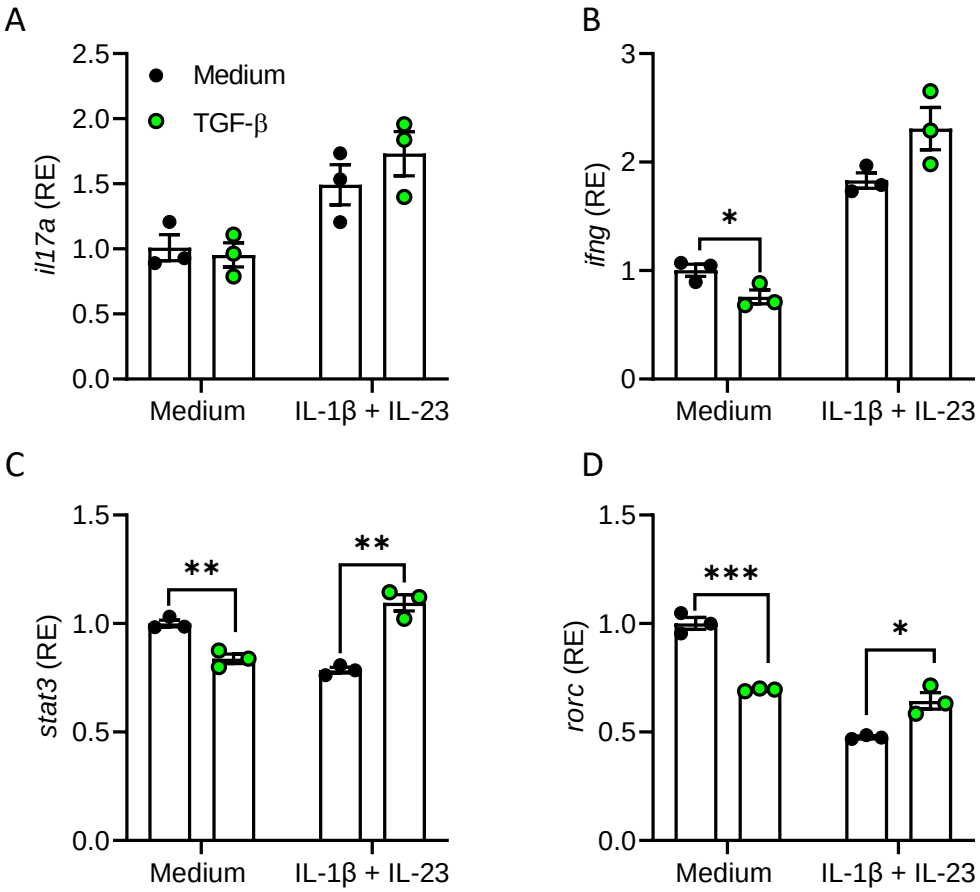

Figure 5.11 TGF-β increases mRNA expression of *rorc* and *stat3* in IL-1β and IL-23-stimulated CD27⁻ γδ T cells. CD27⁻ γδ T cells were FACS-purified from the spleen and LN of naïve C57BL/6J mice. Cells were stimulated with IL-1β (2.5 ng/mL), and IL-23 (10 ng/mL) in the presence or absence of TGF-β (5 ng/mL) for 2 hours. mRNA expression was evaluated by Rt-PCR normalised to 18S rRNA and relative to the medium control. Results are mRNA expression of (A) *il17a*, (B) *ifng*, (C) *stat3,* and (D) *rorc* by CD27⁻ γδ T cells. Data are mean ± SD (n=3) and are representative of three independent experiments. $^{*}p < 0.05$, $^{**}p < 0.01$, $^{***}p < 0.001$ by unpaired Student's *t* test medium control versus TGF-β.

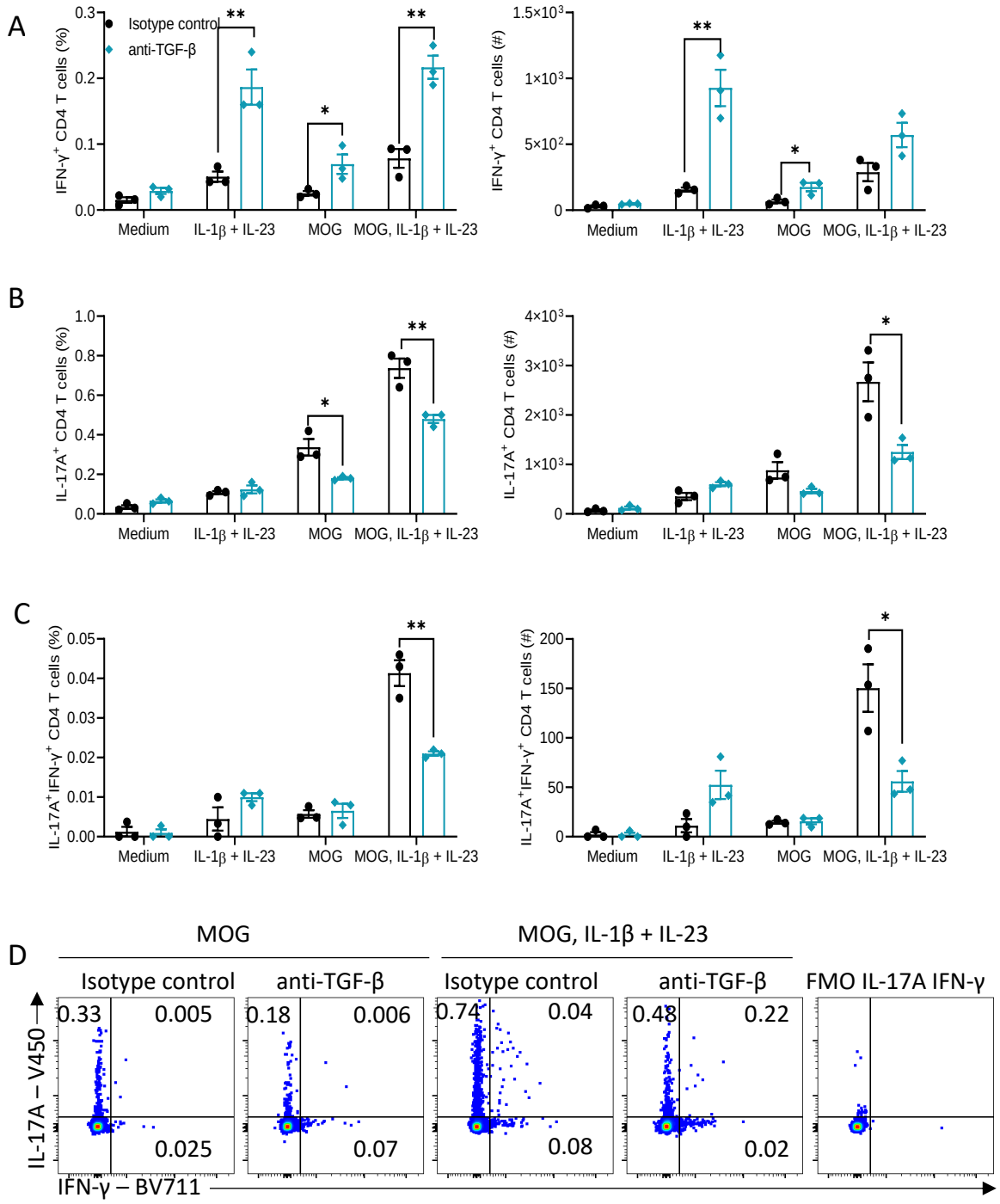

Figure 5.12 Inhibition of TGF-β signalling suppresses IL-17A production by MOG-specific CD4 T cells. C57BL/6J mice were immunised with MOG emulsified in CFA. Axillary, brachial, and inguinal LNs and spleens were harvested from mice 10 days post immunisation. Cells were cultured with MOG (50 µg/mL), IL-1β, and IL-23 (10 ng/mL) in the presence or absence of anti-TGF-β or isotype control antibody. After 72 hours, cells were harvested and incubated with brefeldin A for 4 hours followed by staining for surface CD3, CD4, intracellular IFN-γ, and IL-17A and analysed by flow cytometry. Results are frequency and absolute number of (A) IFN-γ-producing, (B) IL-17A-producing, and (C) IFN-γ$^+$IL-17A$^+$ double-producing CD4 T cells with (D) representative FACS plots. Data are shown as mean ± SD and are representative of three independent experiments. $^*p < 0.05$, $^{**}p < 0.01$ by unpaired Student's *t* test isotype control versus anti-TGF-β.

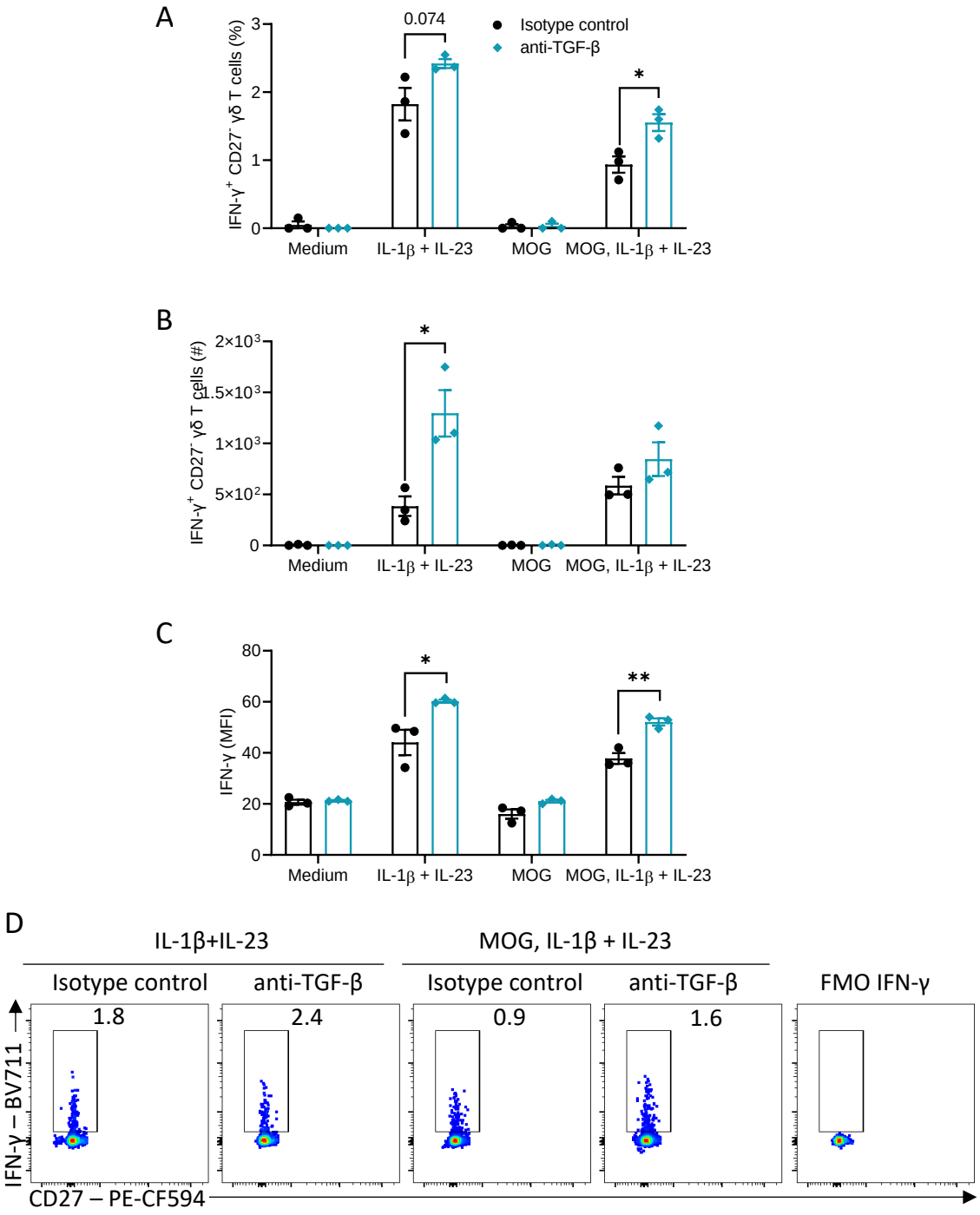

Figure 5.13 Inhibition of TGF-β signalling enhances IFN-γ production by CD27⁻ γδ T cells. C57BL/6J mice were immunised with MOG emulsified in CFA. Axillary, brachial, and inguinal LNs and spleens were harvested from mice 10 days post immunisation. Cells were cultured with MOG (50 µg/mL), IL-1β, and IL-23 (10 ng/mL) in the presence or absence of anti-TGF-β or isotype control antibody. After 72 hours, cells were harvested and incubated with brefeldin A for 4 hours followed by staining for surface CD3, CD27, TCRδ, and intracellular IFN-γ and analysed by flow cytometry. Results are (A) frequency, (B) absolute number, and (C) MFI of IFN-γ expression by CD27⁻ γδ T cells with (D) representative FACS plots. Data are shown as mean ± SD and are representative of three independent experiments. $^{*}p < 0.05$, $^{**}p < 0.01$ by unpaired Student's *t* test isotype control versus anti-TGF-β.

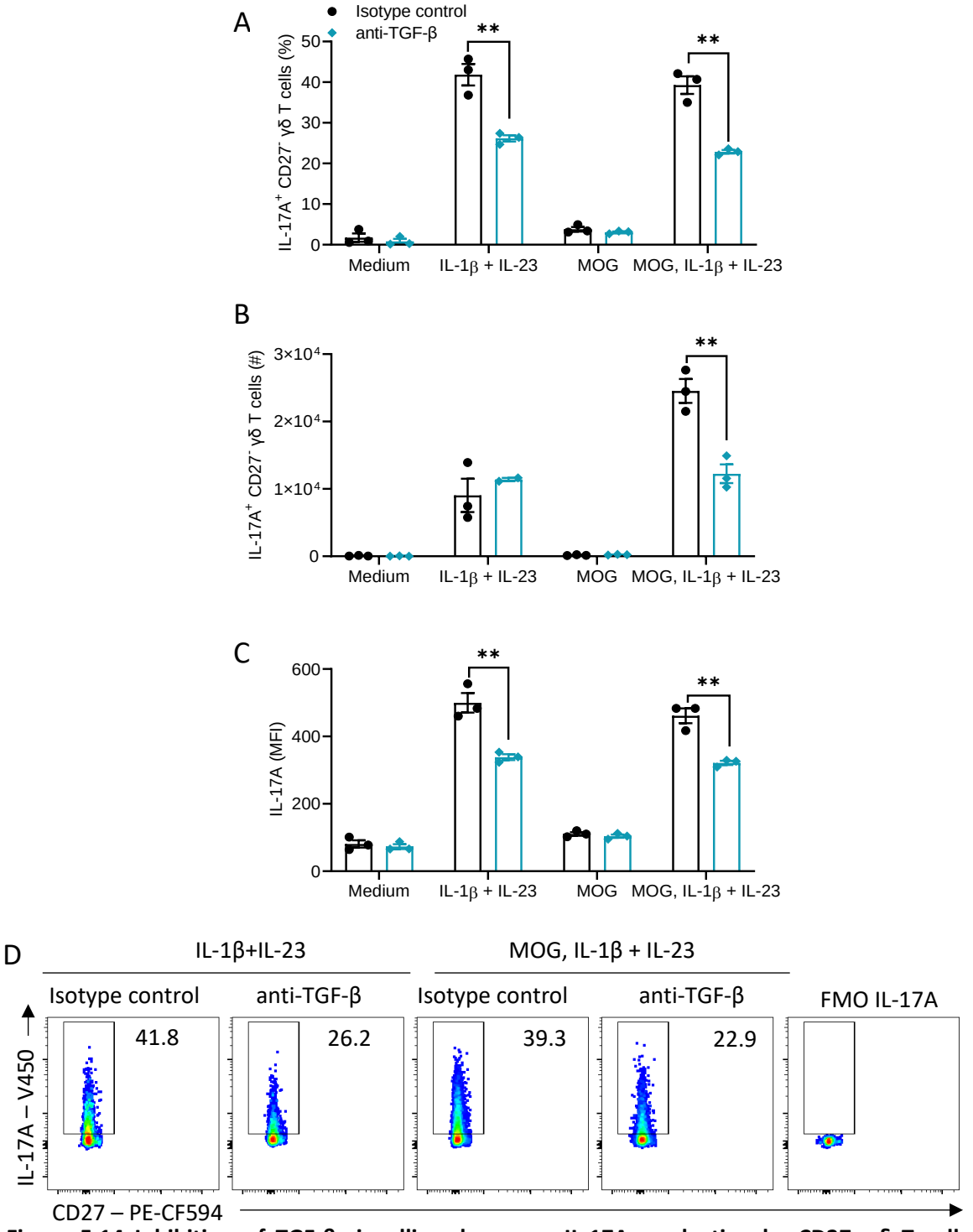

Figure 5.14 Inhibition of TGF-β signalling decreases IL-17A production by CD27⁻ γδ T cells. C57BL/6J mice were immunised with MOG emulsified in CFA. Axillary, brachial, and inguinal LNs and spleens were harvested from mice 10 days post immunisation. Cells were cultured with MOG (50 µg/mL), IL-1β, and IL-23 (10 ng/mL) in the presence or absence of anti-TGF-β or isotype control antibody. After 72 hours, cells were harvested and incubated with brefeldin A for 4 hours followed by staining for surface CD3, CD27, TCRδ, and intracellular IL-17A and analysed by flow cytometry. Results are (A) frequency, (B) absolute number, and (C) MFI of IL-17A-producing CD27⁻ γδ T cells with (D) representative FACS plots. Data are shown as mean ± SD and are representative of three independent experiments. $^{**}p < 0.01$ by unpaired Student's *t* test isotype control versus anti-TGF-β.

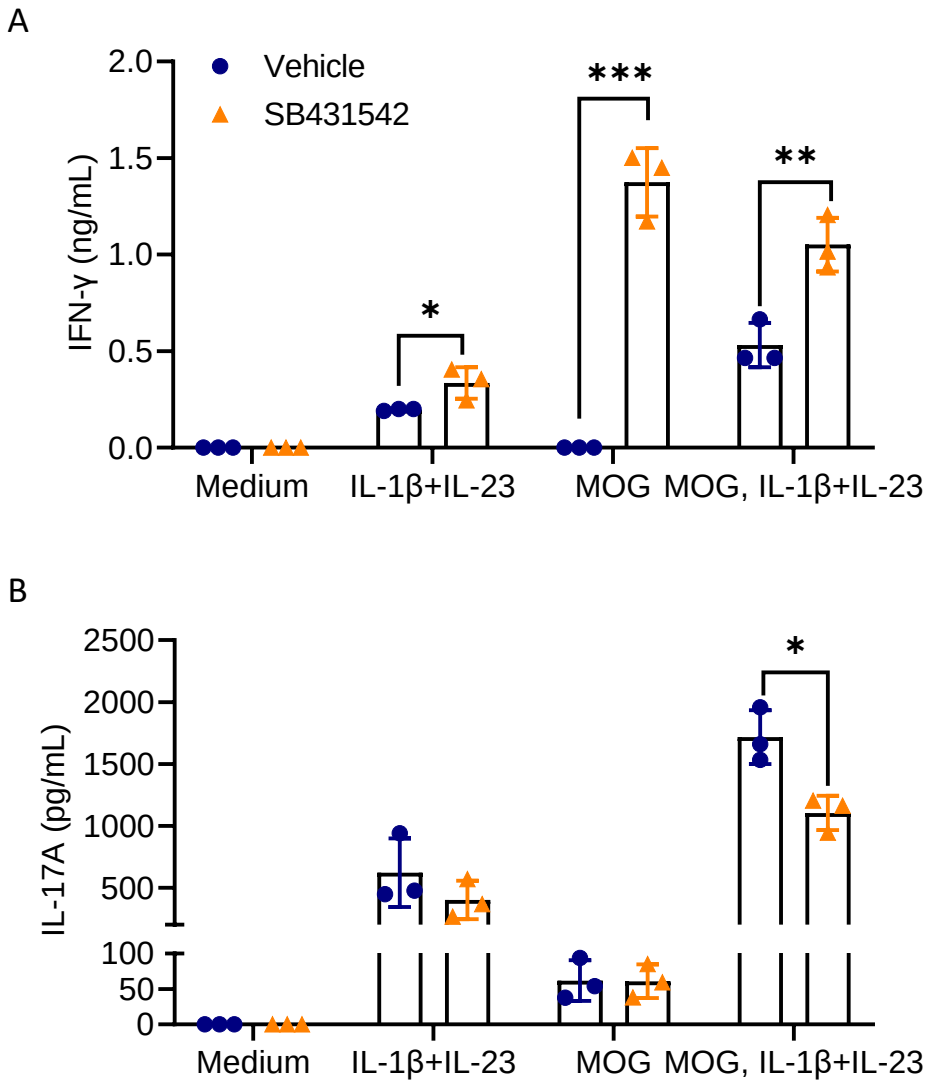

Figure 5.15 Inhibition of TGF-β signalling using a small molecule inhibitor (SB421542) increases MOG-specific IFN-γ and decreases MOG-specific IL-17A production. C57BL/6J mice were immunised with MOG emulsified in CFA. Axillary, brachial, and inguinal LNs and spleens were harvested from mice 10 days post immunisation. Cells were cultured with MOG (50 µg/mL), IL-1β, and IL-23 (10 ng/mL) in the presence or absence of SB431542 (10 µM) or vehicle control. After 72 hours, supernatants were collected and concentrations of (A) IFN-γ and (B) IL-17A were quantified by ELISA. Data are shown as mean ± SD and are representative of three independent experiments. $^{*}p < 0.05$, $^{**}p < 0.01$, $^{***}p < 0.001$ by unpaired Student's *t* test medium versus SB431542.

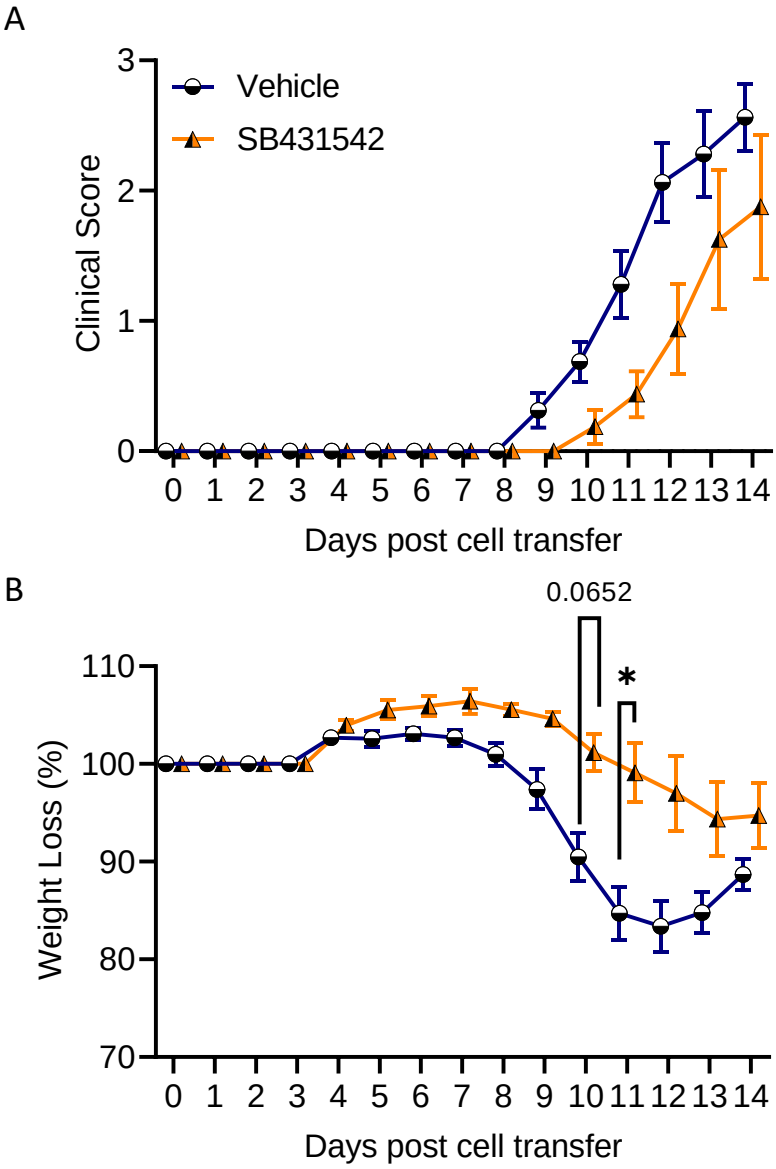

Figure 5.16 SB431542-treated MOG-specific T cells are less pathogenic in the adoptive transfer model of EAE. Donor C57BL/6J mice were immunised with MOG emulsified in CFA. After 10 days, spleen and LNs were harvested from donor mice and cultured with MOG (100 µg/mL), IL-1β, and IL-23 (10 ng/mL) in the presence of SB431542 (10 µM) or vehicle control for 72 hours. Donor cells were harvested and washed thoroughly before being transferred to recipient mice (15 x 10^6 cells per recipient mouse). Recipient mice were assessed daily for the development of EAE by (A) clinical score and (B) % weight loss. Data are mean ± SEM for n=6 mice per group and are representative of two independent experiments. *p < 0.05 by two-way ANOVA with Sidak's multiple comparisons test.

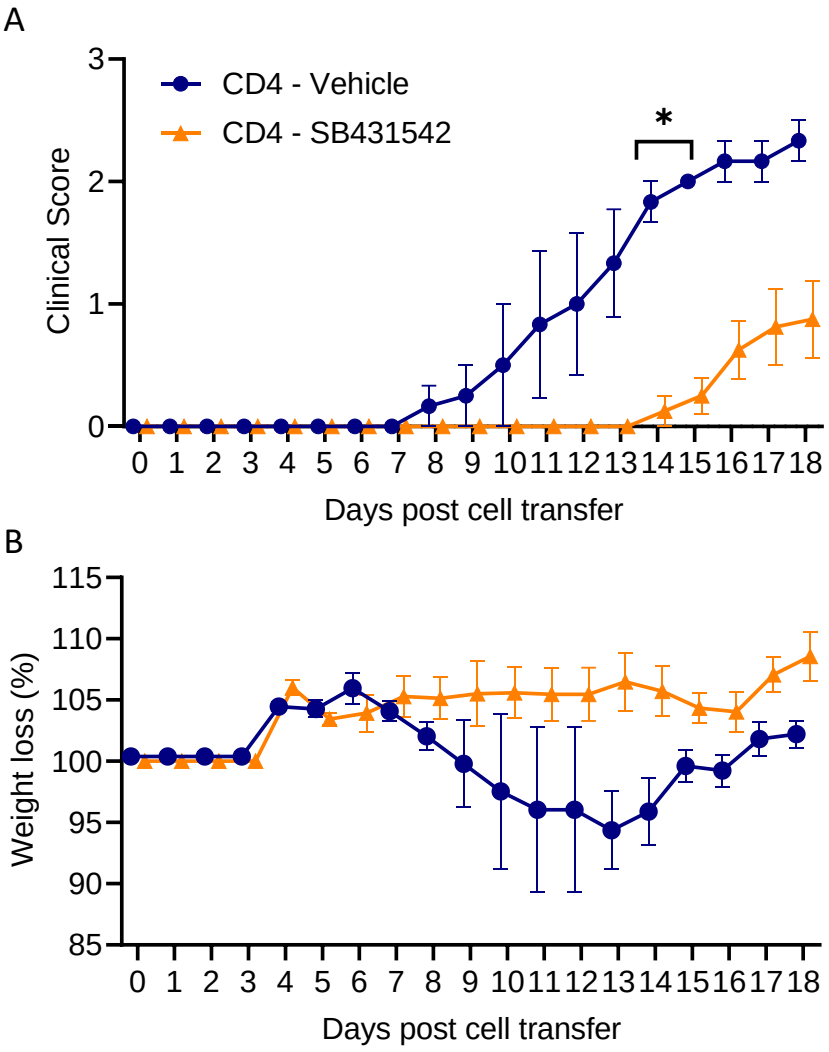

Figure 5.17 SB431542 suppresses the pathogenicity of CD4 T cells in the adoptive transfer model of EAE. Donor C57BL/6J mice were immunised with MOG emulsified in CFA. After 10 days, spleen and LNs were harvested from donor mice. CD4 T cells were separated from spleen and LN cells by magnetic separation. CD4 T cells were treated with SB431542 (10 µM) or vehicle control for 6 hours. CD4 T cells were then washed and recombined with the $CD4^-$ untreated fraction and cultured with MOG (100 µg/mL), IL-1β, and IL-23 (10 ng/mL) for 72 hours. Donor cells were harvested and washed thoroughly before being transferred to recipient mice (10 x 10^6 cells per recipient mouse). Recipient mice were assessed daily for the development of EAE by (A) clinical score and (B) % weight loss. Data are mean ± SEM for n=5 mice per group and are representative of one independent experiment. *$p < 0.05$ by two-way ANOVA with Sidak's multiple comparisons test.

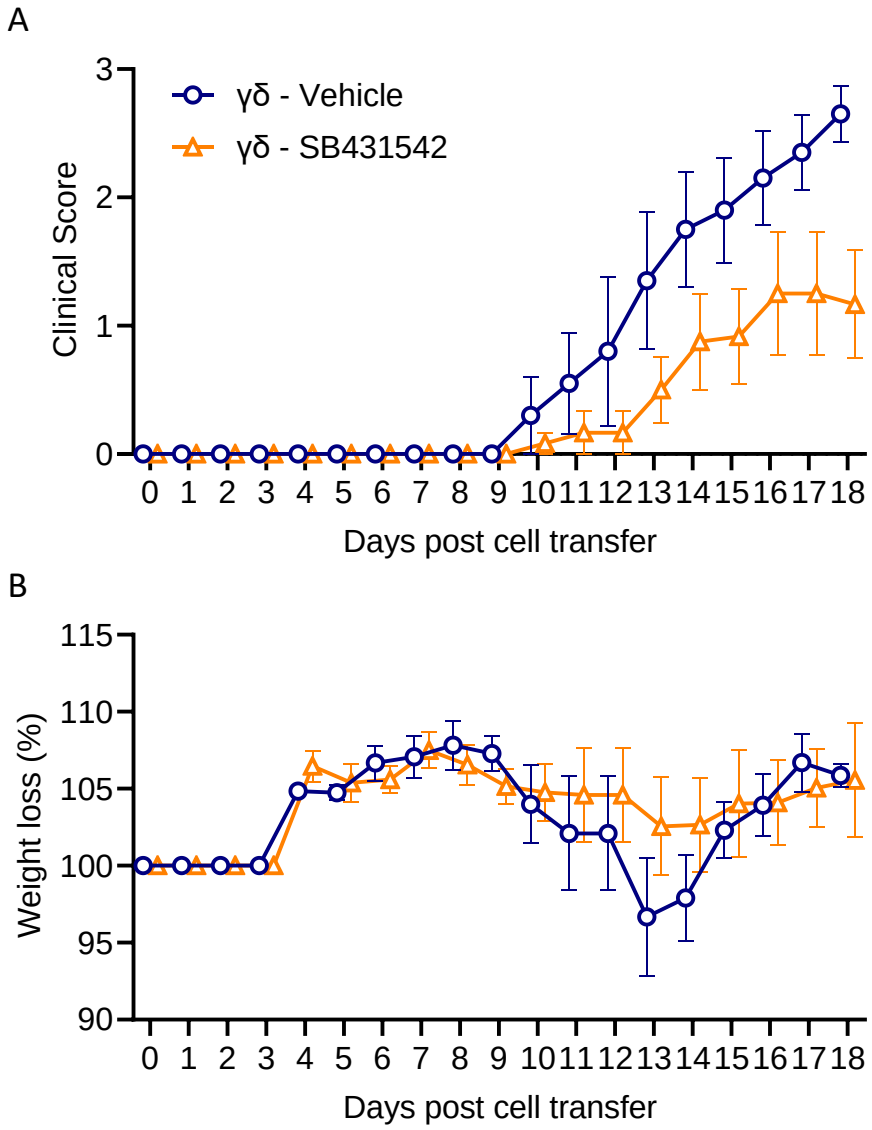

Figure 5.18 SB431542 suppresses the pathogenicity of γδ T cells in the adoptive transfer model of EAE. Donor C57BL/6J mice were immunised with MOG emulsified in CFA. After 10 days, spleen and LNs were harvested from donor mice. γδ T cells were separated from spleen and LN cells by magnetic separation. γδ T cells were treated with SB431542 (10 µM) or vehicle control for 6 hours. γδ T cells were then washed and recombined with the $\gamma\delta^-$ untreated fraction and cultured with MOG (100 µg/mL), IL-1β, and IL-23 (10 ng/mL) for 72 hours. Donor cells were harvested and washed thoroughly before being transferred to recipient mice (10×10^6 cells per recipient mouse). Recipient mice were assessed daily for the development of EAE by (A) clinical score and (B) % weight loss. Data are mean ± SEM for n=5 mice per group and are representative of one independent experiment.

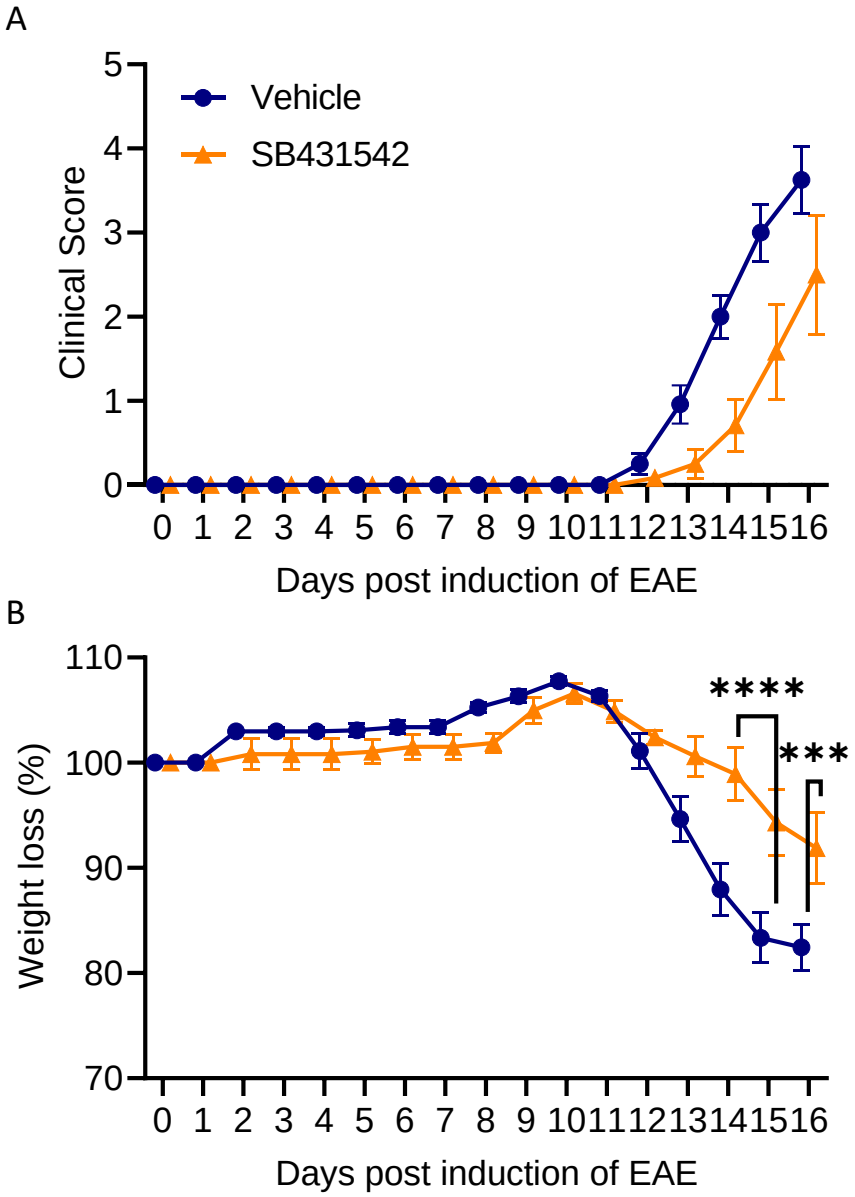

Figure 5.19 SB431542 treatment delays disease onset and severity of active EAE. EAE was induced in C57BL/6J mice by s.c injection with 100 µg MOG emulsified in CFA. Mice were injected i.p with 250 ng PT on days 0 and 2. Mice were injected i.p with 200 µg of SB431542 or vehicle control 1 hour prior to induction of EAE and on days 2, 4, 6, 8, and 10 of EAE. Mice were assessed daily for the development of EAE by (A) clinical score and (B) % weight loss. Data are mean ± SEM for n=6 mice per group and are representative of three independent experiments. ***p < 0.001, ****p < 0.0001 by two-way ANOVA with Sidak's multiple comparisons test.

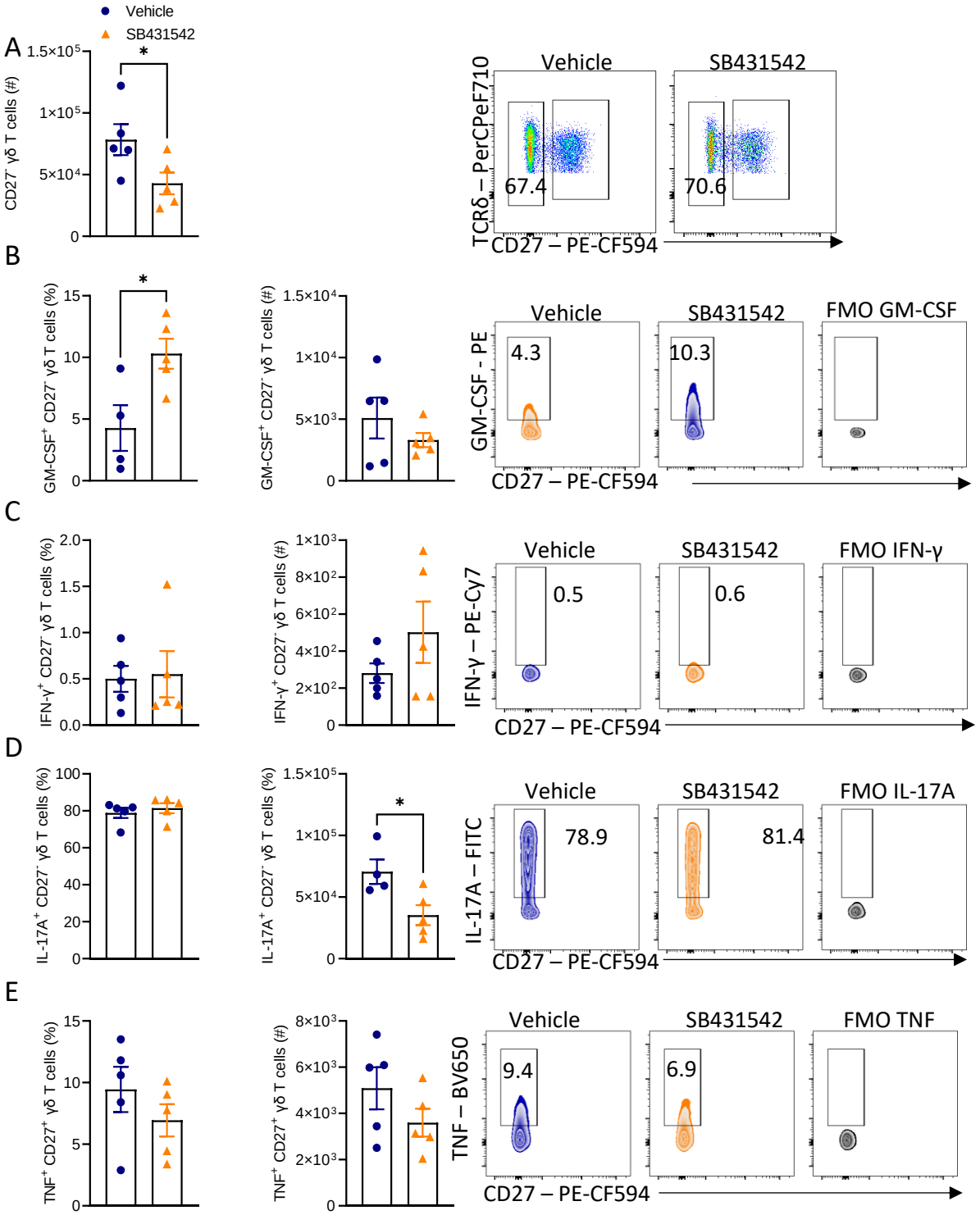

Figure 5.20 SB431542 treatment decreases the number of IL-17A-producing CD27⁻ γδ T cells in the LN at the induction phase of EAE. EAE was induced in C57BL/6J mice. Mice were injected i.p with 250 ng PT on days 0 and 2. Mice were injected i.p with 200 µg of SB431542 or vehicle control 1 hour prior to induction of EAE and on days 2, 4, and 6 of EAE. On day 7 post induction of EAE, mice were sacrificed, and cells were isolated from the LN. Cells were incubated with PMA, ionomycin, and brefeldin A for 4 hours followed by staining for surface CD3, CD27, TCRδ, and intracellular GM-CSF, IFN-γ, IL-17A, and TNF and analysed by flow cytometry. Results are (A) number of CD27⁻ γδ T cells, frequency, and number of (B) GM-CSF-producing, (C) IFN-γ-producing, (D) IL-17A-producing, and (E) TNF-producing CD27⁻ γδ T cells with representative FACS plots. Results are representative of three independent experiments. Data are mean ± SEM (n=5 per group). $^{*}p < 0.05$ by unpaired Student's *t* test.

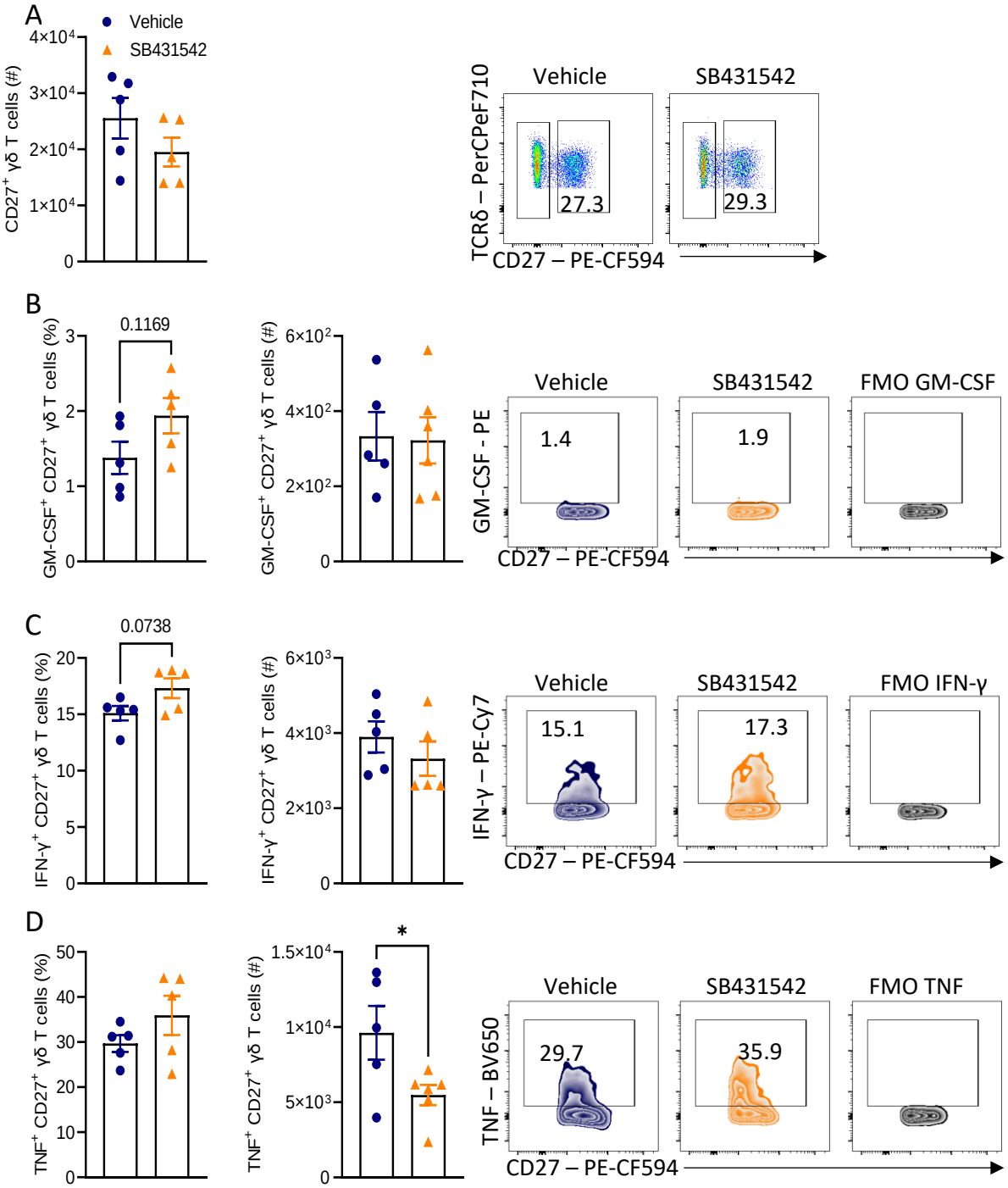

Figure 5.21 SB431542 treatment decreases the number of TNF-producing CD27⁺ γδ T cells in the LN at the induction phase of EAE. EAE was induced in C57BL/6J mice. Mice were injected i.p with 250 ng PT on days 0 and 2. Mice were injected i.p with 200 µg of SB431542 or vehicle control 1 hour prior to induction of EAE and on days 2, 4, and 6 of EAE. On day 7 post induction of EAE, mice were sacrificed, and cells were isolated from the LN. Cells were incubated with PMA, ionomycin, and brefeldin A for 4 hours followed by staining for surface CD3, CD27, TCRδ, and intracellular GM-CSF, IFN-γ, IL-17A, and TNF and analysed by flow cytometry. Results are (A) absolute number of CD27⁺ γδ T cells, frequency, and absolute number of (B) GM-CSF-producing, (C) IFN-γ-producing, and (D) TNF-producing CD27⁺ γδ T cells with representative FACS plots. Results are representative of three independent experiments. Data are mean ± SEM (n=5 per group). $^{*}p < 0.05$ by unpaired Student's *t* test.

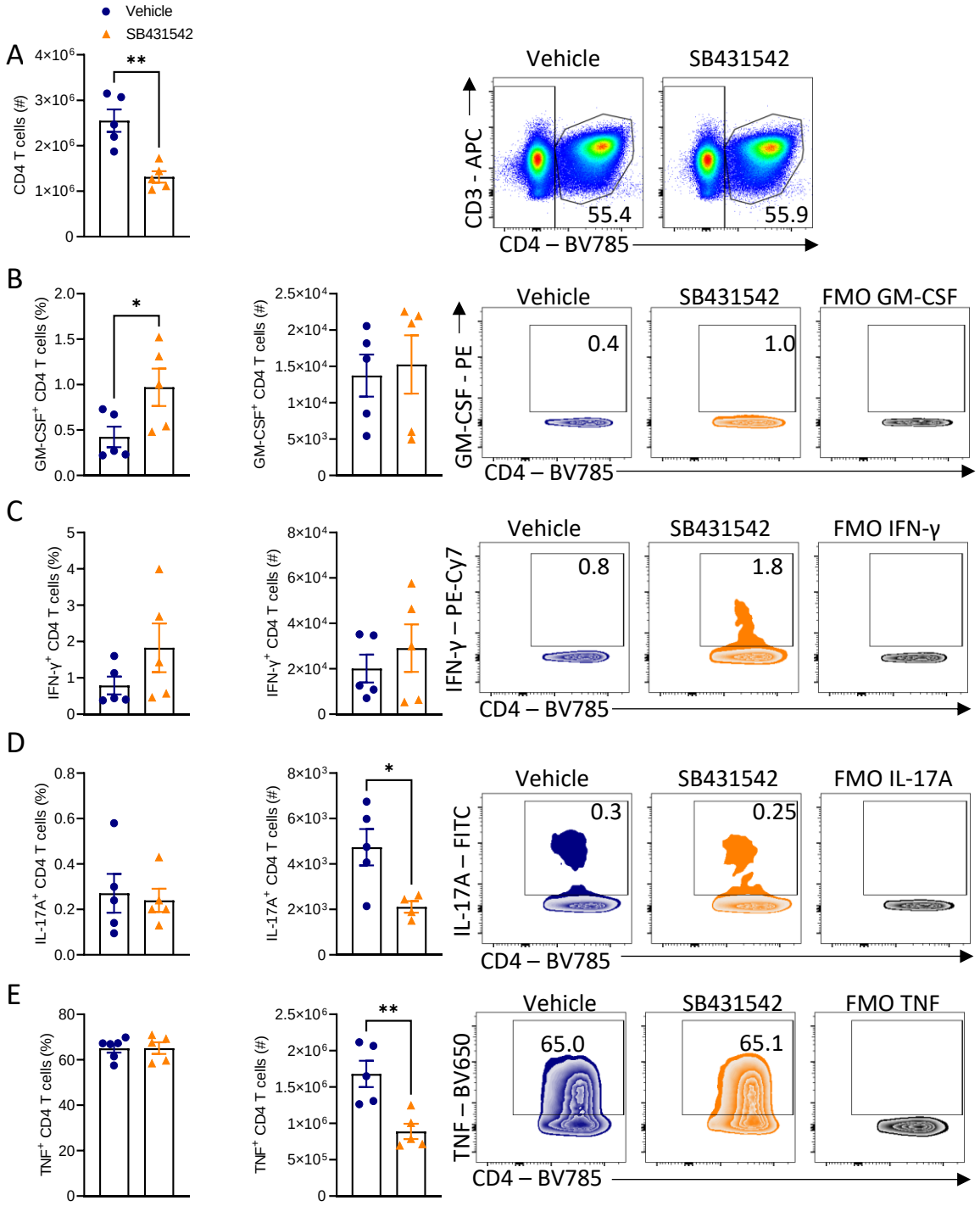

Figure 5.22 SB431542 treatment decreases the number of IL-17A-producing CD4 T cells in the LN at the induction phase of EAE. EAE was induced in C57BL/6J mice. Mice were injected i.p with 250 ng PT on days 0 and 2. Mice were injected i.p with 200 µg of SB431542 or vehicle control 1 hour prior to induction of EAE and on days 2, 4, and 6 of EAE. On day 7 post induction of EAE, mice were sacrificed, and cells were isolated from the LN. Cells were incubated with PMA, ionomycin, and brefeldin A for 4 hours followed by staining for surface CD3, CD4, and intracellular GM-CSF, IFN-γ, IL-17A, and TNF and analysed by flow cytometry. Results are (A) absolute number of CD4 T cells, frequency, and absolute number of (B) GM-CSF-producing, (C) IFN-γ-producing, (D) IL-17A-producing, and (E) TNF-producing CD4 T cells with representative FACS plots. Results are representative of three independent experiments. Data are mean ± SEM (n=5 per group). $^{*}p < 0.05$, $^{**}p < 0.01$ by unpaired Student's *t* test.

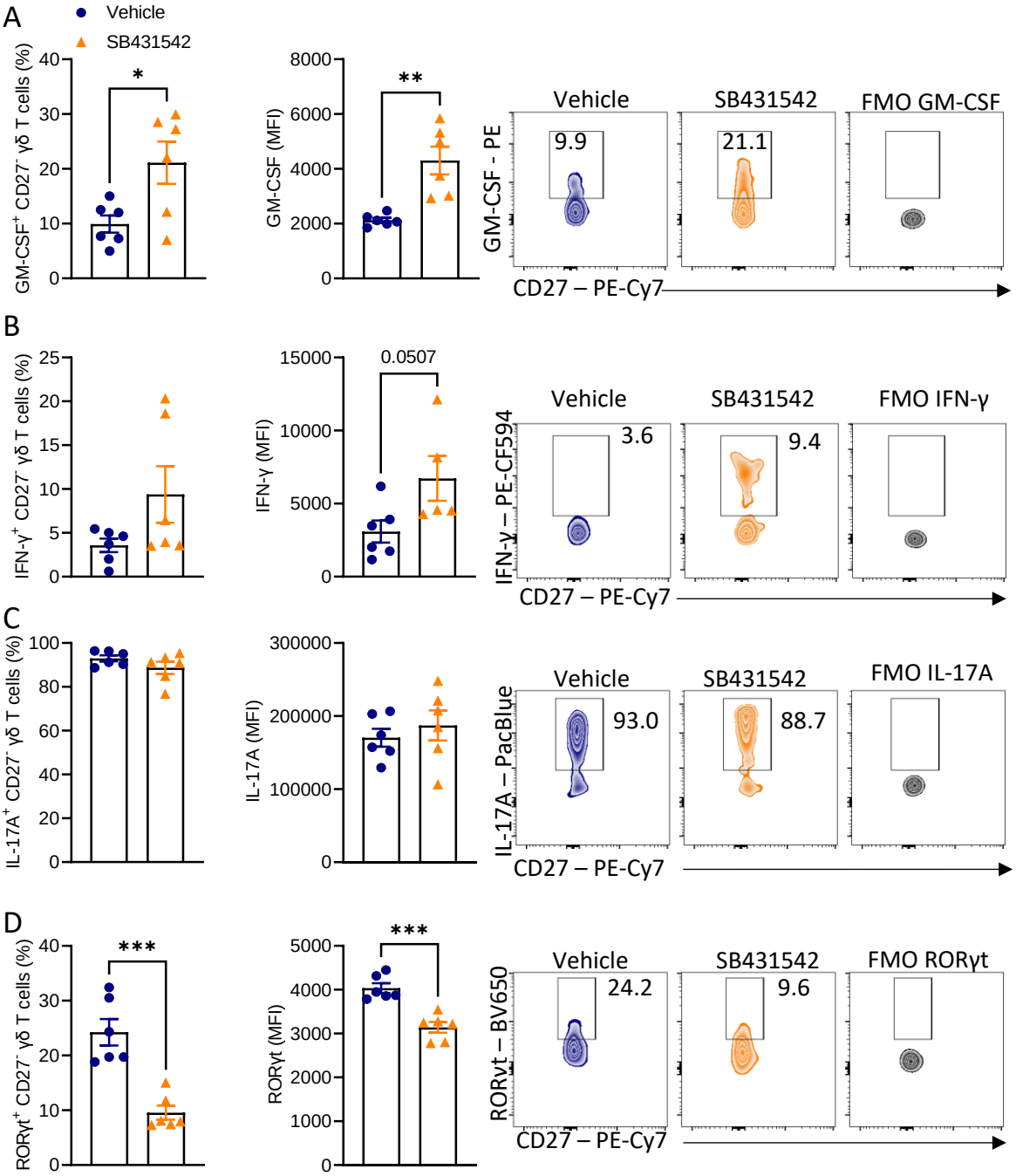

Figure 5.23 Treatment with SB431542 decreases the frequency and MFI of RORγt expression by CD27$^-$ γδ T cells in the brain at the peak of EAE. EAE was induced in C57BL/6J mice. Mice were injected i.p with 250 ng PT on days 0 and 2. Mice were injected i.p with 200 µg of SB431542 or vehicle control 1 hour prior to induction of EAE and on days 2, 4, 6, 8, and 10 of EAE. On day 14 post induction of EAE, mice were sacrificed, and perfused with PBS prior to harvesting of the brain. Mononuclear cells were isolated from the brain and incubated with brefeldin A, alone or in combination with PMA, and ionomycin for 4 hours followed by staining for surface CD3, CD27, TCRδ, and intracellular GM-CSF, IFN-γ, IL-17A, and RORγt and analysed by flow cytometry. Results are frequency and MFI of (A) GM-CSF-producing, (B) IFN-γ-producing, (C) IL-17A-producing, and (D) RORγt-expressing CD27$^-$ γδ T cells with representative FACS plots. Results are representative of three independent experiments. Data are mean ± SEM (n=6 per group). $^*p < 0.05$, $^{**}p < 0.01$, $^{***}p < 0.001$ by unpaired Student's *t* test.

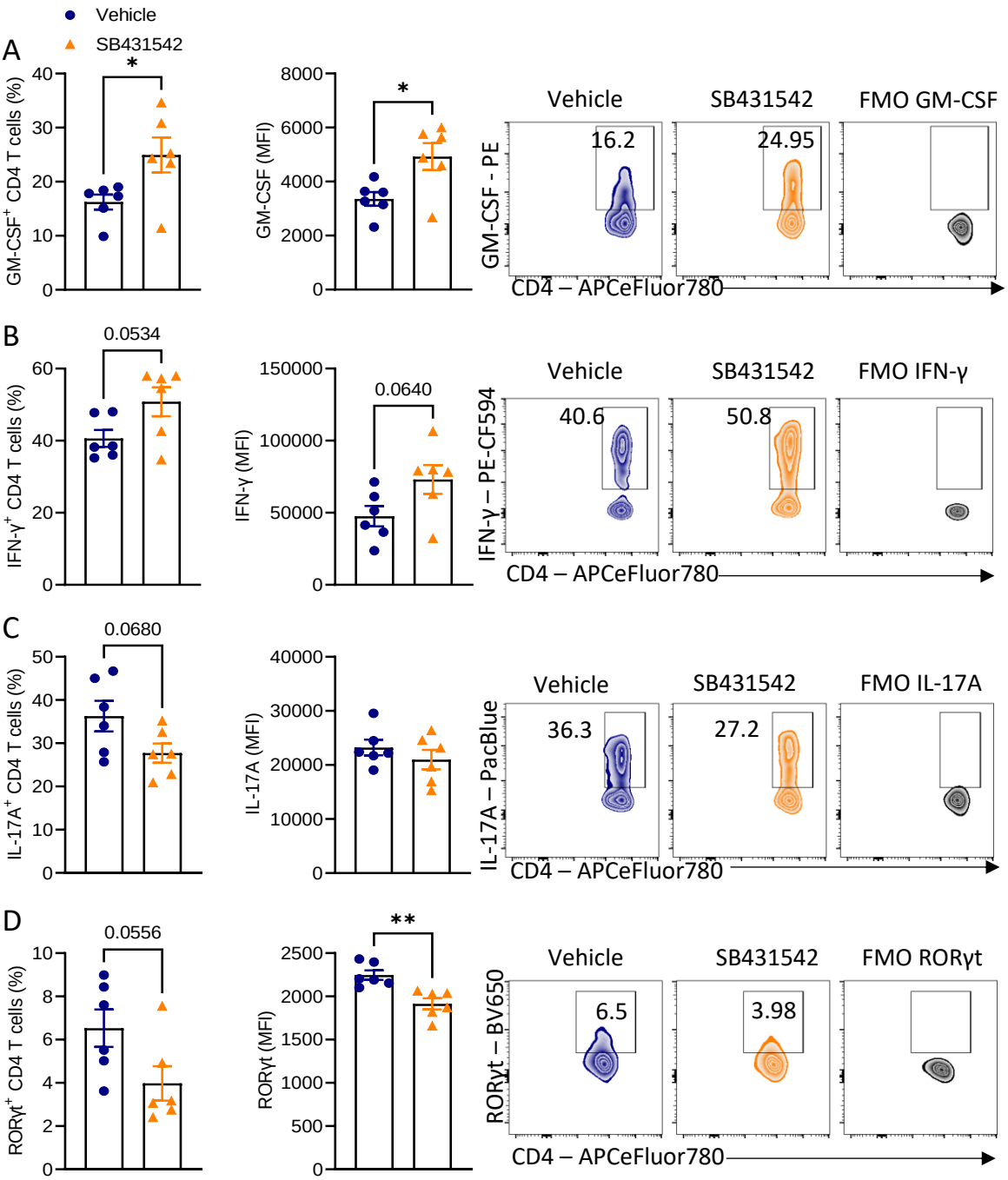

Figure 5.24 Treatment with SB431542 decreases the frequency and MFI of RORγt expression by CD4 T cells in the brain at the peak of EAE. EAE was induced in C57BL/6J mic. Mice were injected i.p with 250 ng PT on days 0 and 2. Mice were injected i.p with 200 µg of SB431542 or vehicle control 1 hour prior to induction of EAE and on days 2, 4, 6, 8, and 10 of EAE. On day 14 post induction of EAE, mice were sacrificed, and perfused with PBS prior to harvesting of the brain. Mononuclear cells were isolated from the brain and incubated with brefeldin A, alone or in combination with PMA, and ionomycin for 4 hours followed by staining for surface CD3, CD4, and intracellular GM-CSF, IFN-γ, IL-17A, and RORγt and analysed by flow cytometry. Results are frequency and MFI of (A) GM-CSF-producing, (B) IFN-γ-producing, (C) IL-17A-producing, and (D) RORγt-expressing CD4 T cells with representative FACS plots. Results are representative of three independent experiments. Data are mean ± SEM (n=6 per group). $^{*}p < 0.05$, $^{**}p < 0.01$ by unpaired Student's *t* test.

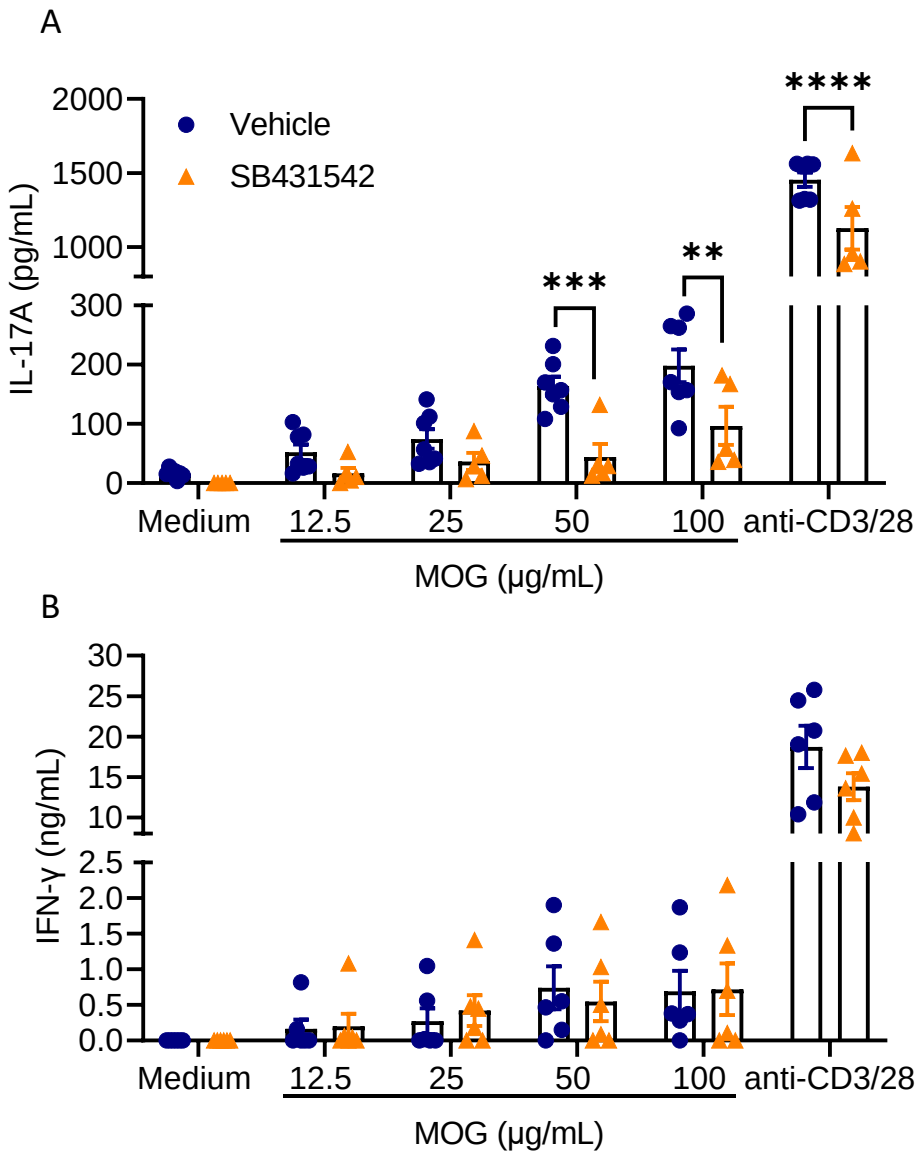

Figure 5.25 Inhibition of TGF-β-mediated signalling decreases MOG-specific IL-17A production. EAE was induced in C57BL/6J mice. Mice were injected i.p with 250 ng PT on days 0 and 2. Mice were injected i.p with 200 µg of SB431542 or vehicle control 1 hour prior to induction of EAE and on days 2, 4, 6, 8, and 10 of EAE. On day 14 post induction of EAE, mice were sacrificed, and axillary, brachial, and inguinal LNs and spleens were harvested. Spleen and LN cells were cultured at a 50:50 ratio (2 x 10^6 cells/mL) with increasing concentrations of MOG peptide (12.5 – 100 µg/mL). After 72 hours, supernatants were collected and concentrations of cytokines in the supernatants were quantified by ELISA. Results are the concentrations of (A) IL-17A and (B) IFN-γ in the supernatants of spleen and LN cells stimulated with MOG and are representative of two independent experiments. Data are mean ± SEM (n=6). $^{**}p < 0.01$, $^{***}p < 0.001$, $^{****}p < 0.0001$ by two-way ANOVA with Sidak's multiple comparisons test.

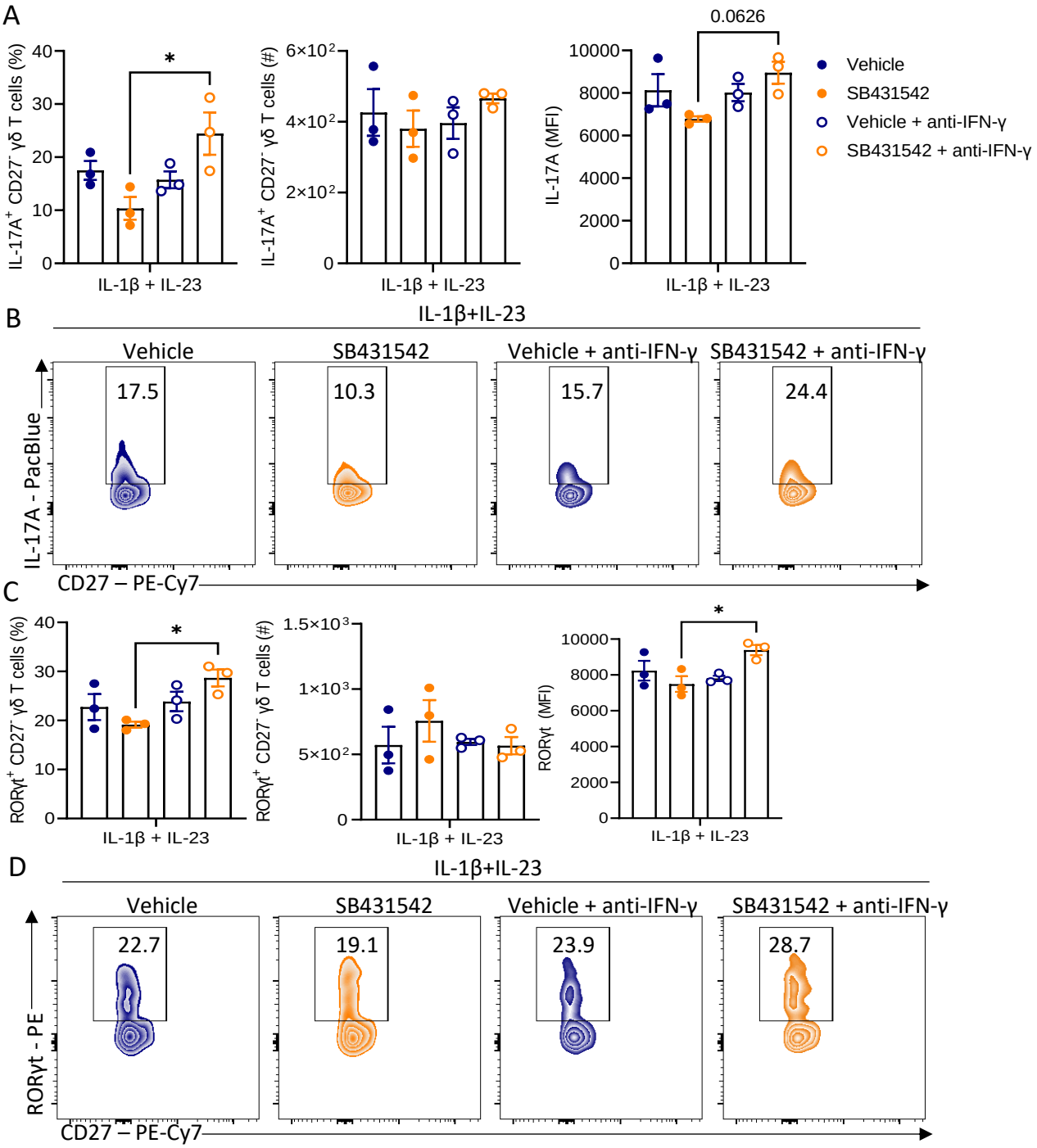

Figure 5.26 Neutralisation of IFN-γ reverses the suppressive effect of TGF-β blocking on CD27$^-$ γδ T cells. C57BL/6J mice were immunised with MOG emulsified in CFA. Axillary, brachial, and inguinal LNs and spleens were harvested from mice 10 days post immunisation. Cells were cultured with IL-1β and IL-23 (10 ng/mL) with or without anti-IFN-γ in the presence or absence of SB431542 (10 µM) or vehicle control. After 24 hours, cells were harvested and incubated with brefeldin A for 4 hours prior to staining for surface CD3, CD27, TCRδ, and intracellular IL-17A, and RORγt. Results are frequency, absolute number, and MFI of (A) IL-17A-producing CD27$^-$ γδ T cells with (B) representative FACS plots and frequency, absolute number, and MFI of (C) RORγt-expressing CD27$^-$ γδ T cells with (D) representative FACS plots. Data are mean ± SD and are representative of two independent experiments. $^*p < 0.05$ by one-way ANOVA with Tukey's multiple comparisons test.

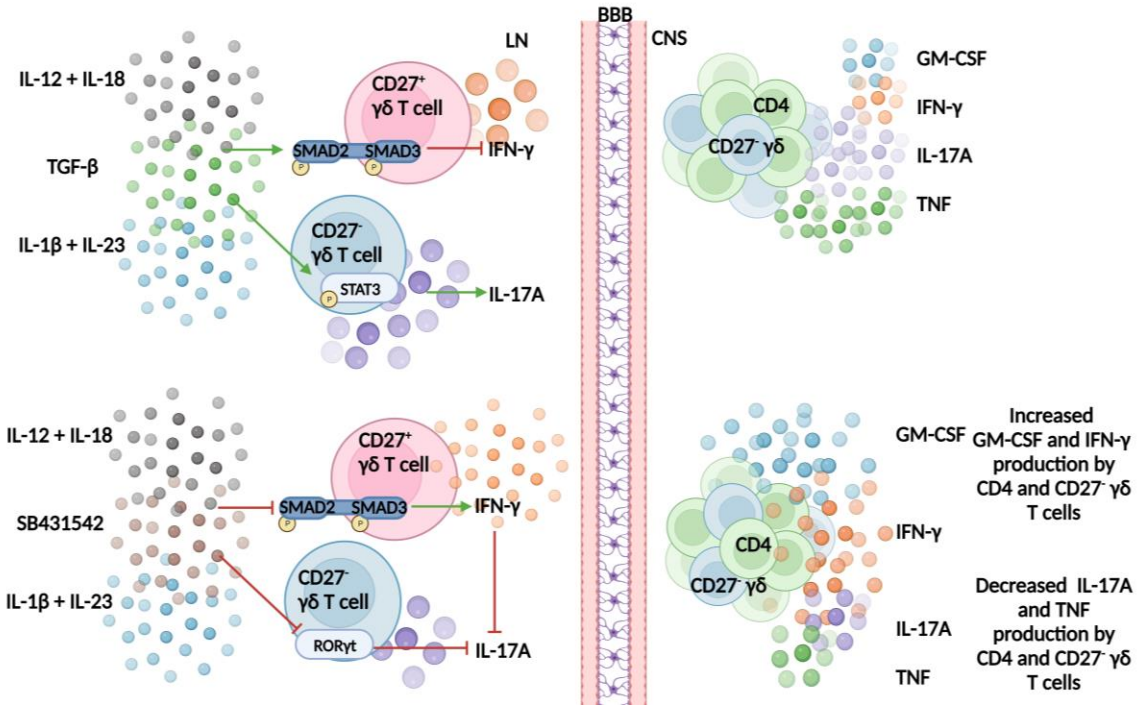

Figure 5.27 Proposed mechanism for the differential regulation of γδ T cell subsets by TGF-β. IFN-γ-production by IL-12+IL-18-activated CD27⁺ γδ T cells is suppressed by TGF-β via phosphorylation of SMAD2/3. Conversely, IL-17A production by IL-1β+IL-23-activated CD27⁻ γδ T cells is promoted by TGF-β via increased phosphorylation of STAT3. This leads to increased IL-17A production in the periphery during the induction of EAE resulting in enhanced infiltration of IL-17A-producing CD4 and γδ T cells into the CNS during EAE. In the case where TGF-β-mediated signalling has been ablated using the small molecule inhibitor SB431542, IFN-γ production by IL-12+IL-18-activated CD27⁺ γδ T cells is enhanced. SB431543 treatment also suppresses IL-17A production by IL-1β+IL-23-activated CD27⁻ γδ T cells in an IFN-γ-dependent manner. SB431542 treatment leads to enhanced production of IFN-γ and GM-CSF by CNS-infiltrating γδ and CD4 T cells and decreased IL-17A and TNF production by CNS-infiltrating γδ and CD4 T cells hence decreasing the severity of EAE.

Chapter 6
General Discussion

MS is a chronic, progressive disease of the CNS, characterised by axonal loss resulting in neurological functional impairment. Disability accumulates over the patient's lifetime and it is estimated that 50% of people living with MS require assistance with walking within 15 years of the onset of disease [365]. MS is the leading cause of neurological disability in young adults with an average age of onset between 20-30 years [366]. As of 2022 , the total societal cost of MS in Ireland has been estimated at 483 million euro per year, increasing by 12% since 2015 [367]. The murine model for MS, EAE, is an important tool for investigating the factors that modulate CNS autoimmunity. EAE is a T cell-mediated autoimmune disease which is characterised by ascending paralysis in the mouse [364]. IL-17A is a crucial mediator of disease that functions by recruiting IL-1β-producing inflammatory monocytes and neutrophils during the induction of EAE, thereby amplifying the pathological immune response [171]. Vγ4 γδ T cells are an important early source of IL-17A in EAE and they expand during disease [368]. Furthermore, depletion of this IL-17A-producing population of γδ T cells during EAE significantly decreases the severity of disease [171]. Little is known about the mechanism whereby γδ T cell function is regulated. The now established role of γδ T cells in the pathology of EAE suggests that these cells could be modulated for therapeutic benefit. The present study investigated regulatory pathways that control γδ T cells and CD4 T cells during the development of EAE.

Findings from the present study demonstrated that the PD-1-PD-L1 pathway is a key regulator of γδ T cell function. PD-1 was highly expressed by $CD27^-$ Vγ4 γδ T cells in the LNs of naïve mice and this was significantly augmented during EAE. PD-1 engagement suppressed IL-17A production by γδ T cells *in vitro* and anti-PD-1 treatment enhanced IL-17A production by Vγ4 γδ T cells *in vivo* during EAE. These data suggest that PD-1 is an important immunoregulatory axis for γδ T cells that can be exploited to modulate the course of autoimmunity. Decreased PD-1 expression and signalling by PBMCs from MS patients has been reported [369]. Decreased *pdcd1* gene expression in PBMCs of MS patients correlated with an increased disability score. Furthermore, reduced expression of PD-1 by CD4 and CD8 Treg cells in PBMCs was reported in the early phase of RRMS [370]. In addition to decreased PD-1 expression identified in MS patients, there was increased IL-17A and IFN-γ concentrations in the serum when compared with healthy

controls. Inherited PD-1 deficiency has been identified in a patient that died from pulmonary autoimmunity [371]. PD-1 deficiency was accompanied by depletion of Vδ2 γδ T cells, mucosal-associated invariant T (MAIT) cells, and NK cells in addition to the expansion of RORγt-expressing $CD4^{-}CD8^{-}$ DN αβ T cells. This study highlights the importance of PD-1 signalling in the development of γδ T cells in humans and in regulating the expansion of RORγt-expressing T cells. While the ablation of PD-1 signalling exhibited in this patient resulted in fatal autoimmunity, increases in PD-1-mediated signalling can also be protective in autoimmunity. In a murine model of imiquimod-induced psoriasis, γδ T cells in the skin expressed high levels of PD-1 and PD-1 engagement suppressed IL-17A production by γδ T cells [372]. Additionally, secretory PD-L1 (sPD-L1) is increased in the CSF of RRMS patients when compared with CSF from SPMS or PPMS patients [123]. This increased PD-1 signalling in RRMS was associated with a decrease in disability score as measured by EDSS.

While decreased PD-1 expression and signalling has a pathogenic role in the context of autoimmunity, suppression of PD-1-mediated signalling represents a major therapeutic strategy for the treatment of cancer [106]. Antibodies targeting the PD-1 signalling pathway via blockade of either PD-1 or PD-L1 have been approved for the treatment of malignances including, non-small cell lung carcinoma, colorectal cancer, and melanoma [373]. Anti-PD-1 treatment reverses the immunosuppressive environment that is induced by tumour cells and allows for reactivation of anti-tumour T cell responses. However, treatment with ICIs such as anti-PD-1 causes autoimmunity in cancer patients [265]. Additionally, anti-PD-1 treatment of advanced melanoma in patients with pre-existing autoimmune diseases induced autoimmune disease flares in 38% of patients [266]. In the present study, anti-PD-1 treatment significantly increased the severity of EAE. Anti-PD-1 treatment increased the number and frequency of $IL\text{-}17A^{+}$ and $ROR\gamma t^{+}$ CD4 T cells and Vγ4 γδ T cells in the LN at the induction of EAE. Increased IL-17A production is pathogenic in EAE and in certain murine cancer models. IL-17A-producing γδ T cells promote breast cancer metastasis and ovarian cancer growth via mobilisation of immunosuppressive neutrophils and small peritoneal macrophages (SPMs), respectively [288, 292]. Anti-PD-1 treatment in a murine lung cancer model did not decrease tumour volume and this was associated with enhanced type 17 responses [295]. This study provides a potential

explanation for the incidence of non-responders to ICI despite enhanced PD-1 and PD-L1 expression in the tumour. In the context of cancer, anti-PD-1 treatment augments pro-tumour type-17 responses, similar to the response observed in the present study which led to an enhancement of the severity of EAE. These data suggest that the efficacy of anti-PD-1/PD-L1-based cancer immunotherapy could be improved by examining PD-1 expression by specific T cell subpopulations. Patients with high PD-1 expression on RORγt^{+} T cells may benefit from dual blockade of IL-17A and PD-1. Blockade of IL-17A improved the efficacy of anti-PD-1 therapy in CRC [296]. Conversely, IL-17A mediated the protective effect of anti-PD-1 and anti-CTLA-4 dual checkpoint blockade in murine melanoma [374]. The conflicting effects of IL-17A in different tumours highlights the need for a personalised approach to treatment of specific cancers with ICIs.

In the present study, anti-PD-1 treatment significantly enhanced antigen-specific T cell responses during EAE. While increased antigen-specific T cell responses are pathogenic in EAE, ICI-induced increases in tumour-specific T cells are associated with enhanced response rates and prolonged survival in melanoma and CRC [375]. DNA mismatch repair deficient (MMR-d) cancers express high levels of tumour antigens and therefore have high responsiveness to ICI [376]. Furthermore, defects in $\beta_2$microglobulin (β_2m) are associated with resistance to ICI [377]. In ICI-resistant melanoma patients, aberration in β_2m prevented the induction of tumour antigen-specific immune responses, which was associated with poorer overall survival. However, there are cases where β_2m defective cancers can respond robustly to ICI suggesting the involvement of another cell type in mediating the anti-cancer effect of ICIs. In MMR-d CRC with defects in antigen presentation, there was a significantly increased infiltration of Vδ1 and Vδ3 γδ T cells into the tumour which was positively associated with responsiveness to ICI [378]. These PD-1-expressing Vδ1 and Vδ3 γδ T cells could kill CRC cells via production of IFN-γ and NCR expression. In this case, ICI treatment re-activated Vδ1 and Vδ3 γδ T cells that were not antigen-specific. Another study demonstrated that, IL-1β+IL-23-activated Vγ6 γδ T cells were regulated by PD-1 which was mediated by expression of FOXO1 [177]. These studies demonstrate how PD-1 can regulate innately activated γδ T cells in both humans and mice. Cytokine-activated γδ T cells could have a potent anti-tumour role in response to ICI treatment in tumours with low expression of tumour-specific antigens (TSAs).

Immune checkpoints suppress T cell responses via downregulation of the components of TCR signalling. In the present study, Vγ4 γδ T cells were regulated by PD-1 during the development of EAE but these cells appeared to be antigen-specific. Conversely, regulation of Vγ6 γδ T cells during EAE was not dependent on MOG. Furthermore, TCR-activated Vγ6 γδ T cells were not regulated by PD-1. Intracellular Ca^{2+} flux is associated with TCR signalling. TCR activation of $CD27^-$ γδ T cells does not induce Ca^{2+} flux, which may explain why TCR-activated Vγ6 γδ T cells are not regulated by PD-1 [379]. Data from the present study suggests that IL-17A-producing Vγ4 γδ T cells that are pathogenic in EAE are MOG-specific. Anti-PD-1 treatment did not enhance IL-17A production by Vγ4 γδ T cells from mice that were immunised with CFA alone but did enhance IL-17A production by Vγ4 γδ T cells from mice immunised with MOG+CFA. Furthermore, TCR-activated Vγ4 γδ T cells were regulated by PD-1 *in vitro;* PD-1 engagement of TCR-activated Vγ4 γδ T cells suppressed gene expression of *rorc* and *il17a*. These data suggest that Vγ4 γδ T cells are activated via their TCR in an antigen-dependent manner and PD-1 regulates their function by suppressing TCR signalling. Further investigation to confirm this mechanism could include assessment of Ca^{2+} flux in MOG-stimulated Vγ4 γδ T cells purified from mice with EAE. These findings also highlight the importance of profiling PD-1-expressing cells in cancer patients. Anti-PD-1 treatment could have increased potential to cause autoimmunity or enhance cancer progression in patients that have antigen-specific IL-17A-producing γδ T cells. Conversely, PD-1 expressing γδ T cells also have the capacity to kill tumour cells and need to be considered in the context of ICI treatment in cancer patients.

While suppressing the PD-1 pathway in cancer blocks suppression of T cell responses and increases anti-tumour immune responses, increasing PD-1 signalling has recently emerged as a novel therapeutic strategy for the treatment of autoimmune diseases. Peresolimab, an agonistic anti-PD-1 monoclonal antibody, has been demonstrated to be effective in treating RhA in a phase II clinical trial. This PD-1 agonistic monoclonal antibody decreased RhA disease activity when compared with the placebo group with no severe adverse events [298]. Since defective PD-1 signalling is associated with disease progression in MS patients, PD-1 agonists could potentially be beneficial in the treatment of MS [270]. Furthermore, defective Treg cells that produce IFN-γ instead of IL-10 or TGF-

β have been identified in MS and these cells express high levels of PD-1 [380]. PD-1 agonist therapy could suppress defective Treg cells in MS patients and decrease autoimmune inflammation.

In addition to increased checkpoint expression, Treg cells also express the immunoregulatory cytokines IL-10 and TGF-β. Hyper-inflammatory Th17 cells that lack co-expression of IL-10 with IL-17A are present in RRMS patients [381]. Furthermore, increased IL-10 expression by Th17 cells in RRMS patients is associated with periods of remission rather than relapse. Effective treatment of MS symptoms with IFN-β was associated with an increase in the number of IL-10-producing leukocytes in PBMCs from MS patients [324]. In the present study, neutralisation of the IL-10R enhanced the severity of EAE. However, this enhancement of disease severity was not mediated by a direct effect of IL-10 on T cells. IL-10R was highly expressed by monocytes, macrophages, and DCs in the spleen at the induction phase of EAE. These data suggest that IL-10 acts on myeloid cells to suppress T cell activation. IL-10 can suppress T cell proliferation via downregulation of MHC-II expression by monocytes [65]. In the present study, IL-10 blockade increased the infiltration of CD49d-expressing CD4, CD8, and γδ T cells into the brain at the peak of EAE. CD49d forms part of the VLA-4 integrin dimer and has been targeted therapeutically for the treatment of MS. Natalizumab is a monoclonal antibody that inhibits VLA-4-mediated migration of immune cells. However, reactivation of the neurotropic JC virus resulting in progressive multifocal leukoencephalopathy (PML), is a serious and fatal risk of natalizumab treatment in MS patients [329]. The present study demonstrated a potential role for IL-10 signalling in regulating T cell migration into the CNS during EAE and possibly MS. As natalizumab treatment has such serious adverse effects it is possible that IL-10 represents a safer pathway to target in the treatment of MS. While natalizumab appears to completely exclude immune cells from the CNS, IL-10 signalling during EAE suppresses integrin expression by T cells in the periphery, resulting in decreased infiltration into the CNS. It is possible that increased IL-10 in MS could provide a less drastic decrease in the infiltration of immune cells into the CNS, thereby preventing the reactivation of opportunistic pathogens. IL-10 also has a protective role in the CNS as it limits neuronal damage following spinal cord injury [382]. IL-10 has a further

anti-inflammatory role in the CNS by promoting TGF-β production by astrocytes, which limits microglial activation and suppresses CNS inflammation [383].

TGF-β is an immunosuppressive cytokine that was discovered as a factor produced by cancer cells to promote oncogenesis of fibroblasts [384]. Due to its role in the progression of various malignancies, inhibition of TGF-β-mediated signalling has been explored as a therapeutic strategy in cancer. AVID200 is a selective inhibitor of TGF-β1 and TGF-β3 that is under development for the treatment of solid tumours [385]. While TGF-β-mediated signalling is broadly pathogenic in cancer, the role of TGF-β signalling in CNS autoimmunity is less clear. Serum concentrations of TGF-β are increased during relapse in RRMS and SPMS patients. Treatment with IFN-β augmented TGF-β production in these patients, suggesting a protective role for TGF-β in IFN-β treatment of MS [386]. The association between increased TGF-β expression with relapse in MS patients suggests that TGF-β may promote autoimmune inflammation. In the present study, TGF-β did not suppress IL-17A-producing $CD27^-$ γδ T cells. On the contrary, TGF-β enhanced RORγt expression and IL-17A production by IL-1β+IL-23-activated $CD27^-$ γδ T cells. Stimulation of $CD27^-$ γδ T cells with IL-1β and IL-23 induced phosphorylation of STAT3 which was significantly increased following addition of TGF-β. These data suggest that TGF-β promotes activation of IL-17A-producing $CD27^-$ γδ T cells by increasing STAT3 phosphorylation. Neutralisation of TGF-β also decreased the induction of RORγt-expressing and IL-17A-producing MOG-specific CD4 T cells. It appears that TGF-β supports the induction of Th17 cells that are pathogenic in EAE. TGF-β was elevated in the CSF of MS patients when compared with CSF from patients with non-inflammatory neurological disease [387]. Furthermore, the current study demonstrated that neutralisation of TGF-β-mediated signalling reduced the severity of EAE. This decrease in severity of EAE was accompanied by decreased antigen-specific IL-17A production and decreased numbers of IL-17A-producing CD4 and γδ T cells at both the induction and effector phases of EAE. These findings suggest that TGF-β plays a pathogenic role in EAE and that neutralisation, rather than enhancement, of TGF-β signalling could possibly be protective in MS.

While data from the present study demonstrated that TGF-β inhibition suppressed type 17 responses, it enhanced IFN-γ production by CD4 and γδ T cells. The role of TGF-β in the induction of Th17 cells is to suppress Th1 and Th2 cells [45]. In the present study, TGF-β

inhibition suppressed RORγt expression and IL-17A production by IL-1β+IL-23-stimulated γδ T cells. However, inhibition of TGF-β-mediated signalling did not suppress IL-1β+IL-23-stimulated γδ T cells when IFN-γ was neutralised. These data suggest that IFN-γ is a key player in the TGF-β-mediated suppression of type 17 responses. IFN-γ has a temporal role in EAE [357]. Neutralisation of IFN-γ during EAE delayed the onset of disease but increased the severity of disease. Furthermore, treatment with IFN-γ during the active phase of disease suppressed the severity of EAE [388]. Adoptive transfer of T cells deficient in IFN-γ-mediated signalling transferred more severe EAE. These data show that IFN-γ regulates the induction of pathogenic type 17 responses. It appears that, TGF-β increases IL-17A production by decreasing IFN-γ production. The application of IFN-γ for the treatment of MS has not been successful [389]. However, it is possible that the timing of IFN-γ treatment is crucial to its suppression of CNS inflammation. Dungan and colleagues demonstrated that IFN-γ is protective during the induction phase of EAE but exacerbates disease at the later stages [357]. Since IL-17A plays such an important role during the induction of EAE, it is possible that early IFN-γ treatment suppresses early IL-17A to reduce the severity of EAE [171].

There are several limitations to using the MOG-induced model of EAE to study the pathogenesis of MS. Active EAE models severe disease where mice do not experience relapses in symptoms unlike during MS where relapses are followed by periods of remissions and disability accumulates over time. Mice used in this study were between 6-12 weeks old which is another limitation to the study as these mice are immunologically immature when compared with MS patients where the average age of onset is between 20-30 years of age. The present study also used female mice exclusively and therefore did not examine the differences that may be observed between males and females during MS. Furthermore, mice used in this study were bred under SPF conditions and therefore did not have any underlying infections. As the pathogenesis of MS has been associated with viral infections such as EBV [390], the MOG-induced model of EAE does not take pre-existing exposure to viruses into account. Additionally, treatment with either small molecules or monoclonal antibodies were initiated prior to the induction of disease, which differs from how disease-modifying therapies are used during MS as their use follows

diagnosis. However, the EAE model does represent a useful tool for examining the activation states of IL-17A-producing T cells and their regulation *in vivo.*

Current therapies for MS target pro-inflammatory axes rather than regulatory pathways. The success of ICIs in the cancer immunotherapy field and the associated side effects of enhanced autoimmunity suggests that agonists of immune checkpoints may be effective in treating autoimmune diseases. The use of agonistic antibodies to activate checkpoint-mediated signalling and increase immunosuppression has great potential for the treatment of MS. Future work investigating the expression of various checkpoints in MS patients during relapse and remission would provide greater clarity as to the specific receptors that could be successfully targeted for the treatment of MS. Furthermore, the use of immunosuppressive cytokines for the treatment of MS requires more research. Blocking the infiltration of encephalitogenic T cells into the CNS during autoimmunity by promoting IL-10 production has therapeutic potential for the treatment of MS. Therapeutics that target TGF-β have been investigated thoroughly in the context of cancer, but this study highlights the possible requirement for repurposing of these drugs for the treatment of IL-17-mediated autoimmunity.

Chapter 7
References

1. Janeway, C.A., Jr., *How the immune system works to protect the host from infection: a personal view.* Proc Natl Acad Sci U S A, 2001. **98**(13): p. 7461-8.
2. Janeway, C.A., Jr., *The immune system evolved to discriminate infectious nonself from noninfectious self.* Immunol Today, 1992. **13**(1): p. 11-6.
3. Akira, S., S. Uematsu, and O. Takeuchi, *Pathogen Recognition and Innate Immunity.* Cell, 2006. **124**(4): p. 783-801.
4. Roh, J.S. and D.H. Sohn, *Damage-Associated Molecular Patterns in Inflammatory Diseases.* Immune network, 2018. **18**(4): p. e27-e27.
5. Zhang, J.-M. and J. An, *Cytokines, inflammation, and pain.* International anesthesiology clinics, 2007. **45**(2): p. 27-37.
6. Peron, G., et al., *Modulation of dendritic cell by pathogen antigens: Where do we stand?* Immunology Letters, 2018. **196**: p. 91-102.
7. Walsh, K.P. and K.H. Mills, *Dendritic cells and other innate determinants of T helper cell polarisation.* Trends Immunol, 2013. **34**(11): p. 521-30.
8. Pennock, N.D., et al., *T cell responses: naive to memory and everything in between.* Advances in physiology education, 2013. **37**(4): p. 273-283.
9. Ma, D., Y. Wei, and F. Liu, *Regulatory mechanisms of thymus and T cell development.* Developmental & Comparative Immunology, 2013. **39**(1): p. 91-102.
10. Nikolić-Žugić, J., *Phenotypic and functional stages in the intrathymic development of αβ T cells.* Immunology Today, 1991. **12**(2): p. 65-70.
11. Starr, T.K., S.C. Jameson, and K.A. Hogquist, *Positive and Negative Selection of T Cells.* Annual Review of Immunology, 2003. **21**(1): p. 139-176.
12. Mandl, J.N., et al., *T cell-positive selection uses self-ligand binding strength to optimize repertoire recognition of foreign antigens.* Immunity, 2013. **38**(2): p. 263-274.
13. Morris, G.P. and P.M. Allen, *How the TCR balances sensitivity and specificity for the recognition of self and pathogens.* Nature Immunology, 2012. **13**(2): p. 121-128.
14. Germain, R.N., *T-cell development and the CD4–CD8 lineage decision.* Nature Reviews Immunology, 2002. **2**(5): p. 309-322.
15. Zhu, J. and W.E. Paul, *CD4 T cells: fates, functions, and faults.* Blood, 2008. **112**(5): p. 1557-69.
16. Zhang, N. and M.J. Bevan, *CD8(+) T cells: foot soldiers of the immune system.* Immunity, 2011. **35**(2): p. 161-168.
17. Boyer, P.D. and E.V. Rothenberg, *IL-2 receptor inducibility is blocked in cortical-type thymocytes.* J Immunol, 1988. **140**(9): p. 2886-92.
18. Palacios, E.H. and A. Weiss, *Function of the Src-family kinases, Lck and Fyn, in T-cell development and activation.* Oncogene, 2004. **23**(48): p. 7990-8000.
19. Balagopalan, L., et al., *The LAT story: a tale of cooperativity, coordination, and choreography.* Cold Spring Harb Perspect Biol, 2010. **2**(8): p. a005512.
20. Zhang, W., et al., *Association of Grb2, Gads, and Phospholipase C-γ1 with Phosphorylated LAT Tyrosine Residues: EFFECT OF LAT TYROSINE MUTATIONS ON T CELL ANTIGEN RECEPTOR-MEDIATED SIGNALING*.* Journal of Biological Chemistry, 2000. **275**(30): p. 23355-23361.
21. Lo, W.L. and A. Weiss, *Adapting T Cell Receptor Ligand Discrimination Capability via LAT.* Front Immunol, 2021. **12**: p. 673196.
22. Locke, F.L., et al., *Conditional deletion of PTEN in peripheral T cells augments TCR-mediated activation but does not abrogate CD28 dependency or prevent anergy induction.* J Immunol, 2013. **191**(4): p. 1677-85.
23. Courtney, A.H., W.L. Lo, and A. Weiss, *TCR Signaling: Mechanisms of Initiation and Propagation.* Trends Biochem Sci, 2018. **43**(2): p. 108-123.
24. Macian, F., *NFAT proteins: key regulators of T-cell development and function.* Nat Rev Immunol, 2005. **5**(6): p. 472-84.

25. Isakov, N. and A. Altman, *Protein kinase C(theta) in T cell activation.* Annu Rev Immunol, 2002. **20**: p. 761-94.
26. Ai, W., et al., *Optimal method to stimulate cytokine production and its use in immunotoxicity assessment.* Int J Environ Res Public Health, 2013. **10**(9): p. 3834-42.
27. Brownlie, R.J. and R. Zamoyska, *T cell receptor signalling networks: branched, diversified and bounded.* Nature Reviews Immunology, 2013. **13**(4): p. 257-269.
28. Lichtenegger, F.S., et al., *CD86 and IL-12p70 Are Key Players for T Helper 1 Polarization and Natural Killer Cell Activation by Toll-Like Receptor-Induced Dendritic Cells.* PLOS ONE, 2012. **7**(9): p. e44266.
29. Szabo, S.J., et al., *A Novel Transcription Factor, T-bet, Directs Th1 Lineage Commitment.* Cell, 2000. **100**(6): p. 655-669.
30. Zheng, W.-p. and R.A. Flavell, *The Transcription Factor GATA-3 Is Necessary and Sufficient for Th2 Cytokine Gene Expression in CD4 T Cells.* Cell, 1997. **89**(4): p. 587-596.
31. Mosmann, T.R., et al., *Two types of murine helper T cell clone. I. Definition according to profiles of lymphokine activities and secreted proteins.* J Immunol, 1986. **136**(7): p. 2348-57.
32. Hirahara, K. and T. Nakayama, *CD4+ T-cell subsets in inflammatory diseases: beyond the Th1/Th2 paradigm.* International immunology, 2016. **28**(4): p. 163-171.
33. Ivanov, I.I., et al., *The Orphan Nuclear Receptor RORγt Directs the Differentiation Program of Proinflammatory IL-17+ T Helper Cells.* Cell, 2006. **126**(6): p. 1121-1133.
34. Veldhoen, M., et al., *TGFbeta in the context of an inflammatory cytokine milieu supports de novo differentiation of IL-17-producing T cells.* Immunity, 2006. **24**(2): p. 179-89.
35. Korn, T., et al., *IL-21 initiates an alternative pathway to induce proinflammatory T(H)17 cells.* Nature, 2007. **448**(7152): p. 484-487.
36. Zhou, L., et al., *IL-6 programs T(H)-17 cell differentiation by promoting sequential engagement of the IL-21 and IL-23 pathways.* Nat Immunol, 2007. **8**(9): p. 967-74.
37. McGeachy, M.J., et al., *TGF-beta and IL-6 drive the production of IL-17 and IL-10 by T cells and restrain T(H)-17 cell-mediated pathology.* Nat Immunol, 2007. **8**(12): p. 1390-7.
38. Weaver, C.T., et al., *Th17: An Effector CD4 T Cell Lineage with Regulatory T Cell Ties.* Immunity, 2006. **24**(6): p. 677-688.
39. Sie, C., et al., *IL-24 intrinsically regulates Th17 cell pathogenicity in mice.* Journal of Experimental Medicine, 2022. **219**(8).
40. Chong, W.P., et al., *The Cytokine IL-17A Limits Th17 Pathogenicity via a Negative Feedback Loop Driven by Autocrine Induction of IL-24.* Immunity, 2020. **53**(2): p. 384-397.e5.
41. Yang, X.O., et al., *STAT3 regulates cytokine-mediated generation of inflammatory helper T cells.* J Biol Chem, 2007. **282**(13): p. 9358-63.
42. Chung, Y., et al., *Critical Regulation of Early Th17 Cell Differentiation by Interleukin-1 Signaling.* Immunity, 2009. **30**(4): p. 576-587.
43. Nurieva, R., et al., *Essential autocrine regulation by IL-21 in the generation of inflammatory T cells.* Nature, 2007. **448**(7152): p. 480-483.
44. McGeachy, M.J., et al., *The interleukin 23 receptor is essential for the terminal differentiation of interleukin 17-producing effector T helper cells in vivo.* Nat Immunol, 2009. **10**(3): p. 314-24.
45. Das, J., et al., *Transforming growth factor β is dispensable for the molecular orchestration of Th17 cell differentiation.* Journal of Experimental Medicine, 2009. **206**(11): p. 2407-2416.
46. Sakaguchi, S., et al., *Immunologic self-tolerance maintained by activated T cells expressing IL-2 receptor alpha-chains (CD25). Breakdown of a single mechanism of self-tolerance causes various autoimmune diseases.* The Journal of Immunology, 1995. **155**(3): p. 1151.

47. Lee, W. and G.R. Lee, *Transcriptional regulation and development of regulatory T cells.* Experimental & Molecular Medicine, 2018. **50**(3): p. e456-e456.
48. Dhamne, C., et al., *Peripheral and thymic foxp3(+) regulatory T cells in search of origin, distinction, and function.* Frontiers in immunology, 2013. **4**: p. 253-253.
49. Jonuleit, H. and E. Schmitt, *The Regulatory T Cell Family: Distinct Subsets and their Interrelations.* The Journal of Immunology, 2003. **171**(12): p. 6323.
50. Chihara, N., et al., *Differentiation and Characterization of Tr1 Cells.* Current protocols in immunology, 2016. **113**: p. 3.27.1-3.27.10.
51. Carrier, Y., et al., *Th3 cells in peripheral tolerance. I. Induction of Foxp3-positive regulatory T cells by Th3 cells derived from TGF-beta T cell-transgenic mice.* J Immunol, 2007. **178**(1): p. 179-85.
52. Collison, L.W., et al., *The inhibitory cytokine IL-35 contributes to regulatory T-cell function.* Nature, 2007. **450**(7169): p. 566-569.
53. Shevach, E.M., *Mechanisms of Foxp3+ T Regulatory Cell-Mediated Suppression.* Immunity, 2009. **30**(5): p. 636-645.
54. Pandiyan, P., et al., *CD4+CD25+Foxp3+ regulatory T cells induce cytokine deprivation–mediated apoptosis of effector CD4+ T cells.* Nature Immunology, 2007. **8**(12): p. 1353-1362.
55. Wing, K., et al., *CTLA-4 control over Foxp3+ regulatory T cell function.* Science, 2008. **322**(5899): p. 271-5.
56. Freeman, G.J., et al., *Engagement of the Pd-1 Immunoinhibitory Receptor by a Novel B7 Family Member Leads to Negative Regulation of Lymphocyte Activation.* Journal of Experimental Medicine, 2000. **192**(7): p. 1027-1034.
57. Liang, B., et al., *Regulatory T cells inhibit dendritic cells by lymphocyte activation gene-3 engagement of MHC class II.* J Immunol, 2008. **180**(9): p. 5916-26.
58. Shimizu, J., et al., *Stimulation of CD25+CD4+ regulatory T cells through GITR breaks immunological self-tolerance.* Nature Immunology, 2002. **3**(2): p. 135-142.
59. Sharon, E., et al., *Immune checkpoint inhibitors in clinical trials.* Chin J Cancer, 2014. **33**(9): p. 434-44.
60. Gagliani, N., et al., *Coexpression of CD49b and LAG-3 identifies human and mouse T regulatory type 1 cells.* Nature Medicine, 2013. **19**(6): p. 739-746.
61. Brockmann, L., et al., *Molecular and functional heterogeneity of IL-10-producing CD4(+) T cells.* Nat Commun, 2018. **9**(1): p. 5457.
62. Mills, K.H., *Regulatory T cells: friend or foe in immunity to infection?* Nat Rev Immunol, 2004. **4**(11): p. 841-55.
63. Groux, H., et al., *A CD4+T-cell subset inhibits antigen-specific T-cell responses and prevents colitis.* Nature, 1997. **389**(6652): p. 737-742.
64. McGuirk , P., C. McCann , and K.H.G. Mills *Pathogen-specific T Regulatory 1 Cells Induced in the Respiratory Tract by a Bacterial Molecule that Stimulates Interleukin 10 Production by Dendritic Cells : A Novel Strategy for Evasion of Protective T Helper Type 1 Responses by Bordetella pertussis.* Journal of Experimental Medicine, 2002. **195**(2): p. 221-231.
65. de Waal Malefyt, R., et al., *Interleukin 10 (IL-10) and viral IL-10 strongly reduce antigen-specific human T cell proliferation by diminishing the antigen-presenting capacity of monocytes via downregulation of class II major histocompatibility complex expression.* Journal of Experimental Medicine, 1991. **174**(4): p. 915-924.
66. Song, Y., et al., *Tr1 Cells as a Key Regulator for Maintaining Immune Homeostasis in Transplantation.* Frontiers in Immunology, 2021. **12**.
67. Akdis , M.b., et al., *Immune Responses in Healthy and Allergic Individuals Are Characterized by a Fine Balance between Allergen-specific T Regulatory 1 and T Helper 2 Cells.* Journal of Experimental Medicine, 2004. **199**(11): p. 1567-1575.

68. Mascanfroni, I.D., et al., *Metabolic control of type 1 regulatory T cell differentiation by AHR and HIF1-α.* Nature Medicine, 2015. **21**(6): p. 638-646.
69. Raverdeau, M., et al., *Retinoic acid-induced autoantigen-specific type 1 regulatory T cells suppress autoimmunity.* EMBO reports, 2019. **20**(5): p. e47121.
70. Shouval, D.S., et al., *Interleukin 10 receptor signaling: master regulator of intestinal mucosal homeostasis in mice and humans.* Adv Immunol, 2014. **122**: p. 177-210.
71. Huber, S., et al., *Th17 cells express interleukin-10 receptor and are controlled by Foxp3⁻ and Foxp3+ regulatory CD4+ T cells in an interleukin-10-dependent manner.* Immunity, 2011. **34**(4): p. 554-65.
72. Wei, L., A. Laurence, and J.J. O'Shea, *New insights into the roles of Stat5a/b and Stat3 in T cell development and differentiation.* Seminars in Cell & Developmental Biology, 2008. **19**(4): p. 394-400.
73. Ouyang, W., et al., *Regulation and Functions of the IL-10 Family of Cytokines in Inflammation and Disease.* Annual Review of Immunology, 2011. **29**(1): p. 71-109.
74. Ouyang, W. and A. O'Garra, *IL-10 Family Cytokines IL-10 and IL-22: from Basic Science to Clinical Translation.* Immunity, 2019. **50**(4): p. 871-891.
75. Huynh, J.P., et al., *Bhlhe40 is an essential repressor of IL-10 during Mycobacterium tuberculosis infection.* Journal of Experimental Medicine, 2018. **215**(7): p. 1823-1838.
76. Widodo, S.S., et al., *IL-10 in glioma.* British Journal of Cancer, 2021. **125**(11): p. 1466-1476.
77. Zhang, Z., et al., *Interleukin 10 promotes growth and invasion of glioma cells by up-regulating KPNA 2 in vitro.* Journal of Cancer Research and Therapeutics, 2019. **15**(4).
78. Lamichhane, P., et al., *IL10 Release upon PD-1 Blockade Sustains Immunosuppression in Ovarian Cancer.* Cancer Research, 2017. **77**(23): p. 6667-6678.
79. Pflanz, S., et al., *IL-27, a heterodimeric cytokine composed of EBI3 and p28 protein, induces proliferation of naive CD4+ T cells.* Immunity, 2002. **16**(6): p. 779-90.
80. Stumhofer, J.S., et al., *Interleukins 27 and 6 induce STAT3-mediated T cell production of interleukin 10.* Nature Immunology, 2007. **8**(12): p. 1363-1371.
81. Yoshida, H. and C.A. Hunter, *The Immunobiology of Interleukin-27.* Annual Review of Immunology, 2015. **33**(1): p. 417-443.
82. Perona-Wright, G., et al., *Persistent loss of IL-27 responsiveness in CD8+ memory T cells abrogates IL-10 expression in a recall response.* Proceedings of the National Academy of Sciences, 2012. **109**(45): p. 18535-18540.
83. Kelly, A.M., et al., *Staphylococcus aureus-induced immunosuppression mediated by IL-10 and IL-27 facilitates nasal colonisation.* PLOS Pathogens, 2022. **18**(7): p. e1010647.
84. Fitzgerald, D.C., et al., *Suppression of autoimmune inflammation of the central nervous system by interleukin 10 secreted by interleukin 27-stimulated T cells.* Nat Immunol, 2007. **8**(12): p. 1372-9.
85. Sweeney, C.M., et al., *IL-27 mediates the response to IFN-β therapy in multiple sclerosis patients by inhibiting Th17 cells.* Brain, Behavior, and Immunity, 2011. **25**(6): p. 1170-1181.
86. Collison, L.W., et al., *The composition and signaling of the IL-35 receptor are unconventional.* Nat Immunol, 2012. **13**(3): p. 290-9.
87. Shen, P., et al., *IL-35-producing B cells are critical regulators of immunity during autoimmune and infectious diseases.* Nature, 2014. **507**(7492): p. 366-370.
88. Lee, C.C., et al., *Macrophage-secreted interleukin-35 regulates cancer cell plasticity to facilitate metastatic colonization.* Nat Commun, 2018. **9**(1): p. 3763.
89. Dixon, K.O., et al., *Human tolerogenic dendritic cells produce IL-35 in the absence of other IL-12 family members.* Eur J Immunol, 2015. **45**(6): p. 1736-47.
90. Collison, L.W., et al., *IL-35-mediated induction of a potent regulatory T cell population.* Nature Immunology, 2010. **11**(12): p. 1093-1101.

91. Wang, Z., et al., *Tumor-Derived IL-35 Promotes Tumor Growth by Enhancing Myeloid Cell Accumulation and Angiogenesis.* The Journal of Immunology, 2013. **190**(5): p. 2415-2423.
92. Zhang, T., et al., *Correlation Analysis Among the Level of IL-35, Microvessel Density, Lymphatic Vessel Density, and Prognosis in Non-Small Cell Lung Cancer.* Clin Transl Sci, 2021. **14**(1): p. 389-394.
93. Liu, J.Q., et al., *Increased Th17 and regulatory T cell responses in EBV-induced gene 3-deficient mice lead to marginally enhanced development of autoimmune encephalomyelitis.* J Immunol, 2012. **188**(7): p. 3099-106.
94. Travis, M.A. and D. Sheppard, *TGF-β Activation and Function in Immunity.* Annual Review of Immunology, 2014. **32**(1): p. 51-82.
95. Dubois, C.M., et al., *Processing of transforming growth factor beta 1 precursor by human furin convertase.* J Biol Chem, 1995. **270**(18): p. 10618-24.
96. Tran, D.Q., et al., *GARP (LRRC32) is essential for the surface expression of latent TGF-β; on platelets and activated FOXP3+regulatory T cells.* Proceedings of the National Academy of Sciences, 2009. **106**(32): p. 13445-13450.
97. Munger, J.S., et al., *A Mechanism for Regulating Pulmonary Inflammation and Fibrosis: The Integrin αvβ6 Binds and Activates Latent TGF β1.* Cell, 1999. **96**(3): p. 319-328.
98. Mani, V., et al., *Migratory DCs activate TGF-β to precondition naïve CD8(+) T cells for tissue-resident memory fate.* Science, 2019. **366**(6462).
99. Lawler, S., et al., *The Type II Transforming Growth Factor-β Receptor Autophosphorylates Not Only on Serine and Threonine but Also on Tyrosine Residues*.* Journal of Biological Chemistry, 1997. **272**(23): p. 14850-14859.
100. Shi, Y. and J. Massagué, *Mechanisms of TGF-β Signaling from Cell Membrane to the Nucleus.* Cell, 2003. **113**(6): p. 685-700.
101. Flavell, R.A., et al., *The polarization of immune cells in the tumour environment by TGFβ.* Nature Reviews Immunology, 2010. **10**(8): p. 554-567.
102. Calon, A., et al., *Dependency of Colorectal Cancer on a TGF-β-Driven Program in Stromal Cells for Metastasis Initiation.* Cancer Cell, 2012. **22**(5): p. 571-584.
103. Ewen, M.E., et al., *TGF beta inhibition of Cdk4 synthesis is linked to cell cycle arrest.* Cell, 1993. **74**(6): p. 1009-20.
104. Kleiter, I., et al., *Smad7 in T cells drives T helper 1 responses in multiple sclerosis and experimental autoimmune encephalomyelitis.* Brain, 2010. **133**(4): p. 1067-1081.
105. Tauriello, D.V.F., et al., *TGFβ drives immune evasion in genetically reconstituted colon cancer metastasis.* Nature, 2018. **554**(7693): p. 538-543.
106. He, X. and C. Xu, *Immune checkpoint signaling and cancer immunotherapy.* Cell Research, 2020. **30**(8): p. 660-669.
107. Linsley, P.S., et al., *CTLA-4 is a second receptor for the B cell activation antigen B7.* J Exp Med, 1991. **174**(3): p. 561-9.
108. Takahashi, T., et al., *Immunologic self-tolerance maintained by CD25(+)CD4(+) regulatory T cells constitutively expressing cytotoxic T lymphocyte-associated antigen 4.* J Exp Med, 2000. **192**(2): p. 303-10.
109. Zhong, C., et al., *Treatment of experimental autoimmune encephalomyelitis using AAV gene therapy by blocking T cell costimulatory pathways.* Molecular Therapy - Methods & Clinical Development, 2022. **25**: p. 461-475.
110. Huard, B., et al., *Lymphocyte-activation gene 3/major histocompatibility complex class II interaction modulates the antigenic response of CD4+ T lymphocytes.* Eur J Immunol, 1994. **24**(12): p. 3216-21.
111. Guy, C., et al., *LAG3 associates with TCR–CD3 complexes and suppresses signaling by driving co-receptor–Lck dissociation.* Nature Immunology, 2022. **23**(5): p. 757-767.

112. Xu, F., et al., *LSECtin expressed on melanoma cells promotes tumor progression by inhibiting antitumor T-cell responses.* Cancer Res, 2014. **74**(13): p. 3418-28.
113. Kouo, T., et al., *Galectin-3 Shapes Antitumor Immune Responses by Suppressing CD8+ T Cells via LAG-3 and Inhibiting Expansion of Plasmacytoid Dendritic Cells.* Cancer Immunol Res, 2015. **3**(4): p. 412-23.
114. Workman, C.J., K.J. Dugger, and D.A.A. Vignali, *Cutting Edge: Molecular Analysis of the Negative Regulatory Function of Lymphocyte Activation Gene-31.* The Journal of Immunology, 2002. **169**(10): p. 5392-5395.
115. Yokosuka, T., et al., *Programmed cell death 1 forms negative costimulatory microclusters that directly inhibit T cell receptor signaling by recruiting phosphatase SHP2.* Journal of Experimental Medicine, 2012. **209**(6): p. 1201-1217.
116. Hui, E., et al., *T cell costimulatory receptor CD28 is a primary target for PD-1-mediated inhibition.* Science, 2017. **355**(6332): p. 1428-1433.
117. Patsoukis, N., et al., *Selective effects of PD-1 on Akt and Ras pathways regulate molecular components of the cell cycle and inhibit T cell proliferation.* Sci Signal, 2012. **5**(230): p. ra46.
118. Sheppard, K.A., et al., *PD-1 inhibits T-cell receptor induced phosphorylation of the ZAP70/CD3zeta signalosome and downstream signaling to PKCtheta.* FEBS Lett, 2004. **574**(1-3): p. 37-41.
119. Sharpe, A.H. and K.E. Pauken, *The diverse functions of the PD1 inhibitory pathway.* Nature Reviews Immunology, 2018. **18**(3): p. 153-167.
120. Damsky, W., et al., *B cell depletion or absence does not impede anti-tumor activity of PD-1 inhibitors.* Journal for ImmunoTherapy of Cancer, 2019. **7**(1): p. 153.
121. Wölfle, S.J., et al., *PD-L1 expression on tolerogenic APCs is controlled by STAT-3.* Eur J Immunol, 2011. **41**(2): p. 413-24.
122. Kummer, M.P., et al., *Microglial PD-1 stimulation by astrocytic PD-L1 suppresses neuroinflammation and Alzheimer's disease pathology.* Embo j, 2021. **40**(24): p. e108662.
123. Linnerbauer, M., et al., *PD-L1 positive astrocytes attenuate inflammatory functions of PD-1 positive microglia in models of autoimmune neuroinflammation.* Nature Communications, 2023. **14**(1): p. 5555.
124. Nishimura, H., et al., *Development of lupus-like autoimmune diseases by disruption of the PD-1 gene encoding an ITIM motif-carrying immunoreceptor.* Immunity, 1999. **11**(2): p. 141-51.
125. Salama, A.D., et al., *Critical role of the programmed death-1 (PD-1) pathway in regulation of experimental autoimmune encephalomyelitis.* J Exp Med, 2003. **198**(1): p. 71-8.
126. Anderson, A.C., N. Joller, and V.K. Kuchroo, *Lag-3, Tim-3, and TIGIT: Co-inhibitory Receptors with Specialized Functions in Immune Regulation.* Immunity, 2016. **44**(5): p. 989-1004.
127. Stanietsky, N., et al., *The interaction of TIGIT with PVR and PVRL2 inhibits human NK cell cytotoxicity.* Proceedings of the National Academy of Sciences, 2009. **106**(42): p. 17858-17863.
128. Yu, X., et al., *The surface protein TIGIT suppresses T cell activation by promoting the generation of mature immunoregulatory dendritic cells.* Nature Immunology, 2009. **10**(1): p. 48-57.
129. Stanietsky, N., et al., *Mouse TIGIT inhibits NK-cell cytotoxicity upon interaction with PVR.* European Journal of Immunology, 2013. **43**(8): p. 2138-2150.
130. Joller, N., et al., *Cutting Edge: TIGIT Has T Cell-Intrinsic Inhibitory Functions.* The Journal of Immunology, 2011. **186**(3): p. 1338-1342.

131. Joller, N., et al., *Treg Cells Expressing the Coinhibitory Molecule TIGIT Selectively Inhibit Proinflammatory Th1 and Th17 Cell Responses.* Immunity, 2014. **40**(4): p. 569-581.
132. Monney, L., et al., *Th1-specific cell surface protein Tim-3 regulates macrophage activation and severity of an autoimmune disease.* Nature, 2002. **415**(6871): p. 536-541.
133. Zhu, C., et al., *An IL-27/NFIL3 signalling axis drives Tim-3 and IL-10 expression and T-cell dysfunction.* Nature Communications, 2015. **6**(1): p. 6072.
134. Zhu, C., et al., *The Tim-3 ligand galectin-9 negatively regulates T helper type 1 immunity.* Nature Immunology, 2005. **6**(12): p. 1245-1252.
135. Gonçalves Silva, I., et al., *The Tim-3-galectin-9 Secretory Pathway is Involved in the Immune Escape of Human Acute Myeloid Leukemia Cells.* EBioMedicine, 2017. **22**: p. 44-57.
136. Huang, Y.-H., et al., *CEACAM1 regulates TIM-3-mediated tolerance and exhaustion.* Nature, 2015. **517**(7534): p. 386-390.
137. Rangachari, M., et al., *Bat3 promotes T cell responses and autoimmunity by repressing Tim-3–mediated cell death and exhaustion.* Nat Med, 2012. **18**(9): p. 1394-400.
138. Dyck, L. and K.H.G. Mills, *Immune checkpoints and their inhibition in cancer and infectious diseases.* Eur J Immunol, 2017. **47**(5): p. 765-779.
139. van Elsas, A., A.A. Hurwitz, and J.P. Allison, *Combination immunotherapy of B16 melanoma using anti-cytotoxic T lymphocyte-associated antigen 4 (CTLA-4) and granulocyte/macrophage colony-stimulating factor (GM-CSF)-producing vaccines induces rejection of subcutaneous and metastatic tumors accompanied by autoimmune depigmentation.* J Exp Med, 1999. **190**(3): p. 355-66.
140. Ganesh, K., et al., *Immunotherapy in colorectal cancer: rationale, challenges and potential.* Nat Rev Gastroenterol Hepatol, 2019. **16**(6): p. 361-375.
141. Ribas, A. and K.T. Flaherty, *Gauging the Long-Term Benefits of Ipilimumab in Melanoma.* Journal of Clinical Oncology, 2015. **33**(17): p. 1865-1866.
142. Weber, J.S., et al., *Ipilimumab Increases Activated T Cells and Enhances Humoral Immunity in Patients With Advanced Melanoma.* Journal of Immunotherapy, 2012. **35**: p. 89–97.
143. Kassardjian, A., P.I. Shintaku, and N.A. Moatamed, *Expression of immune checkpoint regulators, cytotoxic T lymphocyte antigen 4 (CTLA-4) and programmed death-ligand 1 (PD-L1), in female breast carcinomas.* PLOS ONE, 2018. **13**(4): p. e0195958.
144. Liu, J., et al., *PD-1/PD-L1 Checkpoint Inhibitors in Tumor Immunotherapy.* Front Pharmacol, 2021. **12**: p. 731798.
145. Juneja, V.R., et al., *PD-L1 on tumor cells is sufficient for immune evasion in immunogenic tumors and inhibits CD8 T cell cytotoxicity.* Journal of Experimental Medicine, 2017. **214**(4): p. 895-904.
146. Tumeh, P.C., et al., *PD-1 blockade induces responses by inhibiting adaptive immune resistance.* Nature, 2014. **515**(7528): p. 568-571.
147. Wolchok, J.D., et al., *Nivolumab plus Ipilimumab in Advanced Melanoma.* New England Journal of Medicine, 2013. **369**(2): p. 122-133.
148. Kumar, V., et al., *Current Diagnosis and Management of Immune Related Adverse Events (irAEs) Induced by Immune Checkpoint Inhibitor Therapy.* Frontiers in Pharmacology, 2017. **8**.
149. Chien, Y.H., et al., *A new T-cell receptor gene located within the alpha locus and expressed early in T-cell differentiation.* Nature, 1987. **327**(6124): p. 677-82.
150. Davey, M.S., et al., *Recasting Human Vδ1 Lymphocytes in an Adaptive Role.* Trends in Immunology, 2018. **39**(6): p. 446-459.
151. Halary , F., et al., *Shared reactivity of Vδ2neg γδ T cells against cytomegalovirus-infected cells and tumor intestinal epithelial cells.* Journal of Experimental Medicine, 2005. **201**(10): p. 1567-1578.

152. Almeida, A.R., et al., *Delta One T Cells for Immunotherapy of Chronic Lymphocytic Leukemia: Clinical-Grade Expansion/Differentiation and Preclinical Proof of Concept.* Clin Cancer Res, 2016. **22**(23): p. 5795-5804.
153. Harmon, C., et al., *γδ T cell dichotomy with opposing cytotoxic and wound healing functions in human solid tumors.* Nature Cancer, 2023. **4**(8): p. 1122-1137.
154. Li, Y., et al., *The Dual Roles of Human γδ T Cells: Anti-Tumor or Tumor-Promoting.* Frontiers in Immunology, 2021. **11**.
155. Gober , H.-J.r., et al., *Human T Cell Receptor γδ Cells Recognize Endogenous Mevalonate Metabolites in Tumor Cells.* Journal of Experimental Medicine, 2003. **197**(2): p. 163-168.
156. Yuan, L., et al., *Phosphoantigens glue butyrophilin 3A1 and 2A1 to activate Vγ9Vδ2 T cells.* Nature, 2023.
157. Sandstrom, A., et al., *The Intracellular B30.2 Domain of Butyrophilin 3A1 Binds Phosphoantigens to Mediate Activation of Human Vγ9Vδ2 T Cells.* Immunity, 2014. **40**(4): p. 490-500.
158. Mamedov, M.R., et al., *CRISPR screens decode cancer cell pathways that trigger γδ T cell detection.* Nature, 2023. **621**(7977): p. 188-195.
159. Maniar, A., et al., *Human gammadelta T lymphocytes induce robust NK cell-mediated antitumor cytotoxicity through CD137 engagement.* Blood, 2010. **116**(10): p. 1726-33.
160. Lo Presti, E., et al., *Squamous Cell Tumors Recruit γδ T Cells Producing either IL17 or IFNγ Depending on the Tumor Stage.* Cancer Immunol Res, 2017. **5**(5): p. 397-407.
161. Heilig, J.S. and S. Tonegawa, *Diversity of murine gamma genes and expression in fetal and adult T lymphocytes.* Nature, 1986. **322**(6082): p. 836-40.
162. Carding, S.R. and P.J. Egan, *Gammadelta T cells: functional plasticity and heterogeneity.* Nat Rev Immunol, 2002. **2**(5): p. 336-45.
163. Allison, J.P. and W.L. Havran, *The immunobiology of T cells with invariant gamma delta antigen receptors.* Annu Rev Immunol, 1991. **9**: p. 679-705.
164. Lafaille, J.J., et al., *Junctional sequences of T cell receptor γδ genes: Implications for γδ T cell lineages and for a novel intermediate of V-(D)-J joining.* Cell, 1989. **59**(5): p. 859-870.
165. Jensen, K.D.C. and Y.-H. Chien, *Thymic maturation determines γδ T cell function, but not their antigen specificities.* Current opinion in immunology, 2009. **21**(2): p. 140-145.
166. Jensen, K.D., et al., *Thymic selection determines γδ T cell effector fate: antigen-naive cells make interleukin-17 and antigen-experienced cells make interferon gamma.* Immunity, 2008. **29**(1): p. 90-100.
167. Haas, J.D., et al., *CCR6 and NK1.1 distinguish between IL-17A and IFN-γ-producing γδ effector T cells.* Eur J Immunol, 2009. **39**(12): p. 3488-97.
168. Ribot, J.C., et al., *CD27 is a thymic determinant of the balance between interferon-γ- and interleukin 17–producing γδ T cell subsets.* Nature Immunology, 2009. **10**(4): p. 427-436.
169. Sutton, C.E., et al., *Interleukin-1 and IL-23 induce innate IL-17 production from gammadelta T cells, amplifying Th17 responses and autoimmunity.* Immunity, 2009. **31**(2): p. 331-41.
170. Lockhart, E., A.M. Green, and J.L. Flynn, *IL-17 production is dominated by gammadelta T cells rather than CD4 T cells during Mycobacterium tuberculosis infection.* J Immunol, 2006. **177**(7): p. 4662-9.
171. McGinley, A.M., et al., *Interleukin-17A Serves a Priming Role in Autoimmunity by Recruiting IL-1β-Producing Myeloid Cells that Promote Pathogenic T Cells.* Immunity, 2020. **52**(2): p. 342-356.e6.
172. Misiak, A., et al., *IL-17–Producing Innate and Pathogen-Specific Tissue Resident Memory γδ T Cells Expand in the Lungs of Bordetella pertussis–Infected Mice.* The Journal of Immunology, 2017. **198**(1): p. 363-374.

173. Murphy, A.G., et al., *Staphylococcus aureus infection of mice expands a population of memory γδ T cells that are protective against subsequent infection.* J Immunol, 2014. **192**(8): p. 3697-708.
174. Raverdeau, M., et al., *Retinoic acid suppresses IL-17 production and pathogenic activity of γδ T cells in CNS autoimmunity.* Immunol Cell Biol, 2016. **94**(8): p. 763-73.
175. Faustino, L.D., et al., *Interleukin-33 activates regulatory T cells to suppress innate γδ T cell responses in the lung.* Nature Immunology, 2020. **21**(11): p. 1371-1383.
176. Gonçalves-Sousa, N., et al., *Inhibition of murine γδ lymphocyte expansion and effector function by regulatory αβ T cells is cell-contact-dependent and sensitive to GITR modulation.* European Journal of Immunology, 2010. **40**(1): p. 61-70.
177. Edwards, S.C., et al., *PD-1 and TIM-3 differentially regulate subsets of mouse IL-17A–producing γδ T cells.* Journal of Experimental Medicine, 2022. **220**(2).
178. Huang, H.I., et al., *A binary module for microbiota-mediated regulation of γδ17 cells, hallmarked by microbiota-driven expression of programmed cell death protein 1.* Cell Rep, 2023. **42**(8): p. 112951.
179. Yao, Z., et al., *Herpesvirus Saimiri encodes a new cytokine, IL-17, which binds to a novel cytokine receptor.* Immunity, 1995. **3**(6): p. 811-21.
180. Gaffen, S.L., *Structure and signalling in the IL-17 receptor family.* Nature reviews. Immunology, 2009. **9**(8): p. 556-567.
181. Aggarwal, S. and A.L. Gurney, *IL-17: prototype member of an emerging cytokine family.* J Leukoc Biol, 2002. **71**(1): p. 1-8.
182. Chang, S.H. and C. Dong, *A novel heterodimeric cytokine consisting of IL-17 and IL-17F regulates inflammatory responses.* Cell Research, 2007. **17**(5): p. 435-440.
183. Toy, D., et al., *Cutting edge: interleukin 17 signals through a heteromeric receptor complex.* J Immunol, 2006. **177**(1): p. 36-9.
184. Boisson, B., et al., *An ACT1 mutation selectively abolishes interleukin-17 responses in humans with chronic mucocutaneous candidiasis.* Immunity, 2013. **39**(4): p. 676-86.
185. Anderson, P., *Post-transcriptional control of cytokine production.* Nat Immunol, 2008. **9**(4): p. 353-9.
186. Henness, S., et al., *IL-17A augments TNF-α induced IL-6 expression in airway smooth muscle by enhancing mRNA stability.* Journal of Allergy and Clinical Immunology, 2004. **114**(4): p. 958-964.
187. Hartupee, J., et al., *IL-17 enhances chemokine gene expression through mRNA stabilization.* J Immunol, 2007. **179**(6): p. 4135-41.
188. Zrioual, S., et al., *Genome-wide comparison between IL-17A- and IL-17F-induced effects in human rheumatoid arthritis synoviocytes.* J Immunol, 2009. **182**(5): p. 3112-20.
189. Monin, L. and S.L. Gaffen, *Interleukin 17 Family Cytokines: Signaling Mechanisms, Biological Activities, and Therapeutic Implications.* Cold Spring Harb Perspect Biol, 2018. **10**(4).
190. Shen, F., et al., *Cytokines link osteoblasts and inflammation: microarray analysis of interleukin-17- and TNF-α-induced genes in bone cells.* J Leukoc Biol, 2005. **77**(3): p. 388-99.
191. Koenders, M.I., et al., *Interleukin-17 receptor deficiency results in impaired synovial expression of interleukin-1 and matrix metalloproteinases 3, 9, and 13 and prevents cartilage destruction during chronic reactivated streptococcal cell wall-induced arthritis.* Arthritis Rheum, 2005. **52**(10): p. 3239-47.
192. Conti, H.R., et al., *Oral-resident natural Th17 cells and gammadelta T cells control opportunistic Candida albicans infections.* J Exp Med, 2014. **211**(10): p. 2075-84.
193. Cho, J.S., et al., *IL-17 is essential for host defense against cutaneous Staphylococcus aureus infection in mice.* The Journal of Clinical Investigation, 2010. **120**(5): p. 1762-1773.

194. Hirata, T., et al., *Recruitment of CCR6-expressing Th17 cells by CCL20 secreted from IL-1β, TNF-α, and IL-17A-stimulated endometriotic stromal cells.* Endocrinology, 2010. **151**(11): p. 5468-76.
195. Qian, Y., et al., *IL-17 signaling in host defense and inflammatory diseases.* Cellular & molecular immunology, 2010. **7**(5): p. 328-333.
196. Nakae, S., et al., *Suppression of immune induction of collagen-induced arthritis in IL-17-deficient mice.* J Immunol, 2003. **171**(11): p. 6173-7.
197. Mills, K.H., *TLR-dependent T cell activation in autoimmunity.* Nat Rev Immunol, 2011. **11**(12): p. 807-22.
198. Goodnow, C.C., et al., *Cellular and genetic mechanisms of self tolerance and autoimmunity.* Nature, 2005. **435**(7042): p. 590-597.
199. Seddon, B. and D. Mason, *The third function of the thymus.* Immunology Today, 2000. **21**(2): p. 95-99.
200. Brownlee, W.J., et al., *Diagnosis of multiple sclerosis: progress and challenges.* Lancet, 2017. **389**(10076): p. 1336-1346.
201. Efendi, H., *Clinically Isolated Syndromes: Clinical Characteristics, Differential Diagnosis, and Management.* Noro Psikiyatr Ars, 2015. **52**(Suppl 1): p. S1-s11.
202. Freedman, M.S., et al., *Recommended Standard of Cerebrospinal Fluid Analysis in the Diagnosis of Multiple Sclerosis: A Consensus Statement.* Archives of Neurology, 2005. **62**(6): p. 865-870.
203. Confavreux, C., et al., *Relapses and Progression of Disability in Multiple Sclerosis.* New England Journal of Medicine, 2000. **343**(20): p. 1430-1438.
204. Watson, C., et al., *Treatment Patterns and Unmet Need for Patients with Progressive Multiple Sclerosis in the United States: Survey Results from 2016 to 2021.* Neurol Ther, 2023.
205. Lublin, F.D., et al., *Defining the clinical course of multiple sclerosis: the 2013 revisions.* Neurology, 2014. **83**(3): p. 278-86.
206. Kurtzke, J.F., *Rating neurologic impairment in multiple sclerosis: an expanded disability status scale (EDSS).* Neurology, 1983. **33**(11): p. 1444-52.
207. Milo, R. and E. Kahana, *Multiple sclerosis: Geoepidemiology, genetics and the environment.* Autoimmunity Reviews, 2010. **9**(5): p. A387-A394.
208. Walton, C., et al., *Rising prevalence of multiple sclerosis worldwide: Insights from the Atlas of MS, third edition.* Mult Scler, 2020. **26**(14): p. 1816-1821.
209. O'Connell, K., et al., *Incidence of multiple sclerosis in the Republic of Ireland: A prospective population-based study.* Mult Scler Relat Disord, 2017. **13**: p. 75-80.
210. Popescu, B.F. and C.F. Lucchinetti, *Pathology of demyelinating diseases.* Annu Rev Pathol, 2012. **7**: p. 185-217.
211. Tsivgoulis, G., et al., *The Effect of Disease Modifying Therapies on Brain Atrophy in Patients with Relapsing-Remitting Multiple Sclerosis: A Systematic Review and Meta-Analysis.* PLOS ONE, 2015. **10**(3): p. e0116511.
212. Morrow, S.A., et al., *Use of natalizumab in persons with multiple sclerosis: 2022 update.* Multiple Sclerosis and Related Disorders, 2022. **65**.
213. Dendrou, C.A., L. Fugger, and M.A. Friese, *Immunopathology of multiple sclerosis.* Nature Reviews Immunology, 2015. **15**(9): p. 545-558.
214. Hauser, S.L., et al., *B-Cell Depletion with Rituximab in Relapsing–Remitting Multiple Sclerosis.* New England Journal of Medicine, 2008. **358**(7): p. 676-688.
215. Montalban, X., et al., *Ocrelizumab versus Placebo in Primary Progressive Multiple Sclerosis.* N Engl J Med, 2017. **376**(3): p. 209-220.
216. Rangachari, M. and V.K. Kuchroo, *Using EAE to better understand principles of immune function and autoimmune pathology.* J Autoimmun, 2013. **45**: p. 31-9.

217. Miller, S.D. and W.J. Karpus, *Experimental autoimmune encephalomyelitis in the mouse.* Curr Protoc Immunol, 2007. **Chapter 15**: p. Unit 15.1.
218. Levine, S., et al., *Hyperacute allergic encephalomyelitis: adjuvant effect of pertussis vaccines and extracts.* J Immunol, 1966. **97**(3): p. 363-8.
219. Linthicum, D.S., J.J. Munoz, and A. Blaskett, *Acute experimental autoimmune encephalomyelitis in mice. I. Adjuvant action of Bordetella pertussis is due to vasoactive amine sensitization and increased vascular permeability of the central nervous system.* Cell Immunol, 1982. **73**(2): p. 299-310.
220. Ronchi, F., et al., *Experimental priming of encephalitogenic Th1/Th17 cells requires pertussis toxin-driven IL-1β production by myeloid cells.* Nat Commun, 2016. **7**: p. 11541.
221. Dumas, A., et al., *The Inflammasome Pyrin Contributes to Pertussis Toxin-Induced IL-1β Synthesis, Neutrophil Intravascular Crawling and Autoimmune Encephalomyelitis.* PLOS Pathogens, 2014. **10**(5): p. e1004150.
222. McRae, B.L., et al., *Induction of active and adoptive relapsing experimental autoimmune encephalomyelitis (EAE) using an encephalitogenic epitope of proteolipid protein.* J Neuroimmunol, 1992. **38**(3): p. 229-40.
223. Vanderlugt, C.L., et al., *Pathologic Role and Temporal Appearance of Newly Emerging Autoepitopes in Relapsing Experimental Autoimmune Encephalomyelitis1.* The Journal of Immunology, 2000. **164**(2): p. 670-678.
224. Amor, S., et al., *The Biology of Multiple Sclerosis*. 2012, Cambridge: Cambridge University Press.
225. Gerhauser, I., et al., *Facets of Theiler's Murine Encephalomyelitis Virus-Induced Diseases: An Update.* Int J Mol Sci, 2019. **20**(2).
226. Sheahan, B.J., P.N. Barrett, and G.J. Atkins, *Demyelination in mice resulting from infection with a mutant of Semliki Forest virus.* Acta Neuropathol, 1981. **53**(2): p. 129-36.
227. Tarbatt, C.J., et al., *Sequence analysis of the avirulent, demyelinating A7 strain of Semliki Forest virus.* J Gen Virol, 1997. **78 (Pt 7)**: p. 1551-7.
228. Fazakerley, J.K., *Pathogenesis of Semliki Forest virus encephalitis.* J Neurovirol, 2002. **8 Suppl 2**: p. 66-74.
229. Wang, F.-I., S.A. Stohlman, and J.O. Fleming, *Demyelination induced by murine hepatitis virus JHM strain (MHV-4) is immunologically mediated.* Journal of Neuroimmunology, 1990. **30**(1): p. 31-41.
230. Wu, G.F., et al., *CD4 and CD8 T Cells Have Redundant But Not Identical Roles in Virus-Induced Demyelination1.* The Journal of Immunology, 2000. **165**(4): p. 2278-2286.
231. Libbey, J.E. and R.S. Fujinami, *Viral mouse models used to study multiple sclerosis: past and present.* Archives of Virology, 2021. **166**(4): p. 1015-1033.
232. Becher, B., B.G. Durell, and R.J. Noelle, *Experimental autoimmune encephalitis and inflammation in the absence of interleukin-12.* The Journal of clinical investigation, 2002. **110**(4): p. 493-497.
233. Traugott, U. and P. Lebon, *Demonstration of α, β, and γ Interferon in Active Chronic Multiple Sclerosis Lesionsa.* Annals of the New York Academy of Sciences, 1988. **540**(1): p. 309-311.
234. Traugott, U. and P. Lebon, *Multiple sclerosis: Involvement of interferons in lesion pathogenesis.* Annals of Neurology, 1988. **24**(2): p. 243-251.
235. Cua, D.J., et al., *Interleukin-23 rather than interleukin-12 is the critical cytokine for autoimmune inflammation of the brain.* Nature, 2003. **421**(6924): p. 744-8.
236. Langrish, C.L., et al., *IL-23 drives a pathogenic T cell population that induces autoimmune inflammation.* J Exp Med, 2005. **201**(2): p. 233-40.
237. Park, H., et al., *A distinct lineage of CD4 T cells regulates tissue inflammation by producing interleukin 17.* Nat Immunol, 2005. **6**(11): p. 1133-41.

238. Sutton, C., et al., *A crucial role for interleukin (IL)-1 in the induction of IL-17–producing T cells that mediate autoimmune encephalomyelitis.* Journal of Experimental Medicine, 2006. **203**(7): p. 1685-1691.
239. El-Behi, M., et al., *The encephalitogenicity of T(H)17 cells is dependent on IL-1- and IL-23-induced production of the cytokine GM-CSF.* Nat Immunol, 2011. **12**(6): p. 568-75.
240. Durelli, L., et al., *T-helper 17 cells expand in multiple sclerosis and are inhibited by interferon-beta.* Ann Neurol, 2009. **65**(5): p. 499-509.
241. Matusevicius, D., et al., *Interleukin-17 mRNA expression in blood and CSF mononuclear cells is augmented in multiple sclerosis.* Mult Scler, 1999. **5**(2): p. 101-4.
242. Tzartos, J.S., et al., *Interleukin-17 production in central nervous system-infiltrating T cells and glial cells is associated with active disease in multiple sclerosis.* The American journal of pathology, 2008. **172**(1): p. 146-155.
243. Korn, T., et al., *Myelin-specific regulatory T cells accumulate in the CNS but fail to control autoimmune inflammation.* Nature medicine, 2007. **13**(4): p. 423-431.
244. Bailey-Bucktrout, Samantha L., et al., *Self-antigen-Driven Activation Induces Instability of Regulatory T Cells during an Inflammatory Autoimmune Response.* Immunity, 2013. **39**(5): p. 949-962.
245. Korn, T., et al., *IL-6 controls Th17 immunity in vivo by inhibiting the conversion of conventional T cells into Foxp3+ regulatory T cells.* Proceedings of the National Academy of Sciences of the United States of America, 2008. **105**(47): p. 18460-18465.
246. Xiao, S., et al., *Retinoic acid increases Foxp3+ regulatory T cells and inhibits development of Th17 cells by enhancing TGF-β-driven Smad3 signaling and inhibiting IL-6 and IL-23 receptor expression.* J Immunol, 2008. **181**(4): p. 2277-84.
247. Koutrolos, M., et al. *Treg cells mediate recovery from EAE by controlling effector T cell proliferation and motility in the CNS*. Acta neuropathologica communications, 2014. **2**, 163 DOI: 10.1186/s40478-014-0163-1.
248. McGeachy, M.J., L.A. Stephens, and S.M. Anderton, *Natural recovery and protection from autoimmune encephalomyelitis: contribution of CD4+CD25+ regulatory cells within the central nervous system.* J Immunol, 2005. **175**(5): p. 3025-32.
249. Venken, K., et al., *Secondary progressive in contrast to relapsing-remitting multiple sclerosis patients show a normal CD4+CD25+ regulatory T-cell function and FOXP3 expression.* J Neurosci Res, 2006. **83**(8): p. 1432-46.
250. Basdeo, S.A., et al., *Polyfunctional, Pathogenic CD161+ Th17 Lineage Cells Are Resistant to Regulatory T Cell-Mediated Suppression in the Context of Autoimmunity.* J Immunol, 2015. **195**(2): p. 528-40.
251. Komuczki, J., et al., *Fate-Mapping of GM-CSF Expression Identifies a Discrete Subset of Inflammation-Driving T Helper Cells Regulated by Cytokines IL-23 and IL-1beta.* Immunity, 2019. **50**(5): p. 1289-1304.e6.
252. Shimonkevitz, R., et al., *Clonal expansion of activated γδ T cells in recent onset multiple sclerosis.* Proceedings of the National Academy of Sciences of the United States of America, 1993. **90**: p. 923-7.
253. Schirmer, L., et al., *Enriched CD161high CCR6+ γδ T Cells in the Cerebrospinal Fluid of Patients With Multiple Sclerosis.* JAMA Neurology, 2013. **70**(3): p. 345-351.
254. Zarobkiewicz, M.K., et al., *RORγT is overexpressed in iNKT and γδ T cells during relapse in relapsing-remitting multiple sclerosis.* Journal of Neuroimmunology, 2019. **337**: p. 577046.
255. Petermann, F., et al., *γδ T cells enhance autoimmunity by restraining regulatory T cell responses via an interleukin-23-dependent mechanism.* Immunity, 2010. **33**(3): p. 351-63.

256. Tan, L., et al., *Single-Cell Transcriptomics Identifies the Adaptation of Scart1+ Vγ6+ T Cells to Skin Residency as Activated Effector Cells.* Cell Reports, 2019. **27**(12): p. 3657-3671.e4.
257. Constant, P., et al., *Stimulation of Human γδ T Cells by Nonpeptidic Mycobacterial Ligands.* Science, 1994. **264**(5156): p. 267-270.
258. Decaup, E., et al., *Phosphoantigens and butyrophilin 3A1 induce similar intracellular activation signaling in human TCRVγ9+ γδ T lymphocytes.* Immunology Letters, 2014. **161**(1): p. 133-137.
259. Willcox, C.R., et al., *Butyrophilin-like 3 Directly Binds a Human Vγ4+ T Cell Receptor Using a Modality Distinct from Clonally-Restricted Antigen.* Immunity, 2019. **51**(5): p. 813-825.e4.
260. Girlanda, S., et al., *MICA expressed by multiple myeloma and monoclonal gammopathy of undetermined significance plasma cells Costimulates pamidronate-activated gammadelta lymphocytes.* Cancer Res, 2005. **65**(16): p. 7502-8.
261. Castella, B., et al., *Anergic bone marrow Vγ9Vδ2 T cells as early and long-lasting markers of PD-1-targetable microenvironment-induced immune suppression in human myeloma.* OncoImmunology, 2015. **4**(11): p. e1047580.
262. Hoeres, T., et al., *PD-1 signaling modulates interferon-γ production by Gamma Delta (γδ) T-Cells in response to leukemia.* OncoImmunology, 2019. **8**(3): p. 1550618.
263. Nada, M.H., et al., *PD-1 checkpoint blockade enhances adoptive immunotherapy by human Vγ2Vδ2 T cells against human prostate cancer.* OncoImmunology, 2021. **10**(1): p. 1989789.
264. Shiravand, Y., et al., *Immune Checkpoint Inhibitors in Cancer Therapy.* Curr Oncol, 2022. **29**(5): p. 3044-3060.
265. Darnell, E.P., et al., *Immune-Related Adverse Events (irAEs): Diagnosis, Management, and Clinical Pearls.* Curr Oncol Rep, 2020. **22**(4): p. 39.
266. Menzies, A.M., et al., *Anti-PD-1 therapy in patients with advanced melanoma and preexisting autoimmune disorders or major toxicity with ipilimumab.* Annals of Oncology, 2017. **28**(2): p. 368-376.
267. Fellner, A., et al., *Neurologic complications of immune checkpoint inhibitors.* Journal of Neuro-Oncology, 2018. **137**(3): p. 601-609.
268. Garcia, C.R., et al., *Multiple sclerosis outcomes after cancer immunotherapy.* Clinical and Translational Oncology, 2019. **21**(10): p. 1336-1342.
269. Romeo, M.A.L., et al., *Multiple sclerosis associated with pembrolizumab in a patient with non-small cell lung cancer.* Journal of Neurology, 2019. **266**(12): p. 3163-3166.
270. Kroner, A., et al., *A PD-1 polymorphism is associated with disease progression in multiple sclerosis.* Annals of Neurology, 2005. **58**(1): p. 50-57.
271. Ortler, S., et al., *B7-H1 restricts neuroantigen-specific T cell responses and confines inflammatory CNS damage: Implications for the lesion pathogenesis of multiple sclerosis.* European Journal of Immunology, 2008. **38**(6): p. 1734-1744.
272. Carter, L.L., et al., *PD-1/PD-L1, but not PD-1/PD-L2, interactions regulate the severity of experimental autoimmune encephalomyelitis.* Journal of Neuroimmunology, 2007. **182**(1): p. 124-134.
273. Cao, Q., et al., *The change of PD1, PDL1 in experimental autoimmune encephalomyelitis treated by 1,25(OH)2D3.* Journal of Neuroimmunology, 2020. **338**: p. 577079.
274. Rui, Y., T. Honjo, and S. Chikuma, *Programmed cell death 1 inhibits inflammatory helper T-cell development through controlling the innate immune response.* Proc Natl Acad Sci U S A, 2013. **110**(40): p. 16073-8.
275. Hamada, S., et al., *IL-17A produced by gammadelta T cells plays a critical role in innate immunity against listeria monocytogenes infection in the liver.* J Immunol, 2008. **181**(5): p. 3456-63.

276. Homet Moreno, B., et al., *Response to Programmed Cell Death-1 Blockade in a Murine Melanoma Syngeneic Model Requires Costimulation, CD4, and CD8 T Cells.* Cancer Immunol Res, 2016. **4**(10): p. 845-857.
277. Dyck, L., et al., *Anti-PD-1 inhibits Foxp3+ Treg cell conversion and unleashes intratumoural effector T cells thereby enhancing the efficacy of a cancer vaccine in a mouse model.* Cancer Immunology, Immunotherapy, 2016. **65**(12): p. 1491-1498.
278. Lalor, S.J., et al., *Caspase-1–Processed Cytokines IL-1β and IL-18 Promote IL-17 Production by γδ and CD4 T Cells That Mediate Autoimmunity.* The Journal of Immunology, 2011. **186**(10): p. 5738-5748.
279. Billiau, A. and P. Matthys, *Modes of action of Freund's adjuvants in experimental models of autoimmune diseases.* J Leukoc Biol, 2001. **70**(6): p. 849-60.
280. Kosugi, A., et al., *Involvement of SHP-1 tyrosine phosphatase in TCR-mediated signaling pathways in lipid rafts.* Immunity, 2001. **14**(6): p. 669-80.
281. Blackburn, S.D., et al., *Coregulation of CD8+ T cell exhaustion by multiple inhibitory receptors during chronic viral infection.* Nature Immunology, 2009. **10**(1): p. 29-37.
282. Bally, A.P., J.W. Austin, and J.M. Boss, *Genetic and Epigenetic Regulation of PD-1 Expression.* J Immunol, 2016. **196**(6): p. 2431-7.
283. Austin, J.W., et al., *STAT3, STAT4, NFATc1, and CTCF regulate PD-1 through multiple novel regulatory regions in murine T cells.* J Immunol, 2014. **192**(10): p. 4876-86.
284. Yang, X.P., et al., *Opposing regulation of the locus encoding IL-17 through direct, reciprocal actions of STAT3 and STAT5.* Nat Immunol, 2011. **12**(3): p. 247-54.
285. Lu, Y., et al., *PLZF Controls the Development of Fetal-Derived IL-17+Vγ6+ γδ T Cells.* J Immunol, 2015. **195**(9): p. 4273-81.
286. Savage, A.K., et al., *The Transcription Factor PLZF Directs the Effector Program of the NKT Cell Lineage.* Immunity, 2008. **29**(3): p. 391-403.
287. Bertram, T., et al., *Kidney-resident innate-like memory γδ T cells control chronic Staphylococcus aureus infection of mice.* Proc Natl Acad Sci U S A, 2023. **120**(1): p. e2210490120.
288. Rei, M., et al., *Murine CD27(-) Vγ6(+) γδ T cells producing IL-17A promote ovarian cancer growth via mobilization of protumor small peritoneal macrophages.* Proc Natl Acad Sci U S A, 2014. **111**(34): p. E3562-70.
289. Staron, Matthew M., et al., *The Transcription Factor FoxO1 Sustains Expression of the Inhibitory Receptor PD-1 and Survival of Antiviral CD8+ T Cells during Chronic Infection.* Immunity, 2014. **41**(5): p. 802-814.
290. Yamana, T., et al., *IL-17A–Secreting Memory γδ T Cells Play a Pivotal Role in Sensitization and Development of Hypersensitivity Pneumonitis.* The Journal of Immunology, 2021. **206**(2): p. 355-365.
291. Matis, L.A., et al., *Structure and specificity of a class II MHC alloreactive gamma delta T cell receptor heterodimer.* Science, 1989. **245**(4919): p. 746-9.
292. Coffelt, S.B., et al., *IL-17-producing γδ T cells and neutrophils conspire to promote breast cancer metastasis.* Nature, 2015. **522**(7556): p. 345-348.
293. Wakita, D., et al., *Tumor-infiltrating IL-17-producing γδ T cells support the progression of tumor by promoting angiogenesis.* European Journal of Immunology, 2010. **40**(7): p. 1927-1937.
294. Du, Y., et al., *Cancer cell-expressed BTNL2 facilitates tumour immune escape via engagement with IL-17A-producing γδ T cells.* Nature Communications, 2022. **13**(1): p. 231.
295. Li, Q., P.T. Ngo, and N.K. Egilmez, *Anti-PD-1 antibody-mediated activation of type 17 T-cells undermines checkpoint blockade therapy.* Cancer Immunol Immunother, 2021. **70**(6): p. 1789-1796.

296. Liu, C., et al., *Blocking IL-17A enhances tumor response to anti-PD-1 immunotherapy in microsatellite stable colorectal cancer.* J Immunother Cancer, 2021. **9**(1).
297. Curnock, A.P., et al., *Cell-targeted PD-1 agonists that mimic PD-L1 are potent T cell inhibitors.* JCI Insight, 2021. **6**(20).
298. Tuttle, J., et al., *A Phase 2 Trial of Peresolimab for Adults with Rheumatoid Arthritis.* New England Journal of Medicine, 2023. **388**(20): p. 1853-1862.
299. Rahmani, S., et al., *The expression analyses of RMRP, DDX5, and RORC in RRMS patients treated with different drugs versus naïve patients and healthy controls.* Gene, 2021. **769**: p. 145236.
300. Stathopoulou, C., et al., *PD-1 Inhibitory Receptor Downregulates Asparaginyl Endopeptidase and Maintains Foxp3 Transcription Factor Stability in Induced Regulatory T Cells.* Immunity, 2018. **49**(2): p. 247-263.e7.
301. Kamada, T., et al., *PD-1(+) regulatory T cells amplified by PD-1 blockade promote hyperprogression of cancer.* Proc Natl Acad Sci U S A, 2019. **116**(20): p. 9999-10008.
302. Kumagai, S., et al., *The PD-1 expression balance between effector and regulatory T cells predicts the clinical efficacy of PD-1 blockade therapies.* Nature Immunology, 2020. **21**(11): p. 1346-1358.
303. van Gulijk, M., et al., *PD-L1 checkpoint blockade promotes regulatory T cell activity that underlies therapy resistance.* Science Immunology, 2023. **8**(83): p. eabn6173.
304. Basdeo, S.A., et al., *Ex-Th17 (Nonclassical Th1) Cells Are Functionally Distinct from Classical Th1 and Th17 Cells and Are Not Constrained by Regulatory T Cells.* The Journal of Immunology, 2017. **198**(6): p. 2249-2259.
305. Gao, Y., et al., *Gamma delta T cells provide an early source of interferon gamma in tumor immunity.* J Exp Med, 2003. **198**(3): p. 433-42.
306. Riond, J., et al., *In vivo major histocompatibility complex class I (MHCI) expression on MHCIIow tumor cells is regulated by gammadelta T and NK cells during the early steps of tumor growth.* Cancer Immun, 2009. **9**: p. 10.
307. von Lilienfeld-Toal, M., et al., *Coculture with dendritic cells promotes proliferation but not cytotoxic activity of gamma/delta T cells.* Immunol Lett, 2005. **99**(1): p. 103-8.
308. Bettelli, E., et al., *IL-10 is critical in the regulation of autoimmune encephalomyelitis as demonstrated by studies of IL-10- and IL-4-deficient and transgenic mice.* J Immunol, 1998. **161**(7): p. 3299-306.
309. Cua, D.J., et al., *Central Nervous System Expression of IL-10 Inhibits Autoimmune Encephalomyelitis1.* The Journal of Immunology, 2001. **166**(1): p. 602-608.
310. Wildbaum, G., N. Netzer, and N. Karin, *Tr1 cell-dependent active tolerance blunts the pathogenic effects of determinant spreading.* J Clin Invest, 2002. **110**(5): p. 701-10.
311. Edwards, S.C., S.C. Higgins, and K.H.G. Mills, *Respiratory infection with a bacterial pathogen attenuates CNS autoimmunity through IL-10 induction.* Brain Behav Immun, 2015. **50**: p. 41-46.
312. van Boxel-Dezaire, A.H., et al., *Decreased interleukin-10 and increased interleukin-12p40 mRNA are associated with disease activity and characterize different disease stages in multiple sclerosis.* Ann Neurol, 1999. **45**(6): p. 695-703.
313. Waubant, E., et al., *Relationship between serum levels of IL-10, MRI activity and interferon beta-1a therapy in patients with relapsing remitting MS.* Journal of Neuroimmunology, 2001. **112**(1): p. 139-145.
314. Asseman, C., et al., *An essential role for interleukin 10 in the function of regulatory T cells that inhibit intestinal inflammation.* J Exp Med, 1999. **190**(7): p. 995-1004.
315. Hara, M., et al., *IL-10 is required for regulatory T cells to mediate tolerance to alloantigens in vivo.* J Immunol, 2001. **166**(6): p. 3789-96.

316. Vandenbark, A.A., et al., *Diminished frequency of interleukin-10-secreting, T-cell receptor peptide-reactive T cells in multiple sclerosis patients might allow expansion of activated memory T cells bearing the cognate BV gene.* J Neurosci Res, 2001. **66**(2): p. 171-6.
317. Carter, N.A., E.C. Rosser, and C. Mauri, *Interleukin-10 produced by B cells is crucial for the suppression of Th17/Th1 responses, induction of T regulatory type 1 cells and reduction of collagen-induced arthritis.* Arthritis Res Ther, 2012. **14**(1): p. R32.
318. Radomir, L., et al., *The survival and function of IL-10-producing regulatory B cells are negatively controlled by SLAMF5.* Nature Communications, 2021. **12**(1): p. 1893.
319. Knippenberg, S., et al., *Reduction in IL-10 producing B cells (Breg) in multiple sclerosis is accompanied by a reduced naïve/memory Breg ratio during a relapse but not in remission.* J Neuroimmunol, 2011. **239**(1-2): p. 80-6.
320. Kim, Y., et al., *Restoration of regulatory B cell deficiency following alemtuzumab therapy in patients with relapsing multiple sclerosis.* J Neuroinflammation, 2018. **15**(1): p. 300.
321. Fillatreau, S., et al., *B cells regulate autoimmunity by provision of IL-10.* Nature Immunology, 2002. **3**(10): p. 944-950.
322. Laffer, B., et al., *Loss of IL-10 Promotes Differentiation of Microglia to a M1 Phenotype.* Front Cell Neurosci, 2019. **13**: p. 430.
323. Lobo-Silva, D., et al., *Interferon-β regulates the production of IL-10 by toll-like receptor-activated microglia.* Glia, 2017. **65**(9): p. 1439-1451.
324. Kvarnström, M., et al., *Longitudinal interferon-β effects in multiple sclerosis: Differential regulation of IL-10 and IL-17A, while no sustained effects on IFN-γ, IL-4 or IL-13.* Journal of the Neurological Sciences, 2013. **325**(1): p. 79-85.
325. McKinstry, K.K., et al., *IL-10 Deficiency Unleashes an Influenza-Specific Th17 Response and Enhances Survival against High-Dose Challenge1.* The Journal of Immunology, 2009. **182**(12): p. 7353-7363.
326. Bose, T.O., et al., *CD11a is essential for normal development of hematopoietic intermediates.* J Immunol, 2014. **193**(6): p. 2863-72.
327. Glatigny, S., et al., *Integrin alpha L controls the homing of regulatory T cells during CNS autoimmunity in the absence of integrin alpha 4.* Scientific Reports, 2015. **5**(1): p. 7834.
328. Yednock, T.A., et al., *Prevention of experimental autoimmune encephalomyelitis by antibodies against α4β1 integrin.* Nature, 1992. **356**(6364): p. 63-66.
329. Ransohoff, R.M., *Natalizumab for Multiple Sclerosis.* New England Journal of Medicine, 2007. **356**(25): p. 2622-2629.
330. Calabresi, P.A., et al., *VLA-4 expression on peripheral blood lymphocytes is downregulated after treatment of multiple sclerosis with interferon beta.* Neurology, 1997. **49**(4): p. 1111-6.
331. Huss, D.J., et al., *TGF-β signaling via Smad4 drives IL-10 production in effector Th1 cells and reduces T-cell trafficking in EAE.* European Journal of Immunology, 2011. **41**(10): p. 2987-2996.
332. Jarnicki, A.G., et al., *Suppression of antitumor immunity by IL-10 and TGF-beta-producing T cells infiltrating the growing tumor: influence of tumor environment on the induction of CD4+ and CD8+ regulatory T cells.* J Immunol, 2006. **177**(2): p. 896-904.
333. Ferreira, C.M., et al., *Early IL-10 promotes vasculature-associated CD4+ T cells unable to control Mycobacterium tuberculosis infection.* JCI Insight, 2021. **6**(21).
334. Yi, S., et al., *IL-4 and IL-10 promotes phagocytic activity of microglia by up-regulation of TREM2.* Cytotechnology, 2020. **72**(4): p. 589-602.
335. Yogev, N., et al., *CD4(+) T-cell-derived IL-10 promotes CNS inflammation in mice by sustaining effector T cell survival.* Cell Rep, 2022. **38**(13): p. 110565.
336. Babbe, H., et al., *Clonal expansions of CD8(+) T cells dominate the T cell infiltrate in active multiple sclerosis lesions as shown by micromanipulation and single cell polymerase chain reaction.* J Exp Med, 2000. **192**(3): p. 393-404.

337. Schmidt, A., N. Oberle, and P. Krammer, *Molecular Mechanisms of Treg-Mediated T Cell Suppression.* Frontiers in Immunology, 2012. **3**.
338. Tang, Q., et al., *Distinct roles of CTLA-4 and TGF-β in CD4+CD25+ regulatory T cell function.* European Journal of Immunology, 2004. **34**(11): p. 2996-3005.
339. Choi, G., et al., *A critical role for Th17 cell-derived TGF-β1 in regulating the stability and pathogenicity of autoimmune Th17 cells.* Experimental & Molecular Medicine, 2021. **53**(5): p. 993-1004.
340. Rowan, A.G., et al., *Hepatitis C Virus-Specific Th17 Cells Are Suppressed by Virus-Induced TGF-β1.* The Journal of Immunology, 2008. **181**(7): p. 4485-4494.
341. Walsh, K.P., et al., *Infection with a Helminth Parasite Attenuates Autoimmunity through TGF-β-Mediated Suppression of Th17 and Th1 Responses1.* The Journal of Immunology, 2009. **183**(3): p. 1577-1586.
342. Asad, M., et al., *Effector functions of Th17 cells are regulated by IL-35 and TGF-β in visceral leishmaniasis.* The FASEB Journal, 2021. **35**(9): p. e21755.
343. Perez, L.G., et al., *TGF-β signaling in Th17 cells promotes IL-22 production and colitis-associated colon cancer.* Nature Communications, 2020. **11**(1): p. 2608.
344. Ness-Schwickerath, K.J., C. Jin, and C.T. Morita, *Cytokine Requirements for the Differentiation and Expansion of IL-17A– and IL-22–Producing Human Vγ2Vδ2 T Cells.* The Journal of Immunology, 2010. **184**(12): p. 7268-7280.
345. Casetti, R., et al., *Cutting edge: TGF-beta1 and IL-15 Induce FOXP3+ gammadelta regulatory T cells in the presence of antigen stimulation.* J Immunol, 2009. **183**(6): p. 3574-7.
346. Schmierer, B. and C.S. Hill, *TGFβ–SMAD signal transduction: molecular specificity and functional flexibility.* Nature Reviews Molecular Cell Biology, 2007. **8**(12): p. 970-982.
347. Feng, X.H. and R. Derynck, *Specificity and versatility in tgf-beta signaling through Smads.* Annu Rev Cell Dev Biol, 2005. **21**: p. 659-93.
348. Itoh, S. and P. ten Dijke, *Negative regulation of TGF-beta receptor/Smad signal transduction.* Curr Opin Cell Biol, 2007. **19**(2): p. 176-84.
349. Xu, J., et al., *TGF-β in Mice Ameliorates Experimental Autoimmune Encephalomyelitis in Regulating NK Cell Activity.* Cell Transplantation, 2019. **28**(9-10): p. 1155-1160.
350. Li, M.O., Y.Y. Wan, and R.A. Flavell, *T Cell-Produced Transforming Growth Factor-β1 Controls T Cell Tolerance and Regulates Th1- and Th17-Cell Differentiation.* Immunity, 2007. **26**(5): p. 579-591.
351. Severin, M.E., et al., *MicroRNAs targeting TGFβ signalling underlie the regulatory T cell defect in multiple sclerosis.* Brain, 2016. **139**(Pt 6): p. 1747-61.
352. Agerholm, R., et al., *STAT3 but not STAT4 is critical for γδT17 cell responses and skin inflammation.* EMBO reports, 2019. **20**(11): p. e48647.
353. Veldhoen, M., et al., *Signals mediated by transforming growth factor-β initiate autoimmune encephalomyelitis, but chronic inflammation is needed to sustain disease.* Nature Immunology, 2006. **7**(11): p. 1151-1156.
354. Takimoto, T., et al., *Smad2 and Smad3 Are Redundantly Essential for the TGF-β–Mediated Regulation of Regulatory T Plasticity and Th1 Development.* The Journal of Immunology, 2010. **185**(2): p. 842-855.
355. Ichiyama, K., et al., *Transcription Factor Smad-Independent T Helper 17 Cell Induction by Transforming-Growth Factor-β Is Mediated by Suppression of Eomesodermin.* Immunity, 2011. **34**(5): p. 741-754.
356. Duhen, R., et al., *Cutting edge: the pathogenicity of IFN-γ-producing Th17 cells is independent of T-bet.* J Immunol, 2013. **190**(9): p. 4478-82.
357. Dungan, L.S., et al., *Innate IFN-γ promotes development of experimental autoimmune encephalomyelitis: a role for NK cells and M1 macrophages.* Eur J Immunol, 2014. **44**(10): p. 2903-17.

358. Chakraborty, D., et al., *Activation of STAT3 integrates common profibrotic pathways to promote fibroblast activation and tissue fibrosis.* Nature Communications, 2017. **8**(1): p. 1130.
359. Na, H., et al., *Concomitant suppression of TH2 and TH17 cell responses in allergic asthma by targeting retinoic acid receptor–related orphan receptor γt.* Journal of Allergy and Clinical Immunology, 2018. **141**(6): p. 2061-2073.e5.
360. Ajendra, J., et al., *IL-17A both initiates, via IFNγ suppression, and limits the pulmonary type-2 immune response to nematode infection.* Mucosal Immunology, 2020. **13**(6): p. 958-968.
361. Noster, R., et al., *IL-17 and GM-CSF expression are antagonistically regulated by human T helper cells.* Sci Transl Med, 2014. **6**(241): p. 241ra80.
362. Aram, J., et al., *Increased IL-2 and Reduced TGF-β Upon T-Cell Stimulation are Associated with GM-CSF Upregulation in Multiple Immune Cell Types in Multiple Sclerosis.* Biomedicines, 2020. **8**(7).
363. Batoulis, H., et al., *Blockade of tumour necrosis factor-α in experimental autoimmune encephalomyelitis reveals differential effects on the antigen-specific immune response and central nervous system histopathology.* Clin Exp Immunol, 2014. **175**(1): p. 41-8.
364. Sean Riminton, D., et al., *Challenging Cytokine Redundancy: Inflammatory Cell Movement and Clinical Course of Experimental Autoimmune Encephalomyelitis Are Normal in Lymphotoxin-deficient, but Not Tumor Necrosis Factor–deficient, Mice.* Journal of Experimental Medicine, 1998. **187**(9): p. 1517-1528.
365. Cottrell, D.A., et al., *The natural history of multiple sclerosis: a geographically based study. 5. The clinical features and natural history of primary progressive multiple sclerosis.* Brain, 1999. **122 (Pt 4)**: p. 625-39.
366. McGinley, M.P., C.H. Goldschmidt, and A.D. Rae-Grant, *Diagnosis and Treatment of Multiple Sclerosis: A Review.* JAMA, 2021. **325**(8): p. 765-779.
367. MS Ireland, *Societal Cost of Multiple Sclerosis in Ireland 2022*. 2022: https://www.ms-society.ie/sites/default/files/2022-09/Approved%20report.pdf.
368. Hirota, K., et al., *Fate mapping of IL-17-producing T cells in inflammatory responses.* Nature Immunology, 2011. **12**(3): p. 255-263.
369. Javan, M.R., et al., *Downregulation of Immunosuppressive Molecules, PD-1 and PD-L1 but not PD-L2, in the Patients with Multiple Sclerosis.* Iran J Allergy Asthma Immunol, 2016. **15**(4): p. 296-302.
370. Machcińska, M., et al., *Reduced Expression of PD-1 in Circulating CD4+ and CD8+ Tregs Is an Early Feature of RRMS.* International Journal of Molecular Sciences, 2022. **23**(6): p. 3185.
371. Ogishi, M., et al., *Inherited PD-1 deficiency underlies tuberculosis and autoimmunity in a child.* Nature Medicine, 2021. **27**(9): p. 1646-1654.
372. Imai, Y., et al., *Cutting Edge: PD-1 Regulates Imiquimod-Induced Psoriasiform Dermatitis through Inhibition of IL-17A Expression by Innate γδ-Low T Cells.* The Journal of Immunology, 2015. **195**(2): p. 421-425.
373. Twomey, J.D. and B. Zhang, *Cancer Immunotherapy Update: FDA-Approved Checkpoint Inhibitors and Companion Diagnostics.* The AAPS Journal, 2021. **23**(2): p. 39.
374. Váraljai, R., et al., *Interleukin 17 signaling supports clinical benefit of dual CTLA-4 and PD-1 checkpoint inhibition in melanoma.* Nature Cancer, 2023.
375. He, J., et al., *Defined tumor antigen-specific T cells potentiate personalized TCR-T cell therapy and prediction of immunotherapy response.* Cell Research, 2022. **32**(6): p. 530-542.
376. Germano, G., et al., *Inactivation of DNA repair triggers neoantigen generation and impairs tumour growth.* Nature, 2017. **552**(7683): p. 116-120.

377. Sade-Feldman, M., et al., *Resistance to checkpoint blockade therapy through inactivation of antigen presentation.* Nature Communications, 2017. **8**(1): p. 1136.
378. de Vries, N.L., et al., *γδ T cells are effectors of immunotherapy in cancers with HLA class I defects.* Nature, 2023. **613**(7945): p. 743-750.
379. Wencker, M., et al., *Innate-like T cells straddle innate and adaptive immunity by altering antigen-receptor responsiveness.* Nature Immunology, 2014. **15**(1): p. 80-87.
380. Sambucci, M., et al., *FoxP3 isoforms and PD-1 expression by T regulatory cells in multiple sclerosis.* Scientific Reports, 2018. **8**(1): p. 3674.
381. Hu, D., et al., *Transcriptional signature of human pro-inflammatory TH17 cells identifies reduced IL10 gene expression in multiple sclerosis.* Nature Communications, 2017. **8**(1): p. 1600.
382. Zhou, Z., et al., *IL-10 promotes neuronal survival following spinal cord injury.* Exp Neurol, 2009. **220**(1): p. 183-90.
383. Norden, D.M., et al., *TGFβ produced by IL-10 redirected astrocytes attenuates microglial activation.* Glia, 2014. **62**(6): p. 881-895.
384. Moses, H.L., A.B. Roberts, and R. Derynck, *The Discovery and Early Days of TGF-β: A Historical Perspective.* Cold Spring Harb Perspect Biol, 2016. **8**(7).
385. Yap, T.A., et al., *AVID200, first-in-class TGF-beta 1 and 3 selective and potent inhibitor: Safety and biomarker results of a phase I monotherapy dose-escalation study in patients with advanced solid tumors.* Journal of Clinical Oncology, 2020. **38**(15_suppl): p. 3587-3587.
386. Nicoletti, F., et al., *Blood levels of transforming growth factor-beta 1 (TGF-beta1) are elevated in both relapsing remitting and chronic progressive multiple sclerosis (MS) patients and are further augmented by treatment with interferon-beta 1b (IFN-beta1b).* Clin Exp Immunol, 1998. **113**(1): p. 96-9.
387. Rollnik, J.D., et al., *Biologically active TGF-beta 1 is increased in cerebrospinal fluid while it is reduced in serum in multiple sclerosis patients.* Acta Neurol Scand, 1997. **96**(2): p. 101-5.
388. Naves, R., et al., *The Interdependent, Overlapping, and Differential Roles of Type I and II IFNs in the Pathogenesis of Experimental Autoimmune Encephalomyelitis.* The Journal of Immunology, 2013. **191**(6): p. 2967-2977.
389. Panitch, H.S., et al., *Treatment of multiple sclerosis with gamma interferon: exacerbations associated with activation of the immune system.* Neurology, 1987. **37**(7): p. 1097-102.
390. Bjornevik, K., et al., *Longitudinal analysis reveals high prevalence of Epstein-Barr virus associated with multiple sclerosis.* Science, 2022. **375**(6578): p. 296-301.